

**SYNTHESIS AND CHARACTERIZATION OF NOVEL MOLECULAR
ARCHITECTURES: POLYROTAXANES AND CATENANES**

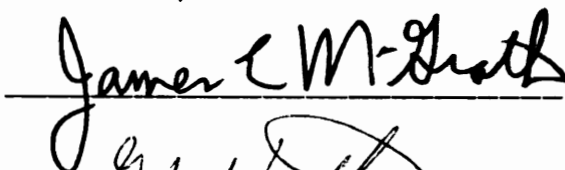
Mukesh C. Bheda

A dissertation submitted in partial fulfillment of
the requirements for the degree of
Doctor of Philosophy
in the
Department of Chemistry

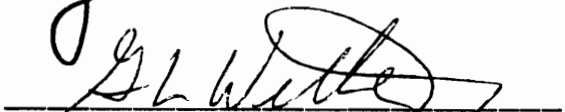
Virginia Polytechnic Institute and State University
Blacksburg, VA-24061
February, 1992



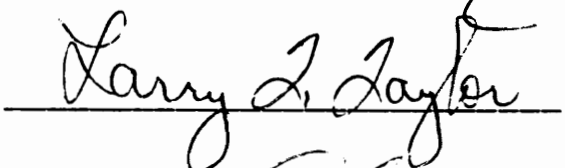
Dr. Harry W. Gibson



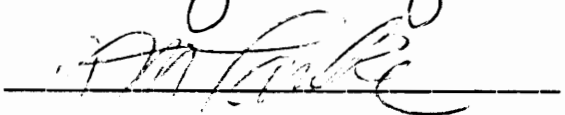
Dr. James E. McGrath



Dr. Garth L. Wilkes



Dr. Larry T. Taylor



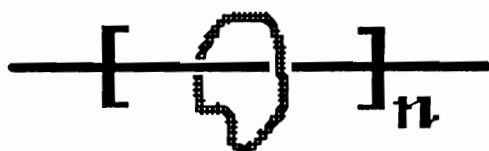
Dr. James M. Tanko



ABSTRACT

SYNTHESIS AND CHARACTERIZATION OF NOVEL MOLECULAR ARCHITECTURES: POLYROTAXANES AND CATENANES

Polyrotaxanes are novel polymer architectures consisting of two components. One component is the macrocycle consisting of 24-60 atoms; it is threaded by the second component, i.e., the linear backbone polymer. Combination of a variety of macrocycles and linear polymers could be used to obtain desired end use properties.



The macrocycles prepared in this investigation are (i) cyclic polystyrene by anionic polymerization (ii) crown ethers such as 30-crown-10 and 60-crown-20 and (iii) bipyridyl (ionic) macrocycle BP-28-N⁺₄, a tetra cationic macrocycle for use in the template threading method.

The linear species used for this investigation are (i) liquid crystalline polyesters (ii) linear polystyrene, (iii) polyaramides, all made by polymerization in the presence of the cyclic species and (iv) preformed polymers such as polybutadiene and poly(tetrahydrofuran) of various molecular weights and (v) small molecules such as 1,8-octanediol and 4,4'-biphenol.

Rotaxanes and polyrotaxanes of small molecules, preformed polymers and polymers have been synthesized using crown ethers. As high as 50 weight % macrocycles has been incorporated into the polymers. It was found that threading of polymeric species proceeds more efficiently than small molecules. Further, it was found that solubility and thermal properties were altered considerably by incorporation of macrocycles. Polyaramide rotaxanes showed

interplay of intermolecular and intraannular hydrogen bonding interactions resulting in behavior analogous to thermosetting polymers. . In the syntheses of polyrotaxanes of polystyrene by anionic polymerization, various factors such as the nature of the solvent, the polymerization temperature, etc., highly influenced the threading yields of the crown ether macrocycles.

Various factors such as size of the macrocycle, length of the linear chain, polarity, compatibility and flexibility or rigidity of two components can play important roles in threading yields. These are discussed in the light of experimental results.

Microstructure of Polystyrene

Model studies of end capping of living polystyryl anions, with and without α -methylstyrene at the chain ends, with chlorotrimethylsilane and chloromethyl methyl ether were done. In ^1H NMR spectra multiple peaks for $-\text{Si}(\text{CH}_3)_3$ and $-\text{CH}_2\text{-O-CH}_3$ group protons were observed. However, $-\text{Si}(\text{CH}_3)_3$ peak patterns for polymers with and without α -methylstyrene at the chain ends were quite different. Trimethylsilyl end group protons and methine or methylene protons of the polystyrene chain were not coupled as determined by decoupling experiments. Various parameters such as initiator, solvent, temperature and molecular weights did not change the peak pattern. This study indicates that the multiple peaks are due to stereoisomerism at the chain ends. Due to steric factors selective stereoisomer formation is indicated when α -methylstyrene is the terminal unit before end capping. Further, the chain end tacticities correspond to bulk tacticities and statistical analyses of multiple peaks gave $P_r = 0.55$, which is consistent with the reported values for anionically prepared polystyrene. These results from the proton nmr analyses were confirmed by integration values of end groups in carbon nmr. Thus, end group spectroscopy provides a means of determining bulk tacticity.

*In the Memory of My Beloved SatGuru
Maharaj Charan Singh Ji*

To

*My Wife Mary Joe,
Our Daughter Priti Beena
and Our Parents*

ACKNOWLEDGEMENTS

I wish to express my gratitude to many people who have contributed to and sacrificed greatly during my pursuit for higher education. First of all, I want to thank my parents for their understanding and loving support in all aspects of my personal development. I would not have made it through this pursuit without the loving care, support and encouragement of my wife Mary Joe. I will always remember your sacrifice of your pursuit so that I could continue.

Further, I want to express my sincere appreciation to Dr. Harry Gibson for providing me the opportunity, continued encouragement and valuable guidance in completing this work; moreover, for having faith in me while things were very bleak for me. A few interesting little facts I would like to mention here. As a member of Dr. Gibson's group I gave about 43 group meeting talks, 5 Saturday group meeting talks, 41 monthly and quarterly reports. It was quite a training !!! Dr. Gibson, you are a 'teacher' in its true meaning.

I would also like to thank Dr. James McGrath, Dr. Herve Marand, Dr. James Tanko, Dr. Yajna Jois, Dr. Jean-Pierre Leblanc, Dr. Yadi Delaviz, Dr. Joe Desimone and members of Dr. Gibson's group for many useful discussions and advice. Special thanks go to Dr. Joe Merola for obtaining X-ray crystal structures of my samples.

Thanks to Mr. Jeff Mecham and Dr. Milos Netopilik for GPC data, Dr. Abaneshwar Prasad for DSC and optical microscopy data, Mr. Paul Vail for DSC data, Mr. Manual Hervas for cyclic voltametry and bulk electrolyses of samples and Analytical Services at Virginia Tech for help with NMR instruments.

Financial support of this work was provided by the Polymers Program of the Division of Materials Research of the National Science Foundation through grant DMR-87-12428 and by the NSF Science and Technology Center for High Performance Adhesives and Composites at Virginia Polytechnic Institute and State University and is gratefully acknowledged.

TABLE OF CONTENTS

I.	HISTORICAL	1
I.1	Introduction	2
I.2	Polymer Topology	2
I.3	Polymer Blends	6
I.4	Polyrotaxane Architectures	7
I.5	Literature Review of Rotaxanes	9
I.6	Theoretical considerations	29
I.7	Practical Considerations	32
II.	OBJECTIVES	42
III.	CROWN ETHER MACROCYCLES AND CATENANE	45
III.1	Introduction	46
III.2	Literature Review	47
III.3	Results and Discussion	52
Characterization of 30-C-10		56
Characterization of 60-C-10		59
III.4	Catenane	60
III.5	Experimental	61
IV.	IONIC BIPYRIDYL MACROCYCLES	79
IV.1	Introduction	80
IV.2	Results and Discussions	81
IV.3	Experimental	87
V.	CYCLIC POLYSTYRENE	94
V.1	Introduction	95
V.2	Literature Review	96
V.3	Characterization of Cyclic Polystyrene	99
V.4	Conclusions	106
V.5	Experimental	106
VI.	BLOCKING GROUPS	119
VI.1	Strategies	120
VI.2	Literature Review	122
VI.3	Results and Discussion	123
VI.4	Experimental	134

VII.	MONOROTAXANES AND POLYROTAXANES	150
VII.1	Introduction	151
VII.2	Results and discussion	152
	Monorotaxanes	153
	Polyrotaxanes of Preformed Polymers	156
VII.3	Experimental	162
VIII.	POLYAMIDE ROTAXANES	177
VIII.1	Introduction	178
VIII.2	Consideration of Polyamides for Polyrotaxane Synthesis	179
VIII.3	Model ODA-I and its Polyrotaxanes	181
VIII.4	Model PPD-T (Kevlar™) and its Polyrotaxanes	190
VIII.5	Model Nylon-6,6 and its Polyrotaxane	194
VIII.6	Experimental	197
IX.	POLYSTYRENE ROTAXANES	210
IX.1	Introduction	211
IX.2	Results and Discussion	213
IX.3	Experimental	219
X.	LIQUID CRYSTALLINE POLYROTAXANES	229
X.1	Introduction	230
X.2	Considerations of LC Systems	232
X.3	Results and discussion	233
	Model LC Polyester	235
	Polyrotaxanes of LC Polyester	238
X.4	Experimental	241
XI	MICROSTRUCTURE OF POLYSTYRENE	250
XI.1	Introduction	251
XI.2	Results and Discussion	252
XI.3	Conclusions	263
XI.4	Experimental	264
XII.	SUMMARY AND PROSPECTS	278
	Appendix A Vacuum Line Set Up and Operation.	284
VITA	288

LIST of FIGURES

Figure III.1	^1H (270 MHz) and ^{13}C NMR of 30-c-10	67
Figure III.2	DSC Trace of 30-c-10	68
Figure III.3	X-Ray Crystal Structure of 30-c-10; Cavity Size: 3.9 °A x 13.6 °A, Unit Cell: Pbc _a (orthorhombic), a = 8.606 (1) °A, b = 8.260 (1) °A, c = 33.310 (4) °A	69
Figure III.4	X-Ray Crystal Structure of 30-c-10:4 H ₂ O; Cavity Size: 7.5 °A x 11.4 °A, Unit Cell: P21/c (monoclinic), a = 8.332 (4) °A, b = 9.083 (2) °A, c = 18.665 (5) °A, $\beta = 90.24^\circ$	70
Figure III.5	^1H (270 MHz) and ^{13}C NMR of 60-c-20	71
Figure III.6	CI Mass Spectrum of 60-c-20	72
Figure III.7	^1H (270 MHz) NMR of [2]catenane of 30-c-10	73
Figure III.8	CI Mass Spectrum of [2]catenane of 30-c-10	74
Figure IV.1	^1H (400 MHz) NMR of IV-4 and IV-7	90
Figure IV.2	FAB Mass Spectra of IV-4 and IV-7	91
Figure V.1	GPC Traces of Linear Precursor Polystyrene and Cyclization Reaction Product (UV Traces)	110
Figure V.2	GPC Traces of Cyclization Reaction Product, MB-125-2C-F1 and MB-125-2C-F2 (UV Traces)	111
Figure V.3	GPC Traces of MB-125-2C-F2, MB-125-2C-F3 and MB-125-2C-F4 (UV Traces)	112
Figure V.4	GPC Traces of MB-125-2C-F4 and MB-125-2L (UV Traces).	113

Figure V.5	^1H (400 MHz), ^{13}C and ^{29}Si NMR spectra of $-\text{Si}(\text{CH}_3)_2$ groups of Cyclic Polystyrene114
Figure V.6	DSC Traces (Second Heat) of Linear Polystyrene (MB-125-2L) and Cyclic Polystyrene (MB-125-2C-F4)115
Figure VI.1	^1H (400 MHz) NMR of VI-14144
Figure VI.2	GPC Trace of VI-14 (RI Trace)145
Figure VI.3	DSC Traces of VI-14146
Figure VI.4	^1H (270 MHz) NMR of VI-15147
Figure VI.5	DSC Trace of VI-15148
Figure VII.1	Schematic of Syntheses of Monorotaxanes from 1,8-octanediol and 4,4'-biphenol166
Figure VII.2	^1H (270 MHz) NMR of the Products of the Monorotaxane Syntheses from 1,8-octanediol and 4,4'-biphenol167
Figure VII.3	GPC Trace of the Product of the Monorotaxane Synthesis from 1,8-octanediol. Insert: (a) 30-c-10 and (b) acid blocking group (VI-7) (RI Trace)168
Figure VII.4	GPC Trace of the Product of the Monorotaxane Synthesis from 4,4'-biphenol (RI Trace)169
Figure VII.5	Schematic of Syntheses of Polyrotaxanes from PBD 2800, PTHF 2900 and PTHF 2000170
Figure VII.6	GPC Trace of the Product of the Polyrotaxane Synthesis from PTHF 2900 (RI Trace)171
Figure VII.7	GPC Trace of the Product of the Polyrotaxane Synthesis from PTHF 2000 (RI Trace)172

Figure VII.8	GPC Trace of the Product of the Polyrotaxane Synthesis from PBD 2800 (RI Trace)173
Figure VII.9	GPC Traces of the Products of the Model Polymer Syntheses from PBD 2800, PTHF 2900 and PTHF 2000 (RI Traces)174
Figure VII.10	¹ H (270 MHz) NMR of the Products of the Polyrotaxane Syntheses from PBD 2800, PTHF 2900 and PTHF 2000175
Figure VIII.1	¹ H (270 MHz) NMR of ODA-I-Rotaxa-30-c-10 and ODA-I-Rotaxa-60-c-20201
Figure VIII.2	GPC Traces of ODA-I, ODA-I-Rotaxa-30-c-10 and ODA-I-Rotaxa-60-c-20, (a) RI Trace and (b) Viscosity Trace202
Figure VIII.3	DSC Traces of ODA-I-Rotaxa-30-c-10203
Figure VIII.4	DSC Traces of ODA-I-Rotaxa-60-c-20204
Figure VIII.5	DTA-TG Traces of ODA-I-Rotaxa-60-c-20205
Figure VIII.6	¹³ C Solid State NMR of PPD-T-Rotaxa-60-c-20206
Figure VIII.7	TGA Traces of PPD-T and PPD-T-Rotaxa-60-c-20207
Figure IX.1	Schematic of the Syntheses of Polyrotaxanes of Polystyrene using 30-c-10 and 60-c-20223
Figure IX.2	¹ H NMR Spectrum of Polystyrene-Rotaxa-30-c-10 (IX-4)224
Figure IX.3	GPC Traces of Polystyrene-Rotaxa-30-c-10 (IX-4) and Polystyrene-Rotaxa-60-c-20 (IX-6) (UV Traces)225

Figure IX.4	GPC Traces of 30-c-10 and 60-c-20 (RI Traces)	. 226
Figure X.1	DSC Traces of Model LC Polyester and its Polyrotaxane	. 246
Figure X.2	^{13}C Solid State NMR Spectra of LC polyester and its Polyrotaxane	. 247
Figure XI.1	Typical ^1H (400 MHz) NMR of Model End Capped Polystyrene	. 266
Figure XI.2	^1H (400 MHz), ^{13}C and ^{29}Si NMR spectra of -Si(CH $_3$) $_3$ groups of model polymers [A] Mn=2200, Mw/Mn=1.15 and [C] Mn=2300, Mw/Mn=1.15	. 267
Figure XI.3	^1H (400 MHz), ^{13}C and ^{29}Si NMR spectra of -Si(CH $_3$) $_3$ groups of model polymers [B] Mn=1800, Mw/Mn=1.10 and [D] Mn=2500, Mw/Mn=1.09	. 268
Figure XI.4	NMR Spectra of -CH $_2$ -O-CH $_3$ groups of model polymer [E] Mn=1800, Mw/Mn= 1.12; (a) ^1H NMR (400 MHz), (b) ^{13}C NMR: -CH $_2$ -O-groups and (c) ^{13}C NMR: -O-CH $_3$ groups	. 269
Figure XI.5	Deconvolution of the ^1H NMR spectrum of -Si(CH $_3$) $_3$ groups of the model polymer [A]. The actual spectrum (top), the deconvoluted peaks (bottom) and full fit (center) are shown	. 270
Figure XI.6	Schematic Representation of Tetrad Structures Observed for Model Polymers [A] and [B]	. 271
Figure XI.7	Schematic Representation of Triad Structures Observed for Model Polymers [C] and [D]	. 272

Figure XI.8	^{13}C NMR Spectra of $-\text{Si}(\text{CH}_3)_3$ End Groups of Model Polymers [A] and [B] and $-\text{CH}_2\text{-O-CH}_3$ End Groups of Model Polymer [E] with Integration Values273
Figure A-1	Vacuum Line Setup287

LIST of TABLES

Table III.1	Reported Syntheses of Crown Ethers . . .	51
Table III.2	Torsional Angles in Anhydrous 30-c-10 . . .	58
Table III.3	Torsional Angles in 30-c-10:4 H ₂ O . . .	59
Table IV.1	400 MHz Proton NMR Chemical Shifts for IV-4 and IV-7	84
Table IV.2	Carbon NMR Chemical Shifts for IV-4 and IV-7	84
Table V.1	Reported Intrinsic Viscosity Data for Cyclic Polystyrene	98
Table V.2	Weights of the Isolated Fractions . . .	103
Table VI.1	Reaction Conditions & Yields of VI-12 . . .	128
Table VII-1	Calculated Molecular Weights of the Products .	155
Table VII-2	Polyrotaxanes from Preformed Polymers . . .	159
Table VII-3	Synthesis and Characterization of Mono- and Poly-rotaxanes	161
Table VIII.1	Precipitation of ODA-I Polyrotaxanes . . .	183
Table VIII.2	Synthesis and Characterization of Polyrotaxanes of Polyamides	196
Table IX-1	Synthesis and Characterization of Polyrotaxanes of Polystyrene	215
Table X.1	One Phase Syntheses of LC Polyester . . .	237

Table XI.1	Frequencies and Integral Values of Deconvoluted peaks	.259
Table XI.2	Statistical Analyses of Deconvoluted peaks	.261

I.	HISTORICAL	1
	I.1	Introduction	2
	I.2	Polymer Topology	2
	I.3	Polymer Blends	6
	I.4	Polyrotaxane Architectures	7
	I.5	Literature Review of Rotaxanes	9
	I.6	Theoretical considerations	29
	I.7	Practical Considerations	32

1.1 Introduction

The increasing use of synthetic polymers by industrialists and engineers to replace or supplement more traditional materials has stimulated the research for even more versatile polymeric structures covering a wide range of properties. To exploit the existing technologies as well as to search efficiently, fundamental knowledge of structure-property relationships has been and is being studied extensively. The structure-property relationships can be dealt with under two broad topics: (i) Chemical aspects of polymers and (ii) Architectural aspects of the polymers (1a).

(i) **Chemical Aspects:** These deal with information on the molecular structure of the macromolecules, including the type of monomer repeat units constituting the chain and the parameters which relates ultimately to the 3-dimensional aggregate structures and physical properties. The solubility properties as well as bulk properties of macromolecules such as glass transition temperature, melting temperatures, crystallinity, modulus depend primarily on the chain flexibility, chain symmetry and intermolecular interactions which, in turn, mainly depend on the chemical nature of the macromolecules.

(ii) **Architectural aspects:** These are concerned with the chain as a whole. Macromolecules in different architectural arrangements (topology) have considerably different properties, for e.g., linear polymers vs networks, branched and cyclic polymers as well as block and graft copolymers.

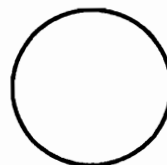
In the following discussion, architectural aspects and the resulting changes in the properties of the polymers are outlined.

1.2 Polymer Topology

Scheme 1-1 shows polymers of different architectures. The structures represented here are of current commercial and academic interest.

Scheme I-1 Polymer Topologies

I Cyclic Polymers (No Chain Ends)



II Linear Polymers (Two Chain Ends)

Homopolymers
Random copolymers



Block copolymers (Di-, Tri-)



Segmented Copolymers



III Branched Polymers

(More than Two Ends)

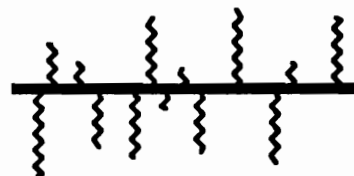
Star Polymers (Homo- or Block-)



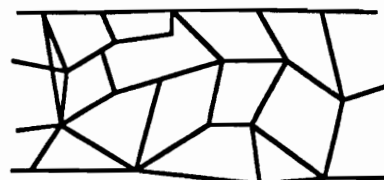
Randomly Branched Polymers



Graft/Comb Polymers
(Long Chain- &
Short Chain- Branching)



IV Network Polymers
(One Enormous Molecule)



Polymer classes are listed in the order of increasing number of chain ends except the network polymer which represents one enormous molecule with relatively few chain ends. Cyclic polymers (Chapter V) represent an extreme case of the broad spectrum of polymer architectures and have no chain ends. Each class of polymer has its unique properties. The unique properties of cyclic polymers include lower hydrodynamic volumes, lower melt viscosities, higher glass transition temperatures at low molecular weights, and low frictional coefficients compared to linear counterparts of similar molecular weights.

The importance of block copolymers can be realized from the fact that depending upon the arrangement of the blocks, compatibility and their crystalline tendencies (T_g and T_m), more versatile high tensile strength materials usable in a relatively larger temperature window than the random copolymer can be produced. Such block copolymers show microphase separation in which glassy or crystalline blocks tend to aggregate in domains and serve to anchor the elastomeric blocks and act as effective physical cross-linking points. These physical crosslinks are reversible. Examples of such thermoplastic elastomers include polyurethanes and polystyrene-polydiene block copolymers (1b).

Block and graft copolymers are also used as blend compatibilizers for two incompatible homopolymers if the respective blocks are compatible with the homopolymers of the blend (1c).

In branched polymers, typically, the main chain is the longest chain with either short or long chains as pendant chains. If the branches of the main chain are themselves branched, then this is known as series branching. With very extensive series branching, the polymer has a kind of fir-tree shaped structure (2a).

Star-shaped polymer have branches of almost equal length radiating out from a single branch point and are characterized by lower hydrodynamic volume due to their lower radius of gyration. This is reflected in the solution properties of the polymer, such as

lower intrinsic viscosity (by ca. 23-38 %) depending on the number of branches. Further, the branches of the star polymer could be homopolymeric or diblock copolymeric (2b).

Graft polymers are branched polymers whereby the branches have constitution which differs from that of the primary or backbone chain (graft base). The graft copolymers are a subgroup in which grafted branches may contain more than one type of monomer repeat unit. Comb shaped polymers, on the other hand, contain branches of generally equal length joined more or less equidistantly along the main chain. Depending on the compatibility, and crystalline tendencies of the grafts and the graft base, phase separated morphologies analogous to the block copolymers and the resultant improvement in the properties can be obtained. One of the important uses of grafting is improved hydrophilicity of the graft base by grafting hydrophilic grafts (1c).

Polyethylene is a good example of branching in polymers (1d). In branched polyethylene, the density and T_m are lower than for the linear counterpart. If a chain is substantially branched, the packing efficiency deteriorates and the crystalline content is lowered. This provides a good handle on lowering the crystalline content of the polymers. Further, T_g of the polymer is significantly affected, depending upon the extent of branching. A small number of branches on a polymer chain are found to reduce the value of T_g due to increased free volume; however, a high branching density has the same effect as side groups in restricting mobility and hence giving higher T_g .

The presence of chemical crosslinks in a polymeric system has the effect of increasing T_g , although when the density of crosslinks is high the range of transition region is broadened and the glass transition may not occur at all. Crosslinking tends to reduce the specific volume of the polymer which means that the free volume is reduced and the molecular motions become more difficult, so the T_g is raised. When the polymer is cross-linked, the dimensional stability, resistance to solvents and heat stability are improved.

Further, the cross-linked thermosetting resins are characterized by high modulus, low damping and low creep rate (1e).

1.3 Polymer Blends

Another approach to improve the properties of a polymer is neither by chemical modification nor by novel polymer architecture, but to blend with another polymer, resulting in a physical mixture of the polymers (2c). The blended polymers may be homopolymers or copolymers or a combination of both. In last two decades, polymer blends have gained more importance since a wide variety of polymers can be utilized to make polymer blends of desired end use property. Further, the cost of developing such blend systems is much lower than that for developing new polymers or to produce and commercialize a known polymer. The new properties of the blend produced such as T_g , T_m , modulus, crystallinity etc., depend on the nature and physical state of the original polymer, on the nature, physical state and means of processing in the added polymer (or additive), on the interaction between polymers, mixing ratio as well on the processing steps to which they are subjected. Further, the properties derived from such blend systems depend also on the microstructure of the resulting blend, i.e., whether the blend is homogeneous (single-phase, compatible) or heterogeneous (micro/macro-phase separated). Blends can be produced for a variety of reasons: to improve mechanical properties, improve processibility, improve heat resistance, improve thermo-mechanical properties or to produce high performance materials. There are a variety of blend systems that are commercialized for use for average requirements to high impact strength thermoplastics to flame proof materials.

One of the major problems in the blend approach is the macro-phase separation (much larger domain sizes) and non mixing of the polymers. Even with detailed structure-property relationships coupled with compatibilization and micro-structural studies of

polymers, polymer blends with significantly improved properties can not be obtained from a wide variety of the polymers. Such examples include polyaramides and some nylons.

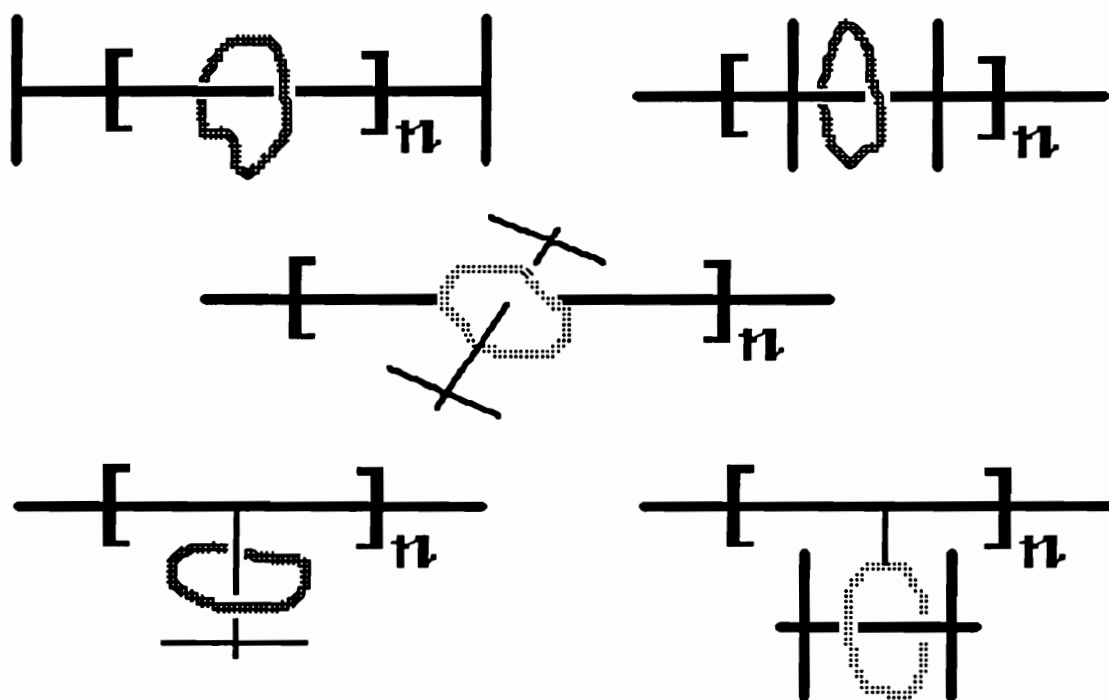
1.4 Polyrotaxane Architectures

To the above list of well studied polymer topologies, we wish to add one more type, i.e., poly(rotaxanes). Polyrotaxanes are two component systems consisting of low molecular weight oligomeric macrocycles threaded onto high molecular weight linear polymers such that there is no covalent bond between the linear and the cyclic components. The term 'rotaxane' is derived from the Latin words for wheel and axle (3). The linear polymer chains (the axles) may be terminated with bulky groups at the chain ends to prevent the dethreading of the macrocycle (the wheel), in the absence of any interactive forces between the macrocycle and the linear polymer chains. Thus, the properties of polyrotaxanes are derived from the two components held together not by a chemical bond but by means of either attractive intermolecular interactions or by the physical barriers to dethreading. Thus, the polyrotaxanes can be compared with blend systems where the linear backbone and the macrocycle components constitute a physical mixture of the two held together by attractive interactions and/or by physical barriers to macro-phase separation. Further, polyrotaxane systems may be compared to block copolymers where one of the block is covalently bonded to either a compatible or non compatible block. In the case of a non-compatible block copolymer, typically the result is micro-phase separation. In polyrotaxanes, if the macrocycle and the linear backbone are not compatible, due to the lack of covalent bond between the two and hence relative freedom of the macrocycles on the linear chain, macrocycles could move along the chain and result in macrocycle aggregation and crystallization as seen in the block copolymers. Thus, a variety of possibilities exists in tailoring the polyrotaxane structures and the resulting novel polymer

architecture is expected to have interesting solid state and solution properties.

Our objective is to explore as well as exploit physical properties resulting from this type of novel polymer architecture. Scheme I-2 shows various possible structures for polyrotaxanes. The macrocycle can be part of a linear polymer or a pendent group or threaded onto the linear polymer, with or without intermittent stops on the chains. The purpose of the intermittent stop is to prevent the aggregation of macrocycles on the polymer chain.

Scheme I-2 Polyrotaxane Architecture



As indicated earlier, oligomeric as well as high molecular weight cyclic polymers have interesting properties such as lower melt and solution viscosities relative to their linear homologues, etc; further, oligomeric macrocycles are soluble in most of the common organic solvents. A wide range of physical properties of practical importance can result from judicious combination of

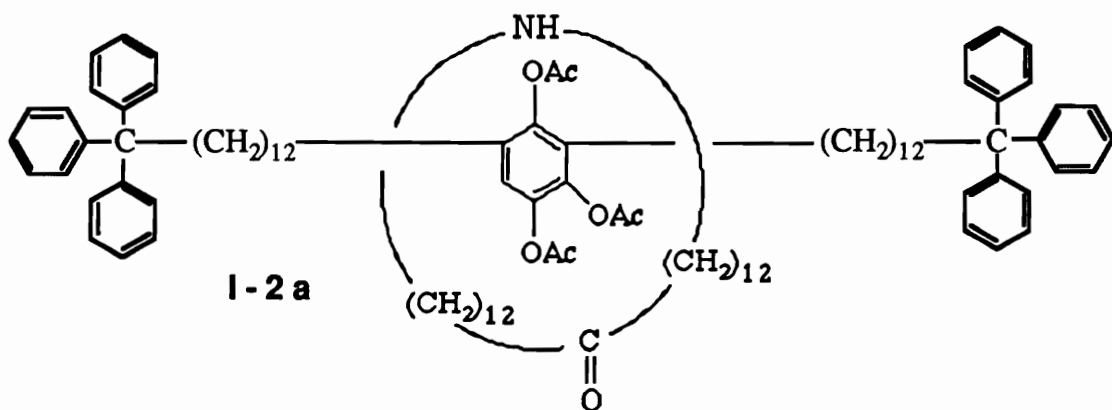
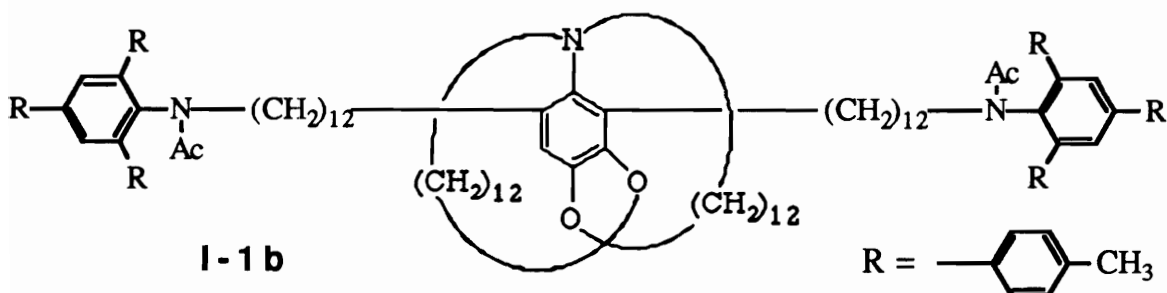
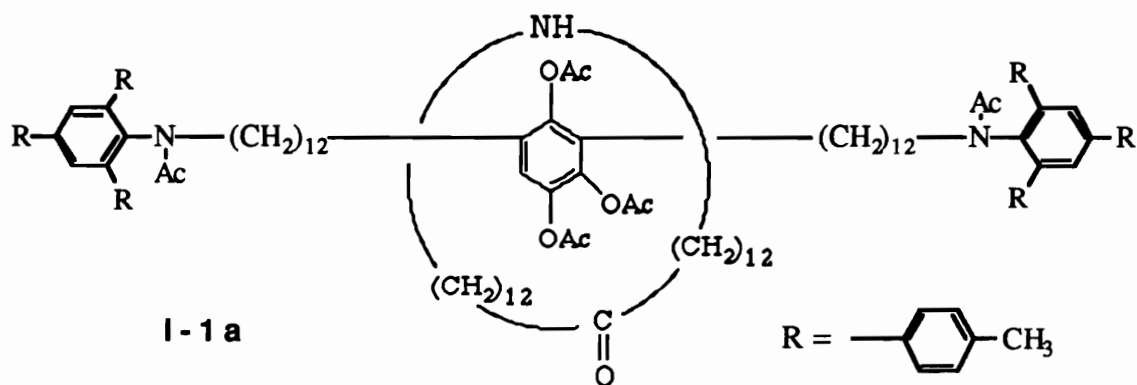
macrocycle as well as backbone linear polymer constituents. For example, the constituents in polyrotaxanes (macrocycle and linear chain) could be compatible in order to achieve systems with increased or decreased crystallinity, obtain tougher systems by introducing intermolecular interactions between macrocycle and the chains. Or they could be noncompatible to obtain micro-phase separated morphologies. Further, high temperature-high performance polymers could be modified to be able to either be melt processed or solution processed by incorporating low melting and highly soluble low molecular weight cyclics onto the polymer chains.

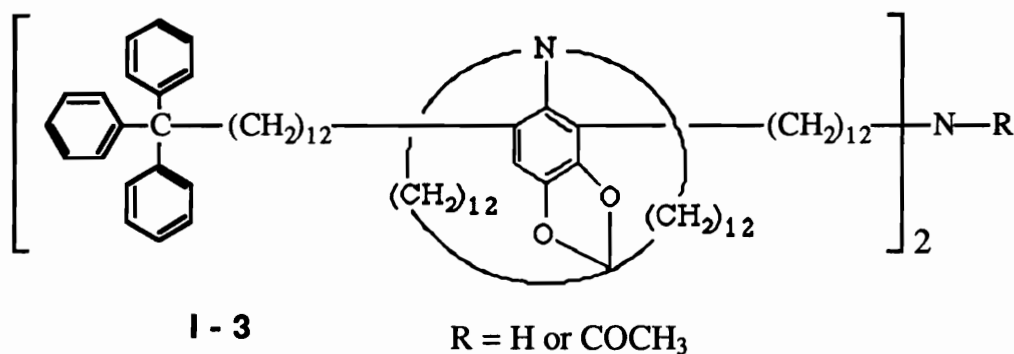
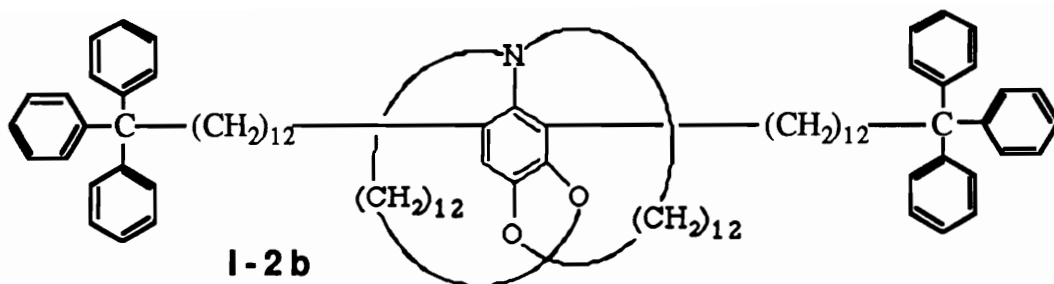
Another novel molecular architecture that has been reported in the literature is interlocked rings (e.g., Olympic games symbol), called catenanes. In catenanes, one or more macrocycles are threaded to one parent macrocycle, thus resulting in interlocked macrocycles. Formation of a rotaxane structure, i.e., a linear species threaded by a macrocycle, is a necessary precursor in the synthesis of a catenane. Typically, the word catenane is preceded by a number in the square bracket indicating the number of macrocycles in the catenane. Included in the following literature review are some of the examples of catenanes that relate to rotaxanes.

I-5 Literature Review of Rotaxane

A stable union of a linear molecule threaded through a macrocycle was first suggested by Frisch and Wasserman (3). The term rotaxane was coined by Schill and Zollenkopf in 1967 (4). They reported a synthesis of **I-1a** and **I-2a** from corresponding pre-rotaxanes **I-1b** and **I-2b** (4). They designed a linear backbone as well as a macrocycle around a phenyl ring followed by end capping the pre-rotaxane. These pre-rotaxanes **I-1b** and **I-2b** were then converted in to corresponding rotaxanes by bond cleavages. Further they reported the synthesis of analogous pre-rotaxane **I-3** of twice the size (5).

The method used in the synthesis of these rotaxanes is called 'Chemical Conversion', in which a well designed molecule containing macrocycle and the linear backbone is chemically converted into rotaxane topology.



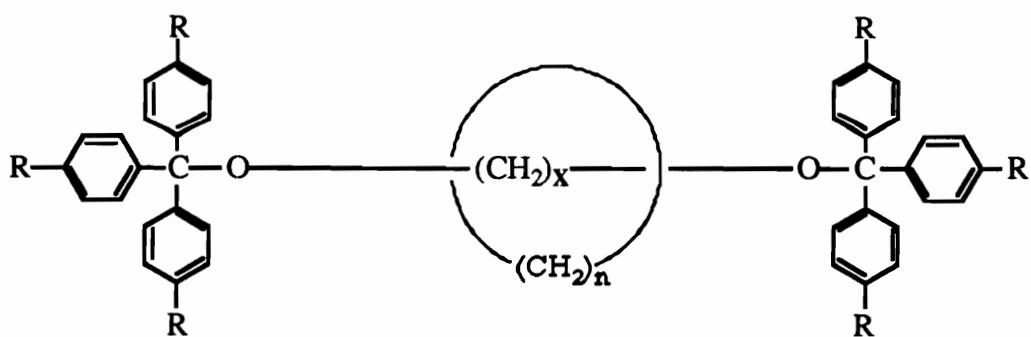
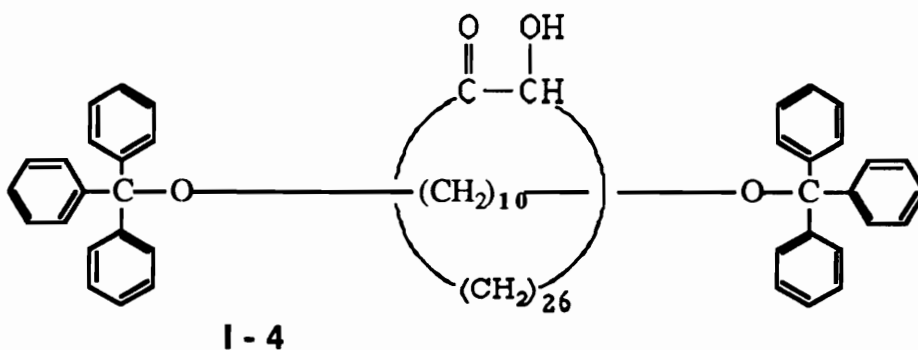


The pre-rotaxane **I-3** is twice the size of **I-1a** and **I-2a** rotaxanes and contains two rings. The concept of the size of the end blocking group in relation to the macrocycle size is illustrated in these examples. In the rotaxane **I-1a** the tri-substituted benzene was used to prevent the dethreading of the macrocycle; however, in the other two rotaxanes the trityl group was used. No indication of the efficiency of the respective blocking groups is reported. The authors reported that in the mass spectrum of **I-1a**, the parent ion peak mass was the sum of the two components and in thin layer chromatography, the rotaxane showed behavior different from that of a mixture of its components.

In 1967 (about the same time as Schill et al.) Harrison and Harrison reported synthesis of an end capped, monomeric rotaxane (**6**). Their work involved immobilizing a 30-carbon alkane macrocycle onto a liquid chromatography column resin via a hydroxyl group present on the macrocycle. This column-macrocycle adduct was treated with 1,10-decanediol followed by end capping the diol

with triphenylmethyl chloride 70 times (to improve the yield) to obtain stable rotaxane I-4. The final rotaxane yield was 6 % .

To identify the rotaxane produced and confirm the topology, they used infrared spectroscopy, chromatographic techniques, melting point experiments and recovery of the individual components after the cleavage of the ether bonds between 1,10 decane diol and the end capped groups. Since the formation of the rotaxane is controlled statistically and the macrocycles are relatively small, the yields were low for the above synthesis. This statistical threading method represents another approach in the synthesis of rotaxanes.



In his later paper (7), Harrison applied the statistical threading method to determine the effect of size of macrocycle in the formation and stability of the rotaxanes. A mixture of

cycloalkane macrocycles comprising 14-42 carbons and 1,10-bis(triphenylmethoxy)decane were heated together at 120 °C, forming small equilibrium concentrations of rotaxanes I-5. Stable rotaxanes were obtained from the 29 membered macrocycle, while unstable rotaxanes (easily dethreadable) of macrocycle sizes 30-32 were obtained. No rotaxanes were obtained for macrocycle sizes 14-28. In another similar experiment in the presence of traces of acid, which reversibly cleaves the ether linkages to allow threading of the macrocycle to take place, stable rotaxanes containing macrocycles of sizes 25-29 were obtained, .

In another similar acid catalyzed statistical synthesis of rotaxane I-6 (8), 1,13-di(tris-p-t-butylphenylmethoxy)tridecane was used with cycloalkane macrocycles. The yields of the rotaxanes increased monotonically from macrocycle size 24 (0.0013 %) to size 33 (1.6 %), with zero yield for larger ring sizes.

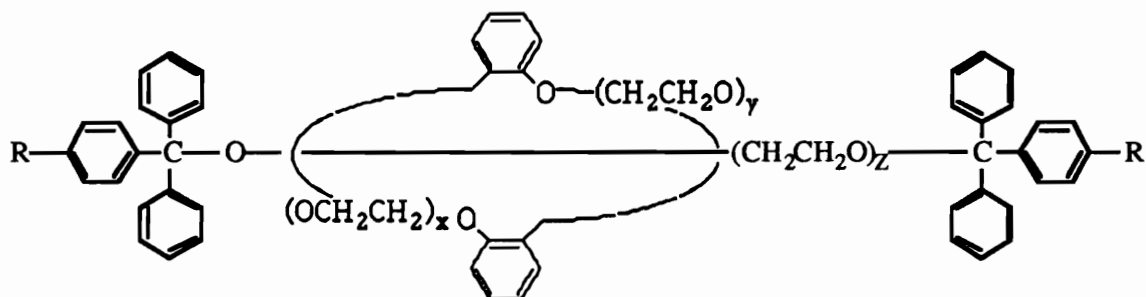
From the above experiments, Harrison concluded that during the statistical synthesis of the rotaxanes, an equilibrium is set up between linear backbone and macrocycle, and that the yield of the stable rotaxane depended on the sizes of the macrocycle and the end blocking groups. Further, it was shown that the macrocycles smaller than 24 atoms were not able to thread on the linear alkane backbone due to the small cavity of the macrocycle. It was further indicated that the triphenylmethyl blocking group can be squeezed through a 29-membered ring, but not through macrocycles of smaller sizes; larger macrocycles can freely thread-dethread over the blocking group, giving rise to unstable rotaxanes. When the larger blocking groups (tris(p-t-butylphenyl)methyl derivatives) were used, stable rotaxanes from macrocycles of sizes from 24-34 were obtained.

Rotaxanes were characterized by spectroscopic techniques, GPC and selective cleavage of the rotaxanes to isolate individual components making up the rotaxanes. In proton nmr spectra, a resonance at 1.25 ppm observed for the macrocycle protons of a 1:1 mixture of the components was shifted to 1.21 ppm for the rotaxane;

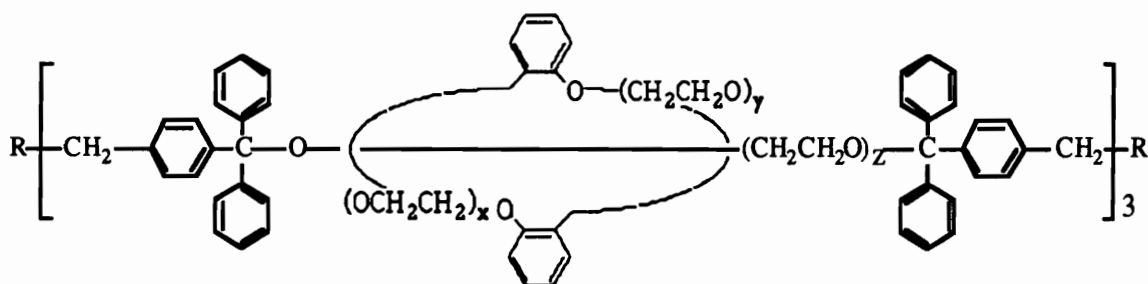
however, the infrared spectrum of the rotaxane was indistinguishable from that of an equimolar mixture of the components. A molecular weight estimation of the rotaxane of molecular weight 1486 by chromatography gave a value of 1300-1600. These rotaxanes are made from hydrocarbon components (linear backbone and macrocycle) and no major changes in the properties of the rotaxanes were observed. Yet in another paper (9), Harrison concluded from the gas chromatographic data on Carbowax 20 M columns for the series of alkane macrocycles of sizes 14-35 and corresponding linear alkanes that threading of the cyclic species with the polymeric stationary phase occurs for macrocycle sizes greater than 26.

In a more detailed study of synthesis and characterization of oligomeric rotaxanes and catenanes, Agam et al. (10) prepared oligomeric rotaxanes using dibenzo-crown ethers and polyethylene glycol. The ends were blocked by trityl groups. By optimization of the statistical threading reaction conditions using molecular models, Agam et al. produced rotaxane I-7 in 15 % yield (10) ($X=Y=Z=8.7$). Further, they accomplished synthesis of I-8 in 18.5 % yield (11) and from I-8 they prepared oligomeric rotaxane, (molecular weight 1200) I-9 in 23 % yield. The rotaxanes were purified by column chromatographic methods, taking advantage of different elution characteristics of the linear, macrocycle and rotaxanes. IR and NMR spectra of the rotaxanes did not show any difference from that of mixtures of components. However, colligative molecular weights of I-7 and I-9 were found to be intermediate between those of the linear and cyclic components. This was claimed to be due to the large size of the macrocycle permitting large freedom of movement of individual components in the rotaxane. However, it was also reported that the activation energies of decomposition (dethreading) and threading were 15.9 kcal/mol and 3.4 kcal/mol, respectively, and that strong dipole-dipole interactions exist between the oxyethylene units of the linear and macrocycles in the rotaxane. Further, the trityl group used to

end block the rotaxane is much smaller relative to the size of the macrocycle and in solution, it will not prevent dethreading of the macrocycle from the linear backbone. This probably explains unusual colligative properties observed for the rotaxanes **I-7** and **I-9**.



I-7 R=H X = Y = Z = 8.7
I-8 R=CH₂Br X = Y = Z = 8.7

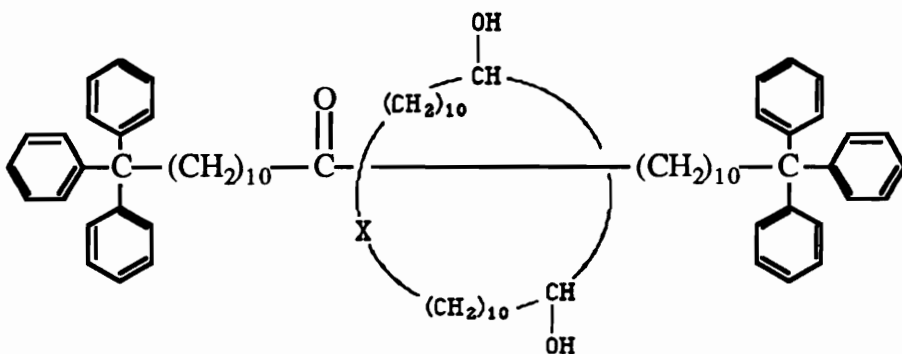


R = -Br X = Y = Z = 8.7
I-9

Schill et al. have reported synthesis of oligomeric rotaxanes **I-10** and **I-11** using a chemical conversion process analogous to the one described before in 0.18 % and 0.12 % yields (12).

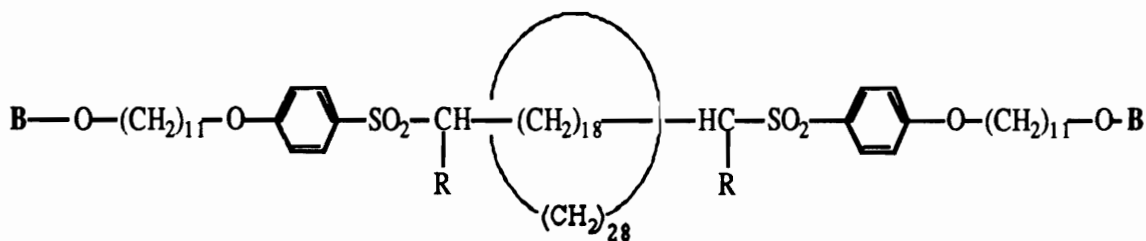
Further, in another study (13), Schill et al. have reported the synthesis of **I-12** using equilibration techniques in the presence of p-toluenesulfonic acid and this rotaxane was converted into translationally isomeric rotaxanes **I-13** and **I-14** by alkylation. In rotaxane **I-13**, the macrocycle is blocked on the chain by the long alkyl groups in the center, while in **I-14**, the macrocycle is forced to be near the chain end due to the physical barrier provided by the

pendant group. The end blocker used in these rotaxanes was triphenylmethane for the 28 membered alkane macrocycle.



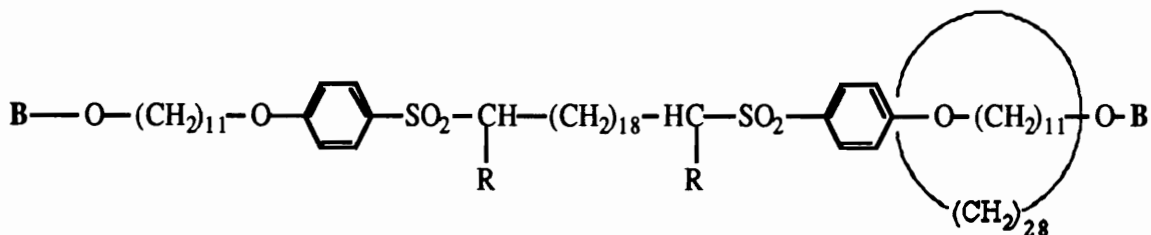
I-10 X = - OC₆H₄O -

I-11 X = - (CH₂)₆ -



B = -C(C₆H₅)₃ I-12 R = H

I-13 R = -(CH₂)₁₁C≡H



I-14 R = -(CH₂)₁₁C≡H

B = -C(C₆H₅)₃

In a recent paper (14), Schill describes the effect of macrocycle size and linear backbone length on the threading efficiency. The effect of macrocycle size was studied by incorporating macrocycles of 21-29 carbons onto dodecane end

capped by trityl groups with sulfide linkages in presence of p-toluenesulfonic acid. The threading yield was found to increase with macrocycle size 21 (0.35 %) to macrocycle size 29 (6.8 %). The effect of length of linear chain was studied by an alkane chain of 10-38 carbons end blocked by trityl groups using the 29-carbon alkane macrocycle. The threading yields were found to increase with chain length of 10 carbons (4.5 %) to 38 carbons (11.3 %).

Very few examples of polymeric rotaxanes have been reported in the literature. The first syntheses of polyrotaxanes were made from naphthalene-1,5-diisocyanate, oligomeric ethylene glycols and dibenzo-crown ethers of different sizes (10). The effect of the molar ratios of rings to chains, length of chain, radius of the ring, volume of the system and temperature on the threading yields were studied and maximum threading yields as expressed in terms of macrocycles/glycol repeat units of 0.63 (i.e., one macrocycle per every 1.6 repeat unit) were obtained (10). Further, no blocking groups were used in the polyrotaxane synthesis and over a 60 day period no dethreading was found to occur, presumably, due to the attractive interactions between the urethane linkages and oxyethylene units. The characterization of the polyrotaxanes have not been reported.

In another attempt to synthesize polyrotaxane, polymerization of ethylene oxide was done by anionic polymerization in the presence of dibenzo-58 crown ether followed by termination with trityl end blockers. The oligomeric rotaxane (molecular weight 700, DP = 15) of the structure I-7, ($X=Y=8.7$, $Z=15$) was produced in 11.2 % yield (10). Further, it has been reported that 60 % dethreading occurs upon heating the polymer at 150 °C for 15 hours.

Synthesis of polyrotaxanes of polyvinylidene chloride by polymerization of the crystalline adduct of vinylidene chloride and β -cyclodextrin by radiation polymerization have been reported (15). The cyclodextrin content in the polymer was found to be about 80 % and the semi-crystalline polymer (molecular weight 20,000) was found to be soluble in DMF while polyvinylidene chloride is not.

Thus, solubility characteristics of a polymer can be altered by polyrotaxane synthesis.

High molecular weight polystyrene rotaxanes using crystalline cyclic urethanes comprising of 34 and 40 atoms have been reported (16). Cyclic urethane swollen by neat styrene was polymerized thermally without any initiator. Further, the authors found that cyclic urethane complexed with $ZnCl_2$ prior to swelling with styrene favors polyrotaxane formation. Lower threading yields were obtained for cyclic urethane with larger number of atoms, suggesting the possibility that unfavorable macrocycle conformations reduce the effective cavity size. The authors found the polyrotaxanes to be insoluble in benzene or DMSO, both of which are good solvents for polystyrene and cyclic urethanes. Further, estimates of the composition of the semi-crystalline polyrotaxanes were obtained by X-ray analyses. It may be possible that cyclic urethanes are distributed along the linear chain and that they aggregate to form ordered regions. No other data on characterization has been reported.

Recent Literature on Rotaxanes and Polyrotaxanes:

After this study on the synthesis and characterization of polyrotaxanes was undertaken, several reports on the synthesis and characterization of rotaxanes, catenanes and polyrotaxanes have appeared the literature. It can be seen from the length of this section that there has been increasing interest in these novel molecular architectures and that various approaches to the synthesis of such architectures have been employed. However, there has been a very limited interest in polyrotaxanes as can be inferred from the number of paper(s) published; actually only one report on polyrotaxanes (besides our group) has been published.

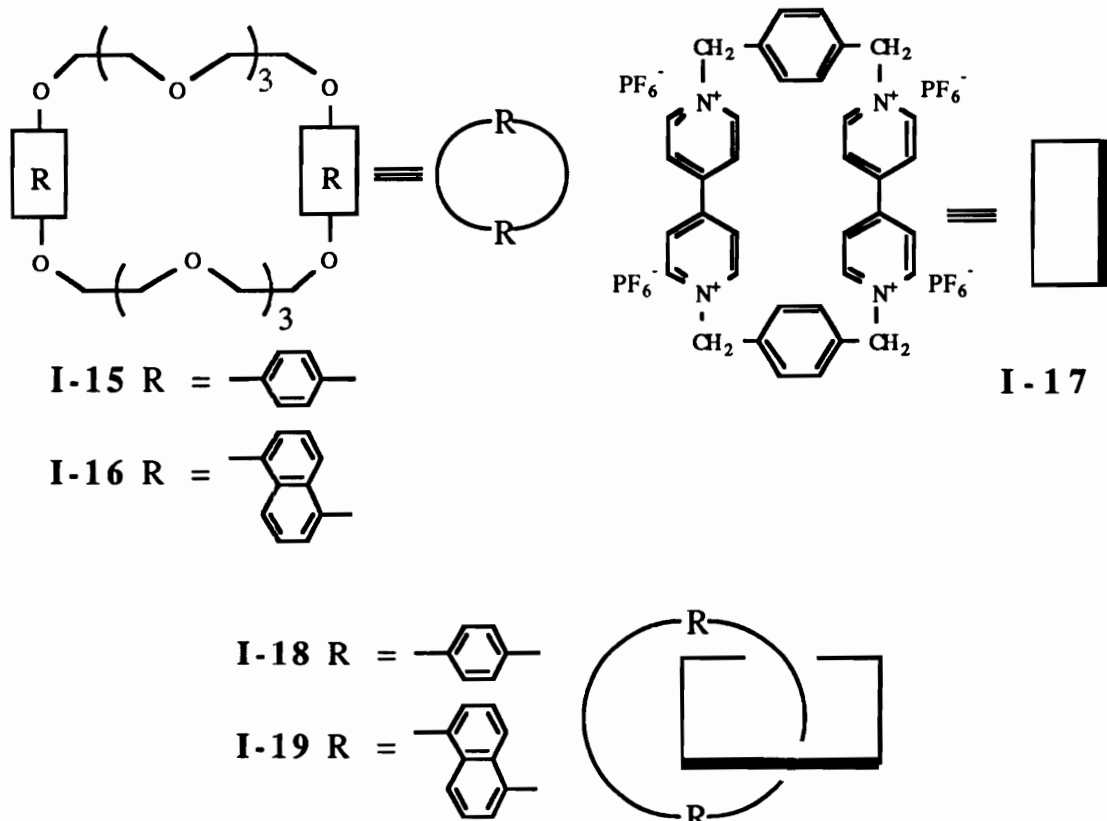
Stoddart and coworkers began studying the formation of complexes of a variety of dibenzo-crown ether (I-15, I-16) and analogous macrocycles with small molecules such as $[diquat]^{2+}$

(N,N'-dimethyl-2,2'-bipyridyl) and [paraquat]²⁺, (N,N'-dimethyl-4,4'-bipyridyl) (17-20) in the mid 1980's. It was found that due to the highly electron deficient nature of the [diquat]²⁺ and [paraquat]²⁺ molecules, 1:1 complexes are preferentially formed with the dibenzo-crown ethers and analogues. This preferential formation of the complex is due to electrostatic and charge transfer interactions with the electron rich aromatic ether units in crown ethers.

In another study (21), Stoddart and coworkers incorporated two [paraquat]²⁺ molecules into a macrocycle, by preparing an ionic bipyridyl macrocycle derived from two 4,4'-bipyridyl units joined by two p-xylene units (BP-28-N₄⁺ : 4 PF₆⁻, I-17, as reported in chapter 4). It was found that macrocycle I-17 preferentially forms a stable complex with hydroquinone ethers such as 1,4-dimethoxybenzene (DMB) and the formation of the complex was preferred as found by the equilibrium constant of $K_a = 17 \text{ M}^{-1}$. Detailed analyses of these complexes showed that neutral DMB is inserted through the center of the centro-symmetric tetracationic macrocyclic receptor (I-17) with the methyl groups of the methoxy substituents protruding above and below the rims of the macrocycle. Such an arrangement of the donor:receptor complex is stable due to the π/π stacking and charge transfer interactions between π -electron rich aromatic ring of the hydroquinone derivative and π -electron deficient bipyridinium units and electrostatic interaction of the ether linkages with the cationic sites. The overall dimensions of the macrocycles do not change due to this complexation. Similar complexation of this macrocycle (I-17) with other molecules is also reported (22-24).

Taking advantage of such preferential interactions between I-17 and hydroquinone ethers they reported synthesis of a [2]catenane (I-18) from I-17 and I-15 in 70 % yield (25)! Further, they also reported synthesis of [2]catenane (I-19) (two interlocked rings) made from I-17 and I-16 in 51 % yield (26). Structures of both the catenanes were confirmed by X-ray crystal structure analyses. Similar [3]catenanes (three interlocked rings) containing two

dibenzo-crown ethers using a macrocycle analogous to **I-17** have been reported in 20-30 % yield (27); further, a [2]- and [3]-catenane using a tetrabenzo-crown ether and **I-17** have been reported in 11-12 % yields (28).

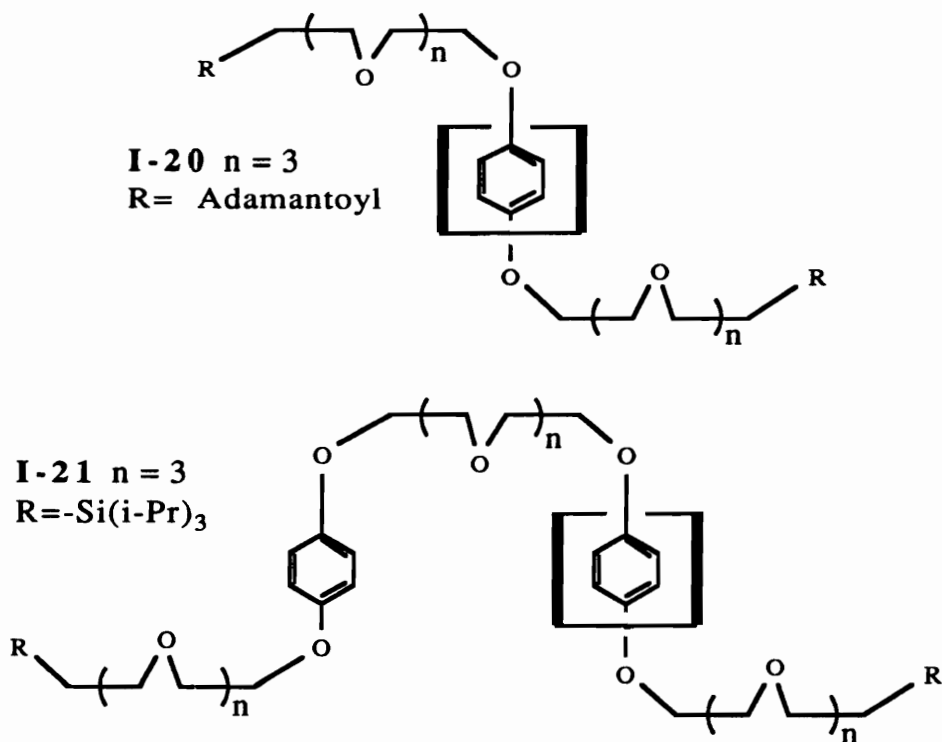


Expanding this concept further, they reported synthesis of rotaxanes using **1-17** and linear molecules having structures analogous to the di-, tri- and tetra-benzo crown ethers. The method employed here in the synthesis of these rotaxanes is called the 'Template Threading' method as opposed to the statistical threading or chemical conversion methods. In the template threading method, there exist attractive interactions between the macrocycle and either the monomeric or oligomeric linear backbone, resulting in formation of a rotaxane structure. Thus, the formation of the

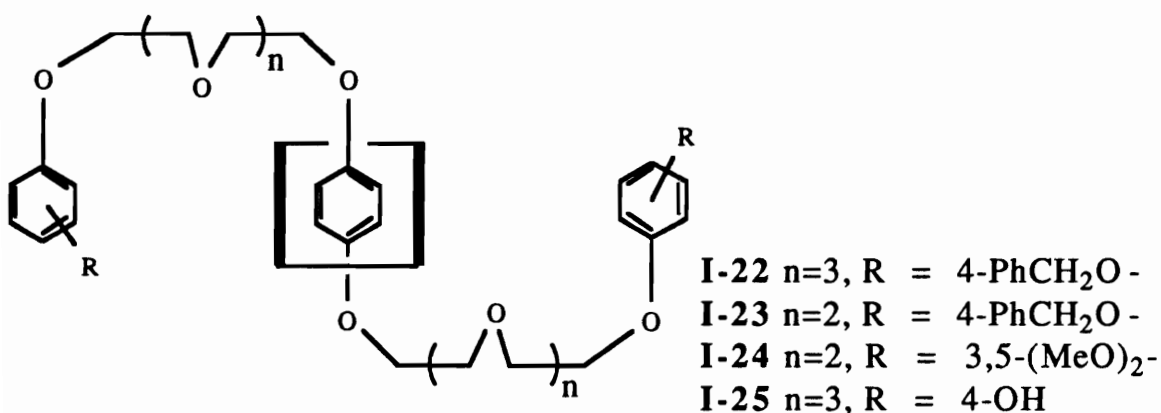
rotaxane structure is enthalpically driven and thermodynamically more stable.

The rotaxanes **I-20** and **I-21** were prepared by synthesizing the macrocycle **I-17** (macrocycle 4,4'-bipyridinium units in the structure are represented by bold lines) in situ around the end capped linear molecule to obtain the rotaxanes in about 10 % yields (29). The structures of the donor:acceptor complex rotaxanes were determined by X-ray crystal structure and NMR spectroscopy. They found that adamantoyl as well as tri-isopropyl silyl groups were bulky enough to prevent the dethreading of the macrocycle.

Another interesting aspect of **I-21** is that the two hydroquinol groups are part of the linear chain. From dynamic NMR studies it was found that at room temperature this rotaxane behaves like a molecular shuttle; the macrocycle moves to and fro at approximately 500 times a second between two identical 'stations' in the shape of hydroquinol rings. The bulky triisopropyl silyl groups act as 'stoppers' (29).

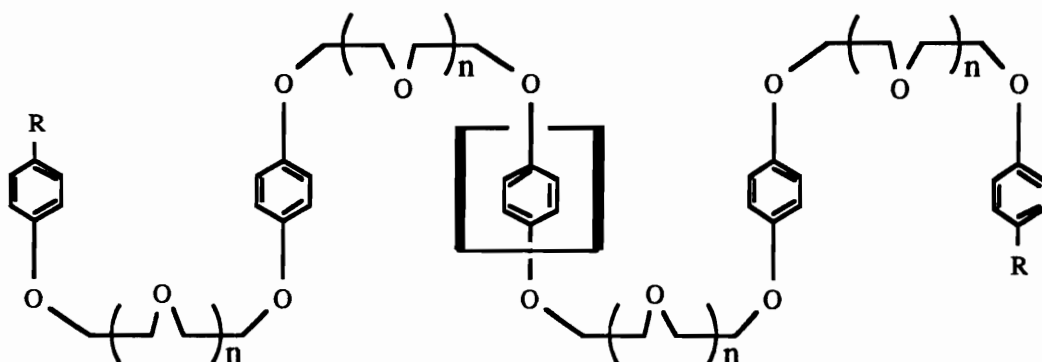


The synthesis of rotaxanes **I-22** to **I-26** is thermodynamically favored, since the formation of complex is enthalpically driven. Synthesis of rotaxanes **I-22** to **I-26** (the authors describe these rotaxanes as pseudorotaxanes due to lack of end blockers) was accomplished by mixing the appropriate linear chains containing the end units with macrocycle **I-17** in equimolar quantities, upon which the color turns red instantly due to charge transfer interactions (30). The rotaxanes were characterized by mass spectroscopy and X-ray crystal structure analyses. X-ray crystal structural analyses of **I-22** and **I-24** show that the polyether linear chain is not only inserted through the center of the tetracationic macrocycle such that the middle hydroquinone ring is encircled but also that linear polyether chains curl back on themselves around the bead enabling the next aromatic donors in both directions to stack against the sides of the π -accepting bipyridinium units of the macrocycle (as shown in the diagram). Further, the polyether chains in **I-22** provide an optimum length and geometry, enabling π/π stacking interactions to occur between donor and acceptor groups, as seen with complexes of **I-17** and DMB; whereas in **I-24**, there was no formation of such continuous stacks within the crystals because the polyether chains are too short.



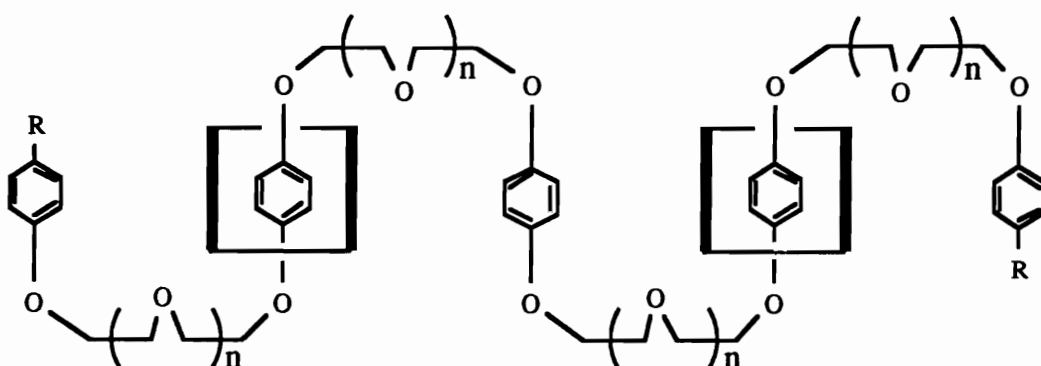
The rotaxane structures of **I-26** and **I-27** were confirmed by mass spectroscopy along with proton NMR spectroscopy (31). **I-27**

was prepared from **I-26** by addition of 1 molar equivalent of **I-17** macrocycle. The low temperature proton NMR analyses suggested that at lower temperatures, the rotaxane exists predominantly as one structure (as shown) and that the macrocycles are immobile.



I-26 $n=3$, $R = -OCH_2Ph$

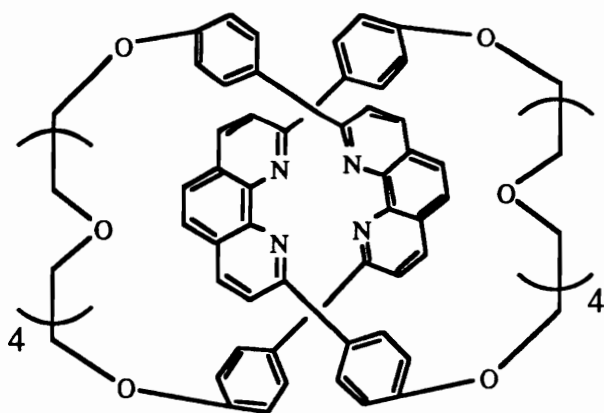
Further, **I-26** showed temperature dependent behavior by the proton NMR spectroscopy; this was rationalized on the basis that the macrocycle travels from the central hydroquinol unit to the ones that are adjacent to the central hydroquinol units, and the system is at equilibrium at room temperature. At lower temperatures, the individual signals can be resolved due to a reduction in the exchange rate.



I-27 $n=3$, $R = -OCH_2Ph$

Taking advantages of such interactions Stoddart and coworkers and our research group have independently prepared derivatized 4,4'-bipyridine having functionalities such as $-\text{COOH}$, $-\text{COOCH}_3$, $-\text{OH}$, etc., (32-33). X-ray crystal structures of donor:acceptor complexes of these molecules with **I-15** have been reported. These complexes with functionalities were polymerized with polyethylene glycol to obtain polyurethane rotaxanes (34).

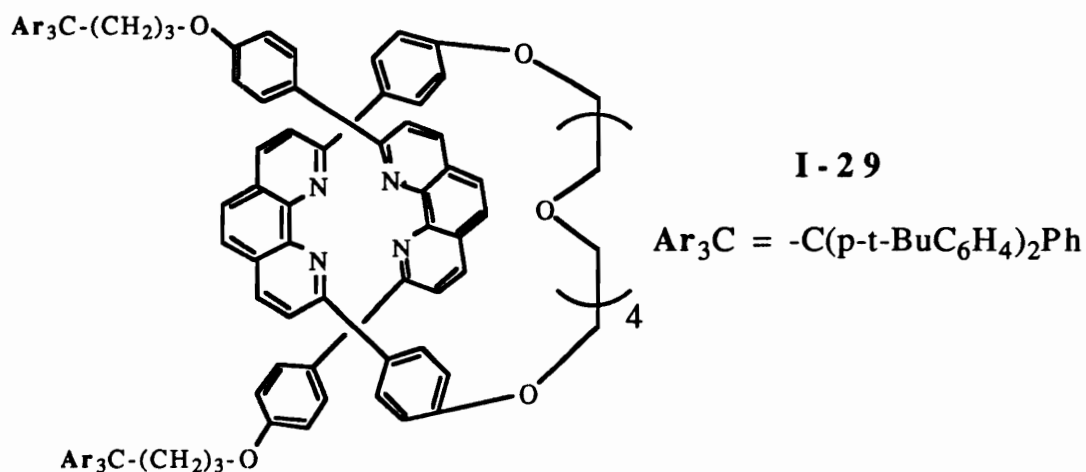
Sauvage and coworkers (35-36 and references therein) reported synthesis of catenanes containing 2 to 7 interlocked rings derived from phenanthroline macrocycles using Cu^+ as a template. Such interlocked rings were synthesized by complexing a template (Cu^+) to the phenanthroline units of one macrocycle and one linear molecule, followed by the cyclization of the linear molecule to yield [2]catenane. In some of the catenanes the template (Cu^+) was not removed, thus giving the metal ion complex of the catenane, also called catenates. One representative example of a [2]catenane (two interlocked rings) without the template is shown below (**I-28**). A detailed and comprehensive literature review of approaches to the synthesis of catenanes has been published (37).



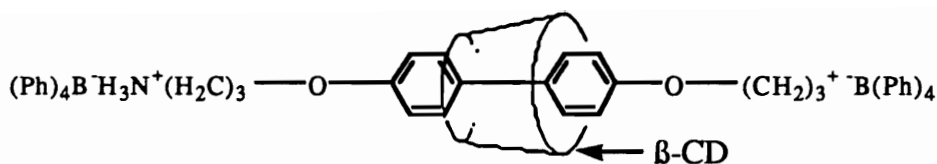
I - 28

By using similar template directed approaches, synthesis of rotaxanes derived from linear chain and macrocycle containing phenanthroline groups (**I-29**) has been reported by our group. The chain ends were blocked by bulky bis(*p*-*t*-butylphenyl)phenyl methyl

derivatives. The rotaxane topology was confirmed by proton NMR and mass spectroscopy (38).

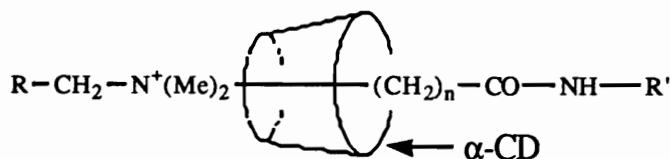


Further, there has been some interest in the synthesis of rotaxanes of cyclodextrin (CD) and linear small molecules containing amines by the template threading method (39,40). It appears from both the reports that CD molecules selectively thread in high yields onto linear molecules containing ammonium ions at the chain end(s). The rotaxane **I-30** made from a diammonium salt and β -cyclodextrin (β -CD) macrocycle was end capped by the tetraphenyl borate anion (39); thus the resulting rotaxane is a salt of end blockers. The synthesis of the rotaxane was accomplished in water and yields as high as 71 % were obtained. The rotaxane structure was confirmed by mass spectroscopy, thin layer chromatography to determine the presence of any unthreaded macrocycles and NMR analyses. It was found that the rotaxane formation is highly favored due to the interactions between the macrocycle and the linear ammonium salt and in a solvent such as acetone at room temperature the rotaxanes were stable, and even in polar aprotic solvents where the ionic end blocking groups and the rotaxane exist as solvent-separated ion pairs. This was due to the solvated positively charged ammonium groups at the chain ends acting as blocking groups.

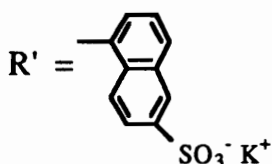


I-30

Similar rotaxanes were made from the α -cyclodextrin (α -CD) macrocycle and the linear chains of two different lengths containing a ferrocene unit attached by ammonium salt formation on one end and a COOH group on the other end. The carboxyl chain ends were end blocked by amidation using 5-amino-2-naphthalenesulfonate as shown in the structures I-31 and I-32. The isolated yields for all the rotaxanes were about 15 %. It was reported (40) that the carboxyl groups on the linear molecule act as an ionizable gate for the threading of α -CD since deprotonation of the carboxyl proton resulted in 6 fold decrease of the binding (threading ?) constant with α -CD.



R = Ferrocene



I-31 n = 7

I-32 n = 11

Further, the authors report isomeric rotaxanes of I-31 and I-32 differing in the arrangement of the macrocycle onto the chain, i.e., whether the narrow end of the macrocycle strip is towards the ferrocene chain end or vice versa. These isomeric structures of the rotaxanes were confirmed by NMR spectroscopy.

In a synthesis of comb-like polyrotaxanes where the β -CD was incorporated on the pendant chains, the linear polymer chain was a

copolymer made from methyl methacrylate (MMA) and 11-methacryloylaminoundecanoic acid by free radical polymerization. Onto the 11-methacryloylaminoundecanoic acid repeat units of this polymer, the pre-rotaxane from β -CD and 4'-triphenylmethyl-4-aminobutanilide or 4'-triphenylmethyl-11-aminoundecanilide was grafted by formation of an amide linkage between the pre-rotaxane and the repeat unit. The resulting polymer had β -CD macrocycles in the pendant chains of the comb shaped polymer. The amount of incorporated macrocycle is not specified; however they report that polymer showed solubility in diethyl ether while the model polymer is insoluble in diethyl ether. Further, from the proton NMR spectrum and reduced viscosity data of the polyrotaxane they suggested that the β -CD macrocycle forms hydrogen bonds with the amide linkage in the pendant chain. No detailed characterization of the polyrotaxane is reported.

Efforts in our groups are directed toward making polymeric rotaxanes using a wide variety of host linear polymer molecules such as polyesters, polyamides, vinylic polymers, liquid crystalline polymers, polyurethanes by using aliphatic macrocycles or dibenzo-crown ethers of various sizes (42-54). Further, functionalized dibenzo-crown ethers macrocycles of various sizes have also been incorporated into polymers as a part of the backbone, thus forming macrocyclic polymers such as polyamides or polyesters (55), which could be used to make polyrotaxanes of the type shown in the center of Scheme 1-2.

Synthesis of polyrotaxanes of poly(triethyleneoxy sebacate) and poly(butylene sebacate) (42-43,50-51) using various mole ratios of monomer to crown ethers such as 30-c-10 and 60-c-20 macrocycles has been reported. The transesterification method was used for the synthesis of polyrotaxanes in the presence of macrocycles. The polyrotaxanes were analyzed using proton NMR, GPC with uv and viscosity detectors to obtain absolute molecular weights, vapor pressure osmometry, optical microscopy, thermal

analyses as well as by recovering the crown ether by hydrolysis of the polymer chain.

The polyrotaxane topology was confirmed by reprecipitation experiments. It was found that in just two precipitation all the free (unthreaded) macrocycle was removed from the polyrotaxane as analysed by proton NMR and a constant ratio of macrocycle/repeat units was found after that; whereas, in a physical blend within two precipitations, all the macrocycles were removed. This conclusion was also confirmed by GPC results since free macrocycles have different retention times than the polymer or its polyrotaxanes and could be easily detected. Further, it was found that polymer morphology is greatly affected by threading of the macrocycles onto the polymer and was distinctly different from that of the corresponding blends.

Furthermore, it was found that larger macrocycles such as 60-c-20 gave much higher threading yields than smaller 30-c-10 and that compatibility of the linear and cyclic components could also play a major role in obtaining higher threading yields. The molecular weights obtained by vapor pressure osmometry correlated fairly well with GPC results suggesting that the polymer behaves as one molecule unlike the results for monorotaxanes reported by Agam et al. (10) that the rotaxane molecular weights were average of the linear and macrocycle molecular weights. Further, it was shown that blocking groups at the end of the polymer chain are not always necessary due to polymer chain entanglements as well as the long chain nature of the polymers.

Other examples of polyrotaxanes synthesized using aliphatic crown ethers in our group include free radically polymerized polystyrene and acrylonitrile using an initiator containing bulky blocking group (54), polyurethanes (34) and liquid crystalline polyazomethines (53). Further, as mentioned earlier polyurethanes derived from ionic 4,4'-bipyridinium derivatives using dibenzo-crown ether have also been synthesized and characterized (34).

In the chapters III to X, my contribution in this group effort to understand and explore properties of rotaxanes and polyrotaxanes is described. Synthesis and characterization of rotaxanes and polyrotaxanes from small molecules such as 1,8-octanediol, 4,4'-biphenol, preformed polymers such as poly(tetrahydrofuran) of different molecular weights, poly(butadiene) as well as polystyrene prepared anionically, polyaramides and nylon-6,6 by condensation polymerization have been described and the results obtained are discussed in the light of possible changes that may occur in the polymer bulk as a result of this novel polymer architecture.

I-6 Theoretical considerations

The first and only major attempt to explain mathematically various questions such as the role of macrocycle size, role of linear chains (length and diameter), molar volumes, effect of ratio of macrocycles/linear molecules on statistical threading efficiency and so on has been made by Agam et al. (10). The statistical threading is very complex not only due to the statistical factors but also due to the geometric factors, energy barriers, flexibility of molecules and so on. The mathematical model described (10) was constructed for such a method and the was compared with the results of threading experiments of dibenzo-crown ether macrocycles (of sizes 30, 44 and 58) using polyethylene glycols (molecular weights 400, 600 and 1000) as linear chains with an accuracy of $\pm 15\%$. Some of the important conclusions and trends of this experiment are presented here.

It was found that in oligomeric rotaxanes of fixed length, the ratio of threaded rings/chain increases with the increase in the initial molar ratio of ring/chain. With increase in the macrocycle size there is an optimum initial ring/chain ratio (between 2-4) to achieve the highest proportion of threaded macrocycles/linear ratio, beyond which it begins to decrease.

When the initial molar ratio of rings/macrocycle is fixed (1:1), it was found that % macrocycle threaded (dibenzo-44-crown ether and dibenzo-58-crown ether) increased with increasing length of the linear chain and optimum values for % threaded rings were obtained for linear chains containing about 41 atoms and above this length the % threaded rings began to decrease. However, for dibenzo-30-crown ether, there was no significant improvement in the % threaded rings above chains containing 27 atoms.

Further, the effect of dilution on % threading was studied by diluting the solution of linear chains in dibenzo-crown ether with another solvent. It was found that % threading decreases proportionately to increasing dilution and for dilution to twice the volume reduces % threading to about one-half.

The effect of temperature on the threading of dibenzo-58-crown and polyethylene glycol (molecular weight 600) was studied. There was no significant change in the % threaded macrocycles when the equilibration temperature of macrocycle and linear chains was increased from 100 °C to 207 °C. This means ΔH for the process is essentially zero and entropy controls the threading equilibrium.

These systematic studies provide an insight into the statistical threading mechanism and suggest that geometrical factors (relative size of the linear and the macrocycle) play a major role.

The mathematical model proposed by Agam et al. (10) considers the macrocycle as being spherical in its influence of the diameter '2r' and that the chain ends of the linear molecules should be in the domain of the sphere within a specific angle range θ (from the plane of the macrocycle) in order to be threaded. In a system where M_c is the number of moles of cyclic component and M_l is the number of moles of linear molecules and V is the total volume of cyclic and linear molecules, the fraction of linear molecules (N) in the domain of the macrocycle to be threaded can be given by:

$$N = K_3 (M_l M_c r^3 \theta) / V \text{ where } K \text{ is a numerical constant.}$$

After some arbitrary modifications and including the number of atoms per linear chain (n_l) and number of atoms in the macrocycle (n_c) the above equation was changed to:

$$N = K_3 [M_l M_c (1 - e^{-n_c/\pi n_l}) n_c n_l^\beta \theta] / V$$

where $K = 0.195$ and $\beta = 1.3$ for the system they studied.

The exponential expression relates to the diameter of the ring with number of atoms in the linear chain in the (multiple) threading process.

The model represented is, if anything, at least a sincere first approach in the direction of understanding various factors affecting the threading of linear molecules with macrocycles in statistical threading process.

There are various fundamental questions that will need to be answered such as:

- 1 How important are interactions between the macrocycle and the linear backbone chain and as a result how independent are the macrocycles from the backbone ?
2. If these macrocycles are independent of the polymer chain do they aggregate or show any unusual behavior ?
3. Are blocking groups always necessary in formation of polyrotaxanes in the presence of attractive interactions between the components ?
4. Does compatibility of the macrocycle and linear backbone play an important role in threading efficiencies ?
5. What is the role of flexibility of rigidity of the linear chains on the ultimate behavior of rotaxane and polyrotaxanes ?

Answers to these fundamental questions were investigated and will be discussed in the light of the experimental results.

I-7 Practical Considerations

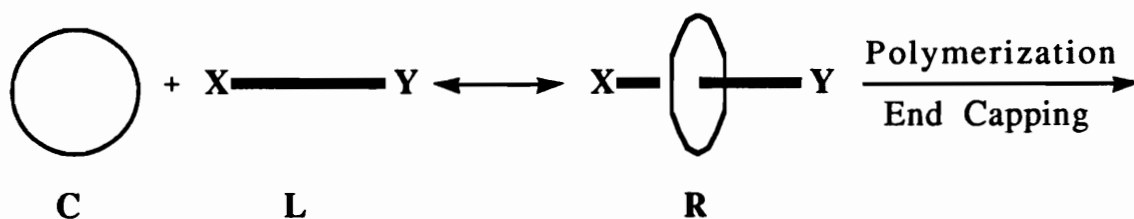
To recap, a variety of methods can be utilized for the synthesis of polyrotaxanes as described in the literature review. These include (i) chemical conversion, (ii) statistical threading and (iii) template directed synthesis.

(i) **Chemical Conversion Method:** In this approach, well designed molecules containing macrocycles and linear molecules called pre-rotaxanes are required and the final rotaxane or polyrotaxane structures can be prepared by either first converting the pre-rotaxanes to rotaxanes followed by polymerization or vice versa. This approach is of limited application for polyrotaxane synthesis since specially designed pre-rotaxanes are required and possible applications to majority of the commercially important polymer would not be possible.

(ii) **Template Threading Method:** As shown earlier by taking advantage of attractive interactions between a small linear molecule such as a monomer and a macrocycle, structures analogous to rotaxanes can be prepared that can be polymerized to obtain polyrotaxanes with much higher yields of threaded macrocycles (Scheme I-3). The nature of these interactions may be varied such as donor:acceptor complexes (Stoddart et al.) or using a metal ion to form ionic complexes (Sauvage et al.) and hydrogen bonding or van der Waal's interactions.

In the formation of pre-rotaxanes by the template threading method, the equilibrium of the reaction (Scheme I-3) will be shifted to right since the formation of such pre-rotaxanes is enthalpically driven (ΔH is negative). This process is much more useful than the chemical conversion method, but its application is still limited to some select group of macrocycles and linear monomeric molecules.

Scheme I-3 Threading Equilibrium



$$K = [R] / [C] [L] \quad RT \ln K = - \Delta G$$

$$\Delta G = \Delta H - T\Delta S$$

(iii) Statistical Threading Method: In this method the threading of macrocycles onto the linear monomers is governed by statistical factors as discussed in above section. There is a true equilibrium formed between the pre-rotaxane and its individual components (Scheme I-3). The reaction is entropically driven if ΔH is either zero or positive (repulsive interactions). The major advantage of this method is that in principle, polyrotaxanes of essentially all polymers can be made by this method including monomers and macrocycles that are non-compatible. The disadvantage of this method is the limited incorporation of macrocycles, but it can be improved by increasing the macrocycle/linear molecule ratio or using a larger macrocycle or both. Thus synthesized polyrotaxane may or may not have attractive interactions between the linear polymer chain and the threaded macrocycle.

Having discussed this, in the following paragraphs the requirements of individual components such as macrocycle, blocking groups and linear chains along with reasons for their synthesis is discussed.

Macrocycles:

One of the major constraints of the synthesis of polyrotaxanes in sufficiently large quantities for full characterization is the

availability of macrocycles, since the rotaxanes and polyrotaxanes were synthesized in this work primarily by the statistical threading method and the macrocycle itself was used as solvent for the linear species (monomeric or polymeric). The macrocycles must be larger than at least 26 carbon atoms, in the case of hydrocarbon macrocycles, or about the same size for aliphatic or dibenzo-crown ethers. A further requirement of macrocycles for the synthesis of polyrotaxanes is that they should be relatively stable at polymerization temperatures. Macrocycles of larger sizes would be very useful to attain higher threading yields; however, larger end blockers would be required to prevent dethreading of the macrocycles. The macrocycles should be easy to prepare and the starting materials can not be too costly since the yields of macrocycles are not very high (ca. 10-40 %). The purity of the macrocycles (greater than 99%) for use in anionic and polycondensation polymerization is critical to obtaining high molecular weight polyrotaxanes

In this study, 30-crown-10 was the choice of macrocycle due to its relative ease of synthesis, polar nature and the fact that its polyrotaxanes can be end blocked using triarylmethane derivatives to prevent dethreading. Further, in the synthesis of 30-c-10 it was found that the macrocycle twice the size, i.e., 60-crown-20, is also formed (as discussed in Chapter III). Thus, 60-c-20 was also used for polyrotaxane synthesis.

Cyclic polystyrene represents the other end of the spectrum in terms of polarity and it would be useful to study polyrotaxanes synthesized from this macrocycle. Thus cyclic polystyrene was made.

Ionic bipyridyl macrocycle I-17 was also prepared since it provides an alternative to statistical threading and ionomeric polyrotaxanes can be prepared from it.

Thus, the macrocycles considered in this study ranged from ionic to polar to non polar.

Blocking Groups:

Blocking groups may be needed at the chain ends so as to prevent dethreading of the macrocycles in the absence of any attractive interactions between the main chain and macrocycles of polyrotaxanes. The end blockers must be large enough to prevent dethreading of reasonably large macrocycles. To recap, blocking groups such as triphenylmethyl can be squeezed through a 29-membered cycloalkane macrocycle but end blockers made from tris(p-t-butylphenyl)methane derivatives were able to block macrocycles up to 42-membered n-alkane macrocycles.

In our study of CPK models it was found that that 30-c-10 can pass over the triphenylmethane blocking group after some manipulation by rotation of phenyl groups; however, the tris(p-t-butylphenyl)methane blocking group was able to effectively block the crown ethers up to 42-membered size. Thus, tris(p-t-butylphenyl)methane blocking group derivatives containing various functional groups such as phenol, acid, acid chloride, hydroxy, halo and vinyl were made.

To make the polyrotaxanes where the blocking groups are an integral part of the linear backbone chain, placed either at regular intervals or at random to prevent the macrocycles from moving along the chain, a bifunctional blocking group is required. Various attempts to make bifunctional blocking groups derived from bis(p-t-butylphenyl)methyl groups were not successful due to steric hindrance coupled with other side reactions (results from our group).

Polymers/Linear Chains:

Rotaxanes from flexible and rigid small molecules were prepared by the statistical threading method to understand the threading behavior of such molecules. Further, polyrotaxanes of preformed polymers of various molecular weight were prepared to study whether compatibility or non-compatibility of the two components caused markedly different threading tendencies.

Polyamides are an important class of commercially important polymers. Polyrotaxanes of polyaramides and nylon-6,6 were prepared to study the changes in the properties obtained by incorporation of macrocycles onto the polymer chain. It was expected that as a result of polyrotaxane formation, properties in bulk as well as solubility characteristics could be significantly altered without compromising the useful properties of such polymers. For similar reasons, the polyrotaxane of liquid crystalline polyester was considered.

Polyrotaxanes of polystyrene were prepared to study the feasibility of the use of crown ether macrocycles in anionic polymerization, to understand the behavior of polar macrocycles on the non polar polystyrene and to study the changes in properties.

References

1. J. M. G. Cowie, Polymers: Chemistry and Physics of Modern Materials, Intertext Books, London, (1973); 1a (p. 263), 1b (p. 271), 1c (p. 100), 1d (p. 193), 1e (283).
2. H. G. Elias, Macromolecules, Plenum Press, New York, NY 10013, (1984); 2a (p.50), 2b (p. 51), 2c (Chapter 34).
3. H. L. Frisch and E. Wasserman, J. Amer. Chem. Soc., 1961, 83, 3789.
4. G. Schill and H. Zollenkopf, Nachr. Chem. Techn., 1967, 79, 149; G. Schill and H. Zollenkopf, Ann. Chem., 1969, 721, 53.
5. G. Schill and C. Zürcher, Chem. Ber., 1980, 113, 2052.
6. I. T. Harrison and S. Harrison, J. Am. Chem. Soc., 1967, 89, 5723.
7. I. T. Harrison, J. Chem. Soc., Chem. Commun., 1972, 231.
8. I. T. Harrison, J. Chem. Soc., Perkin Trans. I, 1974, 301.
9. I. T. Harrison, J. Chem. Soc., Chem. Commun., 1977, 384.
10. G. Agam, D. Gravier and A. Zilkha, J. Am. Chem. Soc., 1976, 98, 5206.
11. G. Agam and A. Zilkha, J. Am. Chem. Soc., 1976, 98, 5214.
12. G. Schill, W. Beckmann and W. Vetter, Chem. Ber., 1980, 113, 941.
13. G. Schill, N. Schweickert, H. Fritz and W. Vetter. Angew. Chem. Int. Ed. Engl., 1983, 22, 889.
14. G. Schill, W. Beckmann, N. Schweickert and H. Fritz, Chem. Ber., 1986, 119, 2647.

15. M. Maciejewski, J. Macromol. Sci.-Chem., 1979, A13(1), 77.
16. T. E. Lipatova, L. F. Kosyanchuk, Yu. and P. Gomza, Polym. Sci., U.S.S.R., (Eng. Tr.), 1985, 27, 622.
17. B. L. Allwood, N. Spencer, H. Shahriari-Zavareh, J. F. Stoddart and D. J. Williams, J. Chem. Soc., Chem. Commun., 1987, 1058.
18. B. L. Allwood, N. Spencer, H. Shahriari-Zavareh, J. F. Stoddart and D. J. Williams, J. Chem. Soc., Chem. Commun., 1987, 1064.
19. P. R. Ashton, A. M. Z. Slawin, N. Spencer, J. F. Stoddart and D. J. Williams, J. Chem. Soc., Chem. Commun., 1987, 1066.
20. B. L. Allwood, N. Spencer, H. Shahriari-Zavareh, J. F. Stoddart and D. J. Williams, J. Chem. Soc., Chem Commun., 1987, 1061.
21. B. Odell, M. V. Reddington, A. M. Z. Slawin, N. Spencer, J. F. Stoddart and D. J. Williams, Angew. Chem. Int. Ed. Engl., 1988, 27(11), 1547.
22. M. V Reddington, A. M. Z. Slawin, N. Spencer, J. F. Stoddart, C. Vincent and D. J. Williams, J. Chem. Soc., Chem. Commun., 1991, 630.
23. P. R. Ashton, B. Odell, M. V. Reddington, A. M. Z. Slawin, J. F. Stoddart and D. J. Williams, Angew. Chem. Int. Ed. Engl., 1988, 27(11), 1550.
24. D. Philp, A. M. Z. Slawin, N. Spencer, J. F. Stoddart and D. J. Williams, J. Chem. Soc., Chem. Commun., 1991, 1584.
25. P. R. Ashton, T. T. Goodnow, A. E. Kaifer, M. V. Reddington, A. M. Z. Slawin, N. Spencer, J. F. Stoddart, C. Vincent and D. J. Williams, Angew. Chem. Int. Ed. Engl., 1989, 28(10), 1396.

26. P. R. Ashton, C. L. Brown, E. J. T. Chrystal, T. T. Goodnow, A. E. Kaifer, K. P. Parry, D. Philp, A. M. Z. Slawin, N. Spencer, J. F. Stoddart, C. Vincent and D. J. Williams, *J. Chem. Soc., Chem. Commun.*, 1991, 634.
27. P. R. Ashton, C. L. Brown, E. J. T. Chrystal, T. T. Goodnow, A. E. Kaifer, K. P. Parry, A. M. Z. Slawin, N. Spencer, J. F. Stoddart, C. Vincent and D. J. Williams, *Angew. Chem. Int. Ed. Engl.*, 1991, 30(8), 1039.
28. P. R. Ashton, C. L. Brown, E. J. T. Chrystal, T. T. Goodnow, A. E. Kaifer, K. P. Parry, M. Pietraszkiewicz, N. Spencer and J. F. Stoddart, *Angew. Chem. Int. Ed. Engl.*, 1991, 30(8), 1042.
29. P. R. Ashton, M. Groguz, A. M. Z. Slawin, N. Spencer, J. F. Stoddart and D. J. Williams, *Tetrahedron Letters*, 1991, 32(43), 6235.
30. L. Anelli, P. R. Ashton, N. Spencer, A. M. Z. Slawin, J. F. Stoddart and D. J. Williams, *Angew. Chem. Int. Ed. Engl.*, 1991, 30(8), 1036.
31. P. R. Ashton, D. Philp, N. Spencer and J. F. Stoddart, , *J. Chem. Soc., Chem. Commun.*, 1991, 1677.
32. P. R. Ashton, D. Philp, M. V. Reddington, A. M. Z. Slawin, N. Spencer, J. F. Stoddart and D. J. Williams, *J. Chem. Soc., Chem. Commun.*, 1991, 1680.
33. P. T. Engen, Y. X. Shen, M. A. G. Berg, J. S. Merola and H. W. Gibson, Submitted to *Macromolecules*.
34. Y. X. Shen, Ph. D. Thesis, Virginia Tech, 1992.
35. F. Bitsch, C. O. Dietrich-Buchecker, A.-K. Khémiss, J.-P. Sauvage and A. V. Dorselaer, *J. Amer. Chem. Soc.*, 1991, 113, 4023.

36. N. Armaroli, V. Balzani, F. Barigelletti, L. De Cola, J.-P. Sauvage, and C. Hemmert, *J. Amer. Chem. Soc.*, 1991, 113, 4033.
37. C. O. Dietrich-Buchecker and J.-P. Sauvage, *Chem. Rev.*, 1987, 87, 795.
38. C. Wu, P. R. Lecavalier, Y. X. Shen and H. W. Gibson, *Chem. Mater.*, 1991, 3, 569.
39. T. Venkata, S. Rao and D. S. Lawrence, *J. Amer. Chem. Soc.*, 1990, 112, 3614.
40. R. Isnin and E. Kaifer, *J. Am. Chem. Soc.*, 1991, 113, 8188.
41. M. Born, H. Ritter, *Makromol. Chem., Rapid Commun.*, 12, 471.
42. C. Wu, M. C. Bheda, C. Lim, Y. X. Shen, J. Sze and H. W. Gibson, *Polym. Comm.*, 1991, 32 (7), 204.
43. H. W. Gibson, M. Bheda, P. T. Engen, Y. X. Shen, J. Sze, C. Wu, S. Joardar, T. C. Ward and P. R. Lecavalier, *Makromol. Chem., Macromol. Symp.*, 1991, 42/43, 395.
44. H. W. Gibson, P. R. Lecavalier and P. T. Engen, *Am. Chem. Soc., Polymer Preprints*, 1988, 29(1), 248.
45. P. R. Lecavalier, P. T. Engen, Y. X. Shen, S. Joardar, T. C. Ward, and H. W. Gibson, *Am. Chem. Soc., Polymer Preprints*, 1989, 30(1), 189.
46. H. W. Gibson, M. C. Bheda, P. T. Engen, Y. X. Shen, J. Sze, C. Wu, S. Joardar, T. C. Ward and P. R. Lecavalier, *Am. Chem. Soc., Polymer Preprints*, 1990, 31(1), 79.
47. M. C. Bheda and H. W. Gibson, *Am. Chem. Soc., Polymer Preprints*, 1990, 31(1), 588.

48. M. C. Bheda and H. W. Gibson, *Macromolecules*, 1991, 24, 2703.
49. H. W. Gibson, P. T. Engen, Y. X. Shen, J. Sze, C. Lim, M. C. Bheda and C. Wu, American Chemical Society, *Polymer Preprints*, 1991, 32(1), 423.
50. H. Marand, A. Prasad, C. Wu, M. Bheda and H. W. Gibson, American Chemical Society, *Polymer Preprints*, 1991, 32(3), 639.
51. C. Wu, Y. X. Shen, M. Bheda, J. Sze, P. Engen, A. Prasad, H. Marand, D. Loveday and G. Wilkes, American Chemical Society, *Polymer Preprints*, 1991, 32(3), 593.
52. H. W. Gibson, C. Wu, Y. X. Shen, M. Bheda, J. Sze, P. Engen, A. Prasad, H. Marand, D. Loveday and G. Wilkes, American Chemical Society, *Polymer Preprints*, 1991, 32(3), 637.
53. J. Sze, M. S. Thesis, Virginia Tech, 1992.
54. P. Engen, Ph. D. Thesis, Virginia Tech, 1991.
55. Y. Delaviz and H. W. Gibson, *Macromolecules*, 1992, 25, 18.

II. OBJECTIVES 42

Objectives

The objectives of this research project were to synthesize rotaxanes and polyrotaxanes in sufficiently large quantities to explore novel physical and solution properties that may result from this novel architecture. Major emphasis was placed on utilizing known chemistry, well characterized macrocycles and polymeric systems from the literature to understand the changes in the properties brought about by the polyrotaxane architecture as well as to expedite the progress. The strategies to prepare rotaxanes and polyrotaxanes in sufficiently large quantities included large scale synthesis of macrocycles having greater than 27 atoms as well as tris(*p*-*t*-butylphenyl)methyl derivatives as blocking groups having various functionalities.

In this study, 30-crown-10 was the macrocycle of choice due to its relative ease of synthesis, polar nature and the fact that its rotaxanes and polyrotaxanes can be end blocked using triarylmethane derivatives to prevent its dethreading. Feasibility of large scale synthesis and purification of 30-c-10 was explored. Further, in the synthesis of 30-c-10 it was found that the macrocycle of twice the size, i.e., 60-crown-20, is also formed. Thus, 60-c-20 was also used for polyrotaxane synthesis.

Diversity in the macrocycle chemical structure, polarity, etc., are important parameters to design and prepare polyrotaxanes with specific properties. Thus other macrocycles such as cyclic polystyrene and ionic bipyridyl macrocycle were also prepared. Cyclic polystyrene represents the other end of the spectrum in terms of polarity compared to crown ethers and the ionic bipyridyl macrocycle (**I-17**) provides an alternative to statistical threading and allows ionomeric polyrotaxanes to be prepared.

As indicated, the tris(*p*-*t*-butylphenyl)methane blocking group was able to effectively block the crown ethers up to 42-membered size. Thus, tris(*p*-*t*-butylphenyl)methane blocking group derivatives

containing various functional groups such as phenol, acid, acid chloride, hydroxy, chloro and vinyl were made.

Fundamental studies on the threading tendencies of flexible and rigid small molecules as well as preformed polymers of various molecular weight were done to understand threading behavior of such monomeric and polymeric molecules in the statistical threading method.

It was expected that as a result of polyrotaxane formation, properties in bulk as well as the solubility characteristics could be significantly altered without compromising the useful properties of polymers. Thus, polymeric systems of commercial importance such as polyamides and liquid crystalline polymers were considered for polyrotaxane synthesis to study the changes in the properties obtained by incorporation of macrocycles onto the polymer chain.

Polyrotaxanes of polystyrene were prepared to study the feasibility of the use of crown ether macrocycles in anionic polymerization, to understand the behavior of polar macrocycles on the nonpolar polystyrene and to study the changes in properties.

III.	CROWN ETHER MACROCYCLES AND CATENANE .	. 45
III.1	Introduction	46
III.2	Literature Review	47
III.3	Results and Discussion	52
	Characterization of 30-C-10	56
	Characterization of 60-C-10	59
III.4	Catenane	60
III.5	Experimental	61

III.1 Introduction

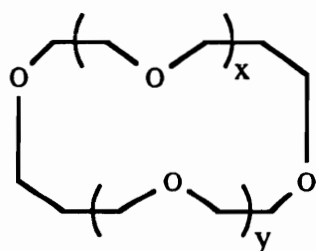
Since the inception, design and first synthesis of dibenzo-18-crown-6, 18-crown-6 and other crown ether macrocycles (1-4) there has been a tremendous growth in the research activities pertaining to synthesis of macrocyclic molecules analogous to the crown ethers. The interest in such macrocycles is derived from the knowledge that such compounds show selectivity in complexing with a variety of neutral and ionic substrates. Modifications of such crown ether structural parameters as size of the cavity, number of ether oxygen atoms, length of aliphatic chains connecting ether oxygens, aromatic groups in the structure and substitution of oxygen by hetero- atoms such as N or S as a part of aliphatic or aromatic units (5-6) have been reported. The selectivity of the complexation is dependent on the above mentioned parameters as well as other chemical interactions that may be present, thus giving new directions to the subject of molecular recognition. Other variations in structures of such macrocyclic molecules include three-sided enclosed cavities (cryptands) (5-6), or Mobius strips, the one-sided, one-edged 'isomer' of a cylinder with a single 180° twist about a long axis (7).

Our interest in crown ethers stems from the fact that such macrocycles are ideally suited for the synthesis of rotaxanes and polyrotaxanes. A variety of aliphatic as well as aromatic crown ethers and analogues with hetero-atoms containing less than 27 atoms have been synthesized and characterized by NMR, X-ray crystal structure analyses and complexation with either neutral or ionic substrates (5-6). However, there are relatively few examples of aliphatic and aromatic crown ethers and analogues containing more than 27 atoms reported in literature. As discussed in the earlier chapter macrocycles containing greater than 27 atoms are needed for significant threading of linear species to take place; thus discussion of such macrocycles will be limited to the larger macrocycles containing 28 atoms or more.

In this chapter, a literature review of some of the crown ethers and analogous macrocycles containing more than 27 atoms and attempts to synthesize crown ethers, particularly 30-c-10 and 60-c-20, in large scale followed by detailed characterization are reported.

III.2 Literature Review

Synthesis and characterization of aliphatic crown ethers of larger sizes (greater than 27 atoms) has been reported in the literature on less than a gram scale (8-9). The syntheses of such macrocycles were accomplished by reacting an appropriate glycol with a base such as sodium hydride or potassium hydride, followed by reaction of this dimetal salt of the glycol with an appropriate ditosylate. Various crown ethers were synthesized with the general structure 3n-crown-n, where n is 10-20, ranging from 30-c-10 (III-1) to 60-c-20 (III-6) using this method (8).



III-1 $x=y= 4$; 30-c-10

III-2 $x=y= 5$; 36-c-12

III-3 $x=y= 6$; 42-c-14

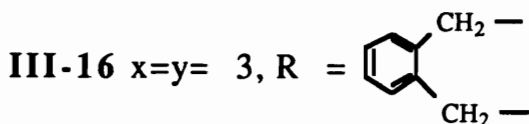
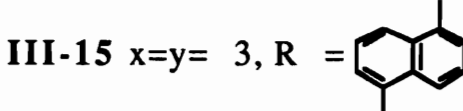
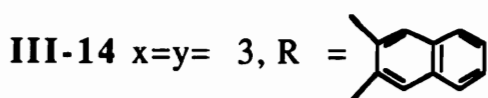
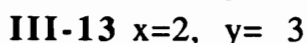
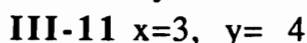
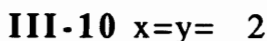
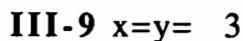
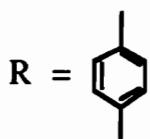
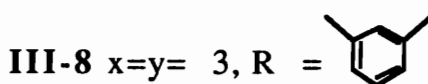
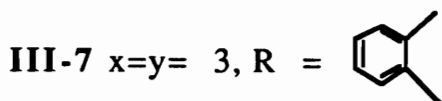
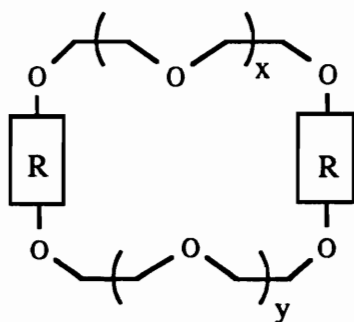
III-4 $x=y= 7$; 48-c-16

III-6 $x=y= 9$; 60-c-20

For 33-c-11 and larger crowns (some of the crown ethers not shown in the above diagram), the yields were in the range of 20-30 % when potassium hydride was used as base and its replacement with sodium hydride did not change the yields significantly. However, for 27-c-9 and 30-c-10, much better yields (about 50 %) were obtained with sodium hydride than with potassium hydride. Further, the authors suggested that much higher yields of the macrocycles are due to double or multiple template effect where more than one metal ion complexes to the precursor ether such that

the uncyclized ends are held in close proximity, resulting in higher yields (8). Less than a gram of each macrocycle was prepared. 27-c-9 and 30-c-10 were reported as oils, while other macrocycles were reported as solids, including 60-c-20 with a melting point of 46-50.5 °C. Macrocycles were purified by column chromatography.

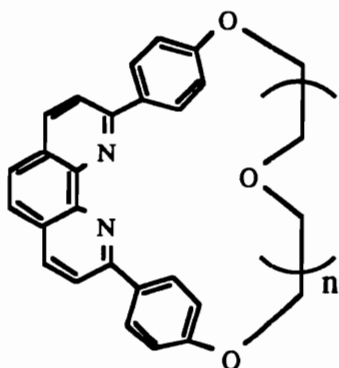
Syntheses and characterization of variety of crown ethers containing aromatic groups have been reported (10-20). Some of the examples of these macrocycles containing 28 atoms or more are shown below.



Synthesis of III-7 to III-15 are reported by Stoddart and coworkers (10-17 and references therein) and overall yields ranged from 7.5-15 %. The synthesis was accomplished in four steps; in the first three steps the linear precursor is prepared, followed by cyclization in the fourth step. In our group, a one step method was

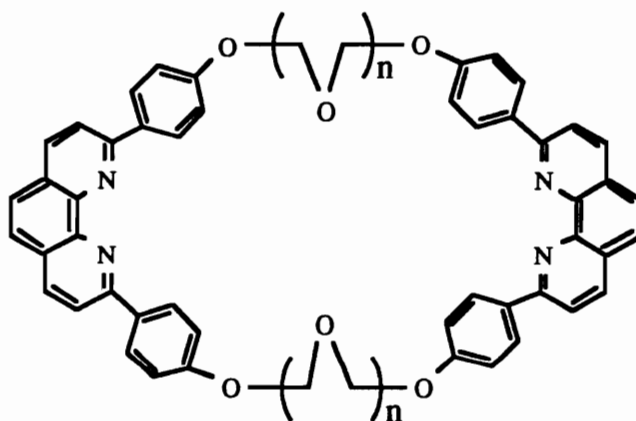
devised for the synthesis of **III-9** and the yields of the macrocycle were 12.5 % (18). In principle, this method can also be used for the synthesis of other macrocycles mentioned above. X-ray crystal structure analyses of these macrocycles showed that most of the macrocycles have cavities open such that they could be utilized for rotaxane synthesis except for **III-14** where the macrocycle is folded in a 'U' shape such that the naphthyl groups are in parallel orientation.

Synthesis of **III-16** was accomplished by reacting α,α' -dibromo-*o*-xylene and tetra(ethylene glycol) in presence of a base (19-20). Yields of the macrocycle varied from 4-25 % depending on the base used; higher yields were obtained with sodium hydride as base. This macrocycle is not very useful in polyrotaxane synthesis since the benzyl ethers linkages are not very stable.



III-17 $n = 3$

III-19 $n = 4$



III-18 $n = 3$

Syntheses of catenanes and rotaxanes derived from macrocycles containing phenanthroline groups have been discussed in chapter I. The phenanthroline groups of the macrocycle can be complexed, using a metal ion such as copper, with another nitrogen containing molecule. The macrocycle **III-17** was synthesized in about 50 % yield and in this synthesis, macrocycle **III-18** is also formed in about 14 % yield; further, macrocycle **III-19** was

synthesized in about 45 % yield (21). Despite the high yields, and added advantage of host-guest complexability of phenanthroline based macrocycles, the starting material is fairly expensive (ca. \$ 1/g). As indicated in Chapter 1, a rotaxane from such a macrocycle has been made in our group.

Calixarenes are cyclic molecules where more than two benzene rings (substituted or unsubstituted) are attached to each other at the meta positions with a methylene group (22-23). The resulting molecules are known as calix[X]arenes where X represent number of benzene groups in the cyclic molecules. Synthesis of calix[8]arene having mp of 410-412 °C has been reported from phenol and formaldehyde in about 70 % yield (23). Such calixarenes would be very useful in the synthesis of polyrotaxanes.

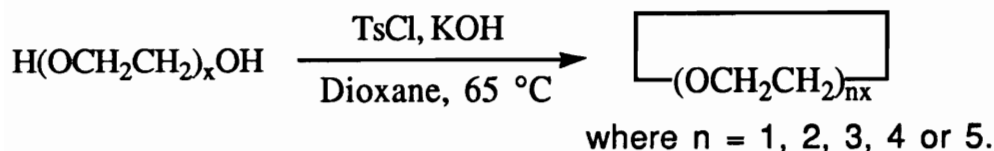
Various reports on other large macrocycles containing more than 27 atoms have appeared in the literature (24-33). These macrocycles vary greatly in their structures as well as complexabilities. These macrocycles were deemed unsuitable for rotaxane synthesis either due to their complex synthetic approach or expensive starting materials.

Thus, crown ethers such as 30-c-10 and higher homologues were the macrocycles of choice mainly due to their simpler synthetic approach, inexpensive starting materials and also because such macrocycles can be prepared in high yields (about 40-50 %). Further, the blocking groups derived from tris(p-t-butylphenyl)methane can be used for the blocking of these aliphatic crown ethers.

After the large scale synthesis of crown ethers was accomplished for this study, a report on synthesis of such large macrocycles was published. In this paper (9), the authors have reported synthesis of crown ethers of various sizes from linear ethylene glycols of various sizes (ca. 36-c-12, 48-c-16, 60-c-20 from tetra(ethylene glycol) and 30-c-10 and 60-c-20 from deca(ethylene glycol) and so on). Of particular interest is the

synthesis of 30-c-10 and 60-c-20. Table III-1 summarizes some of the results obtained by the authors (9).

Table III-1 Reported Synthesis of Crown Ethers (9)



	$\bar{X} =$	Yields (%)		
		<u>4</u>	<u>5</u>	<u>10</u>
12-c-4		1.4		
15-c-5			46.0	
24-c-8	23.0			
30-c-10			12.0	43.0
36-c-12	11.0			
48-c-16	4.3			
60-c-20	1.2		0.7	1.4

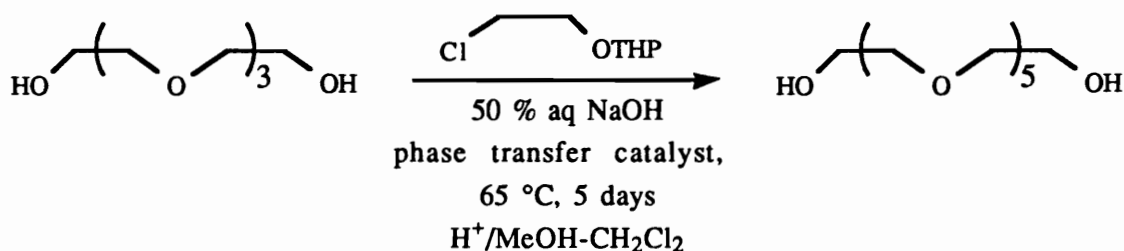
As shown in the Table III-1 crown ethers of larger sizes, up to five times the size of the precursor linear glycol are also formed but the yields of higher homologue crowns are generally much lower (9). An important conclusion of the above study is that the large crown ether macrocycles could be prepared in relatively high yields under appropriate conditions. Similar experiments were repeated using commercial polyethylene glycol of molecular weights 200, 300, 400, 600 and 1000. The crown ethers were purified by either extractions or column chromatography. The yields of crown ethers were determined by gas chromatography using various columns such as glass column packed with 3% OV-17 on 80-100 Supelcoport (1 m x 1/8 in), stainless steel column packed with 5% OV-101 on Chromosorb 100-120 (1 m x 1/8 in) or stainless steel column packed with 10% UCW-982 on Chromosorb 80-100 ((20 in x 1/8 in) using a flame ionization detector (9).

About a gram of each macrocycle was prepared and the purity of 30-c-10 was reported to be about 99 % with a melting point of 35.5-36.8 °C while 60-c-20 was isolated in 85 % purity without reporting any characterization data (9).

III.2 Results and Discussions

Earlier synthesis of hexa(ethylene glycol) was accomplished by the classical Williamson ether synthesis method, where tetra(ethylene glycol) was converted to tetra(ethylene glycol) dichloride followed by reaction of the dichloride with disodium salt of ethylene glycol. The yields of hexa(ethylene glycol) were in the range of 25%. Bartsch et al. have reported phase-transfer-catalysed synthesis of hexa(ethylene glycol) in 80 % yields (34). An organic phase consisting of excess Cl-CH₂CH₂O-THP as solvent and tetra(ethylene glycol) was stirred with 50 % aqueous sodium hydroxide in the presence of tetrabutylammonium hydrogen sulfate as the phase-transfer catalyst at 65 °C for 3 days. Using this procedure, in the present study, hexa(ethylene glycol) was obtained in yields as high as 92 %. The synthesis of hexa(ethylene glycol) is shown in Scheme III-1.

Scheme III-1 Synthesis of Hexa(ethylene Glycol)



Synthesis of 30-c-10 was accomplished by reacting hexa(ethylene glycol) and sodium hydride followed by slow addition of tetra(ethylene glycol) ditosylate under high dilution condition as

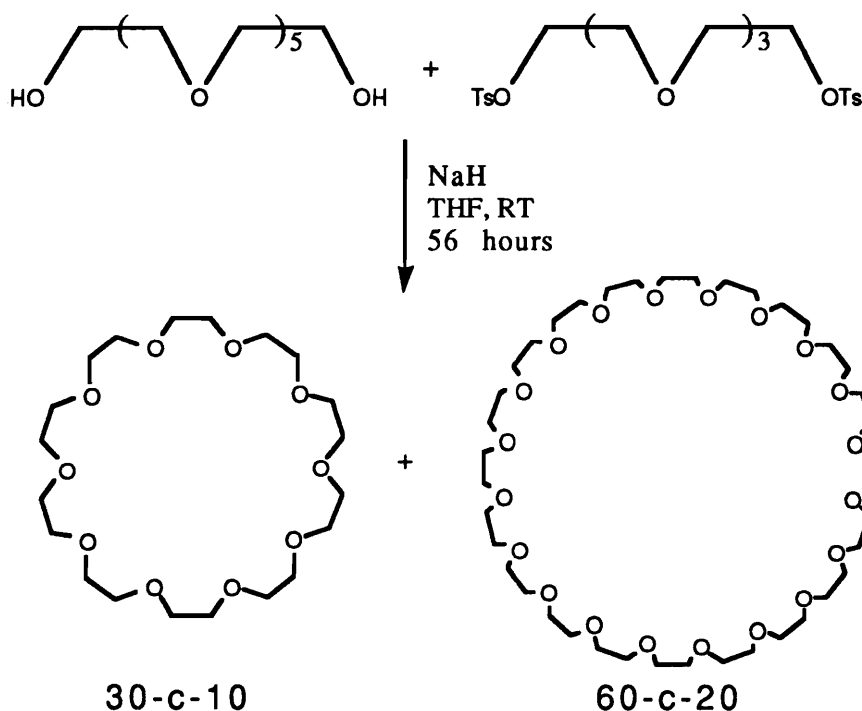
described by Chenevert et al. (8). Since the synthesis of 30-c-10 was done on a very large scale (0.3 moles at a time) relatively higher concentrations were used than reported (8). The overall concentration of hexa(ethylene glycol) in a large scale synthesis of 30-c-10 was 0.12 mole/l in THF (reported (8) dilution for the synthesis of 30-c-10 was 0.04 mole/l of hexa(ethylene glycol) in THF).

30-c-10 prepared in the early stages of the research (small scale synthesis, 0.04 mole/l hexa(ethylene glycol) in THF) was purified by column chromatography using silica gel and ethyl acetate. During the column chromatography most of the linear high molecular weight side product was found to stay on the top of the column and it did not move. Further, to obtain very pure 30-c-10 (99+ %) it had to be purified 3-4 times by column chromatography and the product showed a singlet at 3.67 ppm in the proton NMR spectrum with a melting point of 38.1-40.1 °C. Furthermore, after complete elution of 30-c-10 from the column, another compound (5-7 % yield) was found to elute and in its proton NMR spectrum it showed a singlet at 3.64 ppm. This corresponded to 60-c-20 as reported by Chenevert et al. (8). Later it was confirmed by mass spectroscopy that indeed, it was 60-c-20. Scheme III-2 shows the reaction of hexa(ethylene glycol) and tetra(ethylene glycol) ditosylate to form 30-c-10 and 60-c-20.

In the large scale synthesis, 60-c-20 was formed in about 12 % yield. It is formed by the reaction of two molecules of hexa(ethylene glycol) and two molecules of tetra(ethylene glycol), presumably assisted by the template effect. The first step in the formation of 60-c-20 would be the reaction of one molecule of hexa(ethylene glycol) with a molecule of tetra(ethylene glycol) ditosylate, yielding sodium deca(ethylene glycol) tosylate. This could cyclize to give 30-c-10 or further react with a molecule of hexa(ethylene glycol) and a molecule of tetra(ethylene glycol) ditosylate followed by cyclization of the resulting molecule. Formation of 60-c-20 must be assisted by multiple template effects

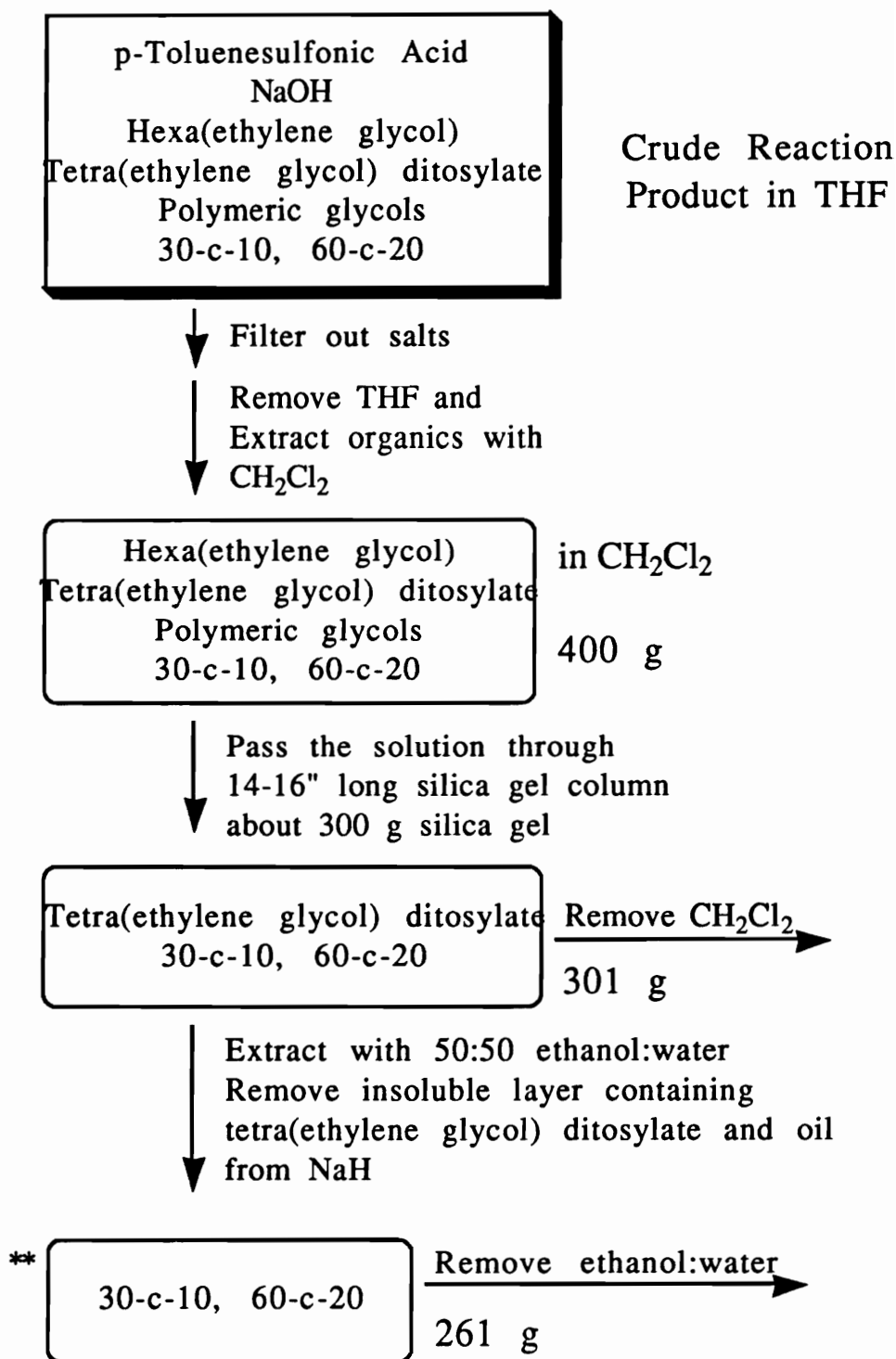
along with the relatively higher concentration of the reaction mixture; as in the absence of any template effect, such high yields of 60-c-20 would not be obtained.

Scheme III-2 Synthesis of 30-c-10 and 60-c-20



Based on the above observations, crude product from three large scale reactions (400 g crude product) was purified by filtering a solution in dichloromethane through a 14-16" long silica gel column to remove linear glycols. Further, after removal of dichloromethane, the filtered crude product was extracted with 50:50 water:ethanol to remove oil (from sodium hydride) and any unreacted tetra(ethylene glycol) ditosylate. Scheme III-3 shows the purification of crude reaction product. The resulting product free of linear impurities was analysed by proton NMR and two major peaks of about equal integral values at 3.64 and 3.67 were observed, corresponding to 30-c-10 and 60-c-20. Further, a small peak at 3.65 ppm was also seen, which is believed to be due to formation of

Scheme III-3 Purification of 30-c-10 and 60-c-20



a catenane (discussed later in the next section). The 30-c-10 and 60-c-20 were separated by crystallization from 60:40 carbon tetrachloride and petroleum ether. 30-c-10 was further purified by crystallization from dichloromethane:hexanes (40:60). 60-c-20 was purified by filtering the solution in dichloromethane through a silica gel column, followed by removal of the solvent and crystallization of 60-c-20 from acetone. The yields of isolated pure crown ethers were: 30-c-10, (110 g) 28 % yield; 60-c-20, (95 g) 12 % yield. The third compound, a catenane, was isolated in about 1 % yield (2.5 g). (More of each compound was present in 40-50 g of oily mixture, which also contained 2-4 additional components as analysed by proton NMR).

Another method that was found to work best in the separation of 30-c-10 and 60-c-20 is extraction of 30-c-10 by hot hexanes. 30-c-10 is soluble in hot hexanes while 60-c-20 is not; thus, very pure 30-c-10 was obtained by just a few extractions of the crude reaction mixture. The 60-c-20 thus isolated can be purified by recrystallization from acetone.

Characterization of 30-C-10

In the proton NMR spectrum, 30-c-10 showed a single peak at 3.67 (3.666 ppm) [reported (8) 3.67 ppm] and a single peak for carbons was seen at 70.67 ppm (reported (8) 70.55 ppm) in the carbon NMR spectrum. Figure III-1 shows the proton and carbon NMR spectra of 30-c-10. Chemical ionization mass spectral data show the parent ion (M+H)⁺ at M/z = 441. Infrared analyses showed no detectable hydroxy groups and a strong peak at 1135-1115 cm⁻¹ is seen for ether linkages.

TGA analyses of 30-c-10 show the onset of decomposition in air at 172 °C and 5 % weight loss was observed at 206 °C. Under nitrogen atmosphere the crown showed onset of degradation at about the same temperature as that in air; however, the 5 % weight loss was observed at 238 °C. DSC analyses of the the crown showed the

glass transition temperature to be $-69\text{ }^{\circ}\text{C}$, crystallization temperature at $-44\text{ }^{\circ}\text{C}$ and melting temperature at $40\text{ }^{\circ}\text{C}$. Figure III-2 show the DSC analyses of 30-c-10 (second scan).

Anhydrous crystals of 30-c-10 for X-ray crystal structure analyses were grown under nitrogen from hexanes. Crystals of 30-c-10 tetrahydrate were grown from dichloromethane:hexanes (30:70) solution by slow evaporation, while exposed to air. Figure III-3 and Figure III-4 show the X-ray crystal structures of anhydrous 30-c-10 and 30-c-10 tetrahydrate, respectively. The X-ray analyses of the anhydrous 30-c-10 crystal showed it to be orthorhombic, belonging to space group *Pbca* having unit-cell parameters of $a = 8.606(1)\text{ }^{\circ}\text{A}$, $b = 8.260(1)\text{ }^{\circ}\text{A}$ and $c = 33.310(4)\text{ }^{\circ}\text{A}$. The 30-c-10 : 4 H_2O crystal was found to be monoclinic, belonging to the space group *P21/c* and having unit-cell parameters of $a = 8.332(4)\text{ }^{\circ}\text{A}$, $b = 9.083(2)\text{ }^{\circ}\text{A}$, $c = 18.665(5)\text{ }^{\circ}\text{A}$ and $\beta = 90.24(3)^{\circ}$. The X-ray crystal structures were solved by direct methods and refined by the full-matrix least-square procedure to $R = 0.0427$, $R_w = 0.0501$ for 1644 independent observed reflections [$F > 4\sigma(F)$] for anhydrous 30-c-10 and $R = 0.0573$, $R_w = 0.0701$ for 1370 independent observed reflections [$F > 4\sigma(F)$] for 30-c-10 tetrahydrate

The anhydrous 30-c-10 crystals have a cavity size of $3.9\text{ }^{\circ}\text{A} \times 13.6\text{ }^{\circ}\text{A}$ and a melting point of $43.8\text{ }^{\circ}\text{C}$ (DSC peak maxima, heating rate $2.5\text{ }^{\circ}\text{C}/\text{min}$). The C-C bonds in three oxyethylene units from O(1) up to O(4) are in trans conformations (O-C-C-O torsional angles range from 167° - 179° , Table III-2) while the C-C bonds of the other two oxyethylene units from O(4) to O(1) have gauche(-) (g-) conformations (torsional angles are -66° and -75°). The rest of the five oxyethylene units are the same as the above five oxyethylene units due to the symmetry of the molecule. The first three oxyethylene units described above behave as if they are a part of linear chain and are in the extended (trans) conformation. This is markedly different behavior of the oxyethylene units since in small macrocycles such as 12-c-4 in which the predominant conformation

is gauche(+) (g+) while in 18-c-6 alternate g+ and g- conformations are predominant (5).

Table III-2 Torsional Angles in Anhydrous 30-c-10

O(1)-C(1)-C(2)-O(2)	-174.9°
O(2)-C(3)-C(4)-O(3)	179.8°
O(3)-C(5)-C(6)-O(4)	-179.0°
O(4)-C(7)-C(8)-O(5)	-66.2°
O(5)-C(9)-C(10A)-O(1A)	-75.4°

In the crystal structure of 30-c-10 tetrahydrate, four molecules of water are intermolecularly bound to each other as well as to four oxygen atoms of the crown ether. In a recent study of the crystal structure of 18-c-6 containing 6 carboxyl groups was found to encapsulate two water molecules that were hydrogen bonded to each other (35). The authors report the distances of the macrocyclic oxygen to the hydrogen that connects the dimer, range from 2.75 Å to 2.78 Å. It would be an interesting study to see if the four water molecules complexed with 30-c-10 could meet the definition for a 'water tetramer'. More refined X-ray structure analyses data are needed to account for exact location of the hydrogen atoms.

Further, due to the inclusion of water molecules, the cavity of 30-c-10 is wide open as compared to the anhydrous structure. The dimensions of the cavity are 7.5 Å x 11.4 Å; this corresponds to about 1.2-1.6 times the area of anhydrous 30-c-10. The tetrahydrate had a melting point of 46-48 °C. Conformational analyses of 30-c-10 tetrahydrate show that only two of the ten oxyethylene units are in trans conformations (O-C-C-O torsional angle $\pm 177.4^\circ$, Table III-3). The rest of the oxyethylene units have g conformations (O-C-C-O torsional angles range from 70°-66°). The larger cavity size of the tetrahydrate compared to anhydrous 30-c-10 is due to large number of g conformations in the tetrahydrate.

Table III-3 Torsional Angles in 30-c-10 : 4 H₂O

O(1)-C(1)-C(2)-O(2)	177.4°
O(2)-C(3)-C(4)-O(3)	-70.0°
O(3)-C(5)-C(6)-O(4)	-70.4°
O(4)-C(7)-C(8)-O(5)	-66.6°
O(5)-C(9)-C(10A)-O(1A)	-65.9°

These X-ray crystal structure analyses of 30-c-10 represent the first such study of a large aliphatic crown ether macrocycle.

Characterization of 60-C-10

The proton NMR spectrum of 60-c-20 showed a single peak at 3.64 ppm (3.6446 ppm, reported (8) 3.64 ppm) while in the carbon NMR spectrum a singlet is seen at 70.53 ppm (reported (8) 70.44 ppm). Figure III-5 shows the proton and carbon NMR spectra of 60-c-20. The crown had a melting point of 53.5-55.1 °C.

The FTIR spectrum of the 60-c-20 does not show any detectable hydroxyl groups and is essentially identical to that of 30-c-10.

The chemical ionization mass spectrum of 60-c-20 shows a peak corresponding to the molecular ion (M+H)⁺ at M/z = 882; however, the peak is not very pronounced. Figure III-6 shows the mass spectrum of 60-c-20; the vertical scale of the mass region from 500 to 1000 is magnified twenty times that from 100 to 500. Various other efforts to see pronounced molecular ion peak by mass spectroscopy were unsuccessful. It has been suggested that large aliphatic crowns typically do not show readily detectable molecular ions and fragments corresponding to the protonated lower homologues of the parent molecule are found in low mass regions only (36).

TGA analyses showed the onset of degradation in air at 169 °C and 5 % weight loss was observed at 198 °C. Under nitrogen

atmosphere, the onset of degradation was observed at 180 °C and 5 % weight loss was observed at 230 °C.

DSC analyses of 60-c-20 showed the glass transition temperature to be about -67 °C and the melting peak is seen at 53 °C (5 °C/min). Various attempts to prepare crystals of 60-c-20 for X-ray crystal structure analyses were unsuccessful.

III.4 Catenane

As indicated in the earlier section, three compounds were observed in the proton NMR spectrum of the worked up product of 30-c-10 synthesis. Two of the compounds with proton NMR singlets at 3.67 ppm and 3.64 ppm were 30-c-10 and 60-c-20, respectively. The appearance of the third compound in very low yield (ca. about 1-4 %) having a proton NMR singlet at 3.65 ppm was surprising. About 2.5 g of this compound (solid, mp = 36.1-38.7 °C; partly soluble in hexanes) was isolated and some more of the compound was found to be mixed with other compounds as an oil. One of the possibilities is the formation of a [2]catenane, interlocked rings, consisting of two 30-c-10 macrocycles or two 60-c-20 macrocycles or a combination of one 30-c-10 and one 60-c-20 macrocycles. The solubility of the isolated compound in hexanes suggests that it could be a [2]catenane of 30-c-10.

The formation of such catenanes seems feasible even under high dilution conditions employed for synthesis of crown ethers due to the template effect. The template effect can be realized when the disodium salt of hexa(ethylene glycol) or sodium salts of higher homologues complex with already formed crown ethers (30-c-10 or 60-c-20) in the reaction mixture. Cyclization of tetra(ethylene glycol) ditosylate by this sodium salt of hexa(ethylene glycol) or higher homologue complexed with crown ether would yield a catenane. Formation of a catenane has been suggested in the synthesis of cyclic polystyrene; however, catenanes have never been isolated from the cyclization reaction mixture (37). The difficulty

arises in proving the structures of such catenanes consisting of chemically similar macrocycles of identical sizes.

Some examples of catenanes were shown in Chapter I. Most of the examples of catenanes involve macrocycles of different chemical structures, except **I-28** and other analogous catenanes where two or more macrocycles are identical in chemical structure (38-45). Other examples of catenanes can be found in the literature (46-49).

To confirm the possibility that the isolated compound having a proton NMR singlet at 3.65 ppm is a catenane, synthesis of a catenane of 30-c-10 was attempted using 4.5 equivalent (relative to hexa(ethylene glycol)) of 30-c-10 (35 g) and THF (40 ml) as a reaction solvent mixture. Proton NMR analyses of the partially purified product (containing mainly 30-c-10) did show a peak at 3.65 ppm corresponding to the catenane, in about 5-8 % overall yield. The product mixture was not separated further; instead the catenane isolated from the 30-c-10 syntheses was utilized for the analyses. Figure III-7 show the proton NMR spectrum of purported [2]catenane of 30-c-10.

The mass spectrum of the catenane is shown in Figure III-8. The peak corresponding to the parent ion appears at a mass of 881 along with a peak at a mass of 441. The peak of mass 881 corresponds to the [2]catenane of 30-c-10 and the peak at $M/z = 441$ correspond to the $(M+H)^+$ ion from 30-c-10. Several other peaks are also present between the mass 441 and 881, which correspond to fragments of the catenane. The catenane topology will be confirmed by X-ray crystal structure analyses and at present, efforts are underway to prepare suitable crystals.

III.5 Experimental

Measurements:

Melting Points were taken in capillary tubes with a Haake-Buchler melting point apparatus and have been corrected. TGA data

were obtained using Du Pont TGA 951 and Perkin-Elmer TGA-7 instruments at a scan rate of 10 °C/min. DSC data were obtained using Du Pont DSC 912 and Perkin-Elmer DSC-2 instruments at a scan rate of 10 °C/min. Proton and carbon NMR spectra were obtained on a Bruker WP 270 spectrometer using deuterated chloroform solutions with tetramethylsilane as an internal standard. FTIR spectra were obtained on a Nicolet MX-1 instrument. X-ray crystal structure data were obtained using a Siemens R3m/V diffractometer and the crystal structures were solved using a SHELXTL PLUS software. Mass spectral data were obtained using a VGA 7070E analytical mass spectrometer.

Synthesis of Tetra(ethylene glycol) ditosylate:

In a 2 l, 3-neck flask equipped with mechanical stirring, 106 g NaOH (2.7 moles), 440 ml water, 250 ml THF and 143.0 ml tetra(ethylene glycol) (0.8 moles) was added. The reaction mixture was cooled to about 0°C and 361.0 g (1.9 moles) of p-toluensulfonyl chloride in 500 ml THF was added dropwise over a period of 4 hours and the reaction mixture was stirred for 7 hours. After the reaction was over, the reactor content was poured into cold 10% HCl and extracted thrice with 2 L toluene. The toluene layer was washed with water, dilute potassium carbonate solution and dried over sodium sulfate, filtered and toluene was removed. Traces of unreacted p-toluensulfonyl chloride were removed by extracting the product with petroleum ether. The product was dried in a vacuum oven at 50 °C overnight. The product was then stored in a freezer until used. The ditosylate was a highly viscous light yellow liquid. The reaction is quantitative. FTIR showed no hydroxyl groups. NMR (CDCl₃): 7.77, 7.74; 7.32, 7.35 (aromatic, 2 d, 8H), 4.14 (α -CH₂, t, 4H), 3.60 (β -CH₂, t, 4H), 3.52 (CH₂, s, 8H), 2.41 (CH₃, s, 6H).

Synthesis of hexa(ethylene glycol):

The synthesis of hexa(ethylene glycol) involved two steps: (a) Synthesis of protected chloroethanol (b) Reaction of protected

chloroethanol with tetra(ethylene glycol) followed by deprotection of the resulting hexa(ethylene glycol).

Step-1 Synthesis of protected chloroethanol:

200 ml of 3,4-dihydro-2H-pyran (DHP) (2.20 moles) was cooled to 0 °C; to this 147 ml (2.19 moles) of chloroethanol was added, followed by addition of 3 drops of con. HCl. The reaction mixture was stirred for 15 minutes at 0 °C and then at room temperature for 3 hours. The product was distilled at 63 °C (± 2°C) under a vacuum of 1-2 torr (reported bp = 52 °C, 0.5 torr). Yield = 334 g, 93 % yield. FTIR showed no hydroxyl groups.



Step-1 Synthesis of hexa(ethylene glycol):

194.2 g (1.0 mole) of tetra(ethylene glycol), 657.4 g of THP protected chloroethanol (4.0 mole) and 19.9 g tetrabutylammonium hydrogen sulfate (58.6 m mole) were mixed at room temperature. To this 1506 ml of 50 % aqueous NaOH was added dropwise. The reaction mixture became semisolid; thus, 100 ml water was added to the reaction mixture to dissolve the semisolid. The reaction mixture was then heated to 60-70 °C and stirred vigorously for 5 days. The reaction mixture was cooled, and filtered to remove salt formed in the reaction; the salt was washed with dichloromethane. Dichloromethane was removed from the filtrate on a rotary evaporator and then it was distilled under vacuum to remove excess THP protected chloroethanol at 50-54 °C (0.5 torr); 180 ml of protected chloroethanol were removed by distillation. To the remaining liquid, 1.2 l methanol:dichloromethane (50:50) was added, followed by addition of 55 ml of con. HCl to deprotect hexa(ethylene glycol). The acid was neutralized by addition of sodium bicarbonate and filtered. The filtered solid was washed with dichloromethane. The solvent was evaporated on a rotary evaporator, upon which more

salt formed. The salts were filtered again, followed by washing with dichloromethane. After the complete removal of the solvent, crude hexa(ethylene glycol) was vacuum distilled under a vacuum of about 1-2 torr at 216-220 °C; reported bp = 217 °C /4 torr (Aldrich catalogue). 260.2 g of pure hexa(ethylene glycol) was obtained, yield = 92 %. NMR (CDCl₃): 3.77 (α-CH₂, m, 4H), 3.66 (CH₂, s, 16H), 3.60 (β-CH₂, t, 4H), 3.47 (-OH, t, 2H).

Synthesis and Purification of 30-Crown-10 and 60-c-20:

In a 5 l, 3-neck flask equipped with a mechanical stirrer 2.5 l of dry THF (freshly opened bottle) was placed under nitrogen and 44.01 g of 80 % NaH (1.53 moles) was carefully added and the suspension was stirred for 20 minutes. To this suspension, 84.7 g (0.3 moles) of hexa(ethylene glycol) was added dropwise over a period of 2-3 hours followed by addition of 155.0 g of tetra(ethylene glycol) ditosylate (slight excess, ca. 0.308 moles) in 300 ml THF over a period of 4-5 hours. After the addition was complete, the reaction mixture was stirred for 56 hours at room temperature. The reaction was terminated by very slow addition of 100 ml water to destroy excess NaH.

Three such reactions were done and the combined crude reaction product (about 400 g) was worked up together. A schematic of the work up procedure employed in the purification of crown ethers is shown in Scheme III-3. 261.4 g (65.3 % yield) of product (mainly the mixture of crown ethers) was obtained after the work up. The proton NMR spectrum of this product indicated that there are three compounds present, namely, 30-c-10 (¹H NMR δ = 3.67), 60-c-20 (¹H NMR δ = 3.64) and catenane in very small quantities (¹H NMR δ = 3.65). 30-c-10 was separated by dissolving it in 75:25 CCl₄:petroleum ether (5-8 % solution) and cooling it to -20 °C. 30-c-10 remains in the solution while mainly 60-c-20 separates as solid. 93 g of 30-c-10 fraction and 165 g of 60-c-20 fraction (mixed with catenane, 15-20 % 30-c-10 and other impurities) were isolated.

The 30-c-10 fraction was further purified by dissolving it in CH₂Cl₂:Hexanes (40:60) and cooling it to -20 °C. Beautiful crystals of 30-c-10 formed in the flask. The crystals were separated by decanting the mother liquor and immediately removing the traces of solvents under vacuum. Upon drying, the 30-c-10 crystals collapsed due to removal of the solvent and white powder was obtained (78.5 g). About 30 g more pure 30-c-10 was recovered from the 60-c-20 fraction.

The impure 60-c-20 fraction was purified by dissolving it in acetone and cooling it to -20 °C in the freezer. 60-c-20 forms a white solid gel with some acetone trapped in it, while other compounds remain in the solution which was filtered out using a filtering stick. More acetone was added to dissolve 60-c-20 and the cycle was repeated again. After 5 such cycles, the 60-c-20 was still not pure as indicated by proton NMR. Hence, it was dissolved in dichloromethane and filtered through a 10" long silica gel column. The dichloromethane was removed and very nice powdery 60-c-20 (90-95 g) was obtained after one crystallization from acetone.

Mother liquors from both the fractions were combined and upon evaporation of the solvents from the mother liquors an oily mixture (40-50 g) of several compounds including 30-c-10, 60-c-20 and catenane (as proton NMR analyses showed 5-6 peaks) was obtained. About 2.5 g of catenane (¹H NMR δ = 3.65) was separated from the oily mixture as it formed crystals upon sitting for several months. The rest of the oily mixture was not purified further.

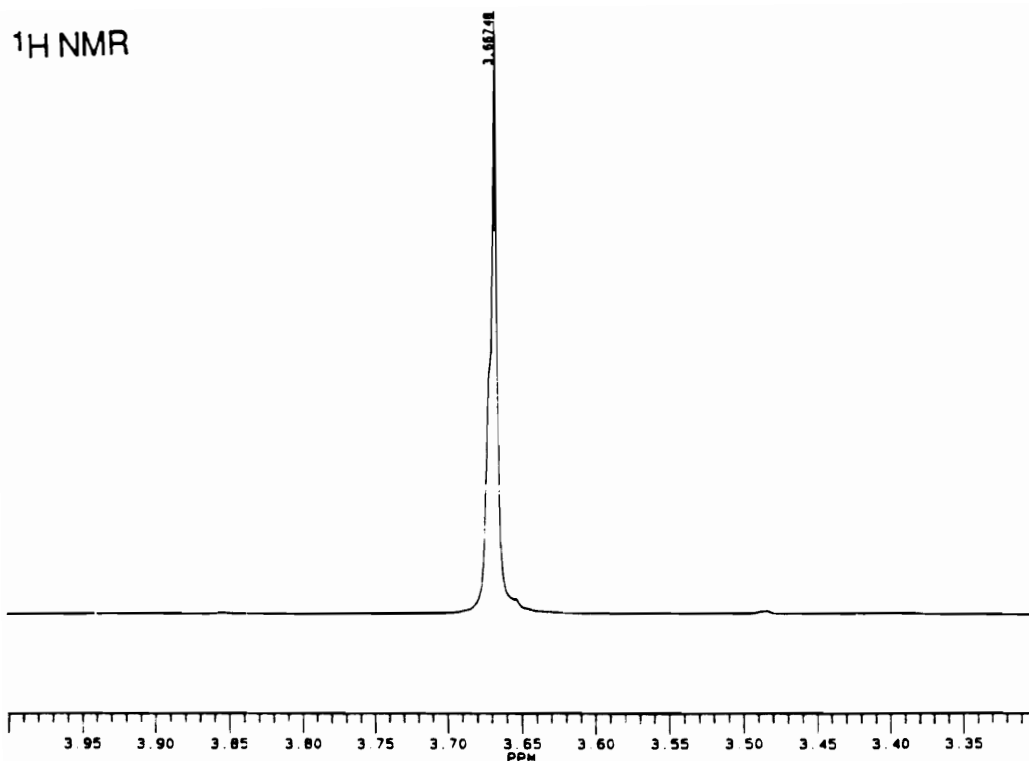
Overall yields of the isolated pure crown ethers are as follows: 30-c-10 (110 g) 28 % yield, 60-c-20 (95 g) 12 % yield. The third compound, the catenane, was isolated in about 1 % yield (2.5 g) (more of each compound was present in the oily mixture).

Synthesis and Purification of the Catenane of 30-c-10:

5.0 g hexa(ethylene glycol) (1.8×10^{-2} mole) and 35.0 g of 30-c-10 (8.0×10^{-2} mole, 4.5 equivalent) were mixed at 50-60 °C and stirred for 41 hours. To this viscous solution 40 ml dry THF was

added, and the reaction mixture was cooled to room temperature, followed by slow addition of 3.0 g of 80 % NaH (0.1 mole, 2.8 equivalent). After complete addition of sodium hydride, a gray colored sticky solid had separated from THF. Upon heating the reaction mixture to about 55 °C, the sticky solid began to dissolve very slowly in THF and it was stirred for 3 hours. To this then, a solution of 8.9 g tetra(ethylene glycol) ditosylate (1.8×10^{-2} mole) in 20 ml THF was added dropwise and addition was completed in 4-5 hours. The reaction mixture was stirred for 74 hours at 50-60 °C. The reaction mixture was cooled and 2 ml of water was added dropwise to destroy excess NaH. The reaction mixture was then extracted with dichloromethane (8 x 100 ml), followed by removal of the solvent on the rotary evaporator. The resulting crude product was extracted twice with hot hexanes (2 x 200 ml) to isolate 30.63 g of pure 30-c-10 (by proton NMR). The rest of the product was a mixture and showed three peaks in a proton NMR spectrum for 30-c-10 ($^1\text{H NMR } \delta = 3.67$), 60-c-20 ($^1\text{H NMR } \delta = 3.64$) and in small quantities catenane ($^1\text{H NMR } \delta = 3.65$). The remainder of the 30-c-10 and catenane (8.43 g) were separated from the mixture by 18 more extractions with hot hexanes. The unextractable portion (4.75 g) was mainly 60-c-20 mixed with linear high molecular weight glycols, as indicated by proton NMR. Catenane was not further separated from 30-c-10. Catenane obtained in the synthesis of 30-c-10 was used for the analyses. FTIR showed no hydroxyl groups.

^1H NMR



^{13}C NMR

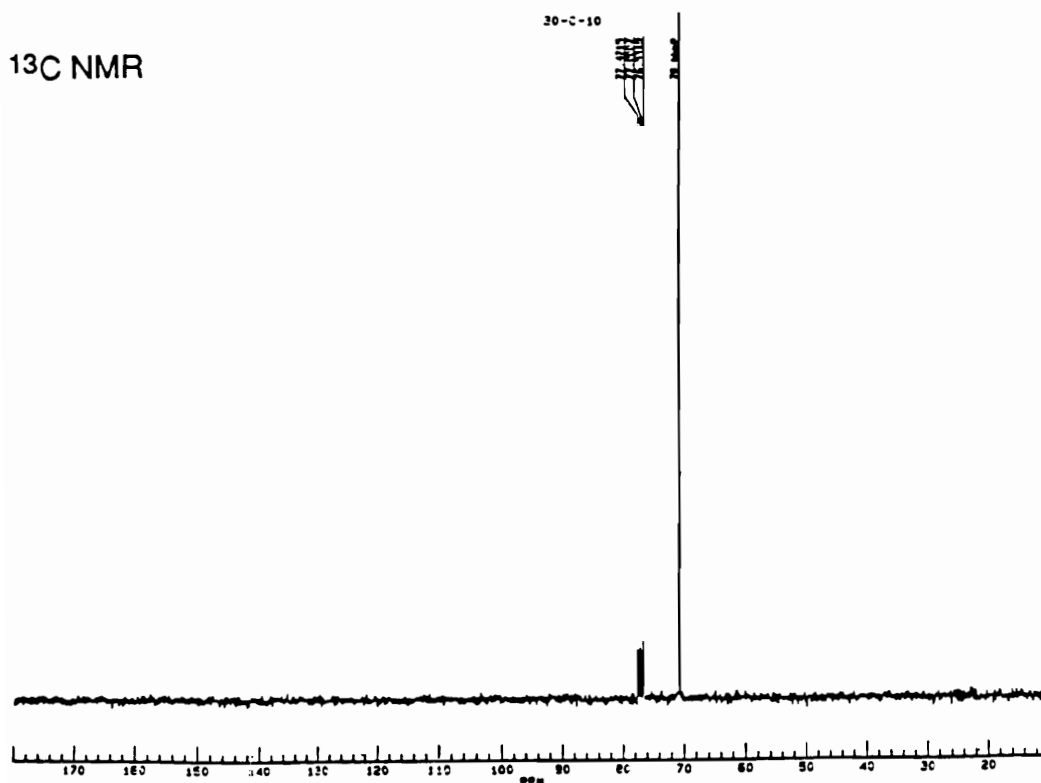


Figure III.1 ^1H (270 MHz) and ^{13}C NMR of 30-c-10

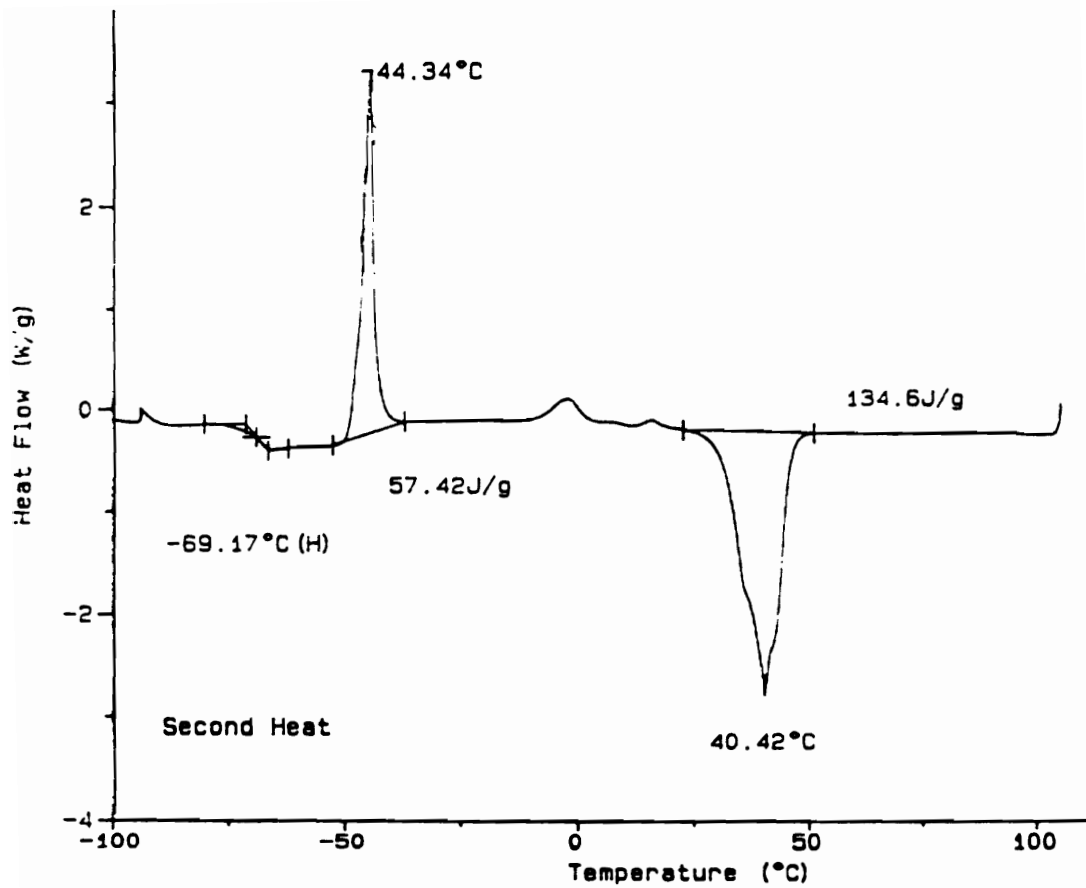


Figure III.2 DSC Trace of 30-c-10

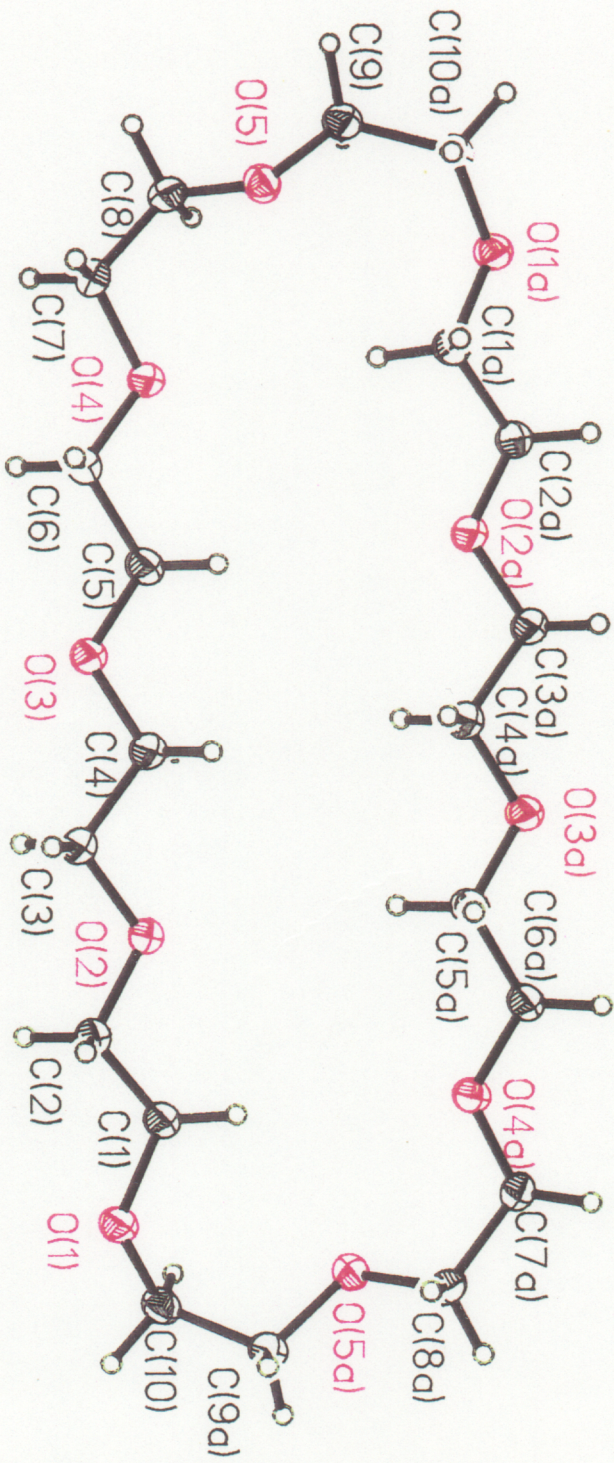


Figure III.3 X-Ray Crystal Structure of 30-c-10; Cavity Size: 3.9 °A x 13.6 °A,
 Unit Cell: Pbc_a (orthorhombic), a = 8.606 (1) °A, b = 8.260 (1) °A,
 c = 33.310 (4) °A

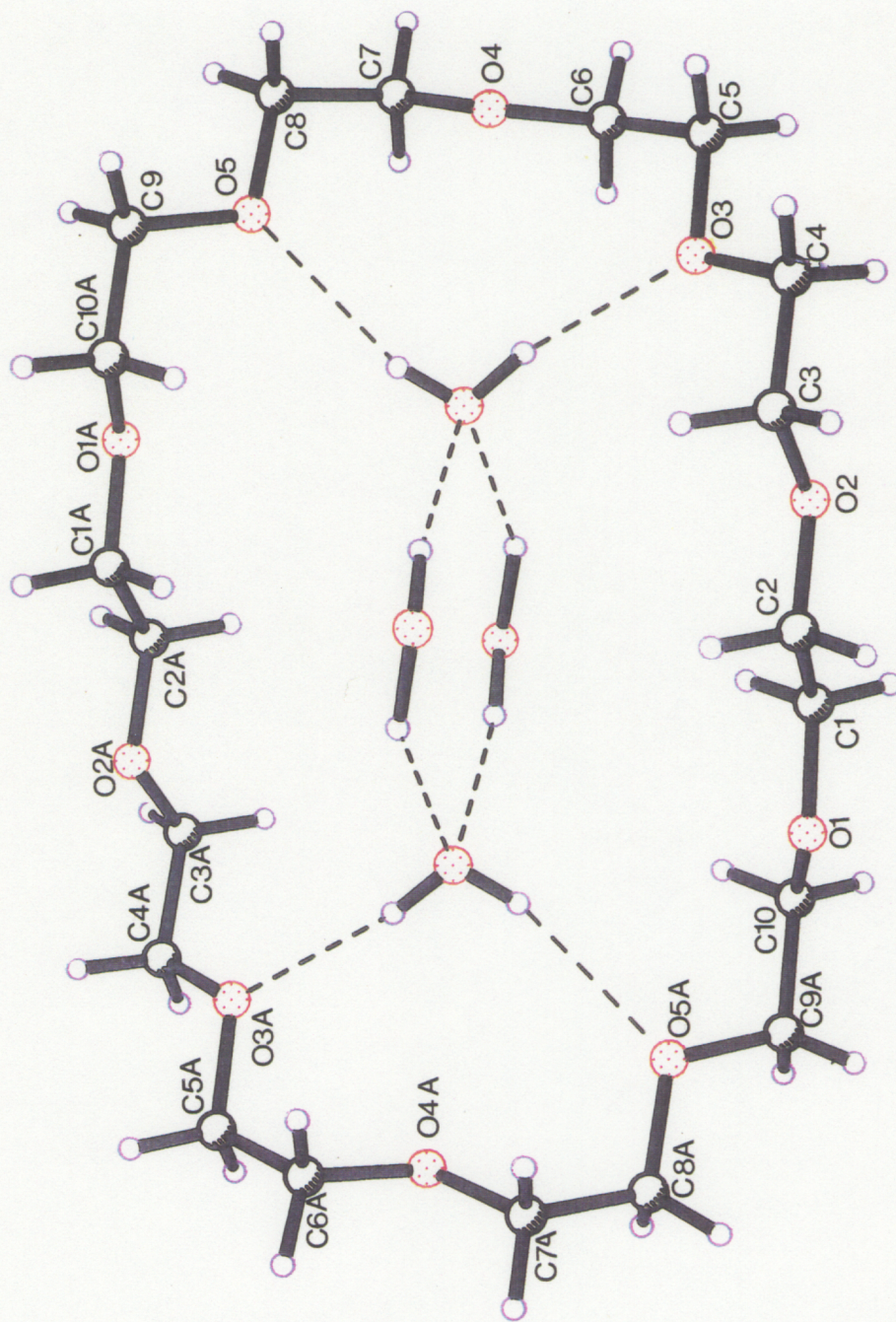
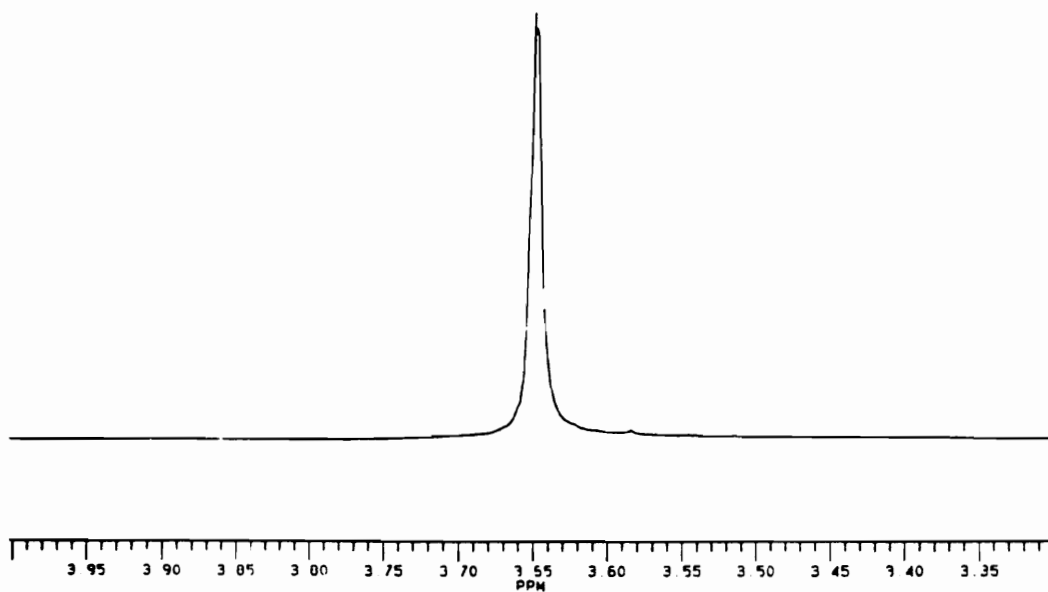


Figure III.4 X-Ray Crystal Structure of 30-c-10:4 H₂O; Cavity Size: 7.5 Å x 11.4 Å,
 Unit Cell: P21/c (monoclinic), a = 8.332 (4) Å, b = 9.083 (2) Å,
 c = 18.665 (5) Å, β = 90.24°

¹H NMR



¹³C NMR

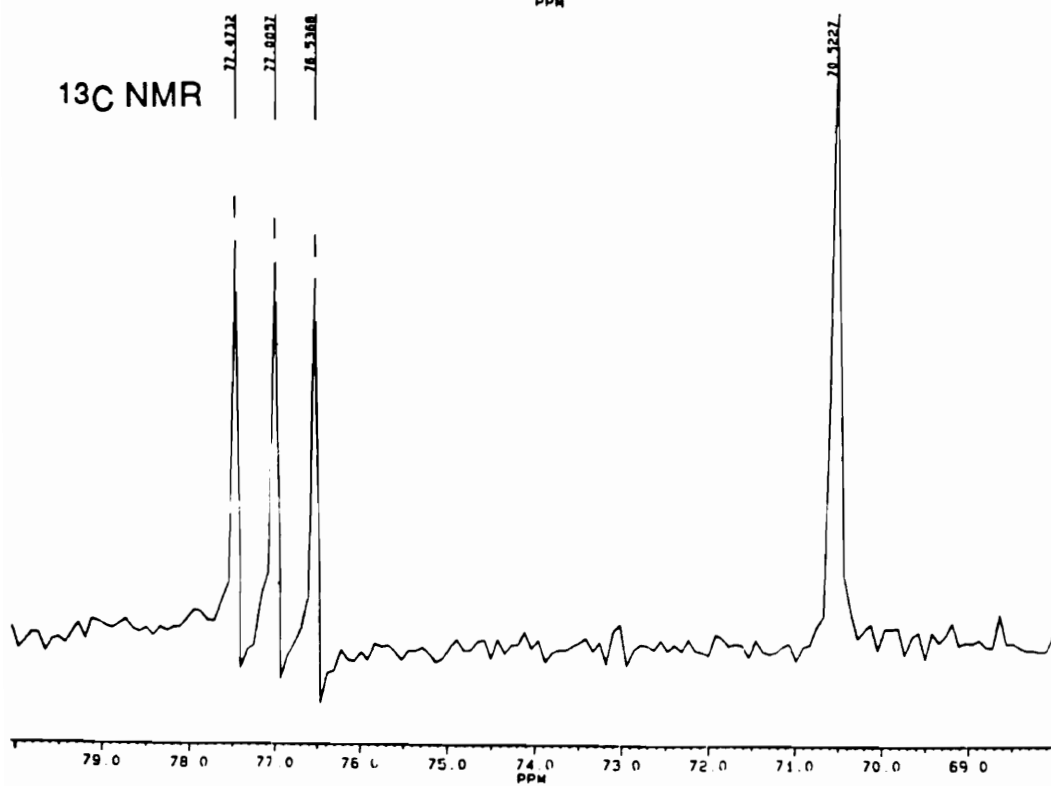


Figure III.5 ¹H (270 MHz) and ¹³C NMR of 60-c-20

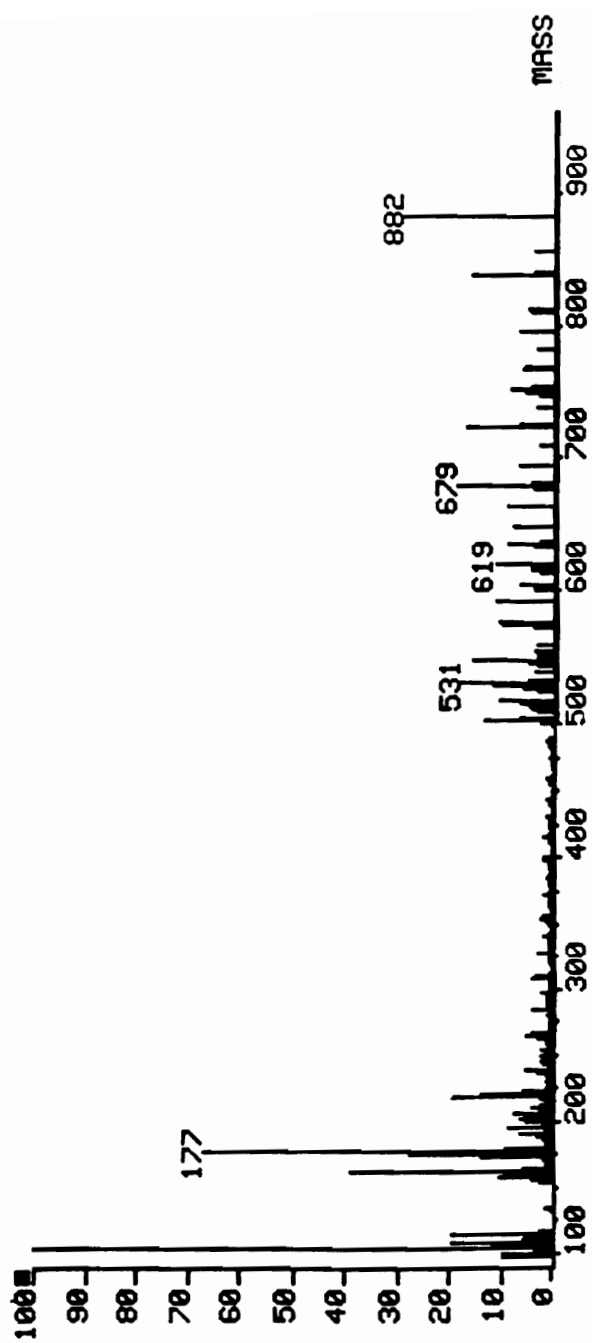


Figure III.6 CI Mass Spectrum of 60-c-20

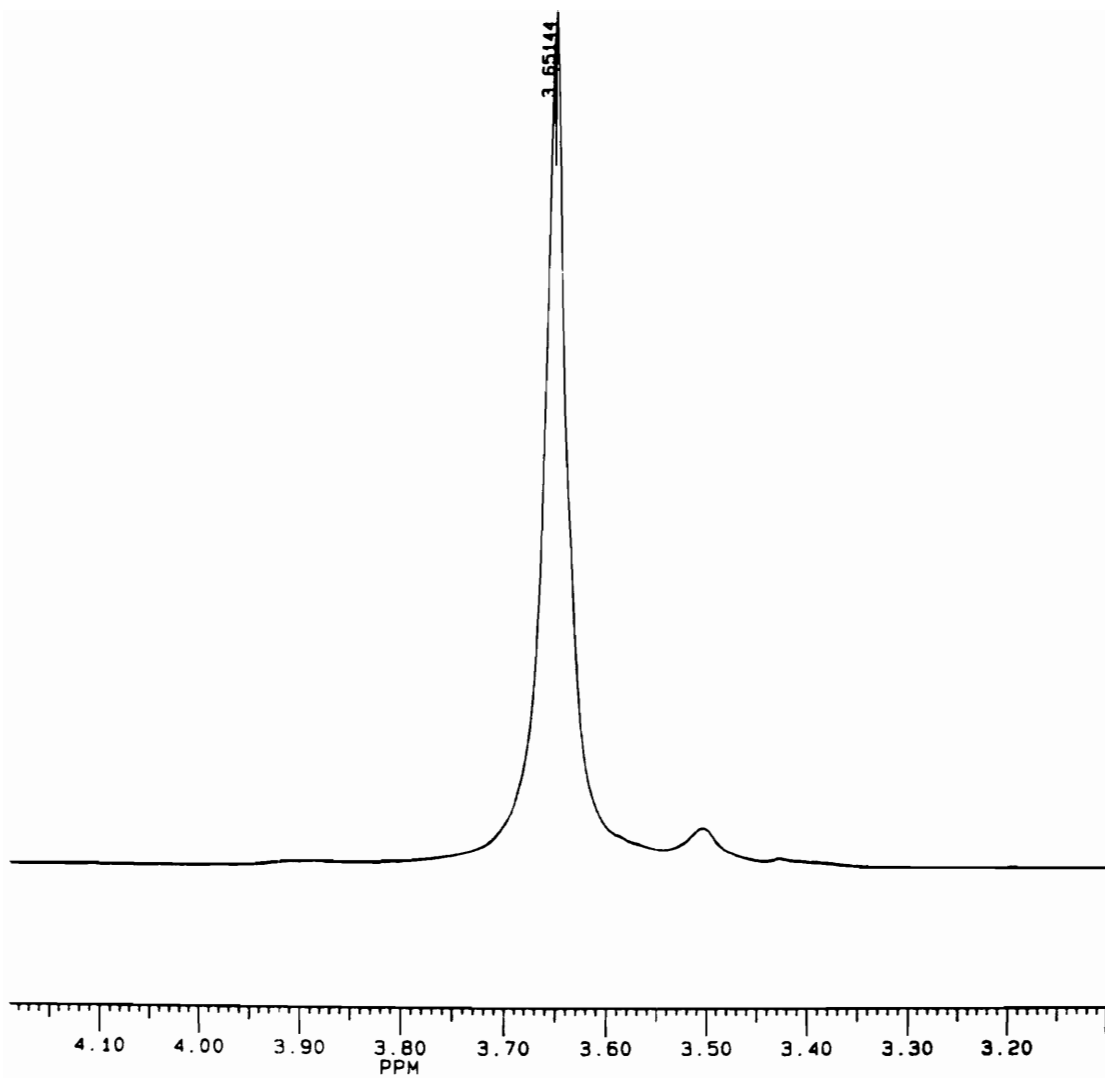


Figure III.7 ¹H (270 MHz) NMR of [2]catenane of 30-c-10

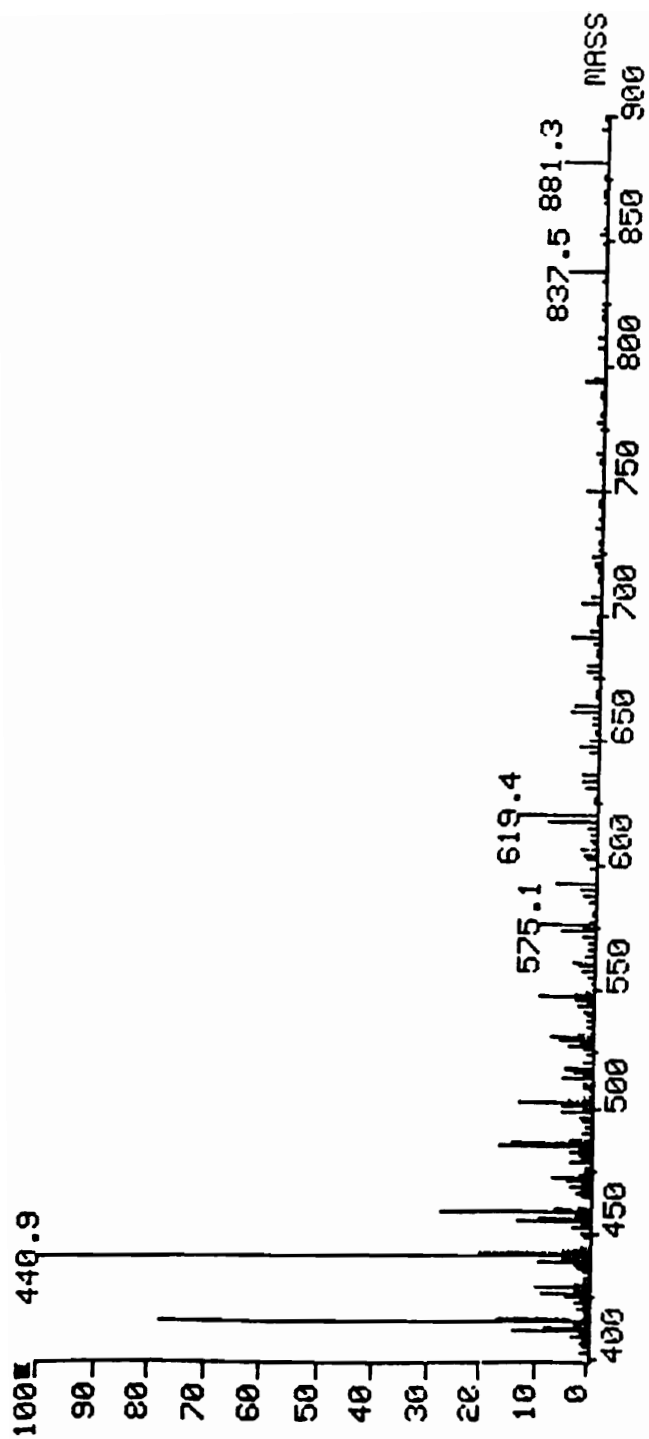


Figure III.8 CI Mass Spectrum of [2]catenane of 30-c-10

References

1. C. J. Pedersen, J. Amer. Chem. Soc., 1967, 89, 2495.
2. C. J. Pedersen, J. Amer. Chem. Soc., 1967, 89, 7017.
3. C. J. Pedersen, Org. Synth., 1972, 52, 66.
4. C. J. Pedersen, J. Am. Chem. Soc., 1970, 92, 391.
5. Crown Ethers and Analogues, S. Patai and Z. Rappoport, Eds., John Wiley & Sons, New York, NY, (1989).
6. Cation Binding by Macrocycles, Y. I. Inoue and G. W. Gokel, Eds., John Wiley & Sons, New York, NY, (1990).
7. D. M. Walba, R. M. Richards and R. Curtis Haltiwanger, J. Am. Chem. Soc., 1982, 104 , 3219.
8. R. Chenevert and L. D'Astous, J. Heterocyclic Chem., 1986, 23, 1785.
9. C. A. Vitali and B. Masci, Tetrahedron, 1989, 45, 2201.
10. B. L. Allwood, H. M. Colquhoun, S. M. Doughty, F. H. Kohnke, A. M. Z. Slawin, J. F. Stoddart, D. J. Williams and T. Zarzycki, J. Chem. Soc., Chem. Commun., 1987, 1054.
11. B. L. Allwood, N. Spencer, H. Shahriari-Zavareh, J. F. Stoddart and D. J. Williams, J. Chem. Soc., Chem. Commun., 1987, 1058.
12. B. L. Allwood, N. Spencer, H. Shahriari-Zavareh, J. F. Stoddart and D. J. Williams, J. Chem. Soc., Chem. Commun., 1987, 1061.
13. B. L. Allwood, N. Spencer, H. Shahriari-Zavareh, J. F. Stoddart and D. J. Williams, J. Chem. Soc., Chem. Commun., 1987, 1064.

14. P. R. Ashton, A. M. Z. Slawin, N. Spencer, J. F. Stoddart and D. J. Williams, *J. Chem. Soc., Chem. Commun.*, 1987, 1066.
15. A. M. Z. Slawin, N. Spencer, J. F. Stoddart and D. J. Williams, *J. Chem. soc., Chem. Commun.*, 1987, 1070.
16. J. F. Stoddart, *Pure & Appl. Chem.*, 1988, 60 (4), 467.
17. J. Y. Ortholand, A. M. Z. Slawin, N. Spencer, J. F. Stoddart and D. J. Williams, *Angew. Chem. Int. Ed. Engl.*, 1989, 28, 1294.
18. Y. X. Shen, Ph.D. Thesis, Virginia Tech, 1992.
19. D. N. Reinhoudt and R. T. Gray, *Tetrahedron Letters*, 1975, 25, 2105.
20. D. N. Reinhoudt and R. T. Gray, C. J. Smith and Ms. I. Venstra, *Tetrahedron*, 1976, 32, 1161.
21. C. O. Dietrich-Buchecker and J. P. Sauvage, *Tetrahedron Letters*, 1983, 24, 5091.
22. J. E. McMurry and C. Phelan, *Tetrahedron Letters*, 1991, 32, 5655.
23. C. D. Gutsche and A. E. Gutsche, *J. of Inclusion Phenomena*, 1985, 3, 447.
24. G. R. Newkome, A. Nayak, G. L. McClure, F. Danesh-Khoshboo and J. Broussard-Simpson, *J. Org. Chem.*, 1977 42(9), 1500.
25. G. R. Newkome, G. L. McClure, J. Broussard-Simpson and F. Danesh-Khoshboo, *J. Am. Chem. Soc.*, 1975, 97 (11), 3232.
26. G. R. Newkome and A. Nayak, *J. Org. Chem.*, 1978 43 (3), 409.

27. M. D. Thompson, J. S. Bradshaw, S. F. Nielsen, C. T. Bishop, F. T. Cox, P. E. Fore, G. E. Maas, R. M. Izatt and J. J. Christensen, *Tetrahedron*, 1977, 33, 3317.
28. S. B. Ferguson, E. M. Seward, F. Diederich, E. M. Sanford, A. Chou, P. Inocencio-Sweda and C. B. Knobler, *J. Org. Chem.*, 1988, 53, 5595.
29. F. Diederich, K. Dick and D. Griebel, *Chem. Ber.*, 1985, 118, 3588.
30. R. Dharanipragada, S. B. Ferguson and F. Diederich, *J. Am. Chem. Soc.*, 1988, 110, 1679.
31. H. Kataoka and T. Katagi, *Tetrahedron*, 1987, 43 (20), 4519.
32. C. A. Hunter, M. Nafees Meah and J. K. M. Sanders, *J. Chem. Soc., Chem. Commun.*, 1988, 694.
33. C. A. Hunter, M. Nafees Meah and J. K. M. Sanders, *J. Chem. Soc., Chem. Commun.*, 1988, 692.
34. R. A. Bartsch, C. V. Cason and B. P. Czech, *J. Org. Chem.* 1989, 54, 857.
35. P. J. Dutton, F. R. Fronczek, T. M. Fyles and R. D. Gandour *J. Am. Chem. Soc.*, 1990, 112, 8984.
36. The Chemistry of Functional Groups: Supplement E: The Chemistry of ethers, crown ethers, hydroxyl groups and their Sulfer Analogues, Part-I, Saul Patai, Ed; John Wiley & Sons, New York, NY, (1980), Page 312.
37. B. Vollmert, J. X. Huang, *Makromol. Chem., Rapid Commun.*, 1981, 2, 467.
38. C. O. Dietrich-Buchecker, J. P. Sauvage, J. P. Kintzinger, *Tetrahedron Letters*, 1983, 24 (46), 5095.

39. C. O. Dietrich-Buchecker and J. P. Sauvage, *J. Am. Chem. Soc.*, 1984, 100 (10), 3043.
40. M. Cesario, C. O. Dietrich-Buchecker, J. Guilhem, C. Pascard and J. P. Sauvage, *J. Chem. Soc., Chem. Commun.*, 1985, 244.
41. J. P. Sauvage and J. Weiss, *J. Am. Chem. Soc.*, 1985, 107, 6108.
42. A. M. Albrecht-Gary, Z. Saad, C. Dietrich-Buchecker and J. P. Sauvage, *J. Am. Chem. Soc.*, 1985, 107, 3205.
43. M. Cesario, C. O. Dietrich-Buchecker, A. Edel, J. Guilhem, J. P. Kintzinger, C. Pascard and J. P. Sauvage, *J. Am. Chem. Soc.*, 1986, 108, 6250.
44. D. K. Mitchell and J. P. Sauvage, *Angew. Chem., Int. Ed. Engl.*, 1988, 27 (7), 930.
45. A. M. Albrecht-Gary, C. Dietrich-Buchecker, Z. Saad and J. P. Sauvage, *J. Am. Chem. Soc.*, 1988, 110, 1467.
46. E. Wasserman, *J. Am. Chem. Soc.*, 1960, 82, 4433.
47. G. Agam and A. Zilkha, *J. Am. Chem. Soc.*, 1976, 98, 5214.
48. T. J. Fyvie, H. L. Frisch, J. A. Semlyen, S. J. Clarson and J. E. Mark, *J. Polym. Sci.: Polym. Chem.*, 1987, 25, 2503.
49. C. O. Dietrich-Buchecker and J.-P. Sauvage, *Chem. Rev.*, 1987, 87, 795.

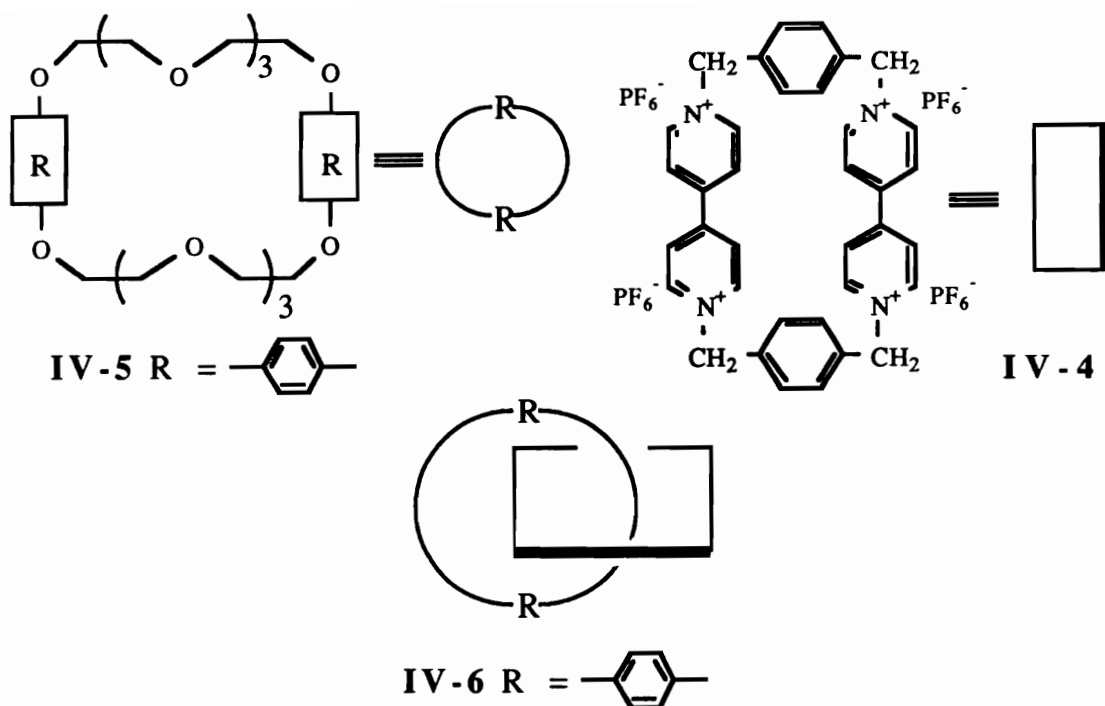
IV.	IONIC BIPYRIDYL MACROCYCLES	79
IV.1	Introduction	80
IV.2	Results and Discussion	81
IV.3	Experimental	87

IV.1 Introduction

To recap, the synthesis of polyrotaxanes can be achieved either by statistical threading or template threading methods. In the statistical threading method (entropically driven) monomers with functional groups are pre-mixed with large macrocycles followed by polymerization of the monomers (1-5). The threading of the cyclic species by the linear species is governed by statistical factors. In a template method (enthalpically driven), there exists a variety of potential attractive interactions (ΔH is negative) between the macrocycle and the monomeric units, resulting in formation of monomeric rotaxanes which can subsequently be polymerized to obtain polyrotaxanes (3,6-8).

In chapter I, a detailed review of syntheses of rotaxanes and catenanes using tetracationic macrocycle **IV-4**, is given. Stoddart and coworkers have reported the synthesis of a 4,4'-bipyridinium macrocycle **IV-4**, called BP-28-N⁺⁴, in 12% pure yield by reaction of salt **IV-3**, derived from 4,4'-bipyridine and α,α' -dibromo-p-xylene **IV-2** (9). They demonstrated that this tetracationic macrocycle forms stable, isolable 1:1 charge complexes with electron donors such as dihydroxybenzene derivatives (9); single crystal X-ray analyses showed that the donor molecules reside within the rather narrow cavity of the very rigid (preorganized) acceptor macrocycle (10). As reported in chapter I, these charge transfer interactions were utilized to synthesize the [2]catenane **IV-6** in 70 % yield, capitalizing on the highly efficient, complexation induced threading of the linear dicationic macrocycle precursor **1** (and/or the tricationic intermediate derived from **IV-2** & **IV-3**) through the cavity of the preformed bis(p-phenylene)-34-crown-10 **IV-5** (11). Further, recently Stoddart and coworkers have reported self assembling of even more elaborate rotaxanes and catenanes (12-14) as reported in chapter I.

In this chapter, synthesis and characterization of macrocycles derived from 4,4'-bipyridyl units is described.

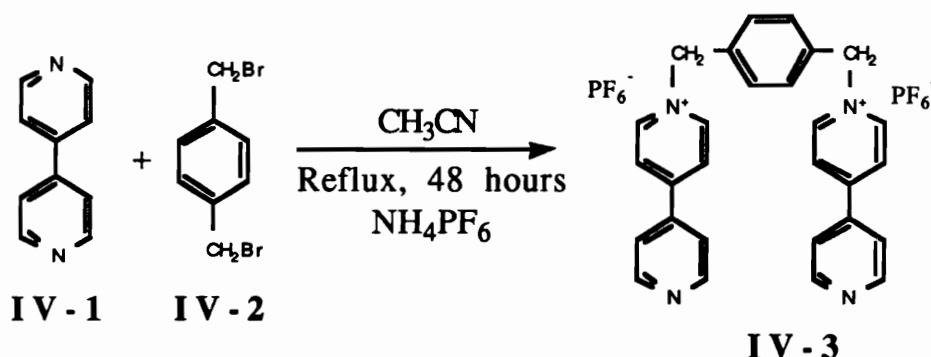


IV.2 Results and Discussions

Thus, the bipyridyl macrocycle BP-28-N⁴⁺ offers an important alternative in the synthesis of polyrotaxanes as an efficiently threadable macrocyclic component. The bipyridyl macrocycle is a very good π -electron acceptor and the charge transfer interactions provide especially favorable enthalpic encouragement for penetration of the macrocycle by monomeric precursors, i.e., α,ω -difunctional linear species containing hydroquinone or other suitable donor moieties. Thus, the high threading equilibrium constant of the macrocycle and difunctional monomeric hydroquinone derivatives lead to monorotaxanes in a highly efficient way which in turn could be utilized to prepare polyrotaxanes. Hence our efforts on the bipyridyl macrocycle synthesis were directed toward such ends.

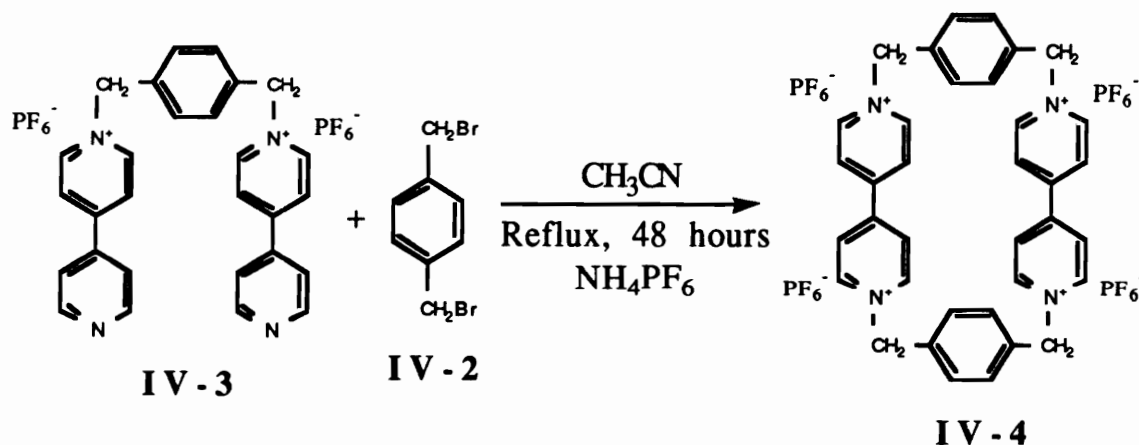
Synthesis of **IV-3** was accomplished in 80 % yield by reaction of 3.3 equivalent of **IV-1** and 1 equivalent of **IV-2**, followed by changing the anion to hexafluorophosphate using the reported procedure (9). Scheme IV-1 shows the synthesis of **IV-3**.

Scheme IV-1 Synthesis of IV-3



The synthesis of IV-4 was duplicated using the reported procedure (9) and the product was isolated in about 10 % yield. Scheme IV-2 shows the synthesis of bipyridyl macrocycle IV-4.

Scheme IV-2 Synthesis of IV-4



It was expected that, as in syntheses of crown ethers and [2]-catenane IV-6, use of the template species to preorganize the reacting species into the conformations favorably disposed for efficient cyclization should lead to higher yields of the macrocycle. To improve the yield of macrocycle IV-4, p-dimethoxybenzene was used as a template to preorganize dicationic salt IV-3 and/or

the intermediate trication derived from its initial reaction with **IV-2**.

In the initial experiment *p*-dimethoxybenzene was employed as the template in a molar ratio of 2.6 relative to dication **IV-3**, whose concentration was 1.1×10^{-2} M (in acetonitrile). However, the yield of **IV-4** was about 10 % (by NMR) and no significant improvement over the earlier procedure of Stoddart and coworkers (9) was observed.

Thus, a 33:1 molar ratio of *p*-dimethoxybenzene to dication **IV-3** was employed, whose concentration was 1.59×10^{-2} M (in acetonitrile). Assuming an association complex equilibrium constant for the threading equal to that reported for *p*-dimethoxybenzene with **IV-4** ($K_a = 17$, acetonitrile, 25 °C (9)), essentially all of **IV-3** would be complexed under these conditions. Slow addition of 1 equivalent of **IV-2** followed by the work up of the reaction product yielded macrocycle **IV-4** in 13 % yield.

In the synthesis of **IV-4** without the template, another compound was isolated in about 24 % yield and this product had similar proton and carbon NMR spectra, except that the peaks for the product were shifted to downfield by about 0.1-0.2 ppm in proton NMR and 0.1-1.0 ppm in carbon NMR spectra. Analogous to these results, synthesis of **IV-4** with 2.6 eq. of the template also yielded the same compound in about 26 % yield. Further, the worked up product of the synthesis of **IV-4** using 33 eq. of the template also contained the same compound in 42 % yield.

Based on the results obtained from crown ethers, it is expected that twice the size macrocycle i.e., BP-56-N⁸⁺, **IV-7**, may be forming. It is suggested that the isolated compound may be **IV-7** having proton and carbon NMR spectra similar to that of **IV-4**. Figure IV-1 shows the proton NMR spectra of **IV-4** and **IV-7**. Although, as shown in Figure IV-1, the proton NMR spectrum of **IV-7** is similar in pattern to that of the smaller and much more rigid macrocycle **IV-4**, all signals of **IV-7** are shifted downfield. Table IV-1 lists the proton NMR chemical shifts observed for the

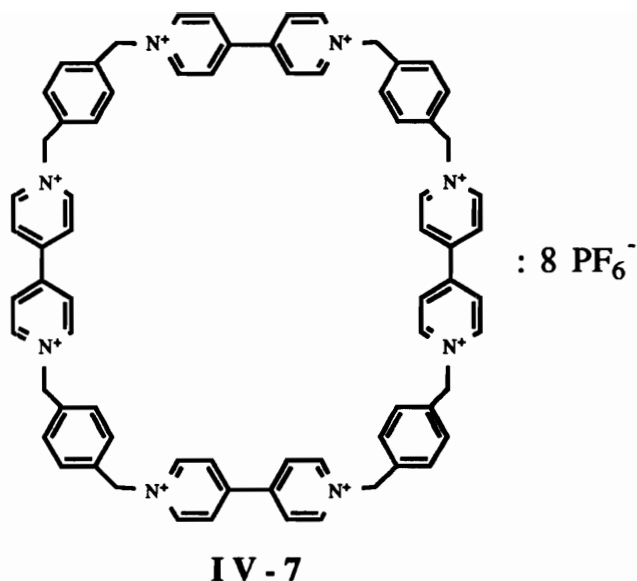
macrocycles **IV-4** and **IV-7** in $\text{CD}_3\text{COCD}_3/\text{D}_2\text{O}$ and CD_3CN along with the reported values (9) for **IV-4** in CD_3CN . Table **IV-2** lists the carbon NMR chemical shifts observed for the macrocycles **IV-4** and **IV-7** in CD_3CN along with the reported values (9) for **IV-4** in CD_3CN .

Table IV-1 400 MHz Proton NMR Chemical Shifts for IV-4 and IV-7

	<u>BP-28-N⁺⁴, IV-4</u>			<u>BP-56-N⁺⁸, IV-7</u>	
	<u>Acetone-d₆/D₂O</u>	<u>CD₃CN</u>	<u>Lit. (9)</u>	<u>Acetone-d₆/D₂O</u>	<u>CD₃CN</u>
-CH ₂ -	6.01 (s)	5.75	5.74	6.17	5.85
-Φ-	7.74 (s)	7.54	7.52	7.78	7.60
4,4'-bipyridyl	8.48 (d)	8.17	8.16	8.74	8.39
(adjacent to N)	8.50	8.18	---	8.77	8.40
4,4'-bipyridyl	9.28 (d)	8.62	8.86	9.42	8.95
(away from N)	9.30	8.88	---	9.45	8.97

Table IV-2 Carbon NMR Chemical Shifts for IV-4 and IV-7

	<u>BP-28-N⁺⁴, IV-4</u>		<u>BP-56-N⁺⁸, IV-7</u>
	<u>CD₃CN</u>	<u>Lit. (9)</u>	<u>CD₃CN</u>
-CH ₂ -	65.75	65.7	65.06
-Φ-	128.37	128.3	128.65
Tertiary (-Φ-)	137.04	137.0	135.35
4,4'-bipyridyl	146.29	146.2	146.75
(adjacent to N)			
4,4'-bipyridyl	131.43	131.4	131.40
(away from N)			
Tertiary (bipyridyl)	150.47	150.4	151.55



The overall yields of the two components (**IV-6** and **IV-7**) were significantly increased (by ca. 30 %) by the use of large excess of the template; however, no significant improvement in the yield of macrocycle **IV-4** was achieved. If indeed the other compound is a macrocycle of twice the size i.e., BP-56-N⁺⁸, **IV-7**, this would be a significant improvement in the synthesis of bipyridyl macrocycle, especially in view of the high cost of 4,4'-bipyridine and the low cost of p-dimethoxybenzene. The template-free product mixture was separated by fractional precipitation from 7:3 acetone:water by the addition of water; **IV-4** is more soluble and preferentially remains in solution, while **IV-7** precipitates. **IV-6** and **IV-7** were finally purified by recrystallization from acetone.

Figure **IV-2** show the FAB mass spectra of the macrocycles **IV-4** and **IV-7**. The lower molecular weight end of the mass spectra (ca., up to $m/z = 350$) of both the macrocycles are almost identical; however, towards the higher mass the spectra are different. The parent ion peaks, if present, are of too low an intensity in both the spectra to be able to unambiguously confirm the structure of the macrocycles; however, the structure of **IV-4** is known from the X-ray crystal structure analyses done by Stoddart and coworkers as well as by the author. The mass spectrum of **IV-7**

at high m/z is complex and peaks are of very low intensity; this may be due due to very high molecular weight of the macrocycle (ca., 2200.2) as well as the ion cluster nature of the macrocycle and resulting fragment ions. Thus, the structure of the large macrocycle has not been confirmed and efforts to make suitable crystals of BP-56-N⁺⁸ for X-ray crystal structure analyses are underway.

In solution, **IV-7** forms charge transfer complexes with hydroquinone and its derivatives, as evident by the instantaneous production of deep visible colors, analogous to the behavior of **IV-4**. Mixing solutions of the larger macrocycle **IV-7** and bisphenol-A does not produce a deep visible color, indicating the absence of charge transfer complex formation; however, mixing solutions of the smaller macrocycle **IV-4** and bisphenol-A produces a deep orange color, evidence of a charge transfer complex. This formation of a charge-transfer complex with the smaller macrocycle and absence of such interactions in the larger macrocycle is surprising, since CPK models studies showed that bisphenol-A with its two methyl groups and an isopropylidene kink is difficult to fit into the cavity of macrocycle **IV-4** to form a threaded complex; further, the kink in the molecule also makes it difficult to form an external complex with the dicationic bipyridyl units. Macrocycle **IV-7**, being much larger and more flexible, should avoid these problems and should form either an external and/or a threaded complex, but it was found not to be the case.

Cyclic voltamograms of the macrocycles exhibited similar characteristics (15). Cyclic voltametry of **IV-4** is characterized by a reversible two electron wave at -0.726 V (vs Ag/0.1 M Ag⁺) [(BP-28-N₄)⁺⁴/(BP-28-N₄)⁺²] and a second reversible two electron wave at -1.157 V [(BP-28-N₄)⁺²/(BP-28-N₄)⁰]. The respective numbers for **IV-7** are -0.717 V and -1.175 V.

To conclude, in the synthesis of BP-28-N⁺⁴ (**IV-4**), the template effect with p-dimethoxybenzene was found to be ineffective. Secondly, formation of a new macrocycle, BP-56-N⁺⁸ (**IV-7**), is indicated and the yield of the larger macrocycle was

increased by the template effect (by about 30 %). Both these macrocycles, BP-28-N⁺⁴ and the new dimer macrocycle BP-56-N⁺⁸, were characterized by NMR, cyclic voltametry and mass spectroscopy and can be utilized in directed syntheses of the rotaxanes and polyrotaxanes.

IV.4 Experimental

Measurements:

Melting Points were taken in capillary tubes with a Haake-Buchler melting point apparatus and have been corrected. Proton and carbon NMR spectra were obtained on a Varian Unity 400 MHz spectrometer using deuterated acetone/water or acetonitrile solutions with tetramethylsilane as an internal standard. Cyclic voltametry of the macrocycles were done using a glassy carbon or gold working electrode and (Ag/0.1 M Ag⁺) reference electrode in 0.5-1.0 mM solutions in DMF with 0.2 M Bu₄NBF₄ supporting electrolyte at 25 °C. Elemental analyses were performed by Atlantic Microlab of Norcross, GA. FAB mass spectral determinations were made at the Midwest Center for Mass Spectrometry with partial support by the National Science Foundation, Biology Division (Grant No. DIR9017262).

Synthesis of IV-3:

50.0 g (0.32 moles) of 4,4'-bipyridyl was dissolved in 600 ml acetonitrile:benzene (4:2, v:v) at room temperature. The solution was refluxed and then 25.0 g (0.1 moles) of α,α' -dibromo-p-xylene dissolved in 180 ml benzene (the solution had to be kept warm with a heat gun to prevent precipitation) was added over 3 hours. The solution was refluxed overnight. The reaction mixture was then cooled, filtered and the precipitate was washed with dichloromethane (100 x 3) to remove unreacted 4,4'-bipyridyl and α,α' -dibromo-p-xylene. The counter anion was changed from bromide to hexafluorophosphate by dissolving the above product in 2.5 ltr

water and filtering to remove insoluble impurities, followed by addition of 30.5 g (2.1 eq.) of NH_4PF_6 dissolved in 250 ml of water. After filtration and drying, 50.0 g (80 % yield) of **IV-3** was obtained, mp = 147 °C decomposed (corrected), reported (16) mp = 145 °C decomposed. Proton NMR (acetone- d_6): δ = 6.16 (s, 4H), 7.81 (s, 4H), 7.94-7.99 (m, 4H), 8.64-8.69 (m, 4H), 8.83-8.89 (m, 4H), 9.31-9.37 (m, 4H).

Synthesis of bipyridyl macrocycles IV-4 and IV-7:

The synthesis of **IV-4** and **IV-7** was done with and without p-dimethoxybenzene as template. The following is the representative procedure using the template. 2.0 g (2.8×10^{-3} mole) of **IV-3** were dissolved in 250 ml acetonitrile (yellow green color) and to this solution 1.0 g (2.6 eq.) of p-dimethoxybenzene was added. The color began to change slowly and after about 10-12 hours the color was slightly orange-yellow. The solution was then heated to reflux and 0.75 g (2.8×10^{-3} mole) of α,α' -dibromo-p-xylene (**IV-2**) was added in three installments over a period of 24 hours and the reaction was continued for 24 hours more. The reaction mixture was cooled and the red precipitate (yellow precipitate in the reaction without a template) was filtered and washed with acetonitrile and air dried (0.95 g). The precipitate was dissolved in hot 70:30 methanol:water mixture and the solution was cooled and filtered. To this 0.6 g of NH_4PF_6 was added. A white precipitate formed, which was stirred for 15 minutes, allowed to stand overnight, filtered, washed with water (4 x 100 ml) and dried under vacuum. The template p-dimethoxybenzene either remained in the methanol:water mixture or was removed under vacuum due to its high volatility, as confirmed by proton NMR.

Total cyclic yield with the template: 1.0 g, 36.4 %,

Total cyclic yield without the template: 0.93 g, 33.8 %

Reported yield of **IV-4** after column purification: 12 %.(9)

Melting Point: degrades above 275 °C; reported (9): same

Both the above products have about 24-26 weight % of the larger macrocycle **IV-7** (BP-56-N⁺⁸); all the corresponding ¹H NMR peaks of **IV-7** are shifted a bit downfield, ca. 0.1-0.2 ppm.

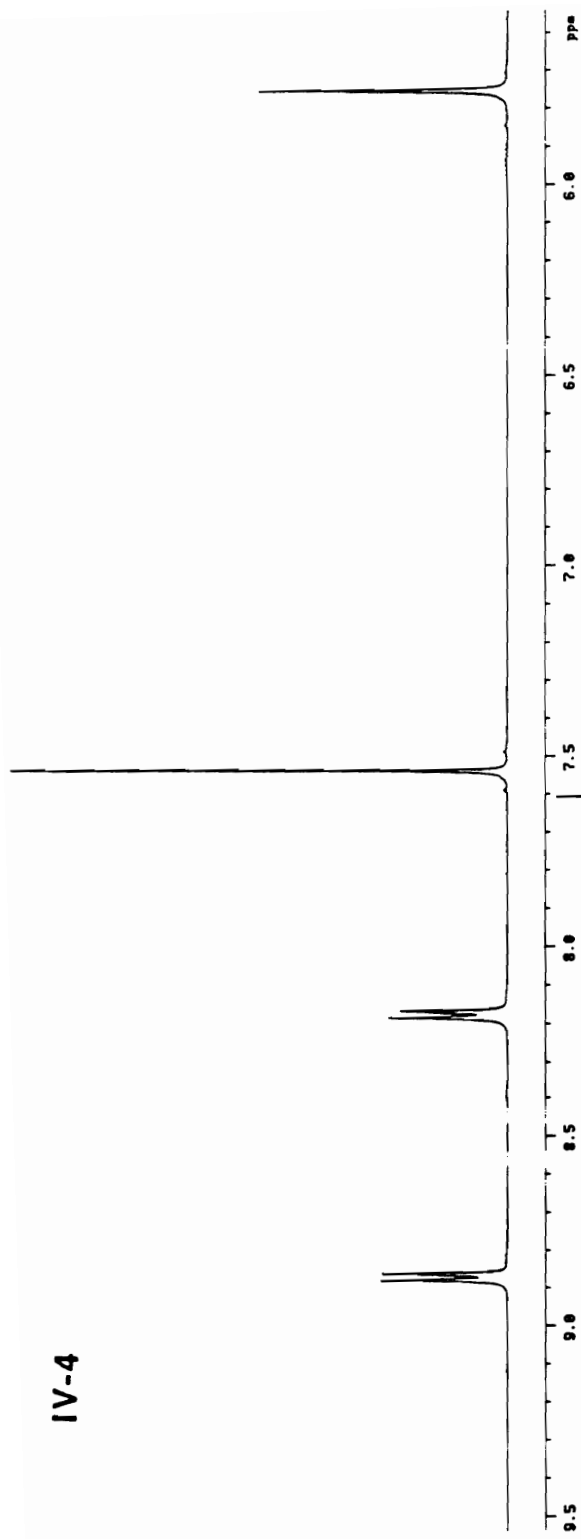
Synthesis of IV-4 and IV-7 Using 33 eq. of The Template:

19.0 g (2.7×10^{-2} mole) of **IV-3** and 123.5 g (0.9 moles, 33 eq.) of p-dimethoxybenzene were dissolved in 100 ml acetonitrile and stirred for 1 hour. The dark red solution was then diluted to 1.7 l with acetonitrile. 7.4 g (2.8×10^{-2} mole) of α,α' -dibromo-p-xylene (**IV-2**) was added in 7 parts at 4-7 hour intervals. The rest of the procedure including the work up was as above.

The p-dimethoxybenzene was removed from the crude mixture by Soxhlet extraction with benzene for 7 days. The uncomplexed bipyridyl macrocycles are light yellow-cream color and degrade at about 275 °C. A total of 16.3 g (55.2 % yield) of template free bipyridyl macrocycles was obtained. The macrocycles were separated by fractionation by dissolution in acetone:water (70:30) and addition of small volumes of water. A fraction rich in BP-56-N⁺⁸ precipitated out. The BP-28-N⁺⁴ is slightly more soluble in water and was the last to precipitate. Each fraction was further purified by crystallization from acetone.

Overall yields were BP-56-N⁺⁸ (**IV-7**) 12.5 g, (42.2 %), m.p.: decomposed above 275 °C and BP-28-N⁺⁴ (**IV-4**) 3.8 g, 13.0 %, m.p.: decomposed above 275 °C (Reported (9): same). ¹H NMR (acetone-d₆/D₂O) BP-56-N⁺⁸: $\delta = 6.17$ (s), 7.78 (s), 8.74 & 8.77 (d), 9.42 & 9.45 (d) with all signals having equal intensities (16 H). BP-28-N⁺⁴: $\delta = 6.01$ (s), 7.74 (s), 8.48 & 8.50 (d), 9.28 & 9.30 (d) with all signals having equal intensities (8 H). Elemental analyses of BP-28-N⁺⁴: C₃₆H₃₂N₄P₄F₂₄: theory: C 39.27, H 2.93, N 5.09; found: C 39.39, H 2.96, N 5.02.

IV-4



IV-7

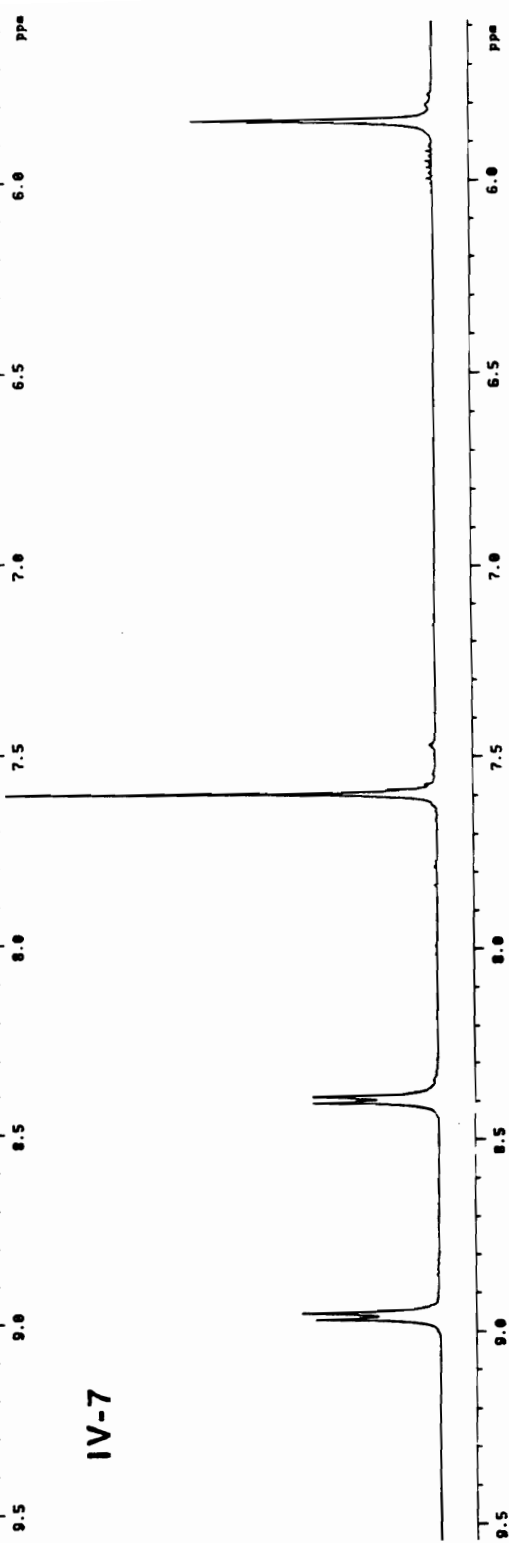


Figure IV.1 ¹H (400 MHz) NMR of IV-4 and IV-7

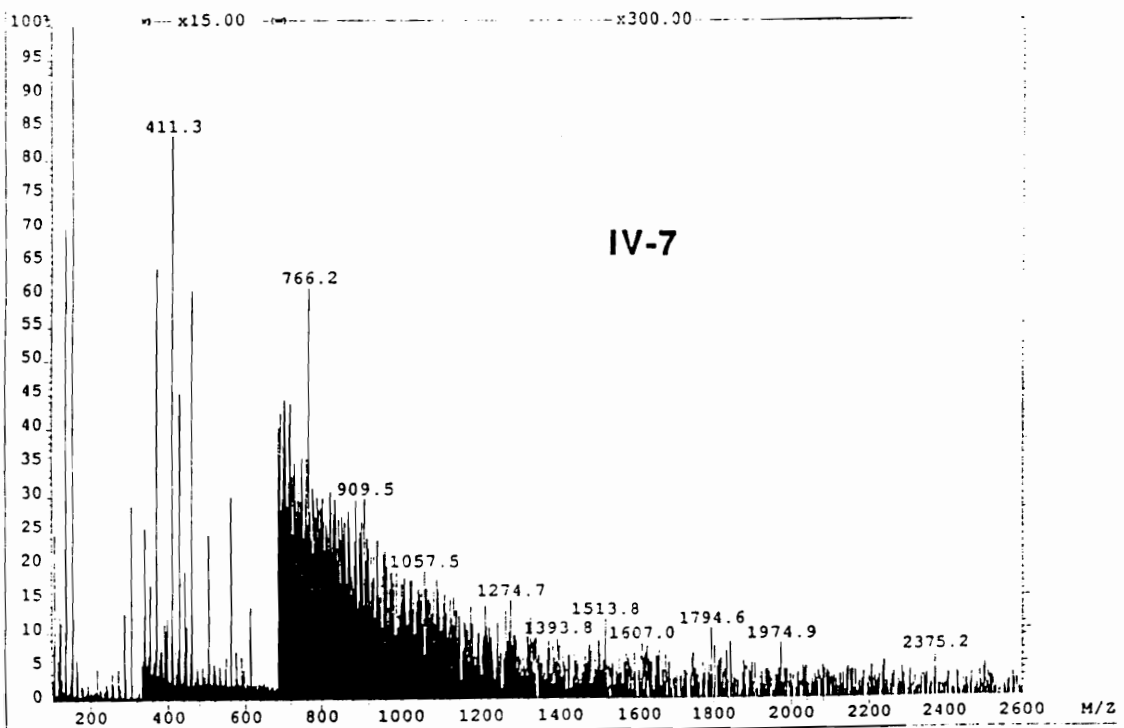
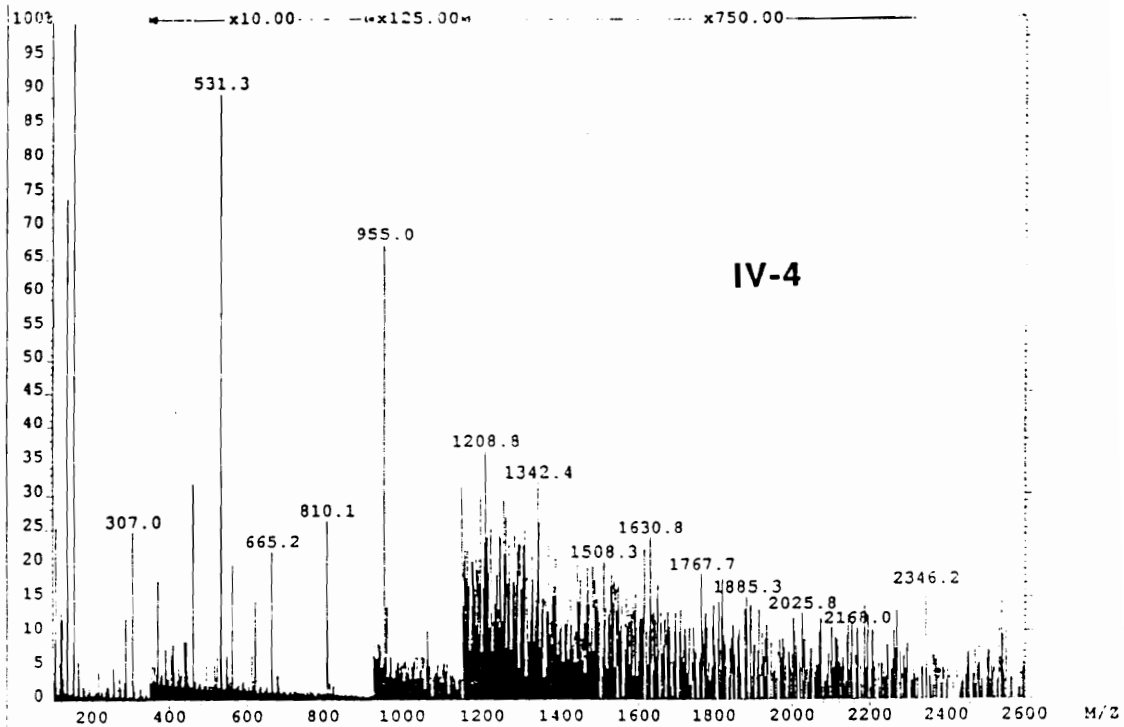


Figure IV.2 FAB Mass Spectra of IV-4 and IV-7

References

1. H. W. Gibson, P. Engen and P. Lecavalier, Am. Chem. Soc., Polymer Preprints, 1988, 29(1),154.
2. P. R. Lecavalier, P. T. Engen, Y. X. Chen, S. Joardar, T. C. Ward and H. W. Gibson, Am. Chem. Soc., Polymer Preprints, 1989, 30(1),189.
3. H. W. Gibson, M. Bheda, P. T. Engen, Y. X. Chen, J. Sze, C. Wu, S. Joardar, T. C. Ward and P. Lecavalier Makromol. Chem , Macromol. Symp. Vol., 1991, 42/43, 395.
4. C. Wu, M. C. Bheda, C. Lim, Y. X. Chen, J. Sze and H. W. Gibson, Polym. Commun., 1991, 32, 204.
5. Y. X. Shen and H. W. Gibson, Macromolecules, submitted.
6. Y. X. Shen and H. W. Gibson, Macromolecules, in preparation.
7. P. T. Engen, Y. X. Shen, M. A. G. Berg, J. S. Merola and H. W. Gibson, Macromolecules, submitted.
8. C. Wu, P. R. Lecavalier, Y. X. Shen and H. W. Gibson, Chem. Mater., 1991, 3, 569.
9. B. Odell, M. V. Reddington, A. M. Z. Slawin, N. Spencer, J. F. Stoddart and D. J. Williams, Angew. Chem. Int. Ed. Engl., 1988, 27, 1547.
10. P. R. Ashton, B. Odell, M. V. Reddington, A. M. Z. Slawin, J. F. Stoddart and D. J. Williams, Angew. Chem. Int. Ed. Engl., 1988, 27, 1550.
11. P. R. Ashton, T. T. Goodnow, A. E. Kaifer, M. V. Reddington, A. M. Z. Slawin, N. Spencer, J. F. Stoddart, C. Vicent and D. J. Williams, Angew. Chem. Int. Ed. Engl., 1989, 28, 1396.

12. P. L. Anelli, P. R. Ashton, N. Spencer, A. M. Z. Slawin, J. F. Stoddart and D. J. Williams, *Angew. Chem. Int. Ed. Eng.*, 1991, 30, 1036.
13. P. R. Ashton, C. L. Brown, E. J. T. Chrystal, T. T. Goodnow, A. E. Kaifer, K. P. Parry, A. M. Z. Slawin, N. Spencer, J. F. Stoddart and D. J. Williams, *Angew. Chem. Int. Ed. Eng.*, 1991, 30, 1039.
14. P. R. Ashton, C. L. Brown, E. J. T. Chrystal, K. P. Parry, M. Pietraszkiewicz, N. Spencer and J. F. Stoddart, *Angew. Chem. Int. Ed. Eng.*, 1991, 30, 1042.
15. Cyclic voltametry of the macrocycles were done using a glassy carbon or gold working electrode and (Ag/0.1 M Ag⁺) reference electrode in 0.5-1.0 mM solutions in DMF with 0.2 M Bu₄NBF₄ supporting electrolyte at 25 °C.
16. P. L. Anelli, P. R. Ashton, R. Ballardini, V. Balzani, M. Delgado, M. T. Gandolfi, T. T. Goodnow, A. E. Kaifer, D. Philip, M. Pietraszkiewicz, L. Prodi, M. V. Reddington, A. M. Z. Slawin, N. Spencer, J. F. Stoddart, C. Vicent and D. J. Williams, *J. Am. Chem. Soc.*, 1992, 114, 193.

V.	CYCLIC POLYSTYRENE	94
V.1	Introduction	95
V.2	Literature Review	96
V.3	Characterization of Cyclic Polystyrene	99
V.4	Conclusions	106
V.5	Experimental	106

V.1 Introduction

Cyclic polymers are of considerable academic as well as industrial importance due to their interesting properties such as lower hydrodynamic volume, lower melt and solution viscosity and lower frictional coefficients than linear polymers of the same molecular weight (1). Our interest in cyclic polystyrene stems from the fact that some of the above mentioned useful properties of oligomeric cyclic polystyrene can be exploited by incorporating it onto linear or crosslinked polymer backbones such that there is no covalent bond between the cyclic and the backbone polymer species, a polyrotaxane (2-10). The oligomeric cyclic polystyrene offers an important alternative as a nonpolar macrocycle over the commonly used macrocycles such as crown ethers or benzo-substituted crown ethers. Further, upon optimization of the synthetic procedure for oligomeric cyclic polystyrene higher yields (up to 70 %) could be obtained and the crude cyclics could be used directly for the polyrotaxane syntheses.

Synthesis and characterization of high molecular weight cyclic polystyrene has been reported in the literature (1,5,10-20). Typically, the bifunctional living polystyrene prepared by anionic polymerization is cyclized under high dilution conditions using various reagents such as dichlorodimethylsilane, α,α' -dibromo-p-xylene or 1,3-bis(α -phenylethenyl)benzene to obtain functionalized or unfunctionalized cyclic polystyrene. To our knowledge there is no mention in literature of well characterized oligomeric cyclic polystyrene of molecular weight lower than 3200.

In this chapter, the synthesis, purification and characterization of cyclic polystyrene of molecular weight 2500 is reported. The salient features of this work are the high yields of the cyclic polystyrene and ease of purification by fractionation (very pure cyclic polystyrene can be obtained in just two fractionations). The lower molecular weights of our cyclic polystyrene allowed us to characterize it at the molecular level

using the NMR techniques described earlier in another study of linear polystyrene (5,6).

V.2 Literature Review

The hydrodynamic volume of the cyclic polystyrene is lower than that of linear polystyrene of the same molecular weight due to the lower radius of gyration (R_g) of the cyclic polymer. In the 1940s, using random-walk chain statistics without consideration of the effects of excluded volume and draining, Zimm and Stockmayer (21-22) and Kramers (23) reported that the ratio of the intrinsic viscosities as well as the ratio of unperturbed mean square radii of gyration of cyclic polymers relative to linear polymers of the same molecular weights should be 0.5. Further, Fukatsu and Kurata (24) predicted the ratio (g) of intrinsic viscosities to be 0.645 under θ conditions, while Bloomfield and Zimm predicted the ratio to be 0.66 (25) in θ solvents and smaller values in good solvents. Further, Casassa estimated the ratio to be greater than 0.5 (26).

According to the Mark-Houwink equation:

$$[\eta] = K_{\theta} M^a \quad \text{at } \theta \text{ condition } a = 0.5$$

where

$$K_{\theta} = 6^{3/2} \Phi_0 \{ \langle R_g \rangle^2 / M \}^{3/2}$$

M = molecular weight and Φ_0 is the universal constant

$$g = [\eta]_{C,\theta} / [\eta]_{L,\theta} = K_{\theta C} / K_{\theta L}$$

and

$$G = \langle R_g \rangle_{C,\theta} / \langle R_g \rangle_{L,\theta}$$

The solution properties of cyclic polystyrene of moderately low and high molecular weights are of considerable interest and have been studied extensively (10-11,13-19,27-32) to determine a

variety of parameters and to verify the theoretical predictions. Further, studies on the solid state properties of cyclic polystyrene such as glass transition temperatures (19,33), melt viscosities (28, 34), viscoelastic properties (35) have been reported. Various studies on other macrocycles such as cyclic poly(2-vinylpyridine) (36-37), poly(dimethylsiloxanes) (38-39) and polycarbonates (40) have also been reported.

There exists a variety of contradictory data on solution properties of cyclic polystyrene and the differences in the results have mainly been attributed to (i) contamination by linear chains in the cyclic fractions and (ii) presence of knots in the cyclic polymer chains (11,32). In most of the reports, the cyclic nature has primarily been deduced from the measurements of intrinsic viscosities at or near θ conditions and in good solvents.

It has been indicated that for cyclic polystyrene in cyclohexane the θ temperature is 28.5 °C, 6 °C lower than that for the linear polymer (34.5 °C) (10,29,31) and that the K_{θ} values for the cyclic and linear polymers are $K_{\theta C} = 5.14-5.76 \times 10^{-4}$ dl/g (cyclohexane 34.5 °C) and $K_{\theta L} = 8.01 \times 10^{-4}$ dl/g, respectively (28). The reported values of the ratios of intrinsic viscosities (g) range from 0.63-0.71 for a broad range of molecular weights of polystyrene in a variety of solvents (10-11,13-19,27-31). For lower molecular weight polymers (3,200-13,000) the g ratio (in cyclohexane at 34-35 °C) reported in the literature varies from 0.64-0.70. The ratio of radius of gyration (G) at θ conditions (28 °C for cyclics) were determined by small-angle neutron scattering and dynamic light scattering experiments and was found to be 0.50 (30).

The reported values of the ratios of intrinsic viscosities of 0.64-0.70 in cyclohexane at 34-35 °C do not represent the θ condition for cyclic polystyrene. Above the θ condition, the exponent 'a' increases from 0.5 and from viscosity measurement of cyclic polymers at 34.5 °C in cyclohexane, the exponent for the viscosity law was found to be 0.53 (28-29) Further, at very low molecular

weights of cyclic polystyrene (ca. 2500) the exponent is expected to be higher than 0.5 in cyclohexane at 34-35 °C, because these conditions may not represent the θ condition. In good solvents (THF, toluene) the exponent for cyclics was found to be 0.70 versus 0.72 (± 0.02) for linears. More detailed and critical evaluation of the intrinsic viscosity data for linear and cyclic polystyrene has been reported (11).

Table V.1 summarizes the intrinsic viscosity data in cyclohexane at 34-35 °C for lower molecular weight cyclic polystyrenes (3,200-13,000) reported in the literature.

Table V.1 Reported Intrinsic Viscosity Data for Cyclic PS

Molecular Linear	Weights Cyclic	$[\eta]$ dl/g Linear	$[\eta]$ dl/g Cyclic	$[\eta]_C / [\eta]_L$	Comments
12500	12500	0.107	0.081	0.76	THF, (14)
3900	4000	0.0533 0.0520	0.0375 0.0395	0.70 0.76	CHX, (15) TLN, (15)
12100	12200	0.0935 0.0986	0.0670 0.0643	0.64 0.65	CHX, (15) TLN, (15)
12500	12600	0.0952 0.1141	0.0617 0.0703	0.64 0.61	CHX, (15) TLN, (15)
10500	11100	0.084 0.103	0.055 0.070	0.66 0.68	CHX, (29) THF, (29)
11200	12500	0.086 0.107	0.0565 0.081	0.66 0.76	CHX, (28) THF, (28)
6900	6900	---	0.045	--	CHX, (31)
12100	12100	---	0.062	--	CHX, (31)

Comments: CHX- Cyclohexane at 34.5 °C; TLN- Toluene, 25 °C;
THF- Tetrahydrofuran, 25 °C.

Not included in the above table is the data from a recent publication (20) where authors have reported synthesis of low molecular weight 1900-7000 cyclic polystyrene and have shown (without any details) the ratio of intrinsic viscosities to be in the range of 0.616-0.710. Further, they found T_g of 92.8 °C for cyclic polystyrene of molecular weight 1900 and that the T_g gradually decreased with increasing molecular weight up to 8700.

V.3 Characterization of Cyclic Polystyrene

A schematic representation of the synthesis of cyclic polystyrene using sodium naphthalide as initiator and dichlorodimethylsilane as the cyclization agent has been shown in Scheme V-1.

As shown in the scheme one of the chain ends of the living bi-ended polystyryl sodium reacts with one molecule of dichlorodimethylsilane to form the intermediate mono-ended living polymer, which then cyclizes, intramolecularly, in high dilution to form cyclic polymer. Further, the same intermediate could react with another molecule of the living bi-ended polystyryl sodium, intermolecularly, to form the linear dimer, which could either cyclize or form higher molecular weight polystyrene by reacting with one or more living (mono-ended or bi-ended) polystyrene chains. Thus concentration of the polystyryl sodium in the cyclization medium plays an important role in the formation of cyclic polymer or linear high molecular weight polymer, since the formation of higher molecular weight linear polymer depends on the square of the concentration as shown below, while the formation of cyclic polystyrene is a unimolecular reaction with respect to the living bi-ended polymer.

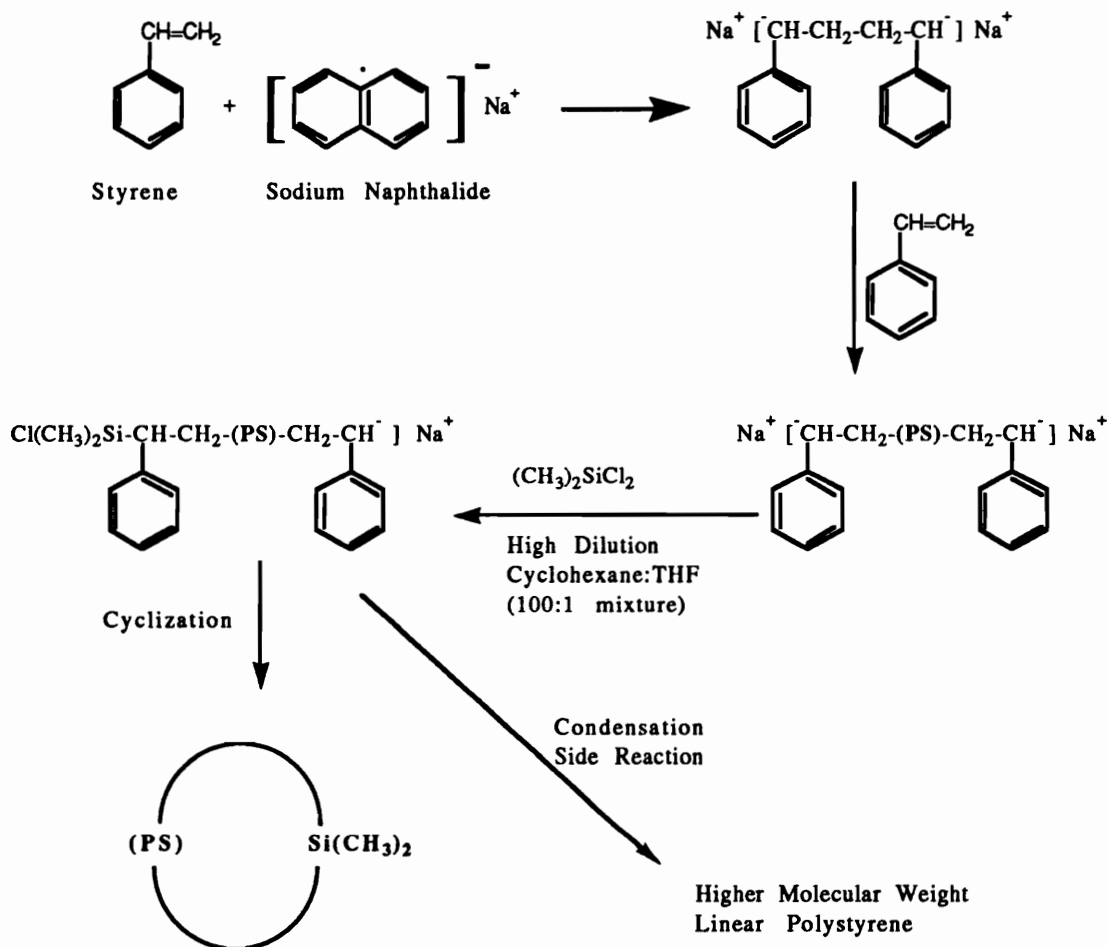
Rate of Formation of Cyclic PS = $k [\text{Na}^+ \text{-PS- Na}^+] [\text{Cl}_2\text{Si}(\text{CH}_3)_2]$

Rate of Formation of Higher Mol. Wt. Linear PS

$$= k [\text{Na}^+ \text{-PS- Na}^+]^2 [\text{Cl}_2\text{Si}(\text{CH}_3)_2]$$

Further, the higher the molecular weight, the lower the chain end concentration necessary for the same proportion of cyclization (11).

Scheme V-1 Synthesis of Cyclic Polystyrene



Another important factor that could affect the yields of the cyclic polymer is the cyclization medium. When the polymer is dissolved in a θ solvent for the polymer, the end to end distance of the polymer chain is minimal and the ends are brought together (decreased chain dimensions). Thus, using a θ solvent as cyclization medium would help in increasing the yields for the cyclic polymer;

however, the effect of living chain ends (ionic) on the end to end distance in a θ solvent has not been explored.

In the present work cyclizations were done by adding small quantities of the polymerization mixture (1-2 ml at a time) into about 1.6 l of the cyclization solvent mixture. Thus, cyclizations were done under very high dilution. The final concentration of the cyclization solution (after the cyclization) was 0.0019 moles of polymer/l, (0.49 weight %).

Earlier cyclization attempts by dropwise addition of bi-ended living polystyrene prepared in THF:benzene (58:42) into a large volume of cyclohexane:THF (90:10) gave light red cloudy solutions. Thus, the cyclization was done in cyclohexane:THF (80:20). Part of the bi-ended living linear precursor polymer was kept aside to serve as a linear reference after termination of living chain ends with methanol. Two samples of cyclic polystyrene MB-125-1C and MB-125-2C were synthesized, fractionated and characterized. The two cyclic samples showed similar properties. The corresponding linear polymers were numbered MB-125-1L and MB-125-2L. In the following discussion, characterization of MB-125-2C has been described.

GPC analyses of the linear polymer showed it to have a number average molecular weight (M_n) of 2500 and a molecular weight distribution of 1.1. The GPC elution peak was at 36.95 ml. The unfractionated cyclic polymer showed a broad distribution and the apparent molecular weight ranged from 2000-9500. The elution peak corresponding to the cyclic polymer was at 37.45 ml, 0.50 ml higher than that for linear precursor, corresponding to a linear polystyrene molecular weight of 2000.

Figure V-1 shows the GPC traces of the linear precursor polymer and crude cyclization product. This indicates that the cyclization has occurred; the cyclic polymer appears at higher elution volumes compared to parent linear polymer, due to its lower hydrodynamic volume. A similar trend was observed for the crude

cyclization reaction product of another reaction and its corresponding linear polymer.

According to the universal GPC calibration, the product $[\eta] M$ (a measure of hydrodynamic volume) determines the chromatographic retention in GPC columns (29). Thus, the apparent molecular weight of the cyclic polymer sample can be expressed by:

$$M_{\text{app}} = M \left[\frac{[\eta]_{\text{C}}}{[\eta]_{\text{L}}} \right]^{(1/1+a)}$$

where a is the exponent of the Mark-Houwink relationship (0.70) and M is the true molecular weight of the macrocycle (29). This predicts an apparent molecular weight of about 2000 for the cyclic polystyrene, which is in agreement with the observed GPC molecular weights.

Yields of the cyclic polystyrene determined from the GPC elution peaks assuming a Gaussian distribution were found to be about 50 %.

In ^1H and ^{13}C NMR spectra, the dimethylsilyl groups of the unfractionated cyclization reaction product show multiple peaks. In proton NMR there were signals from -0.1 to -0.9 ppm. A similar behavior was seen in carbon NMR where two major peaks were seen, each with further splitting. This was expected due to the tacticity effects (5,6).

Both the crude cyclization reaction products MB-125-1C and MB-125-2C were fractionated using a benzene/methanol solvent system to obtain pure cyclic polystyrene from the mixture of cyclic polystyrene and higher molecular weight linear polystyrene. Typically in fractionation, several repeat fractionation are required to obtain final pure product with narrow molecular weight distribution. However, only two fractionations were required to obtain a narrow molecular weight pure cyclic polystyrene fraction. Molecular weight and distribution for each fraction were monitored using GPC. Figure V-2 shows the GPC traces of MB-125-2C-F1, MB-125-2C-F2 and the crude cyclization product. Figure V-3 shows the

GPC traces of MB-125-2C-F2, MB-125-2C-F3, and MB-125-2C-F4. Schematic V-2 shows the fractionation for cyclic polystyrene.

Scheme V-2 Fractionation Scheme

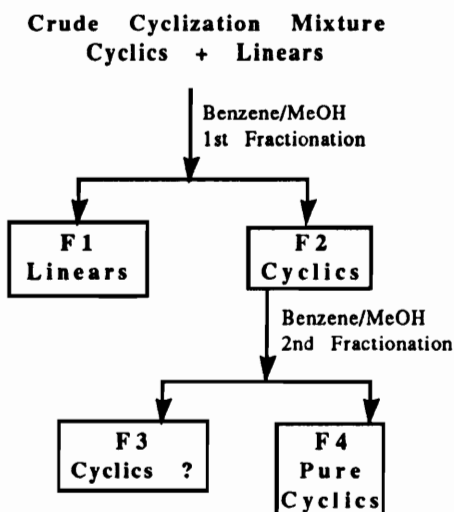


Table V-2 lists the weights of various fractions isolated from MB-125-II-1C and MB-125-II-2C.

Table V-2 Weights of the Isolated Fractions

<u>Fractions</u>	<u>MB-125-1C</u>	<u>MB-125-2C</u>
Linear High Mol Wt Polymer (Fraction F1)	3.77 g	4.07 g
Impure Cyclic Polymer (Fraction F2)	3.78 g*	3.53 g*
Higher Mol Wt Cyclics (?) (Fraction F3)	0.88 g	0.44 g
Pure Cyclic PS (Fraction F4)	2.63 g	2.31 g

* 0.25 and 0.72 g of Fraction F2 of MB-125-II-1C and MB-125-II-2C, respectively, were removed for characterization.

As indicated earlier, the yields determined from GPC were about 50 %. The isolated yields of the pure cyclic polymer fraction were 38 %. Figure V-4 shows the GPC traces of MB-125-2C-F4 and MB-125-2L. Formation of cyclic molecules of twice the size of the precursor linear chain has been indicated in the literature (11,18); however, it has not been isolated or detected previously. Fraction F3 could be the cyclic polymer of twice the size, since the apparent molecular weight was 4000 with a polydispersity index of 1.2, as analysed by GPC.

Further, formation of catena-polystyrene has also been suggested (17); however, under the very dilute conditions employed for cyclization it seems unlikely to form in our system.

Intrinsic viscosity data for both the linear and the pure cyclic polystyrene (MB-125-2L and MB-125-2C-F4, respectively) were obtained in cyclohexane at 34.5 °C using Ubbelohde viscometers. Due to lower molecular weights of the polymers, concentrations as high as 20 mg/ml were used. The conditions used here represent the θ condition for high molecular weight linear polystyrene; however, due to the lower molecular weights of the linear and cyclic polymers, the above mentioned conditions may not be exactly θ conditions. Following is the summary of the data obtained.

MB-125-2L

GPC Mn: 2500

Polydispersity Index: 1.15

Intrinsic Viscosity $[\eta]_L$: 0.070 dl/g (cyclohexane at 34.5 °C)

MB-125-2C-F4

GPC Mn: 2500

Polydispersity Index: 1.20

Intrinsic Viscosity $[\eta]_C$: 0.041 dl/g (cyclohexane at 34.5 °C)*

*Repeat analyses: 0.042 dl/g (cyclohexane at 34.5 °C)

Ratio of Intrinsic Viscosities of Cyclic to Linear:

$$[\eta]_C/[\eta]_L = (0.0415 / 0.070) = 0.59$$

The ratio of intrinsic viscosities of cyclic to linear is 0.59 which is close to the reported values of 0.66. The above ratio could also be considered a measure of the purity of the cyclic fraction; it is the lowest yet reported.

NMR Spectroscopy:

Multiple peaks were observed for the dimethylsilyl groups in the proton NMR spectrum. There were no major differences between the proton NMR peak pattern of the dimethylsilyl groups in the pure cyclic fraction **F4** and that of fraction **F1** or **F3**. This may be due to the fact that in higher molecular weight analogs of the precursor polystyrene the dimethylsilyl moiety is surrounded by the same environment as found in cyclic polystyrene. The ^1H , ^{13}C and ^{29}Si NMR spectra of dimethylsilyl groups are shown in Figure V-5. The proton NMR spectrum of the $-\text{Si}(\text{CH}_3)_2$ groups shows broad and fused multiple peaks from 0.1 ppm to -0.6 ppm. Similarly multiple peaks in carbon NMR as well as silicon NMR were observed from -1.8 ppm to -7.6 ppm and 4.6 ppm to 6.0 ppm, respectively. These multiple peaks arise due to the tacticity of the polymer as explained by model studies of polystyrene chains end capped by trimethylsilyl groups (5-6). The reasons for more peaks observed for cyclic polystyrene than for model end capped linear polymers is that in the cyclic polymer the dimethylsilyl group is surrounded by polymer on both the sides and each side of the chain, in principle, can have different tacticity. Thus, the dimethylsilyl groups would experience many more environments (as many as 64, if expressed in terms of tetrads) depending upon the tacticity of the adjacent polystyrene units on each side.

Thermal Properties:

The pure cyclic polystyrene fraction (**F4**) has a glass transition of 96 °C while the linear precursor has a glass transition

of 68 °C. Figure V-6 shows the DSC traces of the linear and cyclic polystyrenes (second heats). The higher T_g of the cyclic polystyrene compared to its linear counterpart is due to the lower configurational entropy of the cyclic polymer which is the result of lower number of possible configurations available to the cyclic polymer than to a linear polymer of the same number of repeat units (33). Further, smaller cyclics have much lower entropy than the larger cyclics. Typically, for the linear polymer the T_g increases with molecular weight until it reaches a constant value. In the cyclic systems the configurational entropy of the smaller macrocycles is higher, thus, the higher the T_g; the T_g decreases with increasing molecular weight until it reaches a constant value. There is no report of such a high glass transition temperature for cyclic polystyrene of molecular weight 2500. Thus, the high T_g reflects the purity of the cyclic polystyrene fraction F4.

V.4 Conclusions

The cyclic polystyrene prepared represents the lowest molecular weight (ca 2500) well characterized cyclic polystyrene reported to date. High yields (ca 50 %) of the cyclic polymer were obtained; this made it easy to isolate pure cyclic polymer in just two fractionations.

The ratio of intrinsic viscosities of cyclic to linear under identical conditions (in cyclohexane at 34.5 °C) was found to be 0.59. Further, the glass transition temperatures show a big difference (ca. 28 °C) between the cyclic and linear polymers.

V.5 Experimental

Measurements:

GPC analyses of the polymers were done at 30 °C in THF using a Waters system (RI and UV detectors) after calibration with PS standards. TGA data were obtained using Du Pont TGA 951

instrument at a scan rate of 10 °C/min. DSC data were obtained using Du Pont DSC 912 instrument at a scan rate of 10 °C/min. ¹H, ¹³C and ²⁹Si NMR spectra were obtained on a Varian Unity 400 MHz spectrometer using deuterated chloroform solutions with tetramethylsilane as an external standard. Intrinsic viscosity measurements were performed in cyclohexane at 34.5 °C using a Cannon-Ubbelohde viscometer.

Polymerizations as well as cyclizations were done in a Vacuum Atmospheres glove box equipped with a refrigeration unit ([H₂O] = 0.6 ppm, [O₂] = 1.0 ppm).

Purification of Solvents:

Benzene: Benzene from a freshly opened bottle was transferred to a 2 L vacuum flask and about 4.0 ml styrene was added to it followed by addition of 10-15 ml 2.5 M n-butyllithium. The light orange-red color persisted. The solution was placed on the vacuum line, freeze-thawed twice and distilled to another 2 L vacuum flask. The tightly sealed flask was then taken to the glove box. Two such purifications were done for benzene to obtain about 3.5 L of pure solvent.

THF: A total of about 3.2 L of THF was purified as described above for benzene.

Cyclohexane: A total of 3.6-3.8 L of cyclohexane was purified as described above for benzene.

Dichlorodimethylsilane (DCDMS): DCDMS from a freshly opened bottle was distilled and the middle fraction was collected in a vacuum flask which was then freeze-thawed 4 times and transferred by distillation under vacuum to another vacuum flask. It was then taken to the glove box.

Styrene: Styrene (99 %, Aldrich) was passed through a 4" long column of alumina and then collected in a vacuum flask containing calcium hydride. The styrene was freeze-thawed 3 times and then distilled under vacuum to another vacuum flask and taken to the glove box.

Sodium naphthalide was prepared in the glove box by dissolving 2.08 g (9.04×10^{-2} mole) of purified sodium and 20.2 g (1.58×10^{-1} mole) of naphthalene in about 50 ml THF. Within few seconds the green color began to appear and the initiator was allowed to form for 24 hours after mixing. The initiator was titrated against 0.5 N HCl just before the use.

Polymerization and Cyclization of Styrene:

Both the polymerization and cyclization were done in the glove box. All the glassware required in polymerization and cyclization was washed with a dilute solution of sodium naphthalide in THF to prevent termination of living polymer anions by impurities in the glassware. The following conditions were employed for the polymerization:

Target molecular Weight: 2500

Styrene: 10.0 ml (8.73×10^{-2} moles)

Solvents: 150 ml THF + 110 ml benzene

Initiator: Sodium naphthalide,

6.3 ml of 1.113 molar solution (7.0×10^{-3} moles)

Polymerization Time: 30 minutes.

Polymerization Temperature: 10-15 °C

Sodium naphthalide was added to the solvent mixture, using a syringe while stirring vigorously. To this styrene was added very rapidly using a syringe and the polymerization was continued for 30 minutes.

After 30 minutes of polymerization, the living polymer solution was transferred to a 500 ml addition funnel, leaving some behind to serve as the linear reference polymer. 0.50 ml (3.6×10^{-3} moles) of DCDMS was added to another 100 ml addition funnel containing 90 ml THF. Both the solutions were added to a 2 L flask containing 1.6 L of cyclohexane:THF (80:20) at a rate such that there was a slight excess of living anion in the flask (as indicated by the color). The complete addition took about 3 hours. The flask was

then taken out of the glove box. Two such polymerizations and cyclizations were done.

Excess solvent was removed by rotary evaporation and the polymers were precipitated in 10 fold excess methanol. The polymers were then washed with water (3 x 200 ml), ethanol (3 x 200 ml) and then with methanol. The linear reference polymers were also worked up the same way. The polymers were dried under vacuum for 24 hours.

Fractionation of Cyclic Polystyrene:

7.6 g of MB-125-II-1C or MB-125-II-2C was dissolved in 756 ml of benzene. To this 400 ml of methanol was added dropwise using a separatory funnel while stirring. Turbidity began to appear; the turbidity increased as the addition of 600 ml more methanol was continued. After the addition of methanol was complete, the turbid solution was warmed to about 55 °C and left at that temperature for 30 minutes. The turbidity in the solution decreased upon warming. It was then slowly cooled to room temperature (3-4 hours) while stirring. The turbidity reappeared, and solid was allowed to settle at the bottom of the flask for 48 hours. The relatively clear top liquid layer was removed by use of a filtering stick (equipped with a fritted filtering disk). The viscous semisolid polymer at the bottom of the flask (Fraction F1) contained the high molecular weight linear polymer while the liquid contained the impure cyclic fraction (Fraction F2) as determined by GPC.

The fraction F2 (the filtered liquid) was fractionated further by dropwise addition of 250 ml methanol. The rest of the procedure was the same as that described in the first fractionation. The top liquid layer was then filtered out using a filtering stick, leaving the viscous semisolid in the flask. The semisolid fraction (Fraction F3) contained higher molecular weight polymer than that in the top liquid layer (Fraction F4), which contained pure cyclic polystyrene.

All the fractions were then rotary evaporated, dried under vacuum for 24 hours and analysed by GPC and NMR.

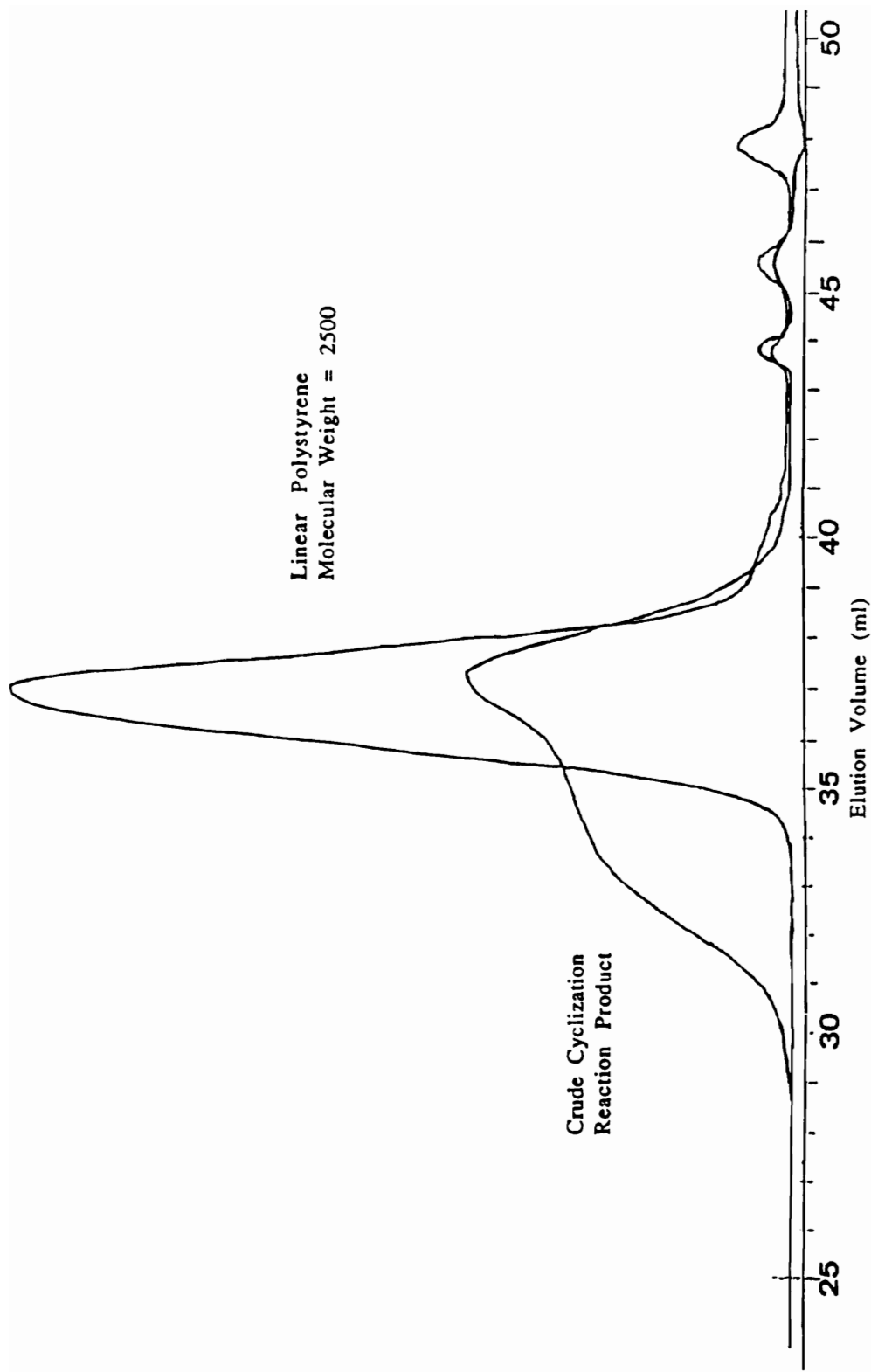


Figure V.1 GPC Traces of Linear Precursor Polystyrene and Cyclization Reaction Product (UV Traces)

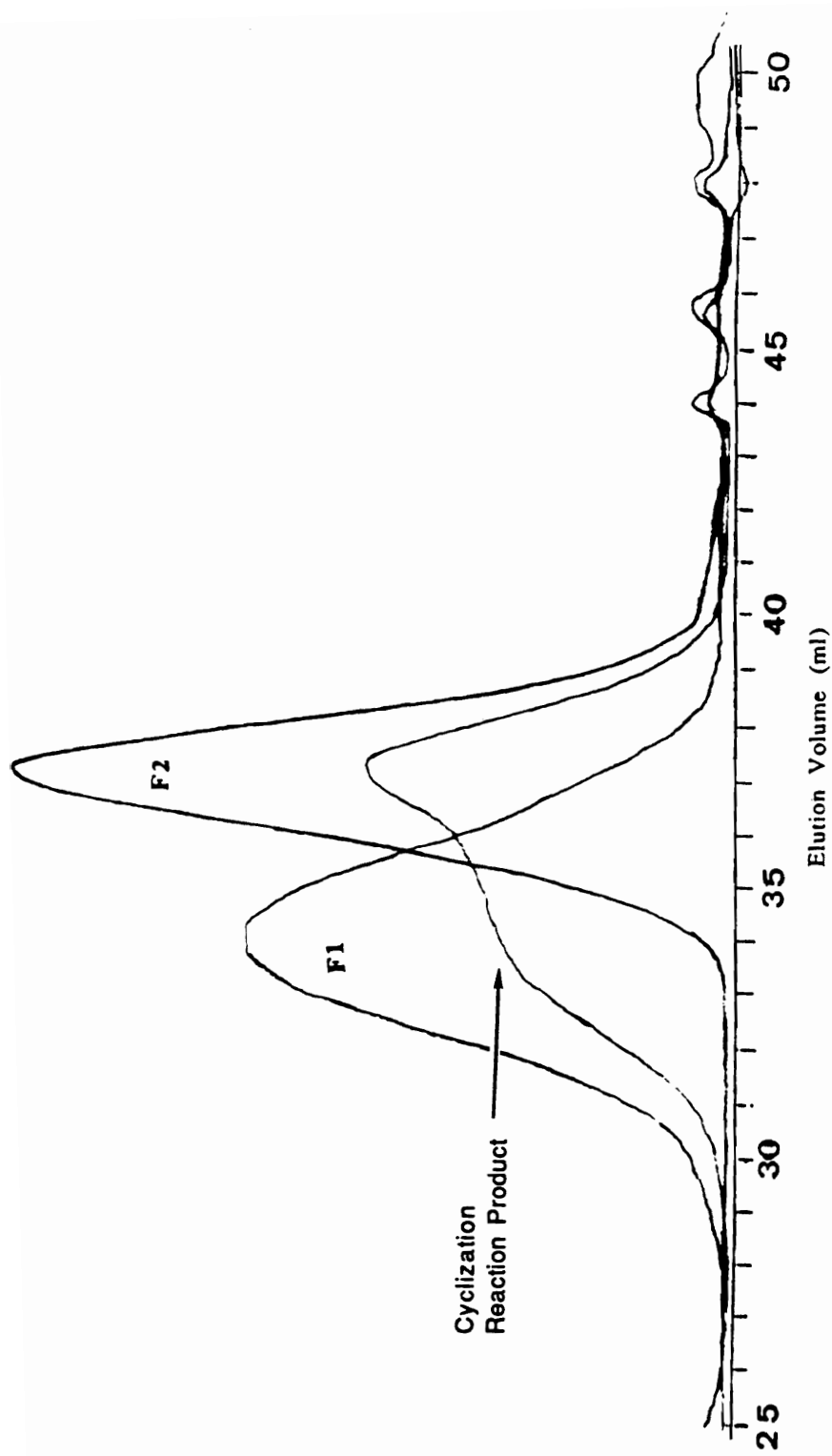


Figure V.2 GPC Traces of Cyclization Reaction Product, MB-125-2C-F1 and MB-125-2C-F2 (UV Traces)

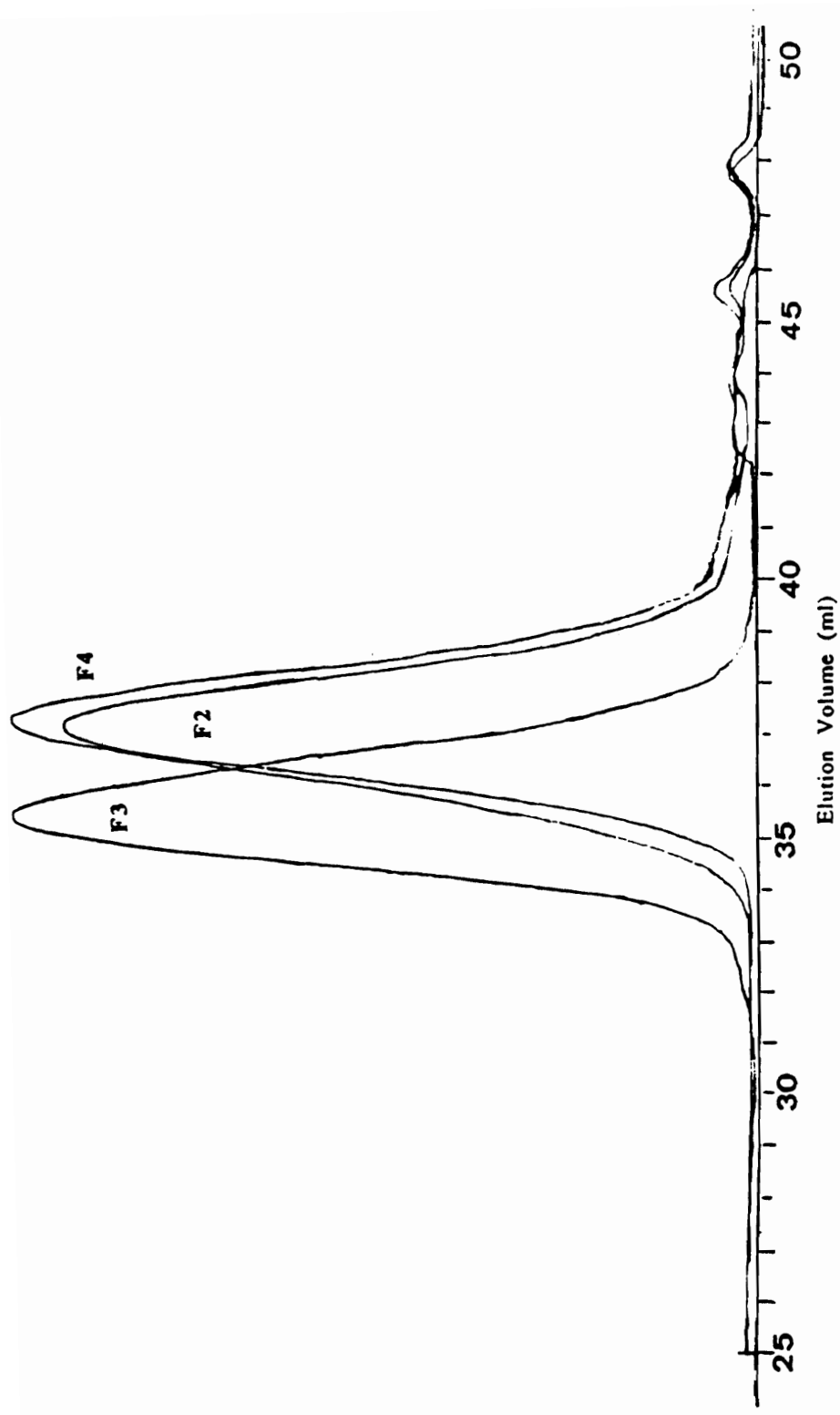


Figure V.3 GPC Traces of MB-125-2C-F2, MB-125-2C-F3 and MB-125-2C-F4 (UV Traces)

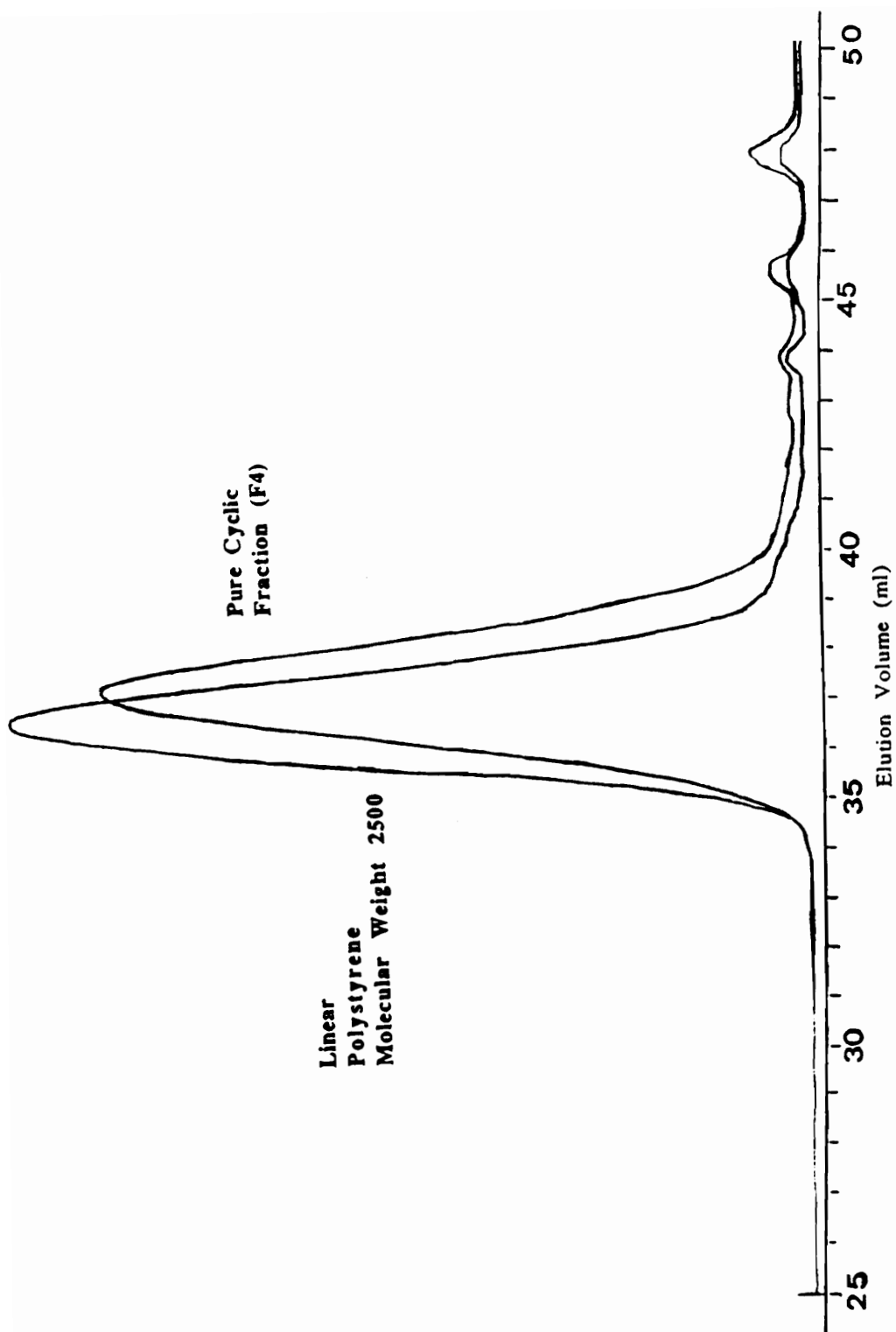


Figure V.4 GPC Traces of MB-125-2C-F4 and MB-125-2L (UV Traces)

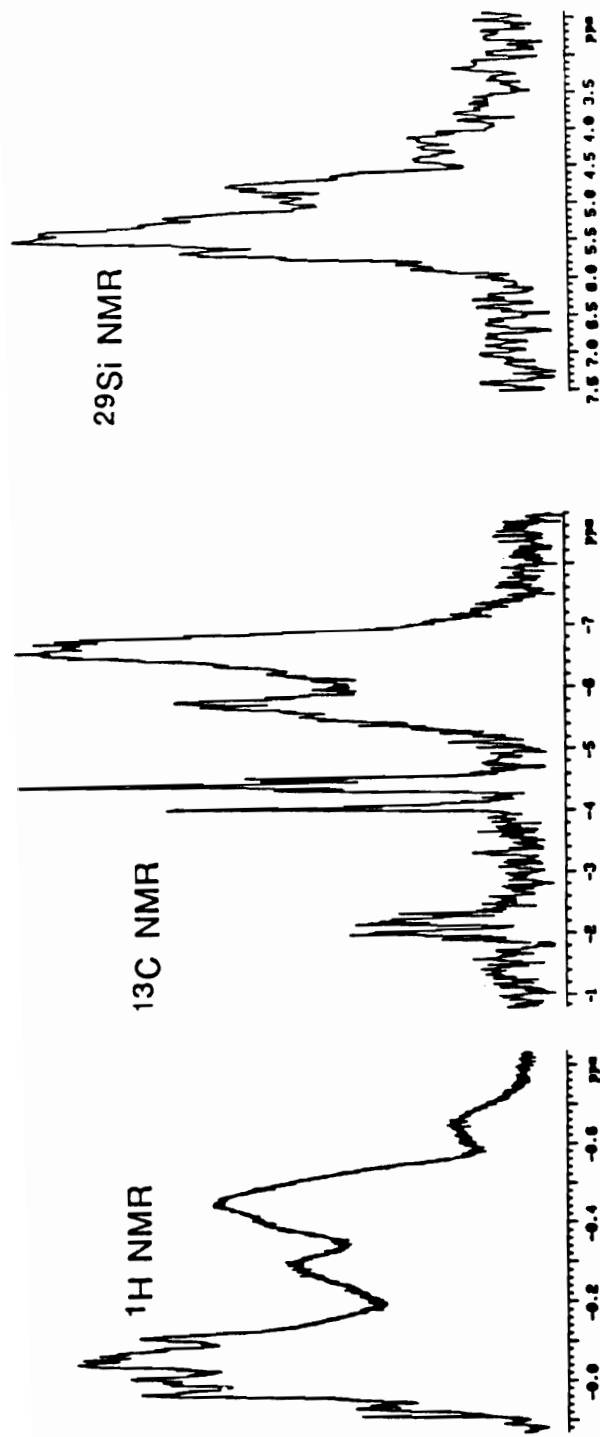


Figure V.5 ^1H (400 MHz), ^{13}C and ^{29}Si NMR spectra of $-\text{Si}(\text{CH}_3)_2$ groups of Cyclic Polystyrene

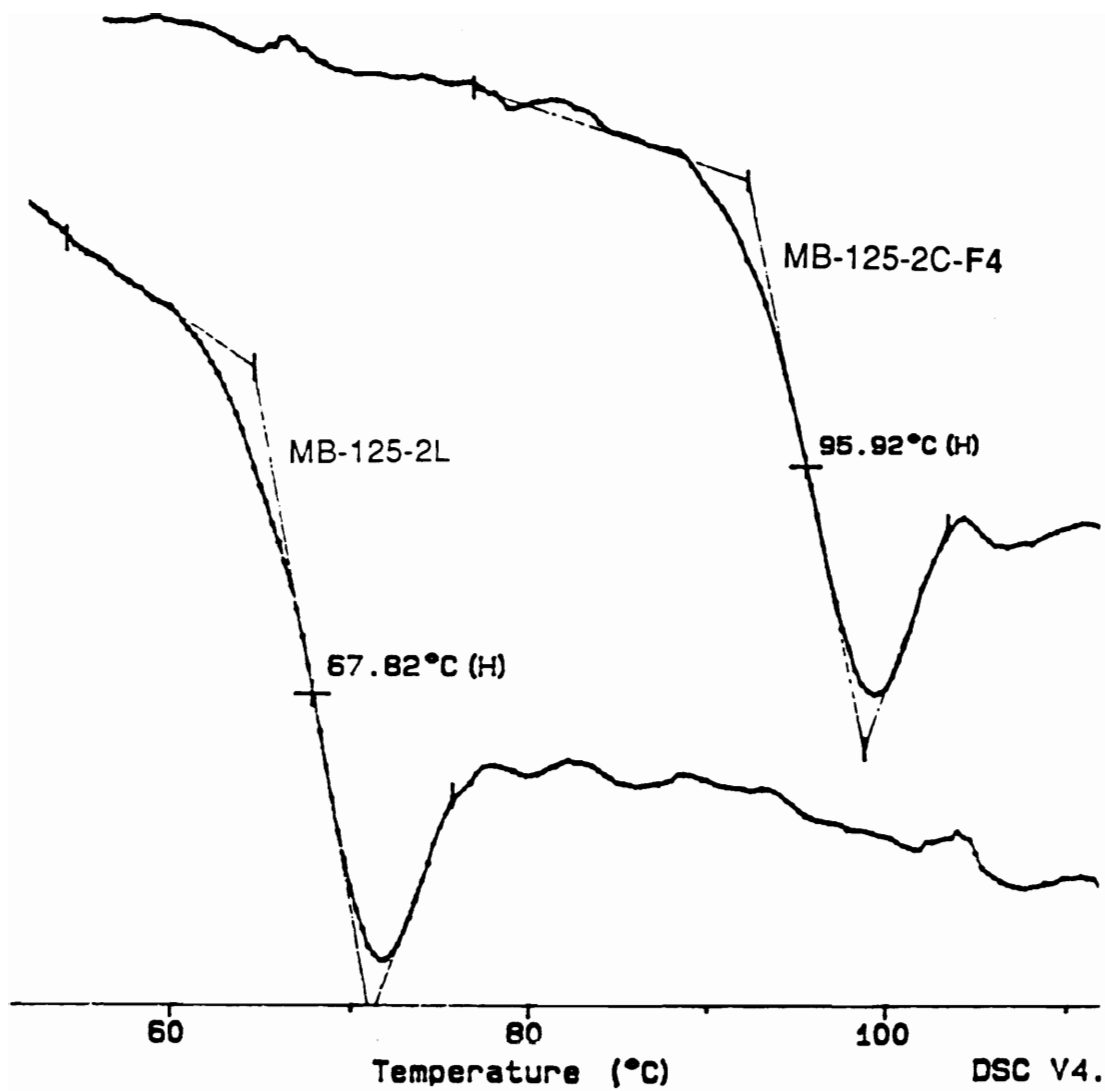


Figure V.6 DSC Traces (Second Heat) of Linear Polystyrene (MB-125-2L) and Cyclic Polystyrene (MB-125-2C-F4)

References

1. P. Rempp, C. Strazielle and P. Lutz, Encyclopedia of Polymer Science and Engineering., John Wiley & Sons, New York., 1987, Vol 9, p 183.
2. H. W. Gibson, P. R. Lecavalier and P.T. Engen, Am. Chem. Soc., Polymer Preprints, 1988, 29(1), 248.
3. P. R. Lecavalier, P. T. Engen, Y. X. Shen, S. Joardar, T. C. Ward, and H. W. Gibson, Am. Chem. Soc., Polymer Preprints, 1989, 30(1), 189.
4. H. W. Gibson, M. C. Bheda, P. T. Engen, Y. X. Shen, J. Sze, C. Wu, S. Joardar, T. C. Ward and P. R. Lecavalier, Am. Chem. Soc., Polymer Preprints, 1990, 31(1), 79.
5. M. C. Bheda and H. W. Gibson, Am. Chem. Soc., Polymer Preprints, 1990, 31(1), 588.
6. M. C. Bheda and H. W. Gibson, Macromolecules, 1991, 24, 2703
7. P. R. Lecavalier, Y. X. Shen, C. Wu and H. W. Gibson, Am. Chem. Soc., Polymer Preprints, 1990, 31(2), 659.
8. H. W. Gibson, M. C. Bheda, P. T. Engen, Y. X. Shen, J. Sze, C.Wu, T. C. Ward and P.R. Lecavalier, Makromol. Chem., Symp. Vol. 1991, 42/43, 395.
9. C. Wu, P. R. Lecavalier, Y. X. Shen and H. W. Gibson, Chem. Mater., 1991, 3, 569.
10. C. Wu, M. C. Bheda, Y. X. Shen and H.W. Gibson, Polymer Communications, 1991, 32(7), 204
11. G. B. McKenna, B. J. Hostetter, N. Hadjichristidis, L. J. Fetters and D. J. Plazek, Macromolecules, 1989, 22,1834.

12. J. J. Ma and R. P. Quirk, Am. Chem. Soc., Polymer Preprints, 1988, 29 (2), 10.
13. J. Roovers and P. Toporowski, Macromolecules, 1983, 16, 843.
14. G. Hild, C. Strazielle and P. Rempp, Eur. Polym. J., 1983, 19, 721.
15. D. Geiser and H. Höcker, Macromolecules, 1980, 13, 653.
16. D. Geiser and H. Höcker, Polymer Bulletin, 1980, 2, 597.
17. B. Vollmert, J. X. Huang, Makromol. Chem., Rapid Commun., 1981, 2, 467.
18. G. Hild, A. Kohler and P. Rempp, Eur. Polym. J., 1980, 16, 525.
19. H. Zhiduan, Y. Meina, Z. Xuanqi, W. Xiaobing and J. Xiaoming, Eur. Polym. J., 1986, 8, 597.
20. X. Liu, D. Chen, Z. He, H. Zhang and H. Hu, Polymer Communications, 1991, 32 (4), 123.
21. W. H. Stockmayer, M. Fixman, J. Polym. Sci., Part C, 1963, 1, 137.
22. B. H. Zimm and W. H. Stockmayer, J. Chem. Phys., 1949, 17, 1301.
23. H. A. Kramers, J. Chem. Phys., 1946, 14, 415.
24. M. Fukatsu and M. Kurata, J. Chem. Phys., 1966, 44, 4539.
25. V. Bloomfield and B. H. Zimm, J. Chem. Phys., 1966, 44, 315.
26. E. F. Casassa, J. Polym. Sci., Part A, 1965, 3, 605.

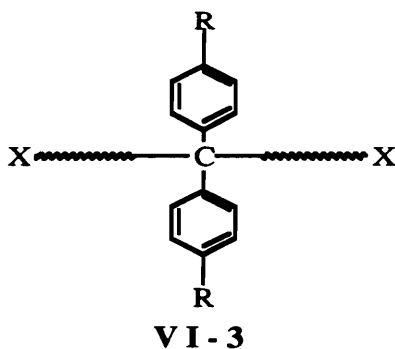
27. B. Vollmert, J. X. Huang, Makromol. Chem., Rapid Commun., 1980, 1, 333.
28. G. B. McKenna, G. Hadziioannou, L. G. Hild, C. Strazielle, C. Straupe, P. Rempp and A. J. Kovacs, Macromolecules, 1987, 20(3), 498.
29. P. Lutz, G. B. McKenna, P. Rempp, C. Strazielle, Makromol. Chem., Rapid Commun., 1987, 7, 599.
30. G. Hadziioannou, P. M. Cotts, and G. ten Brinke, C. C. Han, P. Lutz, C. Strazielle, P. Rempp and A. J. Kovacs, Macromolecules, 1987, 20, 493.
31. J. Roovers, J. Polym Sci., Polym. Physics. Ed., 23, 1117.
32. G. ten Brinke and G. Hadziioannou, Macromolecules, 1987, 20, 480.
33. E. A. Di Marzio and C. M. Guttman, Macromolecules, 1987, 20, 1403.
34. T. Pakula and S. Geyler, Macromolecules, 1988, 21, 1665.
35. Y. Nagasaki, T. Tsuruta, Makromol. Chem. Rapid Commun., 1986, 7, 437.
36. W. Toreki, T. E. Hogen-Esch and G. B. Butler, Am. Chem. Soc., Polymer Preprints, 1987, 28(2), 343.
37. W. Toreki and T. E. Hogen-Esch, Am. Chem. Soc., Polymer Preprints, 1988, 29(2), 416.
38. J. A. Semlyn, Pure. Appl. Chem., 1981, 53, 1797.
39. K. Dodgson, J. A. Semlyn, Polymer, 1977, 18, 1265.
40. A. Horbach, H. Vernaleken, K. Weirauch, Makromol. Chem., 1980, 181, 111.

VI.	BLOCKING GROUPS 119
VI.1	Strategies 120
VI.2	Literature Review 122
VI.3	Results and Discussion 123
VI.4	Experimental 134

be used to make stable polyrotaxanes using crown ethers of various sizes such as 30-c-10, 36-c-12 or 42-c-14. This would enable study of the solid state as well as solution and melt state properties of polyrotaxanes.

Mono- verses Bi-ended

When the blocking group is placed at the chain ends of the linear backbone, to obtain stable polyrotaxane, only a monofunctional blocking group is required. However, to make the rotaxanes where the blocking groups are an integral part of the linear backbone chain, placed either at regular intervals or at random, a bifunctional blocking group of the type **VI-3** is required.



R= t-Butyl, -O-CH₂-C₆H₅; X= -C₆H₅-OH, -C₆H₅-NH₂, -COOH, -OH, -Cl

These bifunctional blocking groups would be very useful in making polyrotaxanes, where macrocycles can be prevented from moving along the chain by the blocking groups that in turn could prevent phase separation of the macrocycles and the backbone polymer in the polyrotaxane. Such systems could be classified as micro-composites where two immiscible components are held together only by physical barriers.

Further, bifunctional blocking groups of the type **VI-3** can be utilized to prepare polyrotaxanes in which the exact location and proportion of the macrocycles are known. Such systems can be prepared by first preparing rotaxanes of a linear difunctional small

molecules end capped by mono-protected bifunctional blocking groups followed by deprotection of the functional groups of the resulting blocked rotaxane and polymerization with a suitable difunctional comonomer.

Various attempts to make such a bifunctional blocking groups were not successful due to steric hindrance coupled with side reactions (2-3). Thus, efforts were directed to prepare mono-functional blocking groups derived from tris(p-t-butylphenyl)methane with a variety of functional groups that could be utilized for end blocking polymer chains of various chemical structures, such as polyesters, polyamides, polyethers, vinylic polymers and more.

Functionality of Blocking Groups

Blocking groups derived from symmetrical tris(p-t-butylphenyl)methane having phenol, amine, carboxyl, and acid chloride functional groups can be used in condensation polymerizations to prepare polyarylether, polyester, polycarbonate, polyamide, polyazomethine, etc., rotaxanes. Further, the acid chloride functional blocking group can be used for blocking polyrotaxanes of preformed polymers having hydroxyl or phenoxy or amine functional groups at the chain ends. Vinyl functional blocking groups would be very useful in the synthesis of polyrotaxanes by chain growth (either anionic, cationic or free radical) polymerization. In this chapter the discussion will focus on pertinent literature, results obtained and experimental approaches to make the mono-ended blocking groups derived from tris(p-t-butylphenyl)methane.

VI.2 Literature Review

A 1941 paper by Marvel et al. (4) proved to be very useful as the starting point toward the synthesis of tris(p-t-butylphenyl)-carbinol. They studied the effect of dissociation of di-, tetra- and

hexa-alkyl substitution on phenyl groups of hexaphenylethane. Syntheses of these substituted hexaphenylethane derivatives were accomplished by first preparing substituted triphenylmethanol derivatives (in about 46 % yield) using Grignard reactions. The substituted methanol derivatives were converted to methyl chloride derivatives followed by coupling of two molecules of methyl chloride derivative using molecular silver in benzene.

Using a Friedel-Crafts type reaction, without the use of the catalyst, Mikroyannidis prepared bis(p-hydroxyphenyl)diphenylmethane using dichlorodiphenylmethane and phenol (5). This reaction is based on the British patent by E. Behr (6). Utilizing this chemistry on substituted triphenylmethyl chloride derivatives would give phenol functional blocking groups. Further, it seems feasible to react the substituted triphenylmethyl chloride derivatives with benzene with electron donating substituents, viz., aniline.

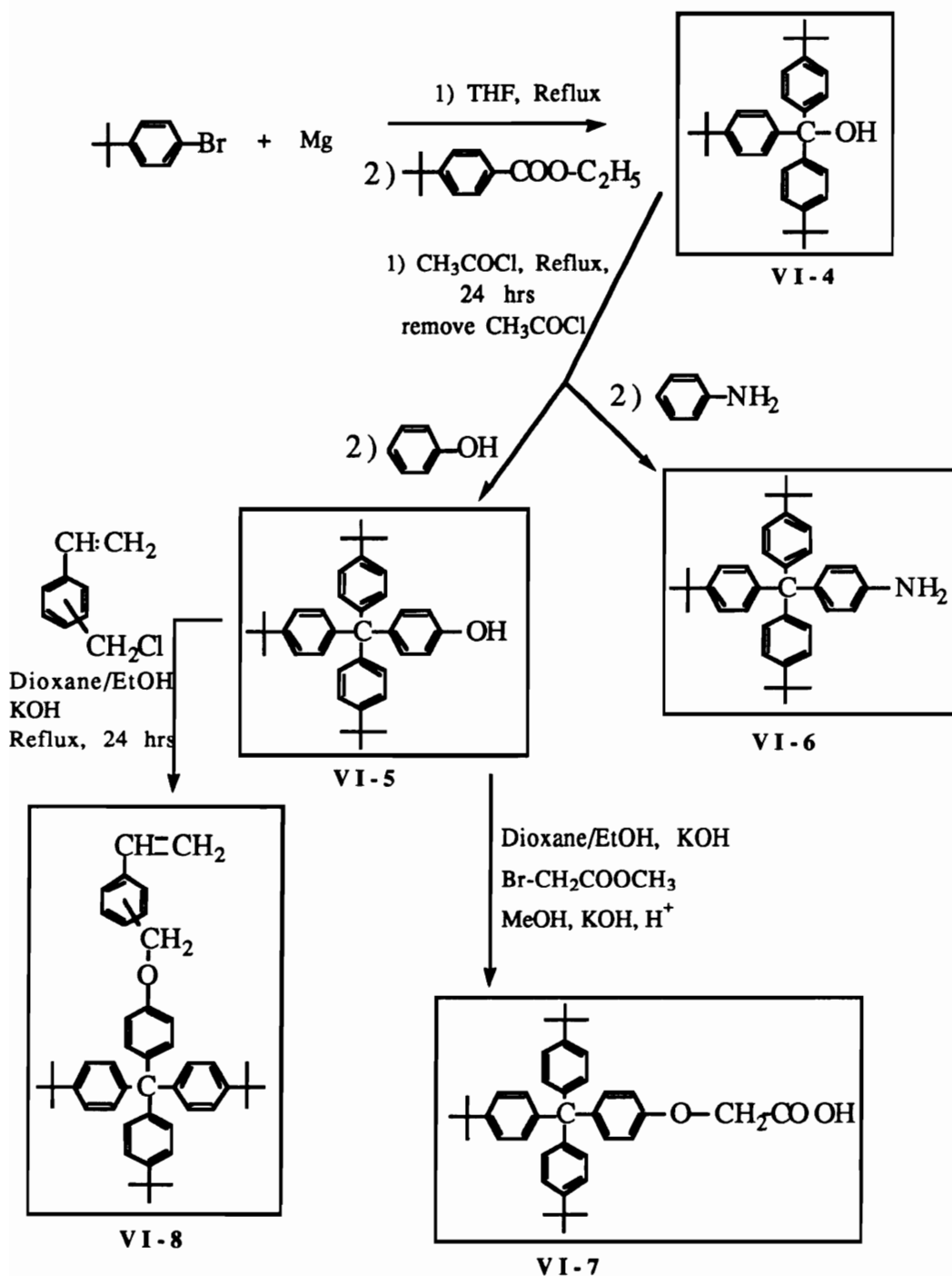
Various reports on reactions of vinylbenzyl chloride and poly(vinylbenzyl chloride) with phenols and other reactive functionalities have been published (7-9). Phenol functional blocking groups can be reacted with vinylbenzyl chloride to yield vinyl functionality on the blocking group. Vinylbenzyl derivatives have been polymerized and copolymerized free radically (7-8). There is no mention of anionic polymerization of vinylbenzyl derivatives. However, the vinyl functional blocking group could be useful for polymerization by either free radical, anionic or cationic methods.

VI.3 Results and Discussion

Blocking Group Synthesis

A schematic of the synthesis of phenol, amine, acid and vinyl functional blocking groups is shown in Scheme VI-1.

Scheme VI-1 Blocking Group Chemistry



Synthesis of **VI-4** was accomplished by Grignard reaction in 70 % yield (30 % side product) using the procedure reported by Marvel and coworkers (4). They reported synthesis of **VI-4** in about 45 % yield. However, they have not commented on rest of the product. Initially it was thought that the remainder (30 %) could be 4,4'-bis-t-butylbiphenyl formed by the coupling of p-t-butylphenyl magnesium bromide. However, the melting point and proton NMR spectrum of 4,4'-bis-t-butylbiphenyl do not match those of the side product. The reported melting point of the 4,4'-bis-t-butylbiphenyl is 129-130 °C while that of the side product is 199.1-200.0 °C. The side product showed sharp peaks at 3582 and 3564 cm^{-1} for hydroxyl groups and peaks at 1107, 1141 and 1015 cm^{-1} corresponding to C-O stretching vibrations. Further, in proton NMR a singlet at 2.97 ppm corresponding to one proton (from integral values) is observed. Elemental analyses showed the empirical formula to be $\text{C}_{20}\text{H}_{26}\text{O}$. These results suggest that the side product may be bis(p-t-butylphenyl)methanol ($\text{C}_{21}\text{H}_{28}\text{O}$).

One of the disadvantages of this chemistry is the high cost of 4-bromo-t-butylbenzene. The yields of **VI-4** can be improved by decreasing the formation of the side product. In our group (10) attempts to make **VI-4** using Friedel-Crafts reaction using t-butylbenzene and carbon tetrachloride have been made. This could decrease the costs considerably. However, loss of t-butyl groups by a retro-Friedel-Crafts process was observed.

In the synthesis of the phenol functional blocking group, information from two different papers was utilized. Marvel et al. (4) have reported the synthesis of tris(p-t-butylphenyl)methyl chloride from **VI-4** (63 % yield). In a paper by Mikroyannidis (5) modification of such chloro derivatives to phenol (81 % yield) has been reported.

The formation of tris(p-t-butylphenyl)methyl chloride by reaction of **VI-4** with acetyl chloride proceeds first by forming acetate, giving off one molecule of HCl, followed by attack of chloride to give off a molecule of acetic acid (11). An earlier

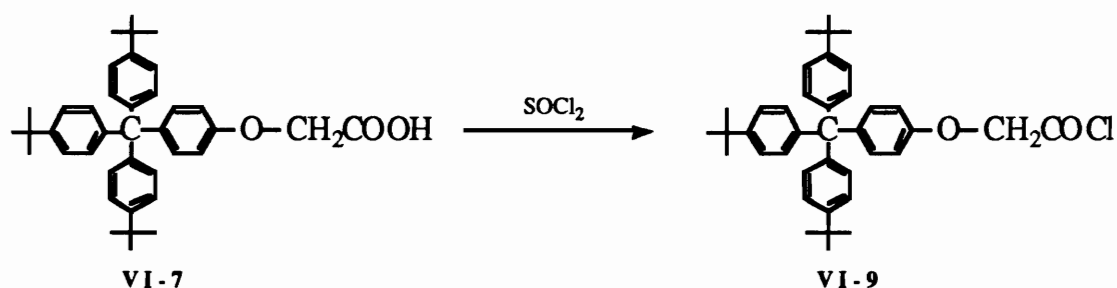
attempt to prepare tris(p-t-butylphenyl)methyl chloride using thionyl chloride and VI-4 was unsuccessful; hence the procedure suggested by Marvel et al. (4) was used. Crude tris(p-t-butylphenyl)methyl chloride thus prepared from VI-4 was reacted with phenol to obtain the phenol functional blocking group (VI-5). Despite lower yields reported for each step, the yield for VI-5 was very high, ca., 97 %. The reaction of the chloro derivative with phenol is a Friedel-Crafts type reaction without the use of catalyst. This reaction also works with benzene substituted with electron donating groups such as aniline to give amino functional blocking group (VI-6). However, the yield of VI-6 was considerably lower (ca., 50 %) than that of VI-5. This may be due to formation of N-tri(p-t-butylphenyl)methyl pyridinium chloride, a salt, that may be soluble in water or methanol and may have been discarded during the work up.

Synthesis of the acid functional blocking group VI-7 was accomplished using two different procedures as reported in the experimental section. Phenol functional blocking group VI-5 was reacted with a base such as KOH (in dioxane:ethanol, 2:1) or NaH (in dry DMF) followed by reaction with 2.6 equivalent of methyl bromoacetate. When excess base was used (greater than 1.2 equivalent) the resulting product had multiple peaks from 3.8-4.8 ppm in proton NMR spectrum. This is due to incorporation of more than one $-\text{CH}_2\text{-COO}-$ groups on the phenol. This is feasible by attack of the enolate of the ester functional blocking group of VI-7 on another molecule of methyl bromoacetate. Upon hydrolysis of this product, acid functional blocking group VI-7 was obtained. The origin of multiple peaks was confirmed by just adding KOH to methyl bromoacetate in THF and refluxing the mixture for 24 hours. The resulting product had similar multiple peaks from 3.8-4.8 ppm. These multiples peaks are due to formation of small oligomers such as dimer, trimer, etc., also termed oligomeric glycolides (12). The ester linkages in the oligomers can be easily hydrolyzed with a base.

Various other attempts to prepare acid functional blocking group in THF and DMF using **VI-10**, 4-chloromethylbenzoic acid and NaH were unsuccessful. No anion formation occurs; there was no color formation. When n-butyllithium was used instead of NaH (reaction done in THF), formation of anions was evident by a dark red color. However, upon addition of much less than stoichiometric quantities of sodium salt of 4-chloromethylbenzoic acid, the color disappeared. The proton NMR spectra of the worked up solids in all the reactions indicated no reaction had occurred and **VI-10** was recovered.

Synthesis of acid chloride functional blocking group **VI-9** is shown in Scheme VI-2. The reaction is straightforward and the yield is quantitative. The crude product from the reaction was not purified further since very pure acid **VI-7** was used. The acid chloride blocking group was used to end block monotaxanes of small molecules as well as polyrotaxanes of preformed polymers.

Scheme VI-2 Acid Chloride Blocking Group (VI-9)



Synthesis of 5,5-bis(p-t-butylphenyl)-5-phenylbutan-1-ol has been reported in about 50 % yield (3). This was accomplished by reacting bis(p-t-butylphenyl)phenylmethane with n-butyllithium in THF at $-78\text{ }^\circ\text{C}$, followed by addition of tetrahydropyran (THP) protected 1-chloropropanol at $0\text{ }^\circ\text{C}$. The resulting product was deprotected to obtain the final product.

Attempts by the author to prepare 5,5,5-tris(p-t-butylphenyl)pentan-1-ol (Table VI-1) using **VI-10** and **VI-11** (THP

protected 4-chlorobutanol) under similar conditions afforded only 5-10 % of **VI-12**. It was surprising to see such a difference in the reactivity of bis(p-t-butylphenyl)phenylmethane and tris(p-t-butylphenyl)methane with n-butyllithium.

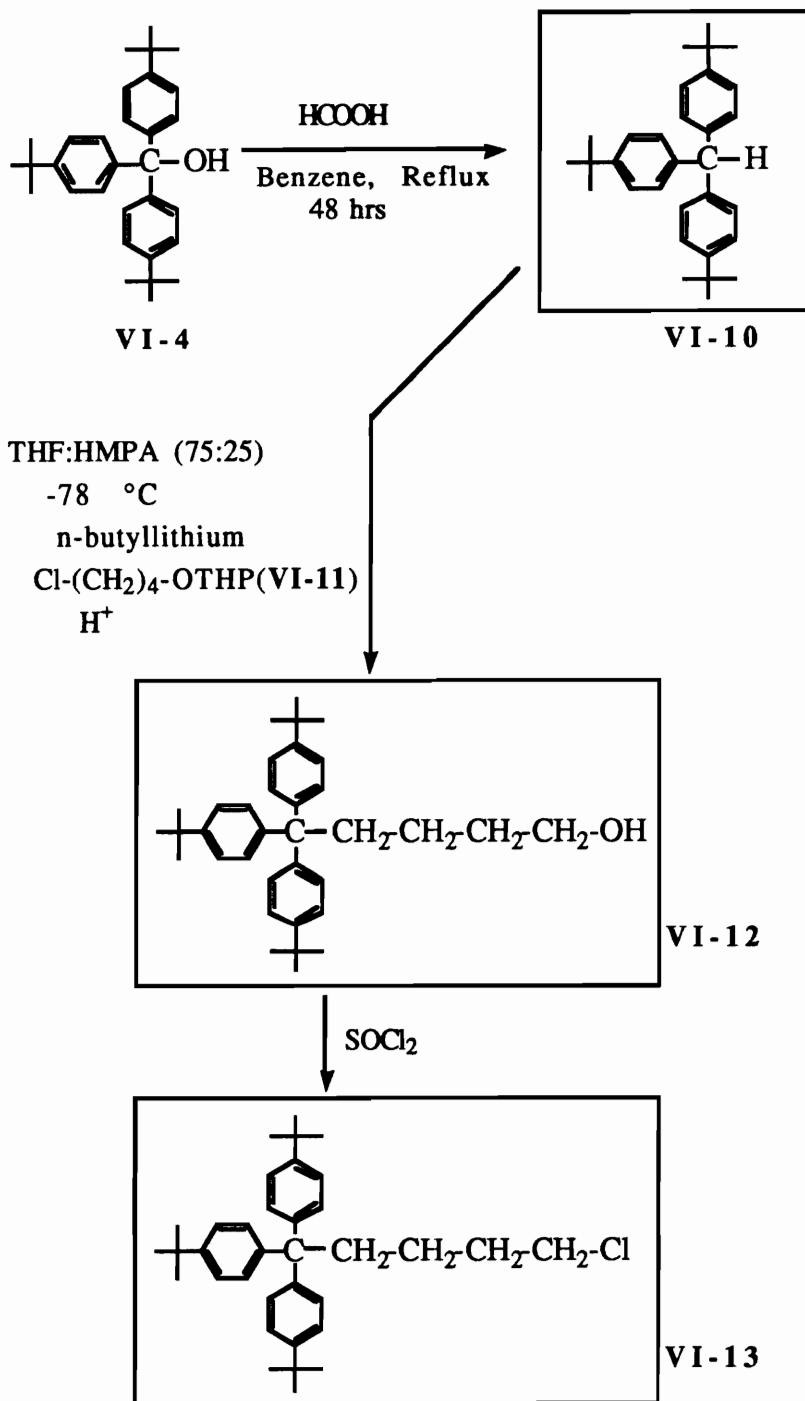
It has been reported by Wang et al. (13) "that in triphenylmethane derivatives, the phenyl groups rotate around the C₆H₅-C bond and that rotation of any phenyl group is affected by the other phenyl groups". Further, "the most favorable conformation of these compound is a propeller-like shape, where phenyl groups are twisted at a 36° angle to each other due to steric hindrance". Furthermore, "the rotation of phenyl groups about the C₆H₅-C bond is prevented if the phenyl groups are substituted by bulky groups". Thus, in the case of tris(p-t-butylphenyl)methane, the steric bulk of three p-t-butylphenyl groups could make the proton less accessible and the resulting anion (by reaction with n-butyllithium) could be less nucleophilic compared to that for bis(p-t-butylphenyl)phenylmethane.

In such S_N2 reactions use of an aprotic, highly polar solvent such as hexamethylphosphoramide (HMPA) could considerably improve the nucleophilicity of the anion and increase the yields of the product (14). In the next attempt to synthesize **VI-12** (Scheme **VI-3**), three equivalents of HMPA (1 eq. of **VI-10**) in THF were used. Anions were formed at -78 °C followed by addition of **VI-11** and gradual warming the reaction mixture yielded product in 33 % yield. When THF:HMPA (75:25) was used as the reaction medium, the yields were significantly higher (ca., 66 %).

Table VI-1 Reaction Conditions and Yields of VI-12

<u>Solvent</u>	<u>Temperature</u>	<u>Results</u>
THF	-78 °C, gradually warmed	5-10 % yield
THF/HMPA(3 eq.)	-78 °C, gradually warmed	33 % yield
THF:HMPA (3:1)	-78 °C, gradually warmed	66 % yield

Scheme VI-3 Synthesis of VI-10, VI-12, and VI-13



Chloro functional blocking group **VI-13** was needed for the end blocking of polystyrene rotaxanes prepared anionically. The living chain ends of polystyrene (polystyryl lithium) can react with chloro functional blocking groups to give lithium chloride and the blocking group is placed at the chain ends. Vinyl functional blocking group **VI-8** could not be used for end blocking of polystyrene rotaxanes prepared anionically due to side reactions as will be discussed in the next section.

Synthesis of **VI-13** was accomplished by reacting hydroxy functional blocking group **VI-12** with thionyl chloride. Pyridine may be added as a catalyst but is not necessary. By mistake excess pyridine was added to the reaction mixture, resulting in the formation of pyridinium salt of the chloro functional blocking group (mp: 260-261 °C (corrected)). The salt forms an emulsion in water.

Polymerization of Vinyl Functional Blocking Group

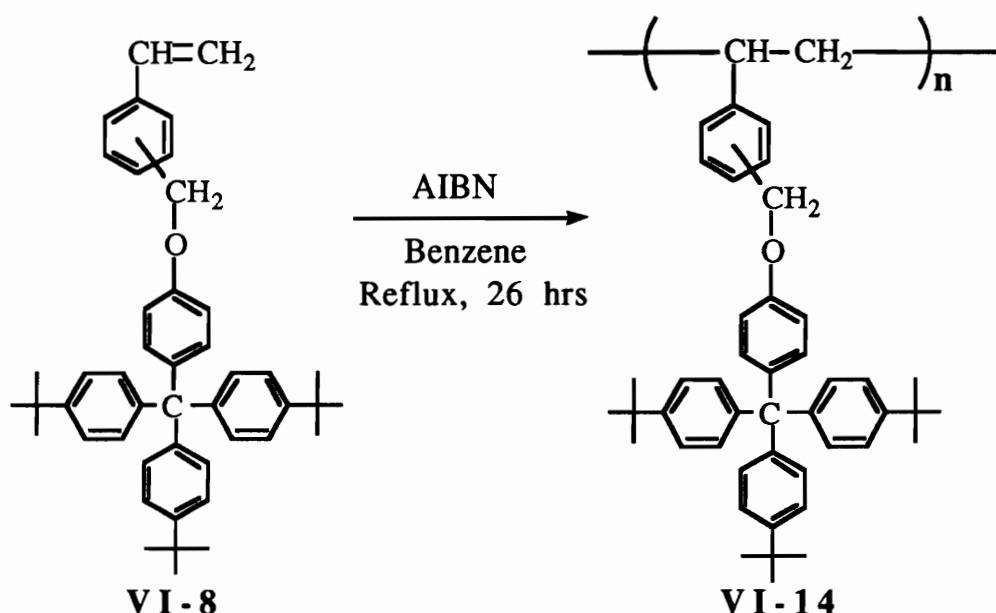
Free radical polymerization as well as modification of vinylbenzyl chloride and its derivatives for a broad range of applications have been reported in the literature (7-9). The specific use of vinylbenzyl chloride monomer in this study was to derivatize phenol functional blocking group **VI-5** so as to generate vinyl functionality on the blocking group **VI-8**. The procedure used for the synthesis of **VI-8** was similar to that reported by Gibson and Bailey (7,8).

Free radical polymerization of **VI-8** (Scheme **VI-4**) was done using azobisisobutyronitrile (AIBN) in benzene to obtain polymer **VI-14**. The number average Molecular weight of the polymer by GPC in THF was found to be 37000 (according to polystyrene standards) with polydispersity index of 1.7. The polymer has T_g of 210 °C and is not crystalline (no T_m).

The T_g of the polymer is higher than typically observed for the vinylic polymers. This is attributable to the reduced polymer chain mobility due to the bulky pendant group. Figures **VI-1**, **VI-2** and **VI-3** show the proton nmr spectra, and GPC and DSC traces (first

and second heat) for polymer **VI-14**. The proton NMR spectrum showed broad peaks for aromatic protons at 7.2-6.3 ppm. The -O-CH₂ protons show a broad peak at 4.8-4.3 ppm and methylene protons at 1.5-1.7 (small peak). Fused multiple peaks are seen 1.29-1.0 ppm for t-butyl groups of the polymer.

Scheme VI-4 Free Radical Polymerization of VI-8



Anionic polymerization of **VI-8** was of interest for several reasons. The first was to study the feasibility of using this monomer to end block living polystyryl anions during the synthesis of polystyrene rotaxanes, since no study on the anionic polymerization of benzyl ether derivatives of vinylbenzyl chloride has been reported. Further, the monomer has a bulky 4-tris(p-t-butylphenyl)methyl benzene group, which due to steric bulk may preferentially orient the living polymer anion and the incoming monomer to give syndiotactic polymer.

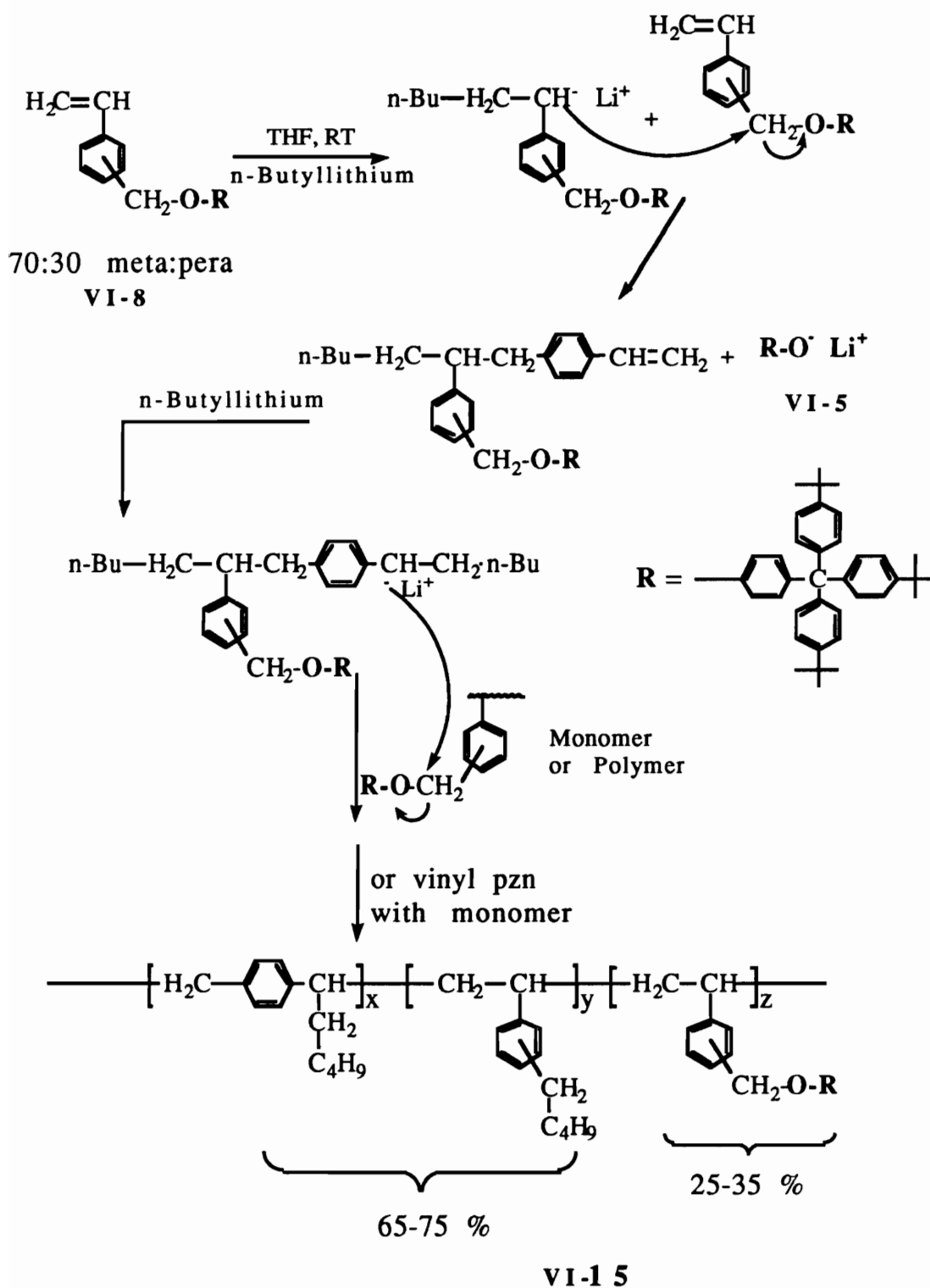
In various attempts to polymerize **VI-8** by n-butyllithium or sodium-naphthalide in THF at 5-10 °C, anions were found to terminate instantly after being formed (evident from occurrence and

disappearance of red color). Initially it was thought that monomer or solvent may be impure; however, after careful purification of both the solvent and monomer the same phenomena was observed. Thus, n-butyllithium was added to the monomer solution in small quantities until the red color of the anion persisted. It took almost the same number of moles of initiator as the number of moles of monomer. During the work up, one of the components of the product was found to have limited solubility in methanol and its proton NMR spectrum was identical to that of phenol blocking group (VI-5) (3.2 g, 73.0 % of the total phenol blocking group). The GPC analyses of the methanol insoluble component showed it to be a polymer VI-15 with number average molecular weight of about 80,000 with polydispersity index of 2.2; the polymer showed Tg at 177 °C by DSC. Figures VI-4 and VI-5 show the proton NMR spectrum and DSC trace (second heat) of the polymer VI-15, respectively.

Scheme VI-5 depicts the formation of the phenol (VI-5) and the possible structure of the polymer.

The formation of phenol blocking group (VI-5) during the polymerization suggests that either n-butyllithium or anions formed by the reaction of n-butyllithium with the vinyl group of the monomer attack the benzyl ether linkages; however, formation of red color upon each addition of n-butyllithium as well as formation of the polymer suggest that styryl anion formation followed by attack on the benzyl ether linkages is predominant. The polymer is soluble in THF, acetone and chloroform, indicating that polymer is not highly crosslinked; this argues for the attack of the styryl anions on benzyl ether linkages. This would lead to the formation of polymer containing phenyl groups in the main chain linked with -CH₂- and -CH(C₅H₉)- groups on the either side as shown in the Scheme VI-5. However, if attack of n-butyllithium on benzyl ether linkages is also occurring then the resulting structure would be a m- or p-substituted n-pentylstyrene, which could copolymerize. Structure VI-15 shows these two types of repeat units containing n-pentyl pendent groups. Further, the yield of the isolated polymer (2.5 g)

Scheme VI-5 Anionic Polymerization of VI-8



was much higher than can be accounted for these two types of the repeat units containing n-pentyl groups. From the yields of the isolated phenol blocking group and the polymer as well as from the proton and semiquantitative DEPT ^{13}C NMR spectra, it was found that about 25-35 % of the repeat units have the benzyl ether linkages intact. Thus, about 25-35 % of the monomer (VI-8) was also incorporated in the polymer without the loss of the phenol blocking group. The exact structure of the polymer is not known. The ratio of integral values of aromatic protons to aliphatic protons is about 0.5-0.6 and the proton NMR spectrum of the polymer is consistent with the suggested structure. The aromatic protons appear as broad peaks from 7.3-6.0 ppm whereas $-\text{CH}_2$ and $-\text{CH}_3$ protons of t-butyl and n-pentyl groups appear at 0.7-1.3 ppm. These assignment was confirmed by DEPT ^{13}C NMR. The methylene and methine groups attached to phenyl groups appear as broad peaks at 1.5-3.0 ppm and the $-\text{O}-\text{CH}_2$ protons appear at 4.2-4.9 ppm. Traces of t-butyl groups from the monomer or phenol functional blocking group are seen as a small sharp singlet at 1.29 ppm.

VI.4 Experimental

Measurements:

Melting Points were taken in capillary tubes with a Haake-Buchler melting point apparatus and have been corrected. Proton and carbon NMR spectra were obtained on a Bruker WP 270 spectrometer or a Varian Unity 400 MHz spectrometer using chloroform solutions with tetramethylsilane as an internal standard. Elemental analyses were performed by Atlantic Microlab of Norcross, GA. DSC data were obtained using a Perkin-Elmer DSC-2 instrument at a scan rate of 10 $^{\circ}\text{C}/\text{min}$. FTIR spectra were obtained on a Nicolet MX-1 instrument. GPC analyses of the polymers were done at 30 $^{\circ}\text{C}$ in THF using a Waters system (RI and UV detectors) after calibration with PS standards.

Synthesis of tris(p-t-butylphenyl)methanol (VI-4):

13.7 g (0.56 moles) of Mg was placed in 150 ml of THF in a 2 l, 3 neck flask and stirred vigorously with a magnetic stirrer. To this mixture about 15 mg of iodine was added. After 5 minutes of stirring 80.0 g (0.38 moles) of 4-bromo-t-butylbenzene, dissolved in 200 ml THF, was added dropwise using an addition funnel. No sign of reaction was observed after adding 20 ml of the solution so the reaction mixture was warmed with a heat gun. The reaction started and the rate of addition was adjusted such that the reaction mixture was at refluxing temperature. The addition was completed in 1 hour. After that the reaction was allowed to stir for 2 hours without heating and then 37.0 g (0.18 moles) of methyl 4-t-butylbenzoate was added to the Grignard reagent. After the addition was complete the mixture was refluxed for 3 more hours.

The reaction mixture was added to cold 5 % HCl to dissolve the salts and then extracted 3 times (3 x 500 ml) with dichloromethane. The dichloromethane was removed by rotary evaporation. The product was crystallized from methanol or ethanol.

This procedure was repeated several times to prepare more tris(p-t-butylphenyl)methanol. In all the cases the yield was about 70 %; mp: 214.6-215.8 °C (corrected); reported 212-213 °C (4). IR (KBr): 3576 (sharp, OH), 3084, 3056, 3029 (aromatic), 2974, 2903, 2865 (aliphatic), 1507, 1470, 1463 (aromatic), 1320, 1306 1268, 1160 (OH bending) 1008, 1019, 1005, 923, 910 (C-O), 841, 834, 821, 705, 582 cm^{-1} . NMR (CDCl_3): 7.32, 7.29; 7.17, 7.20 (aromatic, 2 d, 12H), 1.30 (- CH_3 , s, 27H).

The rest of the product (30 % yield) has mp of 199.6-200.4 °C (corrected). IR (KBr): 3582, 3564 (OH), 3087, 3033 (aromatic), 2955, 2948, 2901, 2863 (aliphatic), 1509, 1476 (aromatic), 1270, 1107, 1141, 1015, 838, 824, 800, 695, 580 cm^{-1} . NMR (CDCl_3): 7.20, 7.17; 7.16, 7.13 (aromatic, 2 d, 8H), 2.97 (? , s, 1H), 1.26 (- CH_3 , s, 18). Elemental analyses of the side product; found: C 85.10 %, H 9.21 %, O 5.69 % (by difference); empirical formula: $\text{C}_{20}\text{H}_{26}\text{O}$. These results suggest that the side product is bis(p-t-butylphenyl)-

methanol. Reported mp: 103-104 °C (15); 220.5-221.2 °C (16). The melting points for this compound do not match with any of the reported values.

Synthesis of p-hydroxyphenyl-tris(p-t-butylphenyl)-methane (VI-5):

20.0 g (4.66×10^{-2} moles) of tris(p-t-butylphenyl)methanol was dissolved in 80.0 ml (21 eq.) acetyl chloride and the reaction mixture was heated to reflux for 24 hours. The reaction mixture was then cooled; excess acetyl chloride was removed using aspirator vacuum. A light cream yellow solid was left in the flask. This crude product was converted to p-hydroxyphenyl-tris(p-t-butylphenyl)-methane by adding 44.0 g phenol (11 eq.) and letting it react for 20 hours at 100 °C. Upon addition of phenol the solution was dark blood red color which disappears in about 2-3 hours and the dirty dark yellow viscous liquid solidifies. The reaction mixture was cooled and the solid was washed with hot and cold (3 x 100 ml) water to remove phenol. The solid was then treated with 1 % sodium hydroxide solution and warmed to remove traces of phenol, filtered, washed with (2 x 50 ml) water and acidified, again washed with water and recrystallized from ethanol. The IR spectrum shows phenol groups at 3400 cm^{-1} distinct from that of the precursor methanol. The yield was 97.0 %, mp: 301-303 °C (corrected, decomposed); reported mp: 304-306 °C (10). IR (KBr): 3473 (OH, broad), 3084, 3029 (aromatic), 2960, 2906, 2880 (aliphatic), 1607, 1593, 1504, 1463 (aromatic), 1265, 1176 (OH bending for phenol), 1019, 841, 824, 705, 595, 575, 527 cm^{-1} . NMR (CDCl_3): 7.24, 7.21; 7.09, 7.06 (aromatic, 2 d, 12H), 7.02 (d, 2H), 6.75, 6.70 (d, 2H) 1.30 ($-\text{CH}_3$, s, 27H).

Synthesis of p-aminophenyl-tris(p-t-butylphenyl)methane (VI-6):

10.0 g (2.33×10^{-2} moles) of tris(p-t-butylphenyl)methanol was dissolved in 40.0 ml of acetyl chloride and the reaction mixture

was heated at reflux for 24 hours. The reaction mixture was then cooled; excess acetyl chloride was removed using aspirator vacuum. A light cream yellow solid was left in the flask. The above crude product was converted directly to p-aminophenyl-tris(p-t-butylphenyl)methane by adding 30 ml dry aniline (14 eq.) and letting it react for 36 hours at 100 °C. Upon addition of aniline the color of the solution changed to dark red-purple and with time became purple. After the reaction was over, the product was precipitated in 800 ml water containing 20 ml con HCl, stirred for 30 minutes, filtered and washed with water. The product was purified by removing unreacted materials in hot methanol; pure yield: 50 %, mp: 283-286 °C (corrected, decomposed); reported mp: 285-287 °C (10). IR (KBr): 3443, 3362 (-NH₂, sharp peaks), 3088, 3026 (aromatic), 2984, 2898, 2866 (aliphatic), 1621, 1507, 1460 (aromatic), 1269, 1187, 1019, 840, 823, 706, 595-577 cm⁻¹. NMR (CDCl₃): 7.23, 7.20; 7.11, 7.08 (aromatic, 2 d, 12H), 6.94, 6.97 (d, 2H), 6.54, 6.57 (d, 2H), 3.56 (-NH₂, s, 2H) 1.30 (-CH₃, s, 27H).

Synthesis of Acid functional blocking group (VI-7):

15.0 g (3.0 x 10⁻² moles) of p-hydroxyphenyl-tris(p-t-butylphenyl)methane (VI-5) were dissolved in 240 ml dioxane and 140 ml ethanol was added. To this 2.85 g of 87 % KOH (1.7 eq) was added and the mixture was allowed to stir and reflux for 14 hours. To this solution 5.7 ml (2.0 eq) of methyl bromoacetate was added and the solution was refluxed for 72 hours. The solution was cooled, acidified with con. HCl and to this 500 ml water was added slowly to precipitate the product. It was stirred for 15 minutes and filtered and washed with warm water (5 x 500 ml) and allowed to air dry and then it was suspended in methanol, stirred for 4 hours and filtered and washed with (4 x 100 ml) methanol and air dried. The NMR spectrum showed multiple peaks from 3.8 ppm to 4.8 ppm. Hence, the product was dissolved in 500 ml hot ethanol and 10 ml water and to this 4.0 g of 87 % KOH was added with stirring. Immediately precipitate began to come out of the solution and it

became difficult to stir. Hence, 400 ml water was added to the mixture and it was stirred overnight. It was filtered and washed with (4 x 500 ml) water. The precipitate was then placed in 600 ml water, acidified using con. HCl, stirred for 2 hours, filtered and washed with (2 x 500 ml) water and dried under vacuum for 24 hours; mp: 297.5-299 °C (corrected, decomposed), yield = 90 %. IR (KBr): 3418 (OH, broad), 3084, 3036 (aromatic), 2960, 2906, 2872 (aliphatic), 1737 (C=O), 1607, 1586, 1504, 1463 (aromatic), 1265, 1169 (broad, OH bending), 1087, 1019, 841, 824, 705, 609, 582, 527 cm^{-1} . NMR (CDCl_3): 7.24, 7.21; 7.08, 7.05 (aromatic, 2 d, 12H), 7.14, 7.11 (d, 2H), 6.80, 6.77 (d, 2H), 4.52 (- CH_2 , s, 2H) 1.30 (- CH_3 , s, 27H). Elemental analyses for $\text{C}_{39}\text{H}_{46}\text{O}_3$; theory: C 83.23 %, H 8.24 %, O 8.53 %; found: C 83.33 %, H 8.25 %.

In another attempt the reaction was done in dry DMF using NaH (1.1 eq) as base and 2.6 eq of methyl bromoacetate. The resulting ester was recrystallized from hot ethanol; mp: 212-213 °C (corrected), yield = 93 %. The IR spectrum shows the carbonyl group at 1764-1744 cm^{-1} . Hydrolysis of the ester afforded the acid with the same melting point reported above. Ester: IR (KBr): 3084, 3029 (aromatic), 2960, 2906, 2865 (aliphatic), 1764, 1744 (C=O), 1607, 1500, 1504, 1463 (aromatic), 1273, 1204, 1183 (broad, OH bending), 1108, 1087, 1019, 841, 821, 705, 609, 582 cm^{-1} . NMR (CDCl_3): 7.25, 7.21; 7.08, 7.04 (aromatic, 2 d, 12H), 7.11 (d, 2H), 6.78, 6.75 (d, 2H), 4.60 (- CH_2 , s, 2H), 3.80 (- CH_3 , s, 3H) 1.30 (- CH_3 , s, 27H). Elemental analyses for $\text{C}_{40}\text{H}_{48}\text{O}_3$; theory: C 83.29 %, H 8.39 %, O 8.32 %; found: C 82.53 %, H 8.37 %. The ester may be solvated with ethanol (3 ester blocking group : 1 ethanol) as it was crystallized from ethanol.

Synthesis of Acid Chloride Functional Blocking Group (VI-9):

7.04 g (1.25×10^{-2} moles) of VI-7 was placed in a 250 ml round bottom flask under nitrogen equipped with a stirring bar, condenser and nitrogen bubbler. To this 13.3 ml of thionyl chloride

was added and stirred for few minutes and a thick pasty liquid formed so 15.0 ml more thionyl chloride was added (total 0.36 moles, 30 equivalents). The mixture was refluxed to obtain a light yellow orange solution, with the evolution of HCl. It was refluxed for 13 hours. It was then cooled and then excess thionyl chloride was removed under aspirator vacuum and gentle heat. A light yellow colored solid was obtained which was first dried under aspirator vacuum for 1 hour and then under vacuum of 0.01 torr for overnight. The crude product was used for the reactions since the starting acid was pure. Yield: quantitative (7.15 g); mp: 270-272 °C (corrected). NMR (CDCl₃): 7.25, 7.22; 7.07, 7.04 (aromatic, 2 d, 12H), 7.14, 7.11 (d, 2H), 6.76, 6.73 (d, 2H), 4.92 (-CH₂, s, 2H) 1.30 (-CH₃, s, 27H).

Synthesis of the Vinyl Functional Blocking Group (8):

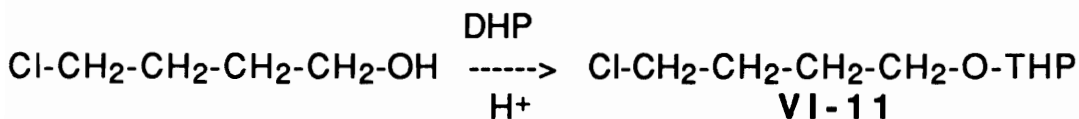
7.0 g (1.4 x 10⁻² moles) of p-hydroxyphenyl-tris(p-t-butylphenyl)methane (VI-5), 1.35 g of 87 % KOH (1.7 eq.), 50 ml dioxane and 25 ml ethanol were placed in a 500 ml round bottom flask. Upon heating p-hydroxyphenyl-tris(p-t-butylphenyl)methane dissolved. The resulting potassium phenolate precipitated and dissolved upon addition of 50 ml dioxane and heating. After 10 minutes, 3.6 ml (1.52 eq) of vinylbenzyl chloride (70 % meta and 30 % para mixture) was added dropwise using a syringe. The reaction mixture was refluxed for a total of 64 hours, cooled and 300 ml water was added. The resultant solid was filtered and then washed with (4 x 400 ml) water. It was then placed in methanol and stirred for 30 minutes, filtered and washed with methanol. The filtrate was light yellow in color; hence, the above step was repeated one more time. The monomer was precipitated from THF into 10 fold excess methanol and dried under vacuum; pure yield: 93.2 % yield of white powdery compound, mp= 233.8-234.6 °C (corrected). Efforts to isolate meta and para isomers using a variety of combination of solvents were not successful. IR (KBr): 3088, 3033 (aromatic), 2960, 2902, 2866 (aliphatic), 1605, 1581, 1507, 1473, 1460 (aromatic), 1223, 1186, 1109, 1019, 987, 906, 841, 825, 712-707, 597-578 cm⁻¹. NMR

(CDCl₃): 7.46-7.33 (m, aromatic, 4H), 7.24, 7.21; 7.09, 7.06 (aromatic, 2 d, 12H), buried under aromatic peaks (d, 2H), 6.83, 6.86 (d, 2H), 5.79-6.67 (=CH, 4s, 1H), 5.80-5.72 (=CH₂, 2d, 1H), 5.28-5.23 (=CH₂, 2d, 1H), 5.01 (-CH₂, s, 2H) 1.30 (-CH₃, s, 27H). Elemental analyses for C₄₆H₅₂O; theory: C 88.98 %, H 8.44 %, O 2.58 %; found: C 88.87 %, H 8.46 %.

Synthesis of tris(p-t-butylphenyl)methane (VI-10):

10.0 g of tris(p-t-butylphenyl)methanol (0.023 moles) was dissolved in 150 ml benzene. To this 100 ml HCOOH was added and the biphasic mixture was refluxed for 48 hours. The color of the solution turned dark yellow during this period. The mixture was washed with water (2 x 100 ml), 5 % KOH (3 x 100 ml) and water (3 x 100 ml). The organic phase was removed by rotary evaporation. Crude product was crystallized once from 50:50 methanol:acetone. Pure yield = 9.3 g (97.2 %), mp 179.5-180.6 °C (corrected). IR (KBr): 3050, 3023 (aromatic), 2961, 2945, 2862 (aliphatic), 1507, 1474, 1464, 1405, 1392 (aromatic), 1267, 1201, 1109, 1019, 956, 840, 819, 792, 695-687, 582, 544 cm⁻¹. NMR (CDCl₃): 7.29, 7.26; 7.06, 7.03 (aromatic, 2 d, 12H), 5.42 (-CH, s, 1H) 1.29 (-CH₃, s, 27H). Elemental analyses for C₃₁H₄₀; theory: C 90.23 %, H 9.77 %; found: C 90.28 %, H 9.81 %.

Synthesis of Protected 4-Chlorobutanol (VI-11):



This reaction was done using procedure similar to that described for the synthesis of protected chloroethanol (in chapter III). The product was distilled at 77- 85 °C, under a vacuum of 0.5-1 torr. After two distillations the yield was 78.6 %. The IR spectrum of the product did not show any -OH groups.

Synthesis of 5,5,5-tris(p-t-butylphenyl)pentan-1-ol (VI-12):

8.0 g (0.019 moles) of tris(p-t-butylphenyl)methane (VI-10) was dissolved in 400 ml of dry THF and 100 ml of hexamethylphosphoramide and cooled to -78 °C. To this 1.3 eq of n-butyllithium was added and the color of the solution turned dark blood red. The solution was stirred for an hour followed by addition of 5.5 g (0.028 moles) of protected chlorobutanol using a syringe. The reaction was allowed to warm up overnight for 12 hours. The dark red blood color had disappeared. To this solution 20 ml con. HCl was added and it was stirred for 30 minutes, after which organic and aqueous layers were separated. The organic layer was rotary evaporated to obtain solid crude product. The product was crystallized from hexanes. Yield: 6.25 g (66 %); mp.: 209.8-210.6 °C (corrected). IR (KBr): 3295 (OH), 3050, 3023 (aromatic), 2955-2868 (aliphatic), 1066-1046 (doublet, C-O-H) cm^{-1} . NMR (CDCl_3): 7.12, 7.16; 7.21, 7.25 (aromatic, 2 d, 12H), 3.55 (α - CH_2 , t, 2H), 2.54 (δ - CH_2 , t, 2H), 1.56 (β - CH_2 , p, 2H), 1.14-1.20 (γ - CH_2 , p, 2H), 1.29 (- CH_3 , s, 27H). Elemental analyses for $\text{C}_{35}\text{H}_{48}\text{O}$; theory: C 86.72 %, H 9.98 %, O 3.3%; found: C 86.46 %, H 10.00 %.

Synthesis of 1-chloro-5,5,5-tris(p-t-butylphenyl)pentane (VI-13)

5.0 g (0.01 moles) of 5,5,5-tris(p-t-butylphenyl)pentan-1-ol (VI-12) was dissolved in 40 ml thionyl chloride. To this 2.0 ml pyridine was added. (This was a mistake and is not needed). The solution was refluxed for 24 hours, cooled and excess thionyl chloride was distilled under aspirator vacuum. The remaining semisolid was poured into cold water and filtered. The solid was dried and product was extracted by hexanes; crude yield 3.11 g (60 %). Product was purified by passing it through a 10 cm long silica gel column using hexanes as the mobile phase. The columned product was purified further by recrystallization from 75:25

methanol:acetone; mp: 138.4-139.2 °C (corrected). IR (KBr): 3050, 3023 (aromatic), 2961-2868 (aliphatic), 727 (CH₂-Cl) cm⁻¹. NMR (CDCl₃): 7.12, 7.16; 7.22, 7.27 (aromatic, 2 d, 12H), 3.44 (α-CH₂, t, 2H), 2.52 (δ-CH₂, t, 2H), 1.75 (β-CH₂, p, 2H), 1.1-1.2 (buried under t-butyl peak and side bands) (γ-CH₂, p, 2H), 1.29 (-CH₃, s, 27H). Elemental analyses for C₃₅H₄₇Cl; theory: C 83.54 %, H 9.41 %, Cl 7.05 %; found: C 83.42 %, H 9.42 %. The rest of the 40 % of the product is the pyridinium salt of 1-chloro-5,5,5-tris(p-t-butylphenyl)pentane mp: 260-261 °C (corrected).

Polymerization of Vinyl Functional Blocking Group (VI-8):

Free Radical Polymerization:

2.17 g (3.5×10^{-3} moles) of VI-8 was dissolved in 25 ml dry benzene at about 60-70 °C (in an oil bath) followed by addition of 7.0 mg (4.0×10^{-5} moles) of azobisisobutyronitrile (AIBN) dissolved in 5 ml dry benzene. The solution was refluxed for 26 hours. The reaction mixture was cooled and precipitated in 10 fold excess methanol, filtered and dried; yield = 2.1 g (97 %). $\langle M_n \rangle = 37,000$ (GPC molecular weight, polystyrene standards); polydispersity index: 1.7. DSC: T_g = 210 °C, no T_m. The FTIR spectrum of the polymer was identical to that of vinyl functional blocking group except that peaks at 987 and 906 cm⁻¹ were absent in the polymer. NMR (CDCl₃): 7.2-6.8; 6.8-6.3 (very broad, aromatic, 16H), 4.8-4.3 (-O-CH₂, very broad, 2H), 1.5-1.7 (broad, -CH₂, 2H), 1.29 (t-butyl of residual monomer, sharp singlet), 1.29-1.0 (t-butyl groups 27H).

Anionic Polymerization:

THF was distilled once from sodium-benzophenone and then styrene and n-butyllithium were added to it; the solution was freeze-thawed on the vacuum line (ca 10⁻⁵ torr) 5-6 times, distilled on the vacuum line and stored in the glove box ([H₂O] = 0.6 ppm, [O₂] = 0.32 ppm).

5.4 g (8.69×10^{-3} moles) of **VI-8** was dissolved in 100 ml THF by warming the mixture using a heat gun in the glove box. Upon addition of 0.5 ml of 0.22 M n-butyllithium (1.08×10^{-4} moles) the red color of the anion formed and disappeared immediately. Thus, more n-butyllithium was added in small quantities until the red color persisted. It took almost 8.7×10^{-3} moles of n-butyllithium to get the red color of the anion to persist. The anions were terminated using methanol and the polymer was precipitated in 1 l methanol followed by purification of the polymer by suspending it in hot ethanol (repeated thrice). Solid was filtered and dried; yield = 2.5 g. GPC $\langle M_n \rangle = 80,000$ (polystyrene standards); polydispersity index: 2.2. NMR (CDCl_3): 7.3-6.0 (broad, aromatic), 4.9-4.2 (-O-CH₂, broad), 1.5-3.0 (broad, -CH₂ and -CH), 1.29 (traces of t-butyl of residual monomer or phenol), 1.3-0.7 (t-butyl and n-pentyl); the ratio of integration values of aromatic protons to aliphatic protons was about 0.5-0.6. DSC: T_g = 177 °C, no T_m. The methanol-ethanol soluble part was recovered and analyzed; yield = 3.2 g (73.0 % of the total phenol blocking group). The proton NMR spectrum of the alcohol soluble solid was identical to that of phenol functional blocking group (**VI-5**).

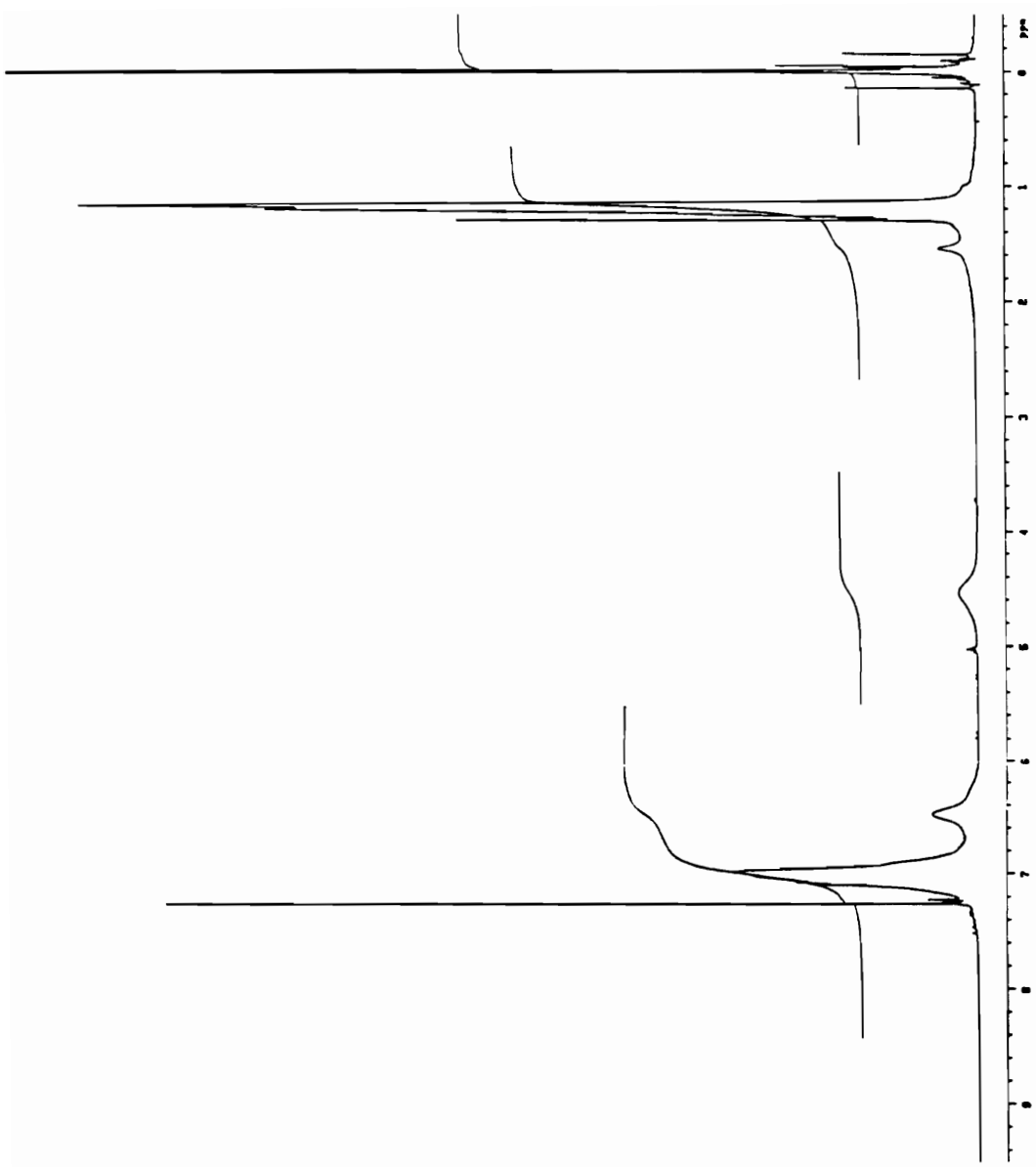


Figure VI.1 ^1H (400 MHz) NMR of VI-14

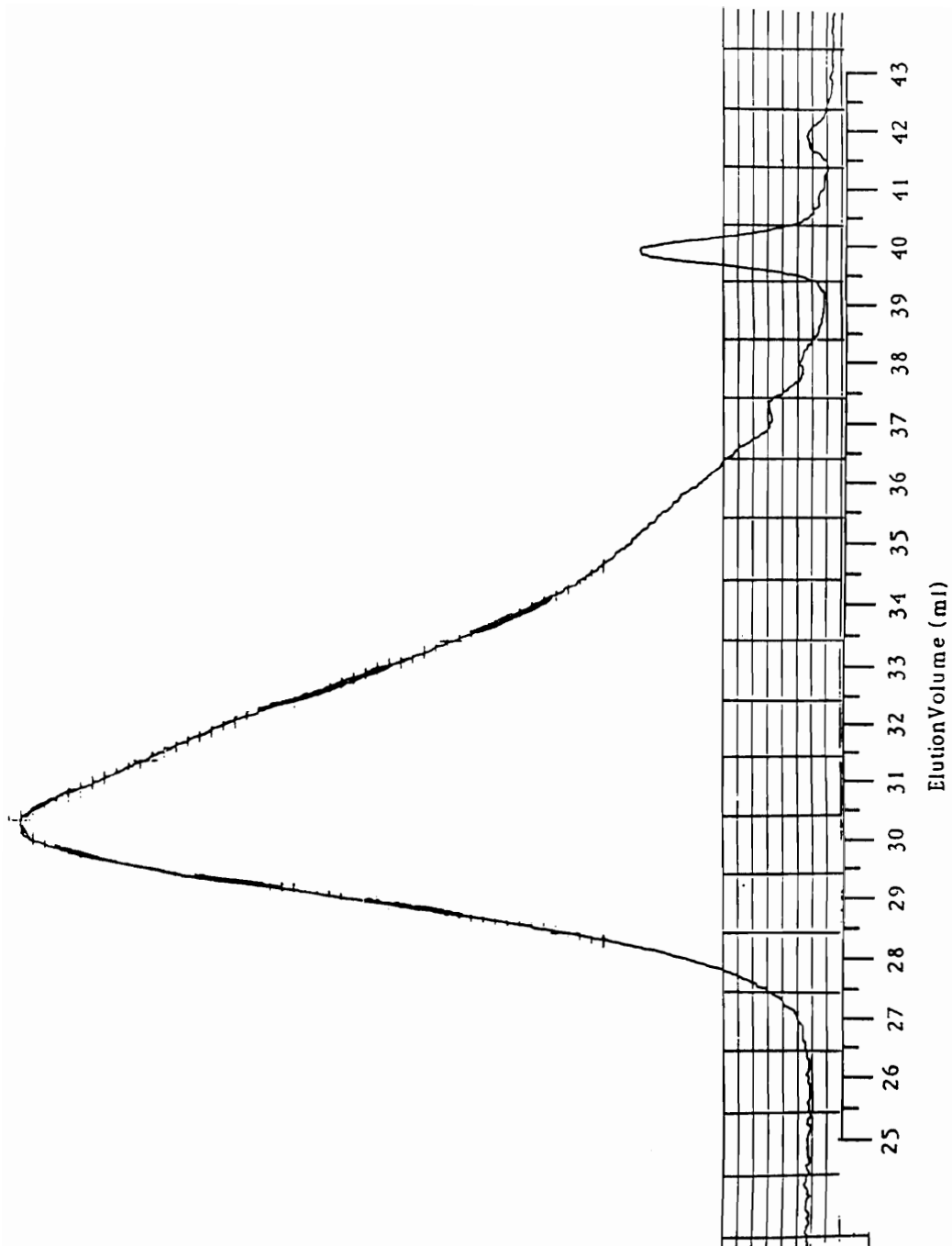


Figure VI.2 GPC Trace of VI-14 (RI Trace)

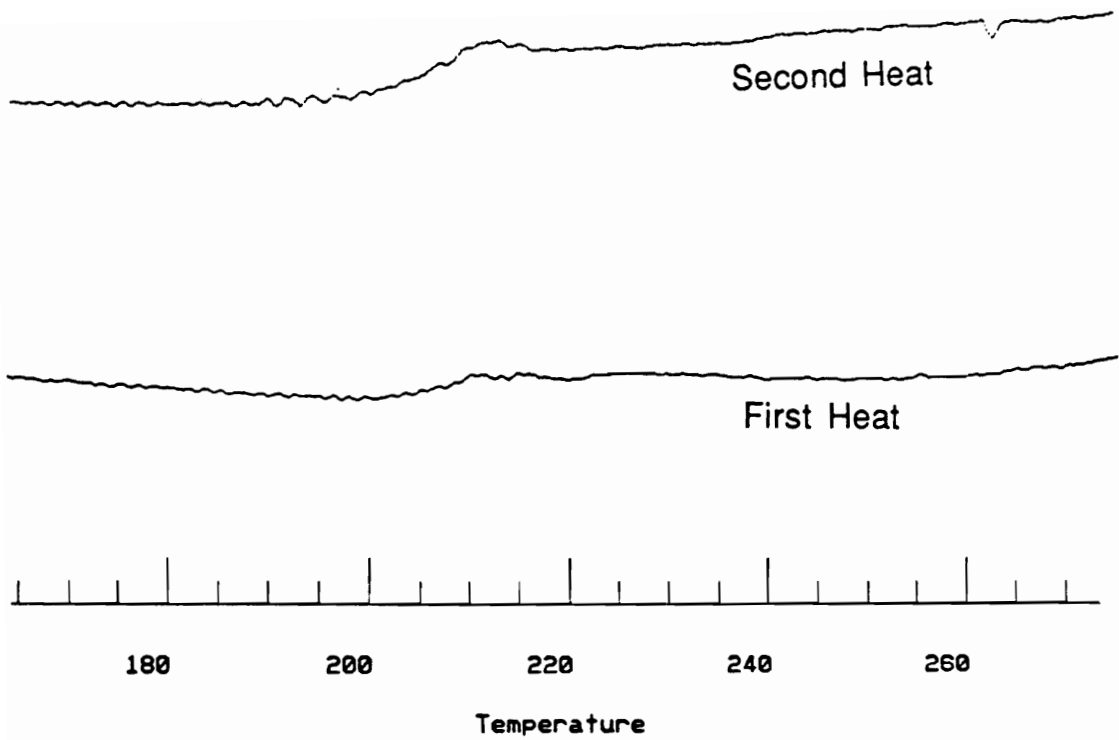


Figure VI.3 DSC Traces of VI-14

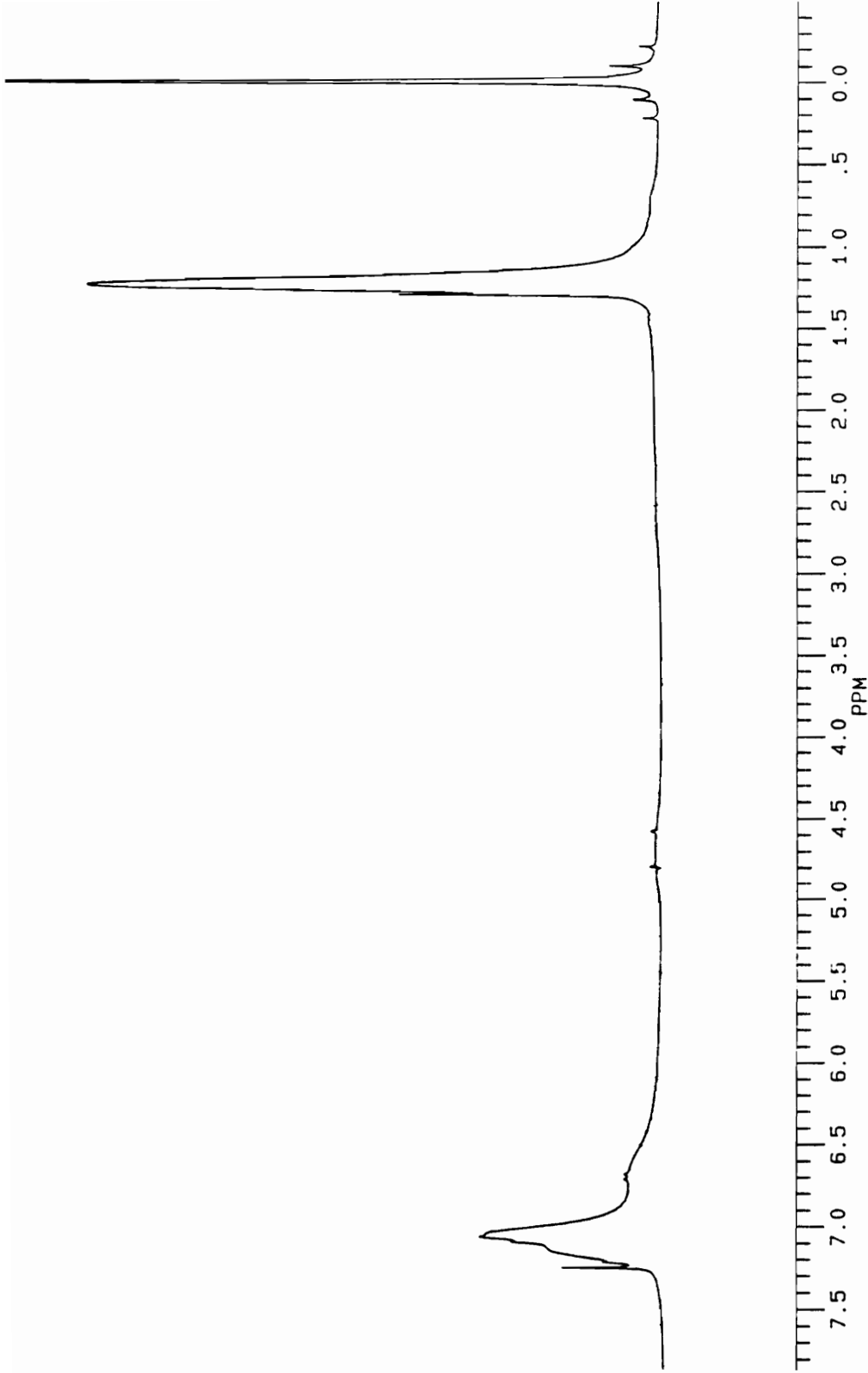


Figure VI.4 ^1H (270 MHz) NMR of VI-15

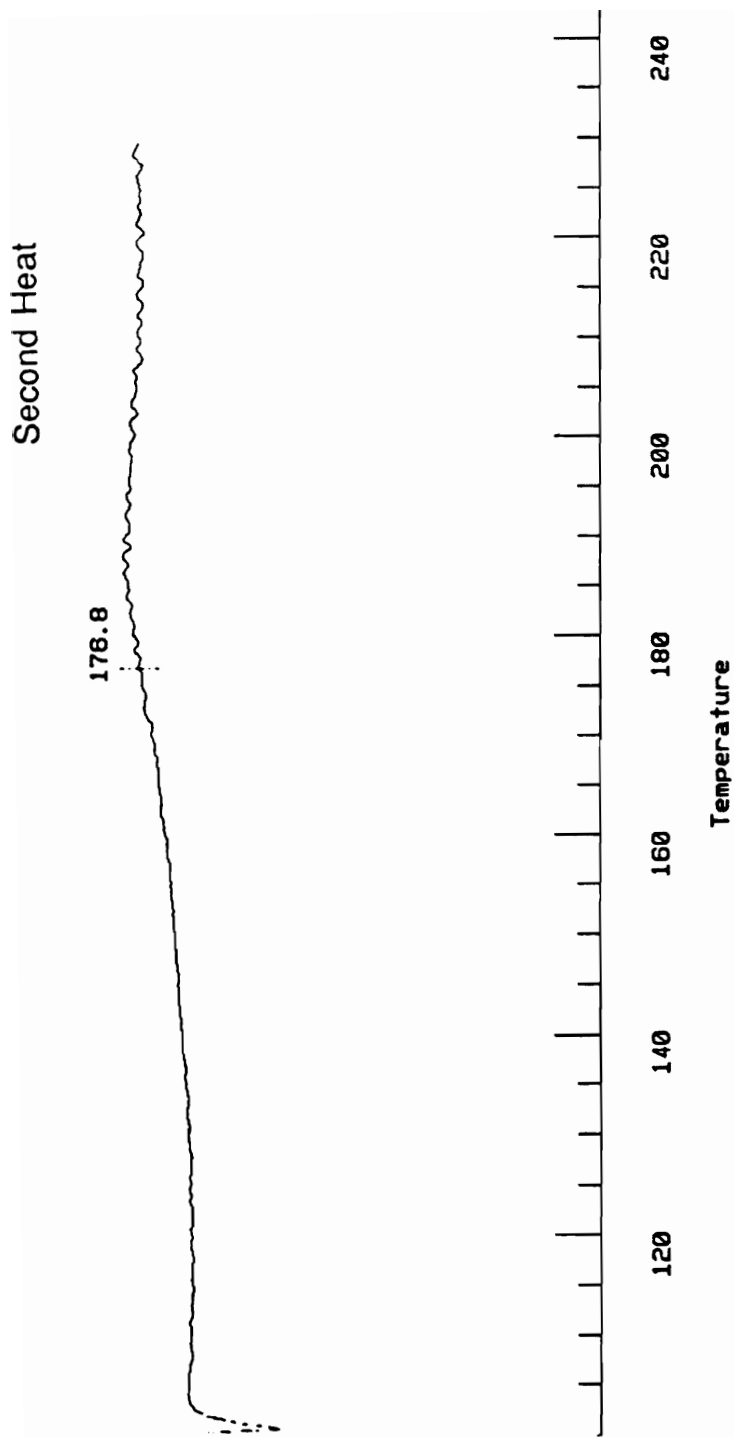


Figure VI.5 DSC Trace of VI-15

References

1. I. T. Harrison, J. C. S. Perkin I, 1974, 301.
2. P. L. Lecavalier, Unpublished Results.
3. Y. X. Shen, Ph.D. Thesis, Virginia Tech 1992.
4. C. S. Marvel, J. F. Kaplan and C. M. Himel,
J. Am. Chem. Soc., 1941, 63, 1892.
5. J. A. Mikroyannidis, Eur. Polym. J., 1985, 10, 895.
6. E. Behr, Br. Pat., 1,184, 289 (1970);
Chem. Abstr., 73, 3657n, 1970.
7. H. W. Gibson, F. C. Bailey, J. Polym. Sci., Poly. Chem. Ed.,
1974, 12, 2141.
8. H. W. Gibson, F. C. Bailey, Macromolecules, 1977, 10, 602.
9. Vinylbenzyl Chloride, Product Brochure, Dow Chemical
U.S.A., Midland, MI-48640, 1988.
- 10 Jean Sze, M. S. Thesis, Virginia Tech, 1992.
- 11 M. Gomberg, Chem. Rev., 1924, 1, 91.
- 12 A. Guido and G. Tagliavini, Ricerca Sci., 1958, 28, 2245.
13. Y. Wang, M. Ding and F. Wang, Makromol. Chem.,
1991, 192, 1769.
14. Jerry March, "Advanced Organic Chemistry", 3rd Ed.,
John Wiley & Sons, New York, NY., p. 316.
15. M. P. Balfe, J. Kenyon, E. M. Thain, J. Chem. Soc., 1952, 790.
16. N. C. Deno, J. J. Jaruzelski, A. Schriesheim,
J. Am. Chem. Soc., 1955, 77, 3044.

VII.	MONOROTAXANES AND POLYROTAXANES 150
VII.1	Introduction 151
VII.2	Results and discussion 152
	Monorotaxanes 153
	Polyrotaxanes of Preformed Polymers 156
VII.3	Experimental 162

VII.1 Introduction

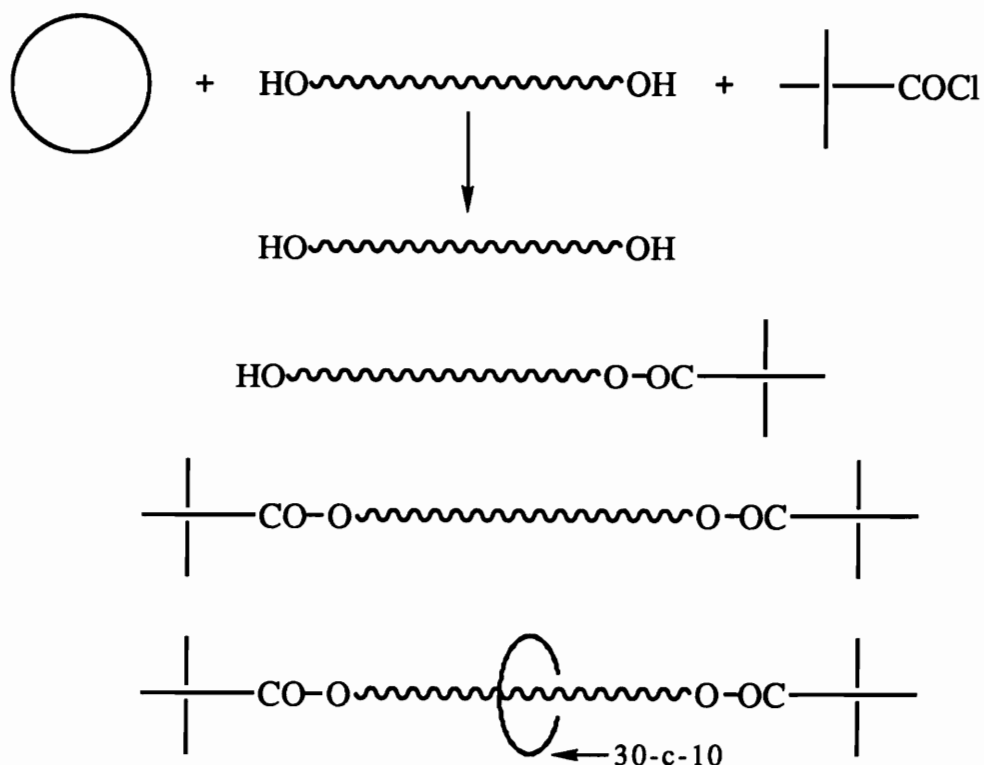
The synthesis and characterization of a variety of monorotaxanes reported in the literature, prepared by statistical threading, template threading or chemical conversion methods, have been described in the historical section of this study. In the syntheses of monorotaxanes by the statistical threading method, the macrocycle and the flexible aliphatic linear backbone were of similar polar nature (1-6). A comparative study of threading efficiencies of flexible and rigid linear backbone by a linear or flexible macrocycles has not been reported. Such a study would be of great importance in the synthesis of polyrotaxanes, since polymer backbones range from flexible to rigid rodlike and it would shed light on feasibility of obtaining polyrotaxanes with high macrocycle incorporation. Thus, the objectives were to study threading behavior of flexible and rigid linear backbones by the synthesis of the end blocked monorotaxanes of 1,8-octanediol and 4,4'-biphenol using flexible 30-c-10 macrocycle as the solvent. The former represents a flexible aliphatic chain while the latter is a rigid aromatic molecule having relatively larger chain diameter.

Another important factor that could significantly affect the threading efficiency is the compatibility of the linear molecules and the macrocycles. Further, the length of the linear backbone also plays an important role in achieving higher threading yields as reported in chapter I. No study on threading efficiencies of a macrocycle with compatible or non compatible linear oligomeric backbones has been reported. Thus, these studies were undertaken to prepare and characterize polyrotaxanes of preformed polymers such as poly(tetrahydrofuran) (PTHF) of molecular weights 2000, 2900 and poly(butadiene) (PBD) of molecular weight 2800 using flexible 30-c-10 macrocycle. The crown ether macrocycle is compatible with PTHF but it is not compatible with PBD. Such a study could also provide helpful hints on the equilibrium dynamics of the statistical threading method.

VII.2 Results and discussion

30-c-10 was used in this study since it can be effectively end blocked by a derivative of tris(*p*-*t*-butylphenyl)-methane. The monorotaxanes and polyrotaxanes were prepared using the statistical threading method, in which 30-c-10 macrocycle and the linear components were equilibrated, followed by the end capping of the α,ω -dihydroxyl linear species by a blocking group derived from tris(*p*-*t*-butylphenyl)methane having an acid chloride moiety. Depending on the efficiency of the end blocking reaction, as shown in Scheme VII-1, a variety of products, such as the desired rotaxanes as well as mono- and di-end blocked linear species can be obtained

Scheme VII-1 Syntheses of Mono- and Poly-rotaxanes



The unthreaded (free) macrocycle was removed from the product mixture either by precipitations of the product into a solvent that is a good solvent for 30-c-10 and a non-solvent for the

product (e.g., water) or by successive washing (or extraction) of the product with such a solvent. GPC analyses proved to be very valuable, because they demonstrate whether the 30-c-10 observed in proton NMR spectra of rotaxanes is threaded or free. The absence of free macrocycle in the product mixtures of the monorotaxanes and polyrotaxanes was confirmed by GPC, since free 30-c-10 macrocycle appears at an elution volume distinctly different from the product mixtures. Estimates on the number of threaded macrocycles were obtained by proton NMR spectroscopy. In the proton NMR spectra of the products, the peak for 30-c-10 was observed at 3.67 ppm. The repeat unit/macrocycle ratio and the amount of blocking group were determined from the proton NMR integrations of (i) the methylene protons alpha to the carbonyl groups (4.55-4.65 ppm) of the blocking group, (ii) protons of the linear chains and (iii) 30-c-10 protons at 3.67 ppm. The model molecules and model polymers consisting of the linear backbone end blocked by acid chloride functional blocking group were also prepared using THF as the solvent.

In the syntheses of the monorotaxanes of small molecules and the polyrotaxanes of low molecular weight preformed polymers, the efficiency of the end blocking reaction plays a major role in achieving high threading yields. If the ends are not blocked, the macrocycles can very easily dethread during the work up, resulting in lower threading yields. Since the syntheses of rotaxanes are done using the macrocycle as a solvent for the linear species, the reaction mixture is highly viscous even at 50-70 °C and this could lead to incomplete or less efficient end blocking reaction. Thus a large excess of the end blocker was used to increase the yield of the end blocking reaction.

Monorotaxanes

1,8-octanediol (mp = 59-61 °C) and 4,4'-biphenol (mp = 280-282 °C) represent flexible and rigid rodlike molecules, respectively, with eight carbons between the terminal hydroxy groups. Syntheses of monorotaxanes from these molecules were accomplished by

mixing the dihydroxy compound with 2.1 eq. of 30-c-10 and stirring each mixture at 50 °C for 36 days to equilibrate and form pre-rotaxanes. The linear chains dissolve in the melted macrocycle and form homogeneous solutions. The resulting pre-rotaxanes were end capped by addition of 1.33 eq. of acid chloride functional blocking group, **VI-9**, per -OH group. Pyridine was used as the acid acceptor in the reactions. To facilitate dissolution of the blocking group in the reaction mixture benzene was added and the reactions were allowed to continue for 36 hours at 80 °C. Figure **VII-1** show the schematic of the syntheses of rotaxanes of 1,8-octanediol and 4,4'-biphenol.

The unthreaded 30-c-10 macrocycle was removed by thoroughly washing the product with water. No attempt was made to isolate pure monorotaxanes from the crude products, since earlier attempts to isolate pure polyrotaxanes of preformed polymers from their crude reaction mixtures were unsuccessful. Using similar conditions, 1,8-octanediol and 4,4'-biphenol were end capped with the blocking group using THF as a solvent. The monorotaxanes and the model molecules were analyzed by NMR spectroscopy and GPC.

Figure **VII-2** shows the proton NMR spectra of product mixtures of monorotaxanes from 1,8-octanediol and 4,4'-biphenol. The NMR spectra of the model molecules were identical, except that the peak corresponding to 30-c-10 at 3.67 ppm was absent. Proton NMR analyses of the monorotaxanes showed the yield of rotaxane from 1,8-octanediol to be about 8-10 % and that from 4,4'-biphenol to be about 10 %.

Figures **VII-3** and Figure **VII-4** show the GPC traces (RI traces) of the monorotaxanes from 1,8-octanediol and 4,4'-biphenol, respectively. Free 30-c-10 appears in GPC traces at an elution volume of 40.5 ml (RI traces) while the acid functional blocking group, **VI-7**, resulting from hydrolysis of **VI-9** during the workup, appears at an elution volume of 39.35 ml. If any free 30-c-10 is present it should appear at the elution volume of 40.5 ml. In the GPC traces of the monorotaxanes, no peak was observed at 40.5 ml,

demonstrating that, indeed, free 30-c-10 has been removed and whatever 30-c-10 that is present, is threaded through the linear species. It was also observed in the GPC traces that unreacted acid functional blocking group is present in each of the isolated products at elution volumes 39.3-39.4 ml. Additional peaks are also present in the GPC traces, indicating the presence of mono- and di-blocked linear backbones along with di-blocked monorotaxanes. The molecular weights obtained from the GPC peaks for mono- and di-blocked components match with the calculated molecular weights (Table VII-1). GPC traces of the model molecules showed similar trends; however, the efficiency of the end blocking reactions were found to be much lower (ca. about 60 %) than that of the rotaxanes (ca. about 75-85 %) since only stoichiometric amounts of acid chloride functional blocking group were used to end block the linear model species.

Table VII-1 Calculated Molecular Weights of the Products

Compound	Mol. Wt.	Mono-End Blocked	Di-End Blocked	Di-End Blocked Monorotaxane
1,8-Octanediol	146.2	719.0	1282.0	1722.0
4,4'-Biphenol	186.2	749.0	1312.0	1752.0
30-c-10 = 440.5		Acid Blk. Gr. (VI-7) = 562.7		

The FTIR analysis of the product mixture from 1,8-octanediol showed peaks at 1765 and 1735 cm^{-1} , corresponding to carbonyl groups of the ester and the acid functional blocking group. Further, a broad peak at 3396 cm^{-1} corresponds to hydroxyl groups of the acid (of the blocking group) or the unblocked hydroxyl groups of 1,8-octanediol. Similarly, hydroxyl groups were also observed in the FTIR spectrum of the product mixture from 4,4'-biphenol. The carbonyl groups of this product mixture appear as a broad peak from 1790-1735 cm^{-1} , indicating formation of ester linkages as well as

the presence of acid functional blocking group and unblocked hydroxy groups of 4,4'-biphenol.

Thus, no significant difference in the threading tendencies of the flexible 1,8-octanediol and rigid 4,4'-biphenol was observed and the threading yields were in the range of 8-10 %. Further, it was found that the yields of the end capping reactions are not quantitative and that a large excess of the blocking group is required to increase the end capping yields. The threading yields could undoubtedly be improved by quantitative end capping of the linear species.

Polyrotaxanes of Preformed Polymers

PBD (molecular weight 2800) and PTHF of two different molecular weights (ca. 2900 and 2000) having terminal hydroxyl groups were obtained from Aldrich (the reported molecular weights are based on hydroxyl contents of the polymers). The polymers (1.0 g) were mixed with 5.0 g of 30-c-10 and stirred for a total of about 3.5 months at 60-70 °C to obtain pre-polyrotaxanes, followed by the addition of excess acid chloride functional blocking group (VI-9) and the reactions were allowed to continue for 22 hours.

Figure VII-5 shows the schematic of the syntheses of polyrotaxanes of preformed polymers. The polymers were purified by precipitations to remove free macrocycle. Due to the similarities in solubilities attempts to separate unreacted excess acid functional blocking group, VI-7, such as precipitation from acetone solutions into methanol:water and adding base to ionize and hence solubilize the blocking group in water, were unsuccessful. Thus, after removing the free 30-c-10, the product mixtures were analyzed by NMR spectroscopy and GPC to determine the amount of 30-c-10 threaded onto the polymers.

Figures VII-6, VII-7 and VII-8 show the GPC traces of the product mixtures from PTHF 2900, PTHF 2000 and PBD 2800 (RI traces). GPC analyses of the product mixtures of the polyrotaxanes did not show unthreaded macrocycles; the unthreaded macrocycle

was removed by two precipitations. However, acid functional blocking group, VII-7, was found to be present in the product mixtures. GPC analyses of the α,ω -dihydroxyl polymers showed broad molecular weight distributions (greater than 2.0) and the elution volumes of these polymers were lower than those of the polyrotaxane product mixture due to association of these polymer chains by hydrogen bonding via the hydroxyl groups at the chain ends. The GPC traces of the polyrotaxane product mixtures are very different from their precursor linear polymers. Tailing of the peaks towards the lower elution volume is observed along with fused multiple peaks at the higher elution volume. The unique shapes of these GPC peaks may be due to a distribution of the number of 30-c-10 macrocycles threaded onto the polymer chains (i.e., one, two, three, or more macrocycles per chain). Figure VII-9 shows the GPC traces of the model polymers. The model polymers prepared by end capping of the terminal hydroxyl groups of the polymers with acid chloride blocking groups do not show fused multiple peaks in GPC traces; instead the peaks are narrower compared to their α,ω -dihydroxyl precursor. Acid functional blocking group is also seen in the GPC traces at elution volume 40.3 ml (calibration is different from the other GPC traces). These results tend to suggest that multiple fused peaks are not be due mono- and di-blocked chains but due to a distribution of macrocycles on the polymers. This possibility will be confirmed by purification of the polyrotaxane products.

Figure VII-10 shows the proton NMR spectra of product mixtures. Table VII-2 lists the weight % macrocycles incorporated onto the polymers along with repeat unit/macrocycle ratio. From the proton NMR integrations of the product mixtures significant incorporation of 30-c-10 macrocycle was found. Proton NMR spectra of the model polymers were similar, except that the peak corresponding to 30-c-10 was absent.

Even though the molar feed ratio of the macrocycle to the linear polymer was lower for PTHF 2000, it showed higher

incorporation of 30-c-10 than PTHF 2900. Due to the lower molecular weight of PTHF 2000, the chain end concentration per unit volume was higher than that of PTHF 2900 and this would lead to higher macrocycle incorporation under kinetic control. These results are consistent with the results obtained (6) for threading of dibenzo-crown ethers with poly(ethylene glycol)s of various molecular weights as described in chapter I. At a similar initial ratio of macrocycle to linear polymer, PTHF 2900 showed lower incorporation of macrocycle than PBD 2800. These results are surprising since PBD was not completely soluble in 30-c-10. It was thought that due to the incompatibility of the linear backbone and the macrocycle lower threading yields would result. These results tend to suggest that incompatibility of the two components may not be a major factor in threading.

Both the PTHF rotaxanes are glue-like while the precursor polymers are more solid and powdery. On the contrary, the polybutadiene rotaxane is a solid compared to the precursor which is a viscous liquid. Further, the polybutadiene rotaxane when placed in water remains as a flaky powder and does not coagulate. This suggests that the surface tension may have been lowered by the incorporation of the hydrophilic crown ether. In a recent report (8), synthesis of styrene-butadiene copolymer was accomplished by emulsion polymerization in the presence of butadiene-ethylene oxide block copolymer (low molecular weight) and the resulting elastomer had durable hydrophilic tendencies. Such polar-nonpolar polyrotaxane systems may be worthwhile to explore as they could prove to be valuable surfactants or blend compatibilizers in a variety of applications.

Table VII-3 summarizes the results obtained for mono- and poly-rotaxanes with 30-c-10. It is clear that threading of the polymers is more efficient than for the small molecules on a macrocycle per backbone atom basis. This may be due to the effects of the blocking groups, which are likely to repel the macrocycles and cause dethreading upon reaction of the first hydroxyl group. This

Table VII-2 Polyrotaxanes from Preformed Polymers

Linear Chain	Feed Ratio Macrocycle per Linear	Feed Ratio Repeat Unit/ Macrocycle	Repeat Unit/ Macrocycle in Polyrotaxane	Macrocycle/ Backbone Atoms	Macrocycle/ Linear Chain	Wt. % Macrocycle
PTHF 2900	33	1.2	10	50	4.0	38 %
PTHF 2000	23	1.2	6.0	30	4.7	50 %
PBD 2800	32	1.6	8.0	33	6.3	48 %

means that 'model' reactions using small molecules may not be very successful in assessing the structures of polyrotaxanes. The results for the polymers are very encouraging in that (i) very high densities of macrocycles threaded per backbone atom are possible and (ii) given enough time even preformed polymers thread efficiently.

The future work in this area includes purification of the rotaxanes of the small molecules and the polyrotaxanes of preformed polymers to isolate the pure mono- and poly-rotaxanes, free from the acid functional blocking group as well as the mono- and di-end capped polymers. This could be accomplished by chromatographic methods. Bulk and solution properties of these rotaxanes and polyrotaxanes need to be explored as well.

**Table VII-3 Synthesis and Characterization of
Mono- and Poly-rotaxanes**

Linear Chain	Feed Ratio Repeat Unit/ Macrocycle	Feed Ratio Backbone Atoms/ Macrocycle	Repeat Unit/ Macrocycle in Polyrotaxane	Macrocycle/ Backbone Atoms
PTHF 2900† ^A	1.2	6.0	10	50
PTHF 2000† ^A	1.2	6.0	6.0	30
PBD 2800† ^A	1.6	6.4	8.3	33
1,8-Octanediol† [#]	0.48	4.8	10* %	100
4,4'-Biphenol† [#]	0.48	4.8	10* %	100

† with blocking group

^A After 2 Precipitations; no free macrocycle as determined by GPC

[#] Purified by washing thoroughly with water; no free macrocycle as determined by GPC

* one molecule out of 10 is threaded (by NMR)

VII.3 Experimental

Measurements:

GPC analyses of the polymers were done at 30 °C in THF using a Waters system (RI and UV detectors) after calibration with PS standards. Proton and carbon NMR spectra were obtained on a Bruker WP 270 spectrometer using deuterated chloroform solutions with tetramethylsilane as an internal standard. FTIR spectra were obtained on a Nicolet MX-1 instrument.

Syntheses of Monorotaxanes from 1,8-octanediol and 4,4'-biphenol:

0.10 g (6.8×10^{-4} moles) 1,8-octanediol and 0.64 g (1.4×10^{-3} moles) 30-c-10 (2.1 eq. of 1,8-octanediol) were mixed and stirred at 50 °C for 36 days to equilibrate and form pre-rotaxanes. Similarly, 0.10 g (5.4×10^{-4} moles) 4,4'-biphenol and 0.50 g (1.1×10^{-3} moles) 30-c-10 (2.1 eq. of 4,4'-biphenol) were mixed and stirred at 50 °C for 36 days to equilibrate and form pre-rotaxanes. The linear chains dissolve in the melted macrocycle and form homogeneous solutions. The resulting pre-rotaxanes were end capped in the presence of stoichiometric amounts of pyridine by addition of 1.06 g (1.8×10^{-3} mole; 1.3 eq. per -OH group) acid chloride functional blocking group, **VI-9**, in 1,8-octanediol pre-rotaxanes and 0.83 g (1.4×10^{-3} moles; 1.3 eq. per -OH group) acid chloride functional blocking group, **VI-9**, in 4,4'-biphenol pre-rotaxanes.

The acid chloride blocking group, **VI-9**, did not melt or dissolve and the reaction mixture became solid; hence, 10 drops of benzene were added to both reactions and the temperature of the oil bath was raised to 95 °C. The reactions were allowed to continue for 36 hours. Then, the reaction mixtures were cooled, diluted with water and stirred for 4-5 hours, filtered, thoroughly washed with water (4 x 100 ml) and dried under vacuum. No attempt was made to isolate pure rotaxanes from the crude products. The products were analyzed by FTIR and NMR spectroscopy and GPC. 1,8-octanediol

rotaxane: FTIR: 3427 (broad), 3089, 3033 (aromatic), 2960, 2903, 2868 (aliphatic), 1765, 1735 (C=O), 1606, 1583, 1506 (aromatic), 1297, 1270, 1183, 1109, 1018, , 841, 823 cm^{-1} ; NMR (CDCl_3): 7.23-6.73 (aromatic, m, 32H), 4.58 (O-CH₂-C=O, s, 4H), 4.17 (O=C-O-CH₂, t, 4H), 3.66 (30-c-10, s, 40H), 1.63 (O=C-O-CH₂-CH₂, m, 4H), 1.5-1.2 (t-butyl and -CH₂, s, 62H).

4,4'-biphenol rotaxane: FTIR: 3396 (broad), 3088, 3035 (aromatic), 2963, 2954, 2903, 2867 (aliphatic), 1786, 1750 (C=O), 1604, 1583, 1504 (aromatic), 1297, 1230, 1188, 1166, 1149, 1107, 1017, , 841, 823 cm^{-1} ; NMR (CDCl_3): 7.54-6.80 (aromatic, m, 40H), 4.64 (O-CH₂-C=O, s, 4H), 3.67 (30-c-10, s, 40H), 1.30 (t-butyl, s, 54H).

1,8-Octanediol and 4,4'-biphenol were end capped with acid chloride functional blocking group (1.03 eq. of -OH groups) in the presence of stoichiometric amounts of pyridine using THF as the solvent. The NMR spectra of these model molecules were similar to those of the rotaxane product mixtures, except that the peak for 30-c-10 was absent. Further, it appears from the NMR spectra that only about 60 % of the acid chloride blocking group had reacted and in GPC traces acid functional blocking group, **VI-7**, resulting from hydrolysis of **VI-9**, was also found to be present. These model molecules were not purified further.

Syntheses of Polyrotaxanes from Preformed Polymers:

1.0 g (3.4×10^{-4} moles) PTHF 2900 and 5.0 g 30-c-10 (1.1×10^{-2} moles) were mixed. Similarly, 1.0 g (5.0×10^{-4} moles) PTHF 2000 and 5.0 g 30-c-10 (1.1×10^{-2} moles) were mixed. Further, 1.0 g (3.6×10^{-4} moles) PBD 2800 and 5.0 g 30-c-10 (1.1×10^{-2} moles) were mixed. These mixtures were stirred at 50-60 °C for a total of 3.5 months. 1.0 g (1.7×10^{-3} moles; 2.5 eq. per PTHF 2900) acid chloride blocking group, **VI-9**; 1.2 g (2.1×10^{-3} moles; 2.1 eq. per PTHF 2000) acid chloride blocking group, **VI-9**, and 1.0 g (1.7×10^{-3} moles; 2.4 eq. per PBD 2800) acid chloride blocking group, **VI-9**, were added to the respective reaction mixtures and the reactions were continued for 22 hours. The PTHF reaction mixtures were

cooled, dissolved in acetone and precipitated in water to remove unthreaded 30-c-10. The polymers were filtered and washed with (3 x 200 ml) water. The polymers were precipitated one more time and filtered. The filtered polymers are mixtures of mono- and di-blocked PTHF, the desired polyrotaxane and acid functional blocking group, **VI-7**. Various attempts to separate acid functional blocking group were unsuccessful. The polyrotaxane product mixture was characterized by NMR and GPC to determine the amount of 30-c-10 threaded onto the polymers. PTHF 2900-Rotaxa-30-c-10: NMR (CDCl_3): 7.24-6.75 (aromatic, m, 32H), 4.63 ($\text{O-CH}_2\text{-C=O}$, s, 4H), 4.4-4.15 (O=C-O-CH_2 , 2t, 4H), 3.63-3.68 (30-c-10, s, 40H), 4.41, 1.62 (PTHF 2m, 216H), 1.30 (t-butyl, s, 54H). PTHF 2000-Rotaxa-30-c-10: NMR (CDCl_3): 7.24-6.75 (aromatic, m, 32H), 4.64 ($\text{O-CH}_2\text{-C=O}$, s, 4H), 4.4-4.15 (O=C-O-CH_2 , 2t, 4H), 3.63-3.68 (30-c-10, s, 40H), 4.41, 1.62 (PTHF 2m, 320H), 1.30 (t-butyl, s, 54H).

The PBD reaction mixture was cooled and dichloromethane was added to dissolve the polymer, but it did not dissolve completely, suggesting that the insoluble part may be crosslinked. The dichloromethane solution was filtered to remove crosslinked polybutadiene. The filtrate was then added slowly to about 1 l of acetone to precipitate the polymer; the mixture was stirred for few hours, diluted with 300 ml water, allowed to sit and then filtered. The solid was washed with water and again dissolved in acetone-dichloromethane and precipitated in acetone-water as before, filtered, washed with water and dried. The filtered solid is a mixture of mono- and di-blocked polybutadiene, the desired polyrotaxane and unreacted acid functional blocking group. Various attempts to separate the acid functional blocking group, **VI-7**, were unsuccessful. The polyrotaxane product mixture was characterized by NMR and GPC to determine the amount of 30-c-10 threaded onto the polymer. PBD 2800-Rotaxa-30-c-10: NMR (CDCl_3): 7.24-6.75 (aromatic, m, 32H), 5.7-5.3 ($=\text{CH}$, m, 104H), 4.8-5.1 ($=\text{CH}_2$, (1,2 BD) m), 4.62-4.59 ($\text{O-CH}_2\text{-C=O}$, m, 4H), 4.3-4.4 (O=C-O-CH_2 , m, 4H), 3.57-

3.71 (30-c-10, s, 40H), 2.25-1.8 (-CH₂, s, 208H), 1.29 (t-butyl, s, 54H),

Model polymers were also prepared from PTHF 2900, PTHF 2000 and PBD 2800 in THF using 1.05-1.01 equivalents of acid chloride functional blocking groups, **VI-9**, relative to -OH groups. The proton NMR spectra of these model polymers were identical to spectra of the rotaxanes except that the peak for crown ether was absent. Further, it appears from the NMR spectra that only about 60-75 % of the acid chloride blocking group had reacted and in GPC traces acid functional blocking group, **VI-7**, was found to be present. These model polymers were not purified further.

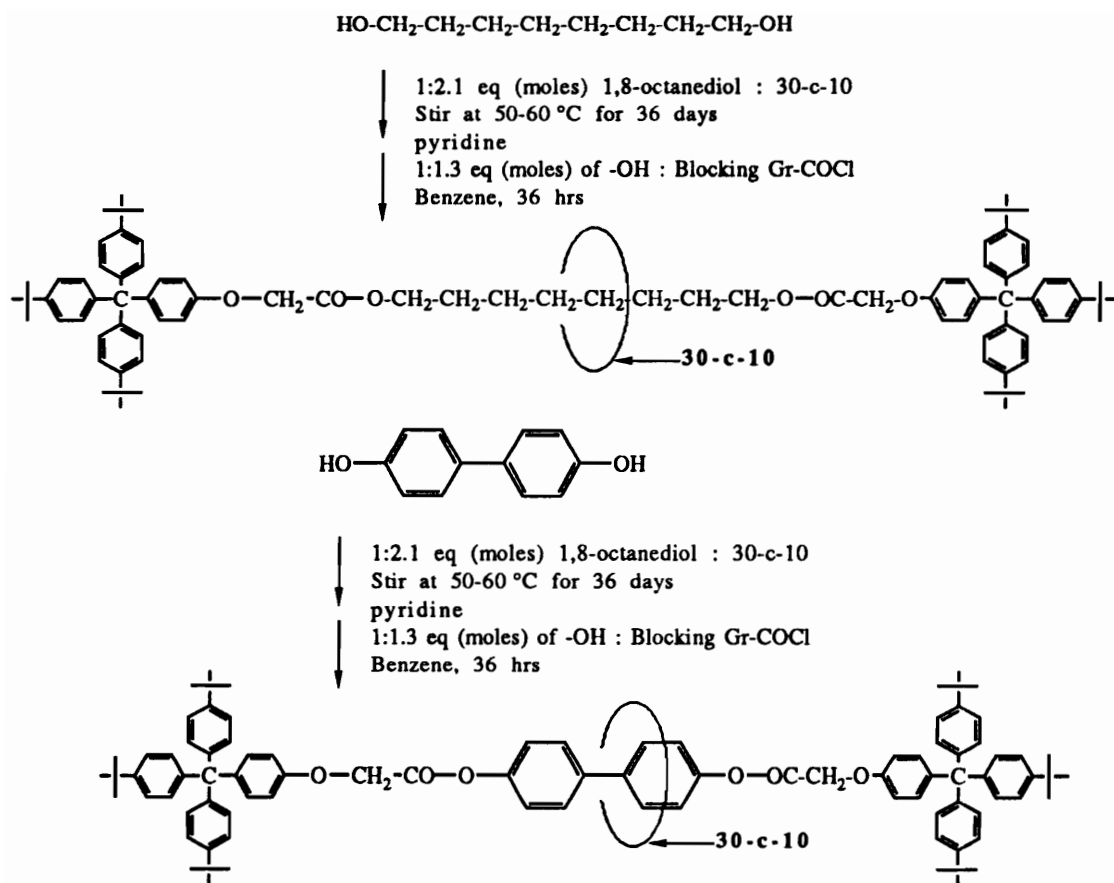


Figure VII.1 Schematic of Syntheses of Monorotaxanes from 1,8-octanediol and 4,4'-biphenol

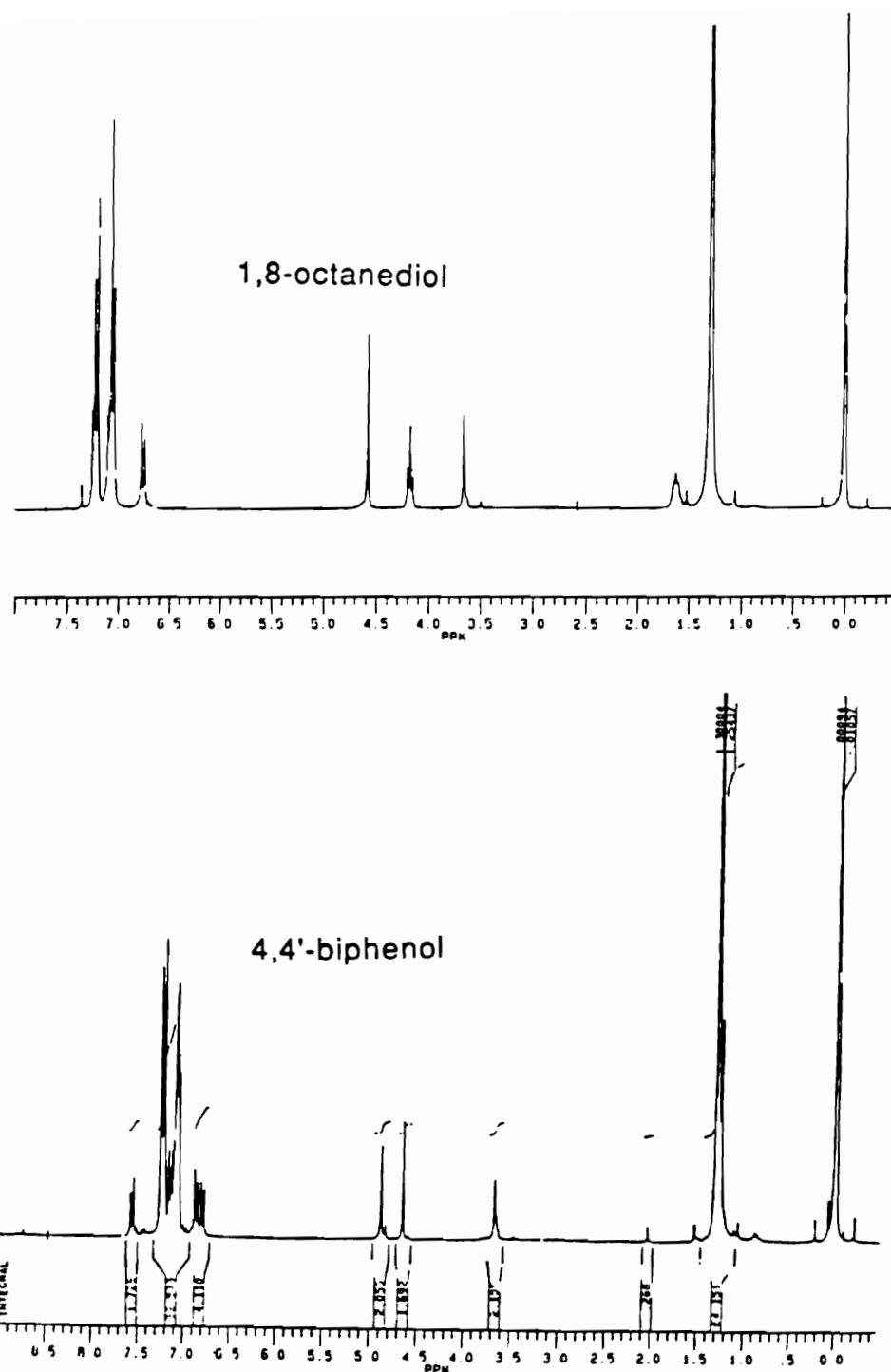


Figure VII.2 ^1H (270 MHz) NMR of the Products of the Monorotaxane Syntheses from 1,8-octanediol and 4,4'-biphenol

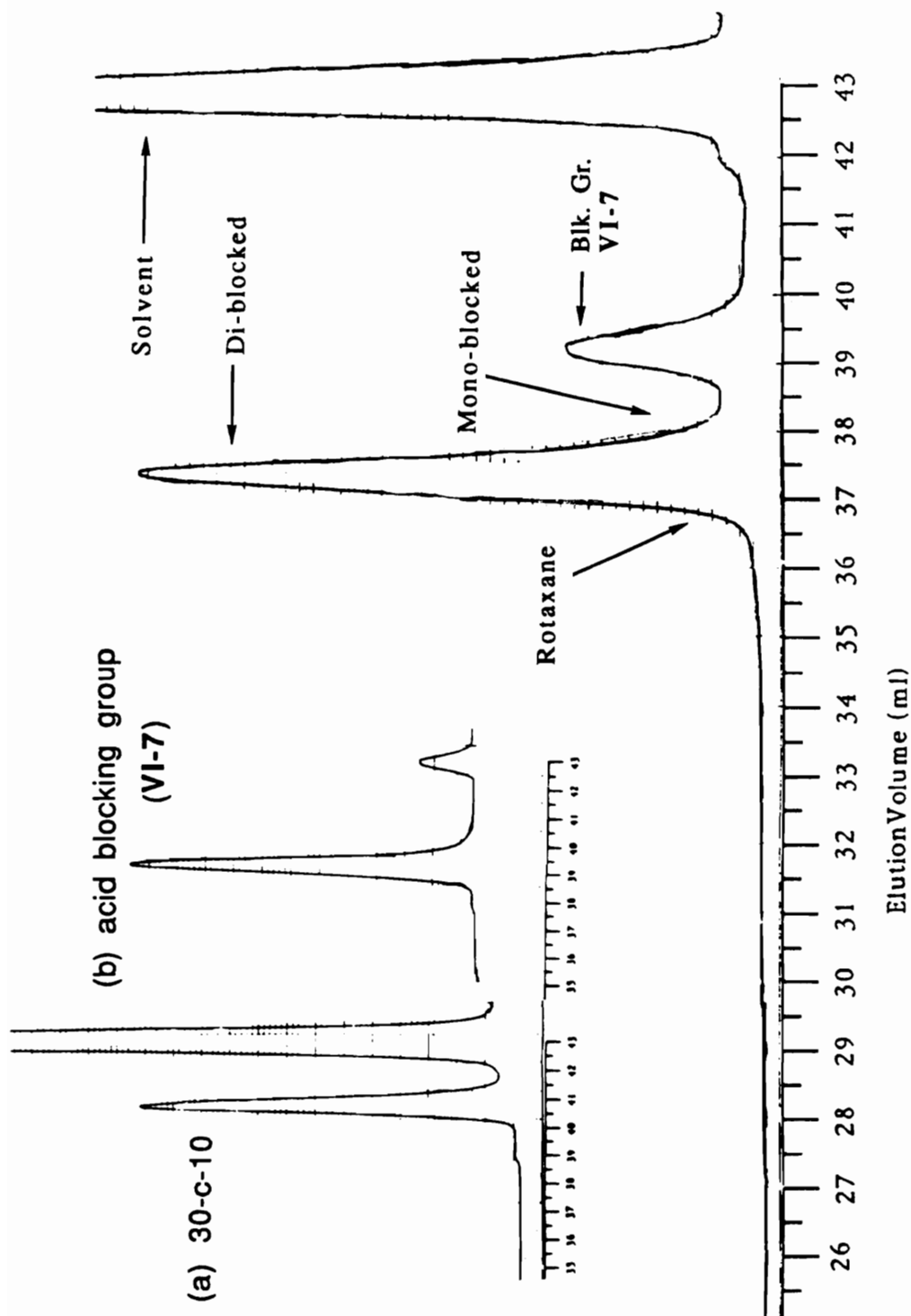


Figure VII.3 GPC Trace of the Product of the Monorotaxane Synthesis from 1,8-octanediol.
 Insert: (a) 30-c-10, (b) acid blocking group (VI-7) (RI Traces)

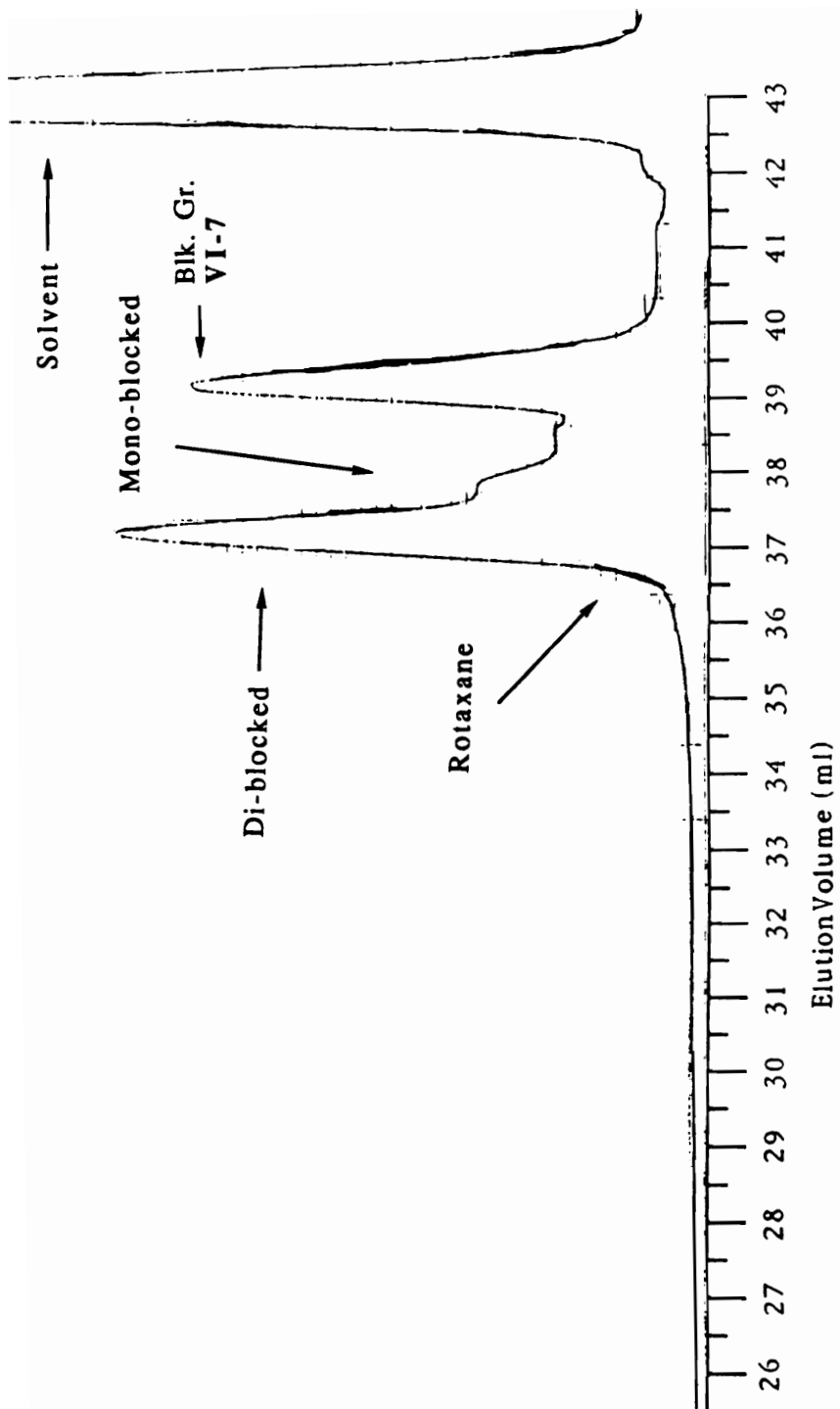


Figure VII.4 GPC Trace of the Product of the Monorotaxane Synthesis from 4,4'-biphenol (RI Trace)

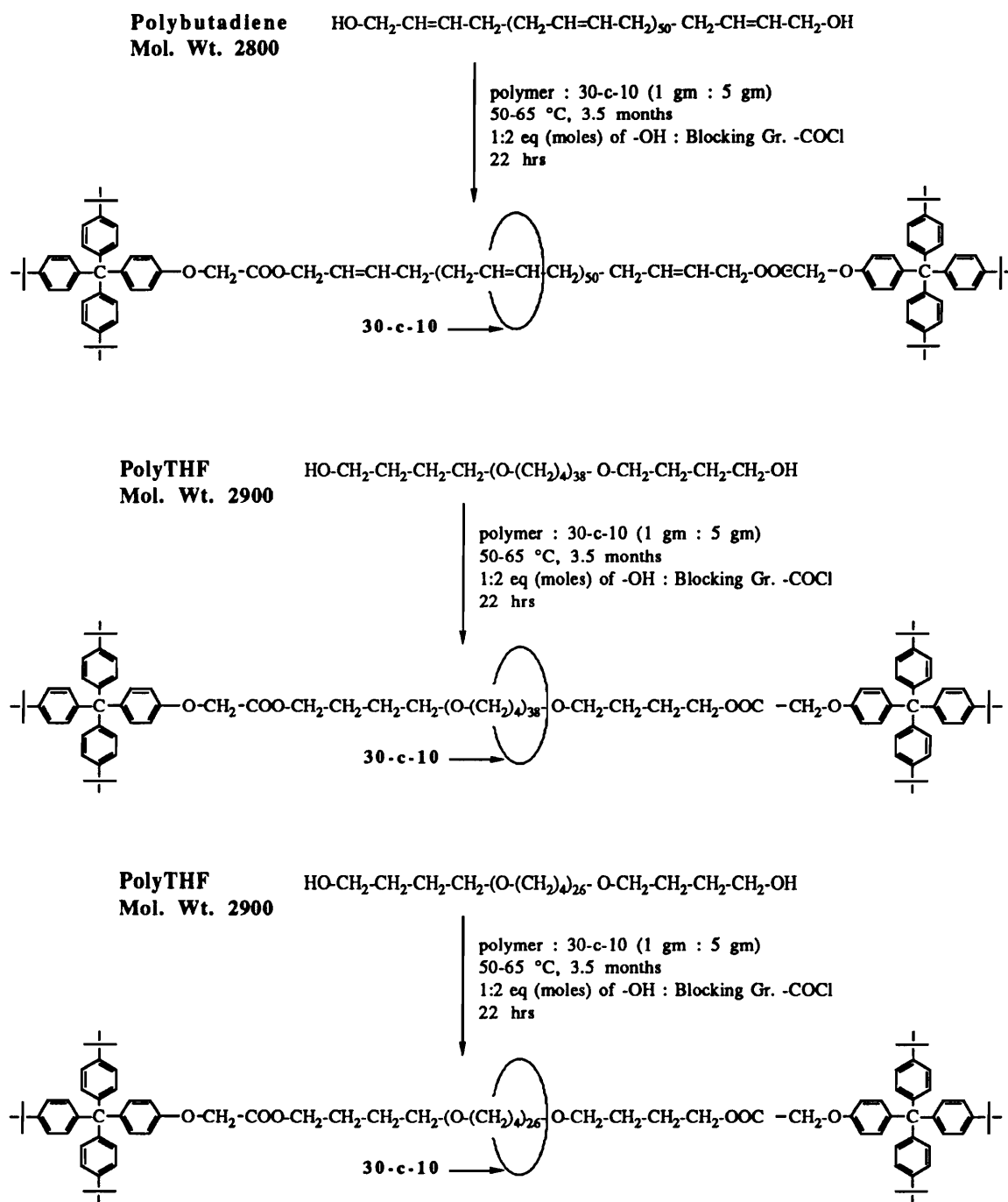


Figure VII.5 Schematic of Syntheses of Polyrotaxanes from PBD 2800, PTHF 2900 and PTHF 2000

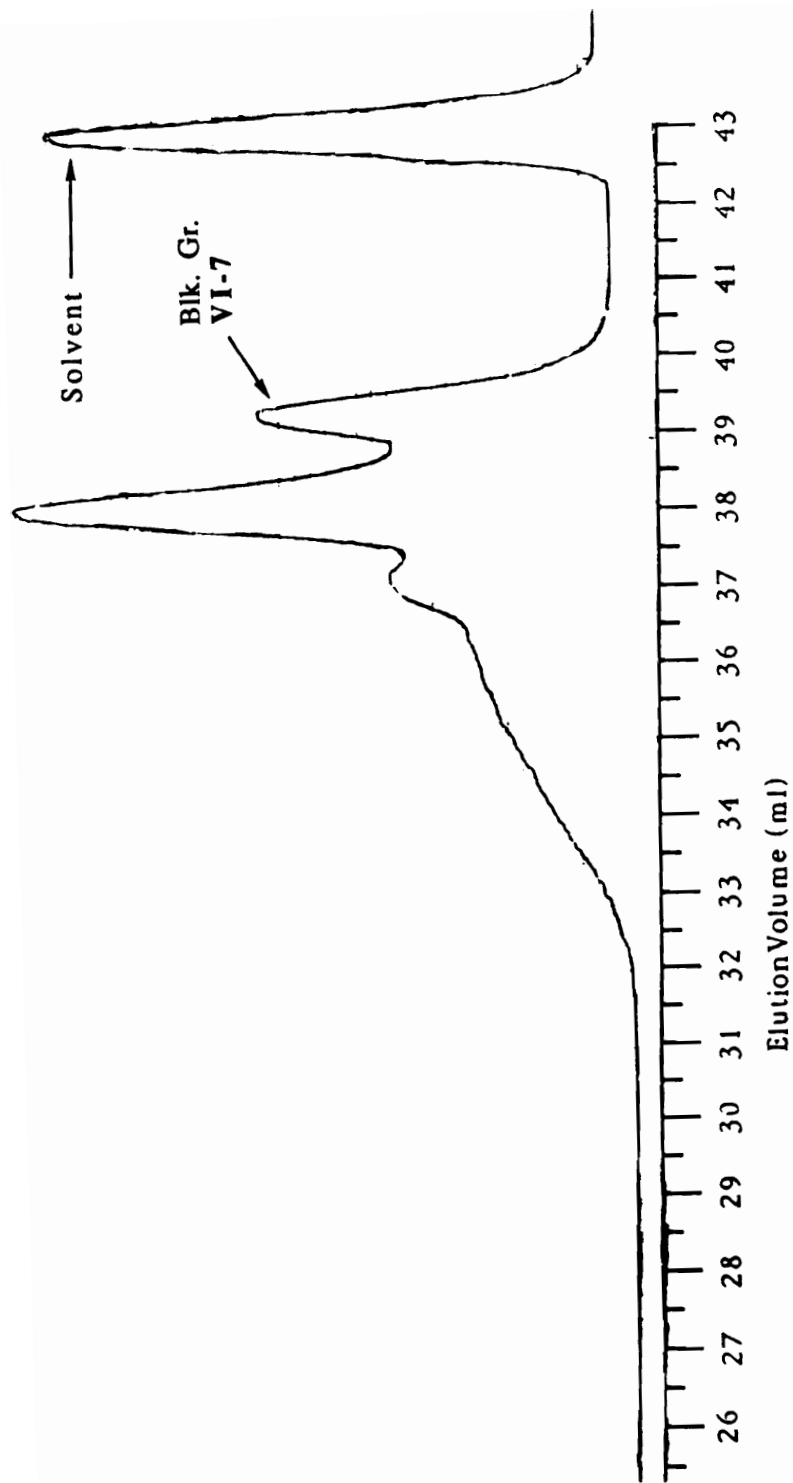


Figure VII.6 GPC Trace of the Product of the Polyrotaxane
Synthesis from PTHF 2900 (RI Trace)

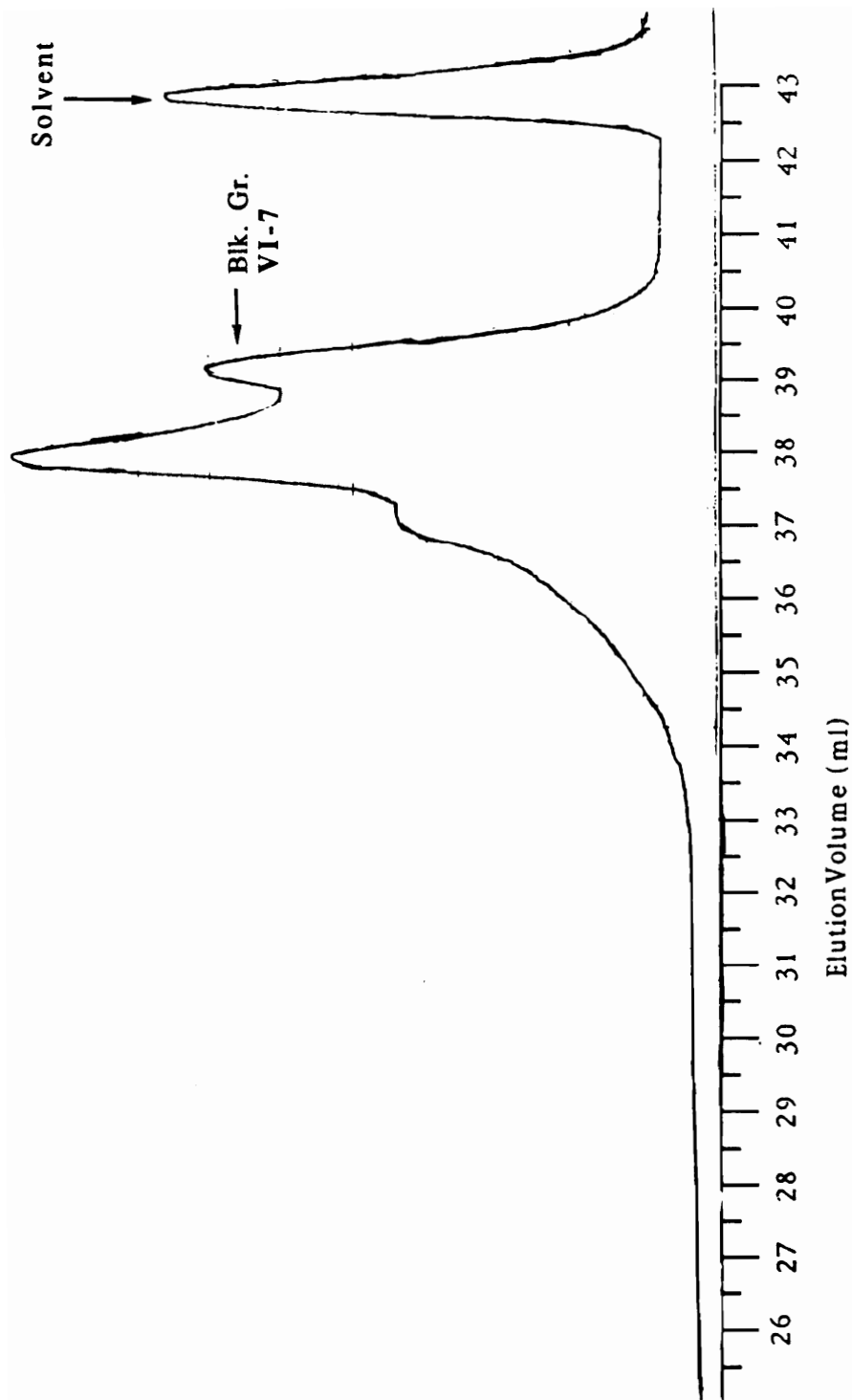


Figure VII.7 GPC Trace of the Product of the Polyrotaxane
Synthesis from PTHF 2000 (RI Trace)

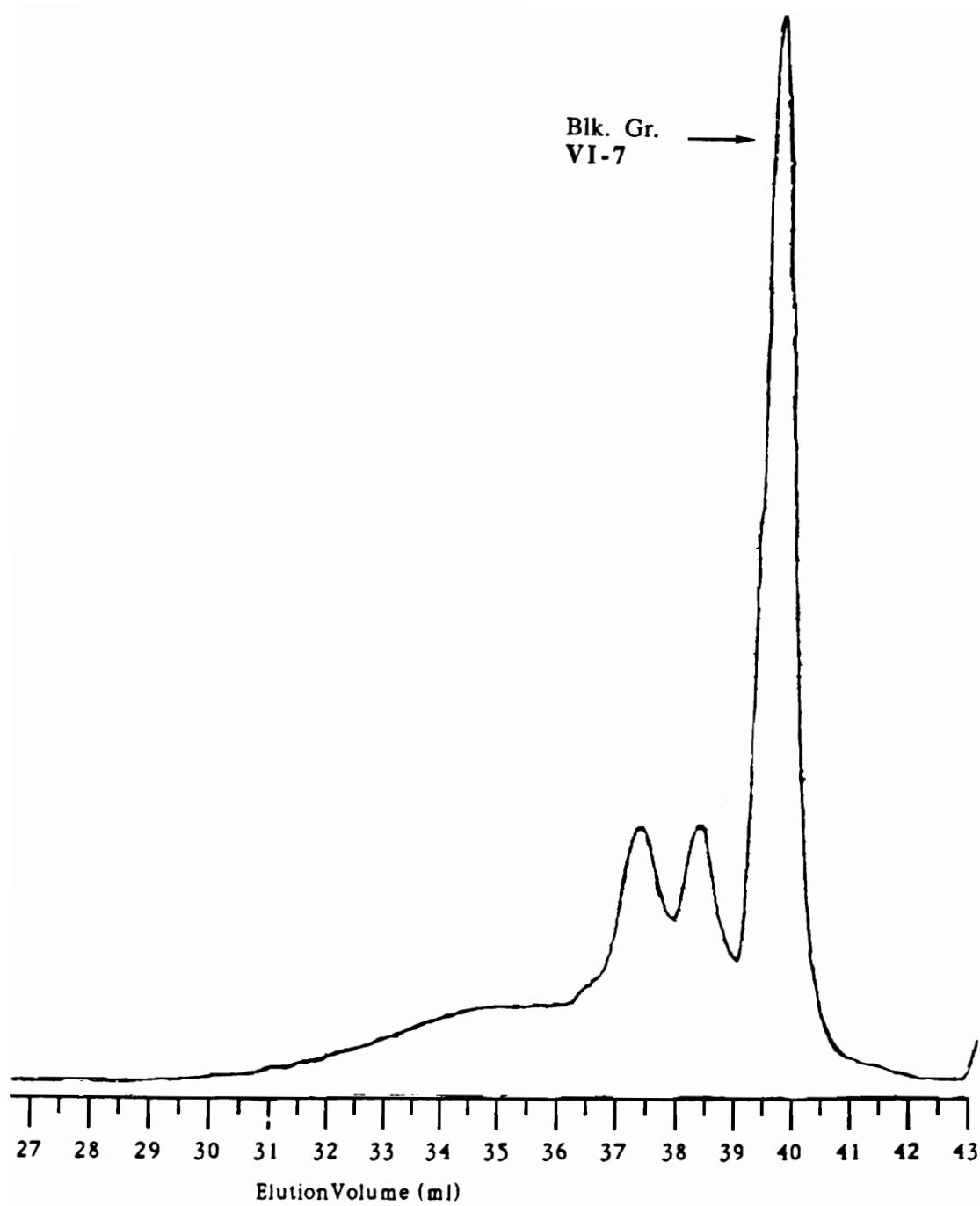


Figure VII.8 GPC Trace of the Product of the Polyrotaxane Synthesis from PBD 2800 (RI Trace)

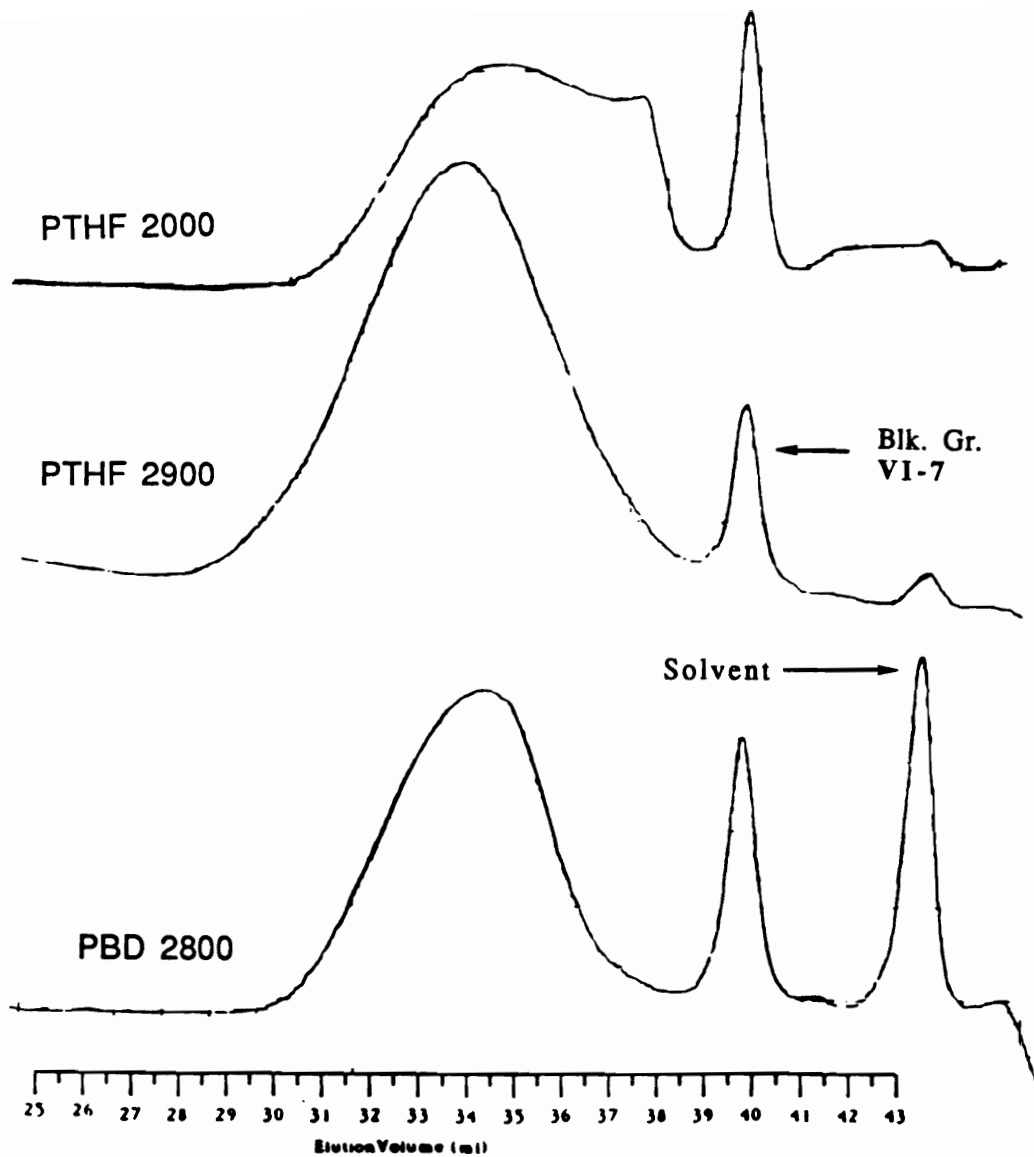


Figure VII.9 GPC Traces of the Products of the Model Polymer Syntheses from PBD 2800, PTHF 2900 and PTHF 2000 (RI Traces)

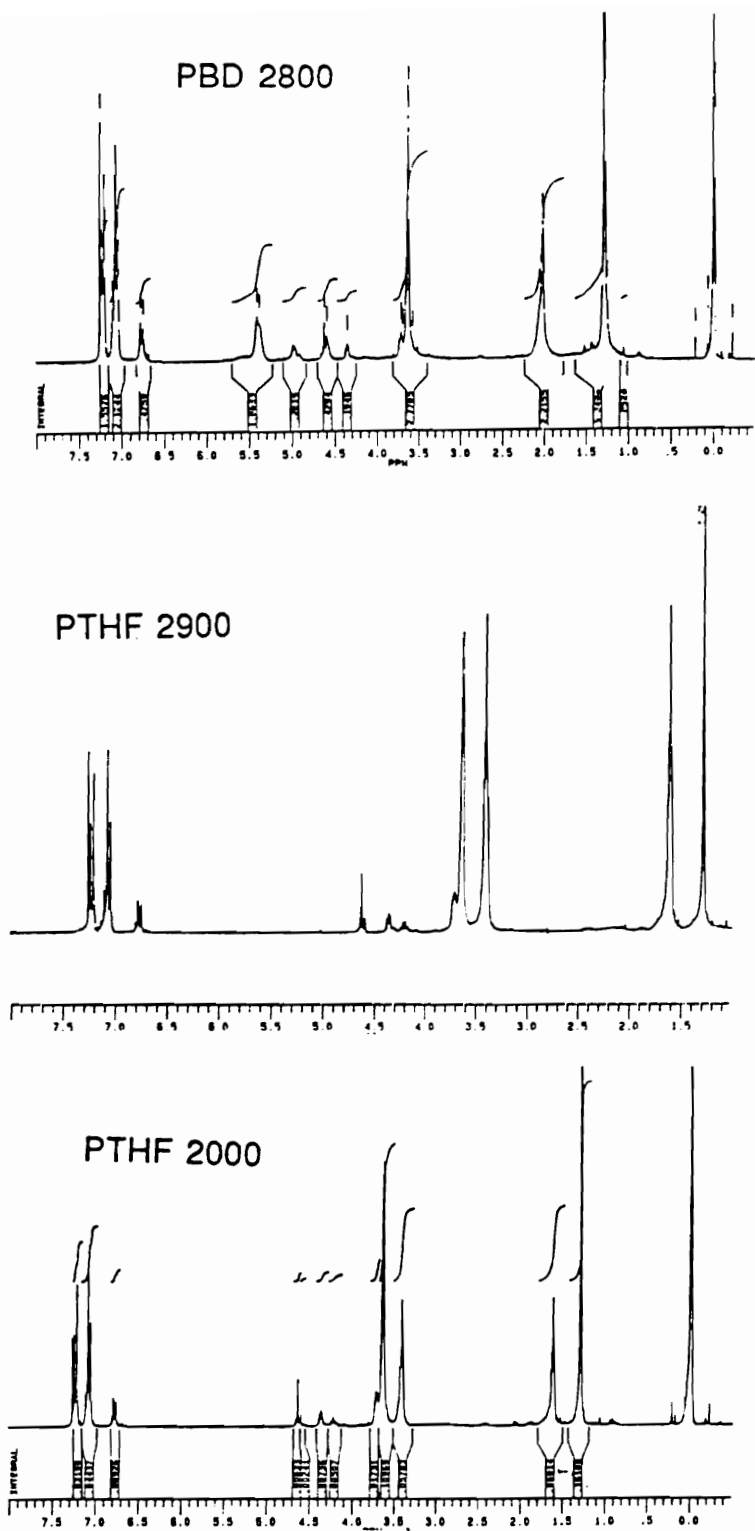


Figure VII.10 ^1H (270 MHz) NMR of the Products of the Polyrotaxane Syntheses from PBD 2800, PTHF 2900 and PTHF 2000

References

1. I. T. Harrison and S. Harrison, *J. Am. Chem. Soc.*, 1967, 89, 5723.
2. I. T. Harrison, *J. Chem. Soc. Chem. Commun.*, 1972, 231.
3. I. T. Harrison, *J. Chem. Soc. Perkin Trans. I*, 1974, 301.
4. I. T. Harrison, *J. Chem. Soc. Chem. Commun.*, 1977, 384.
5. G. Agam, D. Gravier and A. Zilkha, *J. Am. Chem. Soc.*, 1976, 98, 5206.
6. G. Agam and A. Zilkha, *J. Am. Chem. Soc.*, 1976, 98, 5214.
7. G. Schill, W. Beckmann, N. Schweickert and H. Fritz, *Chem. Ber.*, 1986, 119, 2647.
8. I. Noda, *Nature*, 1991, 350, 143.

VIII. POLYAMIDE ROTAXANES 177
VIII.1 Introduction 178
VIII.2 Consideration of Polyamides for Polyrotaxane Synthesis 179
VIII.3 Model ODA-I and its Polyrotaxanes 181
VIII.4 Model PPD-T (Kevlar™) and its Polyrotaxanes 190
VIII.5 Model Nylon-6,6 and its Polyrotaxane 194
VIII.6 Experimental 197

VIII.1 Introduction

Polyamides, aliphatic as well as aromatic, represent an important class of commercially successful polymers. Uses of the polyamides, copolymers of polyamides and polyamide blends range from automotive to fibers to engineering resins. Examples of commercially important polyamides include Nylon-6, Nylon-6,6, Kevlar™, Nomex™, etc. The useful properties of these polymers include relatively high thermal stability, hydrolytic stability, solvent resistance and high modulus in the direction of orientation. These properties are greatly amplified in the aromatic polyamides (polyaramides). The solvent resistance and relatively high thermal stability of these polyamides are due mainly to the frequency and the strength of intermolecular hydrogen bonding in the polymer chains (1,2).

Aliphatic polyamides are typically melt processed even though they have a narrow temperature range available for melt processing. Due to chain stiffness and intermolecular hydrogen bonding, thermal processing of polyaramides has been greatly hindered since their softening or melting temperatures most often coincide with polymer decomposition temperatures.

In N-alkyl substituted polyamides the intermolecular forces contributed by the amide groups are mainly dipolar because the hydrogen bonding offered by the amide groups is lost, and the melting points are greatly reduced while the solubility is improved (1-3). Further, various other efforts to improve the solubility and to lower the thermal transitions, thus improving processability of polyamides have been described (1,3); however, other useful properties such as modulus, etc., have been adversely affected.

For these reasons polyamides are attractive candidates for the purpose of making polyrotaxanes. It was expected that by incorporation of polar, highly soluble oligomeric crown ethers onto the polyamide chains (threading), the net effect of the hydrogen bonding in the polyamides could be altered significantly to yield

more soluble polymers; while retaining other useful properties of the polymers since the polyamide chains themselves are not modified chemically. Thus, commercially available monomers could be used directly.

VIII.2 Consideration of Polyamides

For the synthesis of aliphatic polyamides, a variety of methods such as direct amidation of acid and amine groups, reaction of diacid chlorides with diamines interfacially or in one phase and ring opening polymerization have been employed. In the synthesis of polyaramides, the preferred method is low temperature polycondensation using diacid chloride and diamine. The interfacial polymerization is also employed but it gives broader molecular weight distributions (1,3).

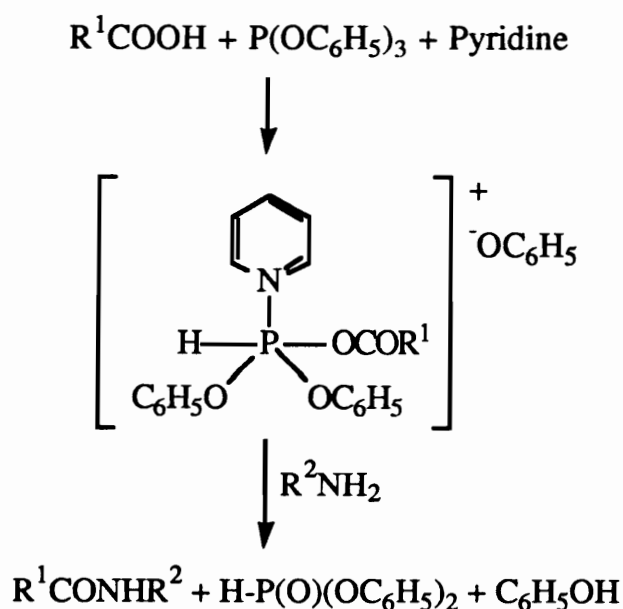
Alternatively, Yamazaki and Higashi et al. have reported syntheses of a variety of polyaramides by direct condensation of aromatic diacids and aromatic diamines in solution using phosphites in the presence of metal salts (4-9). Direct amidation of a diamine occurs via phosphorylation. Further, by this method high molecular weight aliphatic-aromatic polyamides have been prepared using aromatic diamines and aliphatic diacids of 4-10 methylene units (10).

The method described for the synthesis of polyaramides by Yamazaki and Higashi et al. is ideally suited for the synthesis of polyrotaxanes of polyaramides since no acid chloride is required and the polymerization is done in one phase. Amidation of free amine by the carboxyl group is promoted using triphenylphosphite to first form the N-phosponium salt of pyridine that forms the amide link with the amine. Scheme VIII-1 represents the amidation reaction.

Synthesis of polyaramides derived from 4,4'-oxydianiline (ODA) and isophthalic acid [poly(oxydiphenyleneisophthalamide), ODA-I] as well as that derived from p-phenylenediamine and terephthalic acid [(poly(p-phenyleneterephthalamide), PPD-T,

Kevlar™] using Yamazaki and Higashi et al. method have been reported. Both the polymers were selected as the starting point in polyrotaxane study of polyamides. It has been reported (11) that the polyamide ODA-I is soluble in DMAc and in NMP up to certain molecular weights (i.e., up to intrinsic viscosity of 0.95). The polyamide PPD-T (Kevlar™) is completely insoluble in all the organic solvents and is only soluble in sulfuric acid. Thus, comparative study of polyrotaxanes of soluble as well as insoluble polyamide will demonstrate the effect of threading by macrocycles on the solubility and solid state properties. Nylon-6,6 was selected as a representative of aliphatic polyamides to study the effect of macrocycle incorporation on the polymer.

Scheme VIII-1 Amidation via Phosphorylation



For the synthesis of the model polyamide and its polyrotaxanes the Yamazaki and Higashi et al. procedure was slightly modified. It has been shown that polymerization in NMP:pyridine (3:2 to 4:1) and LiCl in 4-5 wt % concentrations yielded high molecular weight polymer. These conditions were used for the synthesis of

model polymer and its polyrotaxane; however, polymerizations were done in more concentrated solutions. Further, crown ether was used as cosolvent, about half of the total solvent in the synthesis of polyrotaxanes. The monomers and crown ether were dissolved in the solvent mixture and stirred for 1-2 hours at 60 °C, followed by addition of LiCl and triphenyl phosphite. In the absence of crown ether, diglyme was used in the synthesis of model polymer due to its structural resemblance to crown ether macrocycles.

VIII.3 Model ODA-I and its Polyrotaxanes

In the initial attempt, monofunctional amine blocking group (VI-6) was used to end block the polyrotaxane of molecular weight 10,000, prepared using 30-c-10 macrocycle (8.4 equivalents per monomer).

The polyrotaxane with blocking group was found to be soluble in DMF, DMAc and partially soluble in THF. Proton NMR data (after 2 precipitations) suggests that there are two blocking groups per every 60 repeat units (molecular weight 20,000); also it suggests that there is one 30-c-10 macrocycle per every 60 repeat units (weight % macrocycle = 2.5 %). GPC analyses showed the molecular weights to be as follows.

Universal Calibration

Mn= 10.2×10^3

Mw= 32.0×10^3

Mw/Mn= 3.15

Polystyrene Standards

Mn= 14.2×10^3

Mw= 43.1×10^3

Mw/Mn= 3.04

The molecular weight distribution is fairly broad; this is due to the presence of low molecular weight polymer which accounts for almost 13 wt %. Also it has about 20 wt % polymer having molecular weight higher than 65000. Further, GPC does indicate the absence of unthreaded macrocycle. Thus, two precipitations are enough to remove unthreaded (free) macrocycle from the polyaramide.

Higher than target molecular weight was obtained; this may be due to the difference in the reactivity between the amine blocking group and the amine groups of ODA. Further, only about one blocking group per polymer chain was found to be present (by NMR). The threading efficiency is very low and this may be due to the small size of the 30-c-10 macrocycle.

Thus polyrotaxanes of ODA-I were prepared using 30-c-10 (4.2 eq. per monomer) and 60-c-20 (2.1 eq. per monomer) without the blocking group. Scheme VIII-2 shows the synthesis of polyrotaxanes of ODA-I using 30-c-10 and 60-c-20.

Scheme VIII-2 Synthesis of Polyrotaxanes of ODA-I

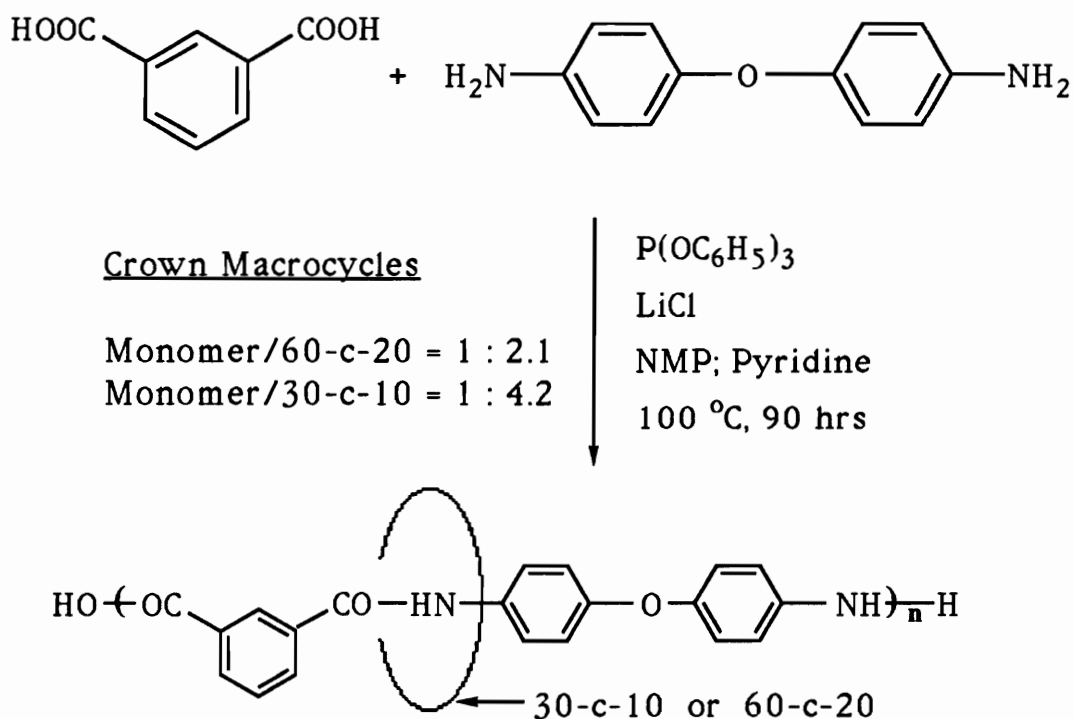


Table VIII-1 shows the macrocycle incorporation (weight %) as well as the ratio of repeat units per macrocycle (R/M) after each precipitation for the polyrotaxanes. The weight % incorporation of macrocycles did not change significantly in two precipitations; this

suggests that all the free macrocycles have been removed from the polymers. Further, in the GPC analyses of the polymers, no free macrocycles were seen. However, the polyrotaxanes did not show any significant improvements in the solubility properties.

Table VIII-1 Precipitation of ODA-I Polyrotaxanes

<u>Precipitation</u>	<u>ODA-I-Rotaxa-30-c-10</u>	<u>ODA-I-Rotaxa-60-c-20</u>
Precipitation 1	13.0 wt. % 9.1 R/M	35.0 wt. % 5.0 R/M
Precipitation 2	9.1 wt. % 13.3 R/M	34.8 wt. % 5.0 R/M

Figure VIII-1 shows the proton NMR spectra for ODA-I-Rotaxa-30-c-10 and ODA-I-Rotaxa-60-c-20. In the polyrotaxanes of 30-c-10 only about 9 wt % macrocycle has been incorporated while almost 35 wt % 60-c-20 is incorporated. This difference in macrocycle incorporation is due to the size of the macrocycles. As the number of atoms in a macrocycle doubles, the area of the macrocycle cavity quadruples assuming that both the macrocycles are in fully expanded state. Whether this assumption is valid is not, the increase in effective macrocycle cavity size available for threading is much higher in 60-c-20 than in 30-c-10 and the threading yields reflects this.

Absolute molecular weights and those from polystyrene standards obtained from GPC are shown below for model polymer and polyrotaxanes. Figure VIII-2 shows the GPC traces for model ODA-I, ODA-I-Rotaxa-30-c-10 and ODA-I-Rotaxa-60-c-20.

ODA-I Model Polymer

Universal Calibration

Mn= 18.7 X 10³
Mw= 33.2 X 10³
Mw/Mn= 1.78

Polystyrene Standards

Mn= 31.7 X 10³
Mw= 54.6 X 10³
Mw/Mn= 1.72

ODA-I-Rotaxa-30-c-10

Universal Calibration

$$M_n = 4.8 \times 10^3$$

$$M_w = 7.1 \times 10^3$$

$$M_w/M_n = 1.49$$

Polystyrene Standards

$$M_n = 7.8 \times 10^3$$

$$M_w = 10.5 \times 10^3$$

$$M_w/M_n = 1.35$$

ODA-I-Rotaxa-60-c-20

Universal Calibration

$$M_n = 7.7 \times 10^3$$

$$M_w = 11.5 \times 10^3$$

$$M_w/M_n = 1.49$$

Polystyrene Standards

$$M_n = 14.2 \times 10^3$$

$$M_w = 20.3 \times 10^3$$

$$M_w/M_n = 1.43$$

The molecular weights for the polyrotaxanes are lower than that for the model polymer. This may be due to traces of water not removed from the crown ethers. The polymerization is typically not affected by the presence of traces of moisture since the reaction is done at about 100 °C; in the literature, neither adverse effects of moisture are discussed nor polymerizations under very dry conditions. Thus, it can be safely concluded that moisture may not have played a major role in obtaining the lower molecular weights for polyrotaxanes. Another possibility is that glycol impurities in the crown ethers may yield lower molecular weights of the polyrotaxanes. However, this was not the case as discussed below.

Synthesis of these polyaramides in the presence of poly(ethylene oxide) (PEO) of different molecular weights using the Yamazaki et al. procedure has been reported (5,6). It was found that the molecular weights of the polymers (as inferred from inherent viscosity data) produced varied with the amount and molecular weight of PEO, which showed maximum values when PEO with a molecular weight of 20,000-500,000 was used in a concentration of 0.5 wt % in the solvent. Molecular weights thus produced were much higher than that in the absence of PEO. It is indicated that the aromatic diacid interacts with oxyethylene repeat units via hydrogen bonding and is adsorbed onto PEO chain, thus increasing

(local) concentration of the diacid to produce higher molecular weight polymer (5).

An increase in concentration of PEO from 0.5 % up to 2 % decreased the molecular weight of the polyaramide. Further, decrease in molecular weight of the PEO from 500,000 to 400 also decreased the molecular weight of the polyaramide produced. In any case the, molecular weights thus produced (0.5 wt % PEO; mol. wt. $(3-5) \times 10^5$) were much higher than that in the absence of PEO.

In the polyrotaxanes produced above, concentrations of the crown ether in the polymerization mixture were as high as 50 %. It is possible that such high concentrations of crown ether may reduce molecular weights of the polyrotaxanes produced.

In reported polymerization of polyaramides in the presence of PEO, the authors report that all the PEO (mol. wt. $(3-5) \times 10^5$) was effectively removed by suspending the polyaramide in boiling water for 1 hour followed by filtration and further suspending the polymer in methanol for one hour. Removal of PEO was confirmed by elemental analyses.

In the case of polyrotaxanes, the low molecular weight highly soluble free macrocycles should be much more easy to remove by precipitation as was found to be the case.

FTIR Analyses

Absorption for carbonyl groups of amide linkages in the IR spectrum of ODA-I-Rotaxa-60-c-20 was seen at 1668 cm^{-1} (resolution of 4 cm^{-1}) along with absorption for the ether linkages of the macrocycles at 1109 cm^{-1} . The IR spectrum of ODA-I-Rotaxa-30-c-10 showed carbonyl groups at 1662 cm^{-1} along with the ether linkages at 1109 cm^{-1} . The model polymer showed carbonyl group absorption at 1662 cm^{-1} . This suggests that some of the carbonyl groups in ODA-I-Rotaxa-60-c-20 are not hydrogen bonded. It may also be the case for ODA-I-Rotaxa-30-c-10; however, due to lower incorporation of 30-c-10, the relative proportion of hydrogen bonded carbonyl groups may be higher. No

significant changes were observed in the absorption of N-H groups of model polymers and its polyrotaxanes. More detailed FTIR studies on these polyrotaxanes may be needed using a high resolution FTIR instrument.

Thermal Analyses:

Polyamides are known for high moisture absorption. It depends on the amide linkage content and typically for nylon-6,6 it ranges from 5-9 % (1) while for polyaramides it is about 5 % (12). Thus all the DSC analyses were done by first heating the sample to 120-130 °C in the DSC pan to remove any absorbed moisture and rapidly cooling it to room temperature and then the first as well as second heating scans in DSC were obtained at a heating rate of 10 °C.

Polyrotaxanes were analysed by DSC immediately after the synthesis and both the polyrotaxanes showed an exothermic peak in the first heat scan, which disappeared in the second scan. The model polymer showed typical glass transition temperature at 253 °C (both first and second scan). The exothermic peak for ODA-I-Rotaxa-30-c-10 was observed at 181 °C while the exothermic peak for ODA-I-Rotaxa-60-c-20 was observed at 160 °C. The presence of an exotherm in polyrotaxanes indicate some sort of crystallization or reorganization occurring in the polymer. These exothermic peaks were found to shift with time at room temperature. In the case of ODA-I-Rotaxa-30-c-10 the peaks shifted to 251 °C in 60 days, while for ODA-I-Rotaxa-60-c-20 the peaks shifted to 177 °C in four months. In the later case, the shift was not as significant as that observed for the 30-c-10 rotaxane. During the above mentioned aging times the polymers were mainly kept at room temperature except that they were dried at 35-40 °C for 48 hours. Figure VIII-3 and VIII-4 show the DSC traces of ODA-I-Rotaxa-30-c-10 and ODA-I-Rotaxa-60-c-20, respectively, before and after the exotherm shift.

DTA-TG Analyses:

To make sure that these exotherms are real and that the exotherms are not due to other reasons such as decomposition etc., differential thermal analyses coupled with TGA were done simultaneously for polyrotaxanes of 60-c-20. Figure VIII-5 shows the DTA-TG traces of ODA-I-Rotaxa-60-c-20. The sample lost about 1.2 % weight up to 145 °C and up to 265 °C it lost a total of 2.8 % weight. Further, a broad peak from 150 °C up to 210 °C, with a peak at 193 °C was observed. This suggests that the exotherm seen in DSC is real and that some type of crystallization or more ordered structure is forming.

Explanation:

Various studies on the interaction of carbonyl containing groups (amides, urethanes, esters, etc) in polymers and polymer blends have been studied using FTIR spectroscopy (13-18). Free carbonyl groups (non hydrogen bonded) absorb at higher wave numbers than hydrogen bonded (16,18). Based on the FTIR studies of the polyamides it was concluded that the predominant effect of increasing temperature is the reduction of the strength of the hydrogen bonds and that the fraction of 'free' N-H groups does not vary significantly over a temperature range between 30-210 °C (17).

As indicated above, the frequency of the absorption of the carbonyl groups of the amide linkage is higher in ODA-I-Rotaxa-60-c-20 than in the model polyamide. A similar effect is not seen in ODA-I-Rotaxa-30-c-10, probably due to the lower incorporation of the crown ether. This suggests that the hydrogen bonding in the bulk polymer is affected by the presence of macrocycles on the polymer chain. It is possible that hydrogen bonding may be taking place between oxygen atoms of the crown ether and N-H groups, intraannularly. Further, the macrocycles around the semi-rigid chains may decrease the strength of intermolecular hydrogen bonds but due to low Tg of the incorporated oligomeric macrocycles (-67 to -70 °C) the Tg of the polyrotaxane is lowered. Thus, the polymer

has a chance to reorganize itself to go to a more ordered state by formation of hydrogen bonds intermolecularly, at the expense of intraannular hydrogen bonding, which may be the driving force.

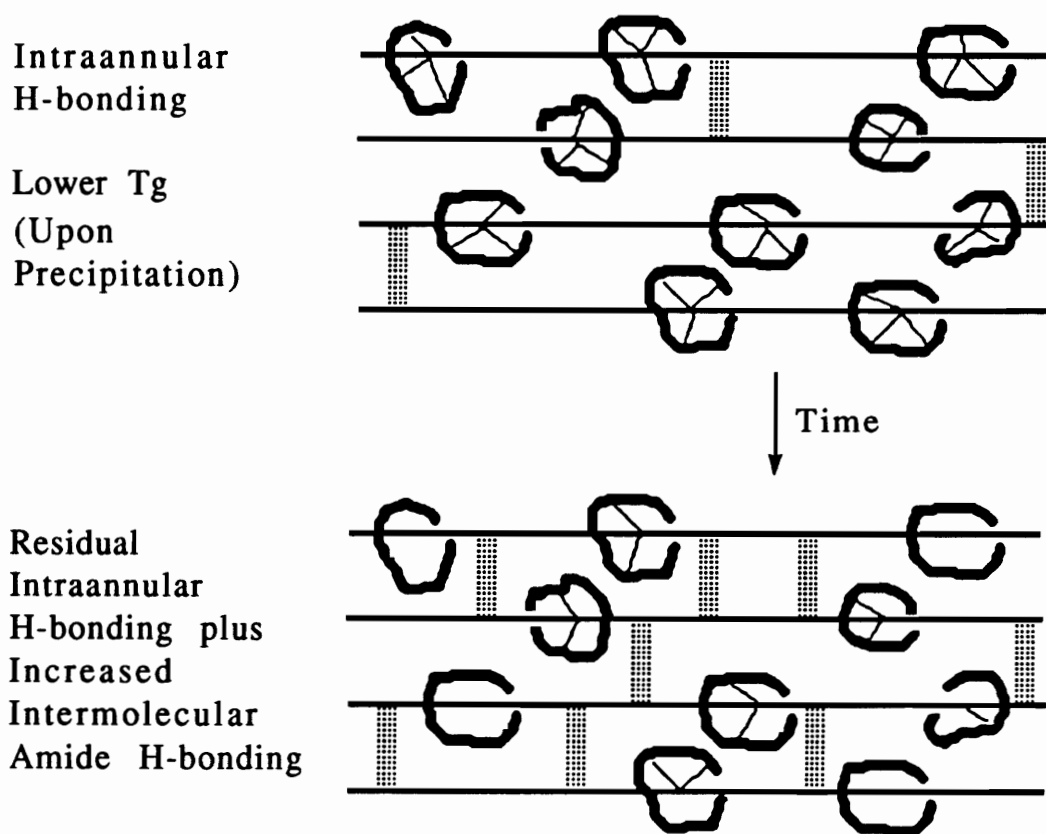
This formation of more ordered state may be less favored entropically; however, the relative strength of crown ether-amide hydrogen bond is much lower than that of the amide-amide hydrogen bond (19) and thus, formation of such an ordered state is more favored. The formation of such ordered structures (analogous to crystallization) would explain exothermic peaks observed at 181 °C and 160 °C in the DSC traces of the polyrotaxanes of ODA-I-Rotaxa-30-c-10 and ODA-I-Rotaxa-60-c-20, immediately after the synthesis (Figures VIII-3 and VIII-4). Further, no more peaks are seen after the exothermic peaks until decomposition (in the first and second heating scan), indicating that melting of the ordered structure may be accompanied by thermal decomposition as seen in most of the rigid or semi-rigid polyaramides. It has also been suggested that for rodlike systems an anisotropic phase or crystallization of some type can occur with minimal intermolecular forces (1).

It was expected that the T_g of the polyrotaxanes must be close to but lower than the observed exothermic peaks. Using the Fox equation, the calculated T_g values were 187 °C for ODA-I-Rotaxa-30-c-10 (9.1 wt % 30-c-10, $T_g = -69$ °C) and 69 °C for ODA-I-Rotaxa-60-c-20 (34.8 wt % 60-c-20, $T_g = -67$ °C). These calculated values for polyrotaxanes of polyaramides are not in agreement with the observed values of exothermic peaks. This deviation may arise from the novel polyrotaxane architecture and/or the intermolecular and intraannular hydrogen bonding.

Scheme VIII-3 describes the changes taking place in polyrotaxanes with time and temperature. The intraannular hydrogen bonding is represented by thin lines connecting the macrocycle and the linear chain. The thick dotted lines between the polymer chains represents the intermolecular hydrogen bonds between the chains. When the polymer is formed in the presence of crown ether

macrocycles in solution, the macrocycles threaded onto polymer chains form intraannular ether-amide hydrogen bonds with the polymer chains; with time in the solid state intermolecular amide-amide hydrogen bonds form at the expense of intraannular hydrogen bonds. As would be expected for a strongly exothermic process such changes occur only once and thus, in DSC traces no such changes are observed in the second heat scans. This result suggests that the reorganization is irreversible and that such polyrotaxane systems are analogous to thermosetting polymers.

Scheme VIII-3 Time and Temperature Dependent Changes in Polyrotaxanes

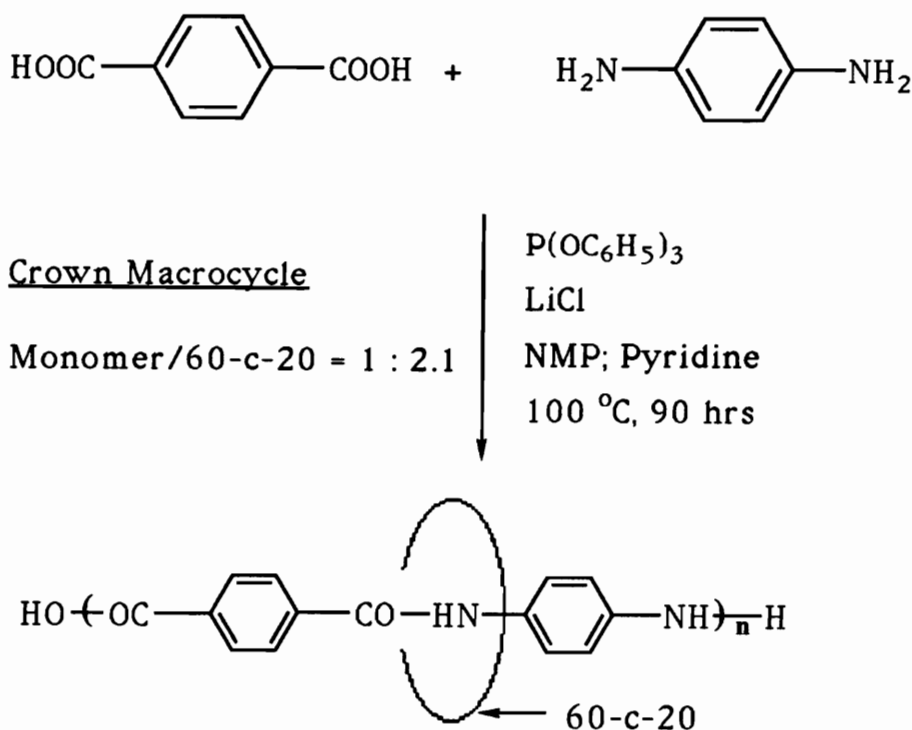


VIII.4 Model PPD-T (Kevlar™) and its Polyrotaxanes

Polyrotaxanes of PPD-T were prepared using 2.1 eq of 60-c-20 per monomer without the blocking group. The model polymer was prepared using diglyme as described earlier. Scheme VIII-4 shows the schematic of the synthesis of PPD-T polyrotaxane.

Polymerizations were continued for 90 hours to obtain high molecular weight polymers. It was observed that the polyrotaxane forms opaque gels in about 11-12 hours while the model polymer formed an insoluble precipitate in about one hour. The model PPD-T was easy to purify by suspending the polymer in methanol followed by filtration. The polyrotaxane formed a very fine suspension in water, methanol, acetone, DMF, NMP and THF and was very difficult to filter; heat had no effect on the suspension.

Scheme VIII-4 Synthesis of Polyrotaxane of PPD-T



Based on these results, it was thought that polyrotaxanes of sufficiently low molecular weight might be soluble. Thus, polymerizations were performed for only 11 hours; the resulting polymer showed no solubility but formed suspensions as indicated above. Optical microscopy of the suspension showed crystalline particles of a few microns size. Further, it was observed that once the polyrotaxanes are worked up and dried, they no longer form fine suspensions.

Quantitative ^{13}C solid state NMR spectra of the polyrotaxanes (both samples) indicate that the macrocycle content is 57-58 weight % (± 10 %). Figure VIII-6 show the ^{13}C solid state NMR spectrum of the PPD-T-Rotaxa-60-c-20.

FTIR Analyses:

In the FTIR spectrum of the model PPD-T, the carbonyl absorption was observed at 1647 cm^{-1} , the same as observed for the polyrotaxane (resolution 4 cm^{-1}). A huge peak for ether linkages was seen at 1109 cm^{-1} in PPD-T-Rotaxa-60-c-20. Additional peaks for polyrotaxanes are observed at 953 cm^{-1} and 1351 cm^{-1} . The rest of the IR spectrum of the polyrotaxane was identical to the model polymer.

Thermal Analyses:

TGA data (in nitrogen) showed the onset of degradation for the the polyrotaxane at about $330\text{ }^\circ\text{C}$ while the model polymer is stable at least up to $450\text{ }^\circ\text{C}$. The char content in the model polymer was found to be 63 % while for the polyrotaxane VIII-6 it was 34 %. Figure VIII-7 show the TGA traces for PPD-T model polymer and its polyrotaxanes. The lower char content in polyrotaxane is due to the 60-c-20 threaded onto the polymer. The char content of the polyrotaxane (ca. 34 %) roughly matches the polyaramide content (43 weight % ± 10 %), assuming low char yield (less than 5 %) for the crown.

DSC analyses did not yield any useful information since no transitions were observed from 30 to 330 °C and above that the polymer began to decompose. However, from DSC it was found that the polymers do absorb significant amounts of moisture. The very different behavior of the PPD-T-Rotaxa-60-c-20 (absence of detectable transitions and exothermic peaks) from that of ODA-I rotaxanes is due to the fact that PPD-T polymer chains are much more rigid than ODA-I polymer chains.

From the characterization data it appears that a very large amount (ca. about 57 ± 10 %) of 60-c-20 was incorporated onto the polymer. However, the polyrotaxanes were insoluble. The fine dispersions obtained for polyrotaxanes may provide aid in the processing of such rigid-rod type liquid crystalline polymers.

Similar results in macrocyclic polymers, where the macrocyclic components were dibenzo- crown ethers of various sizes, were obtained, i.e., they were insoluble in common solvents (20-21). A polymer with macrocyclic diaminodibenzo-18-c-6 linked with isophthalic acid was soluble in very highly polar hexamethylphosphoramide (20), while the macrocyclic polymer derived from relatively flexible ODA and dicarboxyl-dibenzo-32-c-10 was insoluble (21). The insolubility of these systems has been ascribed to the hydrogen bonding interactions between the amide groups.

In rigid rodlike polyaramides such as PPD-T, the chains are rigid as well as symmetrical (para-linked phenyl groups), providing a unique geometry to bring amide groups in close proximity such that the effect of amide-amide interactions is maximized.

An insight in to the nature of amide-amide interactions occurring in biopolymers and biomolecules and quantifications of such interactions are reported (19). Of particular interest are answers to the questions about how a polypeptide remains soluble as well as selectively and reversibly cleaves hydrogen bonds (in replications, etc.) despite its extremely high amide content as well as cross-linking to some extent.

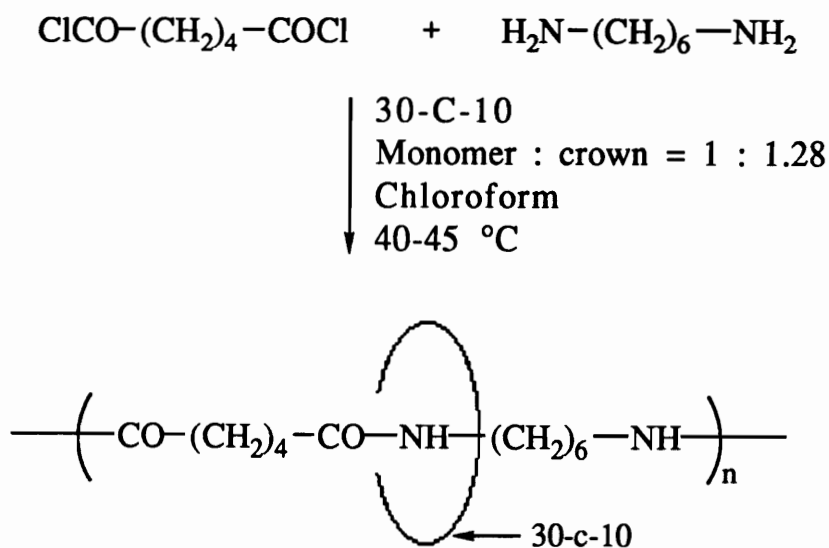
Any bimolecular binding process is entropically unfavorable due to the loss of translational and rotational entropy. However, in aqueous media, as the author suggests based on experimental data, going from two amide groups hydrogen bonded individually to water to two amide groups hydrogen bonded with each other is largely entropy driven due mainly to the increase in entropy by release of two water molecules as bulk water. This favorable entropy change associated with amide-amide hydrogen bonding is closely balanced by unfavorable entropy changes associated with the ordering of the polypeptide chains. The formation of such binding is reduced in nonpolar media by a factor of 10. Further, larger amounts of hydrophobic content in polypeptides reduces the binding energy of such amide-amide interactions.

Due to very high rigidity (as a result of symmetry in the repeat unit components, i.e., para- linkages) and large amide content, the polymer chains in PPD-T do not have very high degrees of translational or rotational freedom, thus resulting in loss of entropy. This loss in entropy is compensated by amide-amide hydrogen bond formation since the unique geometry for the formation of such interactions is available and this seems to be enthalpically favorable. When a crown is present in polyrotaxanes of PPD-T, the strength of hydrogen bonds of amide-crown ether is much lower (about one half) (19) than that of amide-amide hydrogen bonding. These effects together give insoluble polyrotaxanes of PPD-T and the desired results of breaking the amide-amide hydrogen bonds and replacing it with intraannular crown ether-amide bonds to give a soluble polyaramide was not achieved. However, one approach that may be taken to improve the solubility is to incorporate hydrocarbon macrocycles such that hydrophobicity of the polyrotaxane could be increased, resulting in lower amide-amide hydrogen bonding, as indicated above.

VIII.5 Model Nylon-6,6 and its Polyrotaxane

The model polymer and Nylon-6,6-Rotaxa-30-c-10 were prepared from hexamethylenediamine (HMD) and adipoyl chloride using 1.28 eq of 30-c-10 macrocycle per monomer. Scheme VIII-5 shows the synthesis of Nylon-6,6-Rotaxa-30-c-10.

Scheme VIII-5 Synthesis of Polyrotaxane of Nylon-6,6



The model polymer was synthesized in a similar way except that diglyme was used as solvent and polymerization was done at about 80-90 °C due to the insolubility of HMD.

After two purifications, only 4.8 weight % macrocycle was found to be incorporated onto the polymer (by proton NMR in trifluoroacetic acid). Further, the polyrotaxane did not show any changes in solubility, it was found to be insoluble in most of the common organic solvents.

Thermal Analyses

The model polymer begins to degrade at 300 °C and 5 % weight loss is observed at about 330 °C. The polyrotaxane shows the onset

of degradation at about 280 °C. The glass transition temperature (T_g) for the model polymer is not seen either in the first heat or in the second heat. The reported value for the T_g is 65 °C (1). In the second heat a melting transition T_m appears as a strong exotherm at 243 °C. The reported value for the T_m is 265 °C (1). The polyrotaxane showed a broad melting peak from 212 -249 °C, with the maximum at 240 °C. The melting temperatures of the model polymer and its polyrotaxane are comparable.

The low incorporation of macrocycle can be attributed to the lower monomer to macrocycle ratio in the polymerization mixture and lower cavity size of the macrocycle. Further, the polymerization of HMD and adipoyl chloride is very fast (less than a minute) and this may not help in achieving high threading yields. Unlike polyrotaxanes of ODA-I and PPD-T, the end blockers may be needed. More macrocycle needs to be incorporated to effectively change the solution as well as bulk properties in nylon-6,6. This could be accomplished by using higher macrocycle to monomer ratios, using a larger macrocycle and changing the crown ether macrocycle to calix[8]arene (chapter III) so that the polymerization could be done in the melt. Model studies on the synthesis of end blocked low molecular weight (ca. 10,000) nylon-6,6 polyrotaxanes using various macrocycle to monomer ratios will be useful.

Table VIII-2 summarizes the results obtained for polyrotaxanes of polyamides with 30-c-10 and 60-c-20.

Table VIII-2 Synthesis and Characterization of Polyrotaxanes of Polyamides

Linear Chain	Macrocycle	Feed Ratio Macrocycle/ Monomer	Repeat Unit/ Macrocycle in Polyrotaxane	Wt. % Macrocycle
ODA-I [†]	30-c-10	4.2 eq.	60.0 ^{A*}	2.5 %
ODA-I	30-c-10	4.5 eq.	13.3 ^{A*}	9.1 %
ODA-I	60-c-20	2.2 eq.	5.0 ^{A*}	34.8 %
Kevlar	60-c-20	2.1 eq.	2.7 ^B	57.8 %
Kevlar	60-c-20	2.1 eq.	2.8 ^C	56.9 %
Nylon 6,6	30-c-10	1.3 eq.	41.0 ^A	4.8 %

† with blocking group

* No free macrocycle as determined by GPC

A After 2 Precipitations

B After 3 purifications with methanol

C After 3 purifications with Acetone:water:methanol using centrifugation followed by suspending the polymer in methanol

VIII.5 Experimental

Measurements:

Melting Points were taken in capillary tubes with a Haake-Buchler melting point apparatus and have been corrected. TGA data were obtained using Du Pont TGA 951 and Perkin-Elmer TGA-7 instruments at a scan rate of 10 °C/min. DSC data were obtained using Du Pont DSC 912 and Perkin-Elmer DSC-2 instruments at a scan rate of 10 °C/min. GPC data were obtained in 0.5 % LiBr solutions in NMP at 60 °C using a Waters 150-C ALC/GPC instrument equipped with refractive index and online viscometer detectors. Molecular weights of the soluble polymers according to polystyrene standards as well as absolute molecular weight (based on hydrodynamic volume) were obtained. Proton and carbon NMR spectra were obtained on a Bruker WP 270 spectrometer using deuterated dimethyl sulfoxide, dimethyl formamide and CF₃COOD solutions with tetramethylsilane as an internal standard. Solid state ¹³C NMR data were obtained using a Bruker MSL-300 instrument. FTIR spectra were obtained on a Nicolet MX-1 instrument.

Synthesis of Poly(oxydiphenyleneisophthalamide):

0.4485 g (2.7×10^{-3} moles) of isophthalic acid, 0.5406 g (2.7×10^{-3} moles) of oxydianiline (ODA), 6.0 ml of diglyme, 1.5 ml pyridine, 2.5 ml NMP and 0.4 g dry LiCl were mixed under nitrogen and heated to 100 °C using an oil bath (oil bath temperatures was 110 °C). At this temperature everything had dissolved; to this 1.42 ml (1.67 g, 2.7×10^{-3} moles) triphenylphosphite was added and the polymerizations were continued for 90 hours. The gelled polymer was dissolved by addition of 20-40 ml DMF or NMP (warmed if necessary) and precipitated into acetone:methanol (60:40), filtered, washed several times with acetone, water and methanol and dried under vacuum at room temperature for 36 hours. Isolated yield was about 96-97 %. The polymer was characterized using GPC, TGA, DSC, FTIR and NMR.

Polyrotaxanes of Poly(oxydiphenyleneisophthalamide):

For the synthesis of polyrotaxanes the procedure described above was utilized. Equal moles of both the monomers, blocking group (if used), pyridine, NMP and crown ether (30-c-10 or 60-c-20) were mixed and the reaction mixture was stirred for 1-3 hours at 60 °C. To this LiCl and triphenylphosphite were added and the polymerization was continued for 90 hours. Work up of the polymer was as described above; however, the rotaxanes were further purified by one more precipitation from DMF into 10 fold excess methanol to remove any free macrocycle. The polymers were characterized using GPC, TGA, DSC, FTIR and NMR.

Kevlar Polymer and its Polyrotaxanes using 60-c-20:

The procedures used for the synthesis of polyrotaxanes of Kevlar using 60-c-20 and the model polymer were similar to that described above; however, 6.5 g of 60-c-20 in polyrotaxane synthesis was substituted by 6.5 ml of diglyme for the model Kevlar polymer synthesis. 0.5814 g (3.5×10^{-3} moles) of terephthalic acid, 0.3785 g (3.5×10^{-3} moles) of p-phenylenediamine and 6.5 g 60-c-20 (5.67×10^{-3} moles; 2.1 eq. of monomer) were used for the synthesis of the polyrotaxane. It took about 10-12 hours for the polyrotaxane reaction mixture to gel while the Kevlar model polymer was insoluble as it began to form. Polymerizations were continued for 90 hours at 100 °C.

After the polymerization, the mixture was put in methanol for 2-3 hours and stirred to obtain a very fine suspension which was difficult to filter. Hence, the polymer was purified by adding about 200 ml methanol and storing the suspension in the freezer at -20 °C for 2 days and then filtered. This purification was repeated two more times to remove any free macrocycle. The model polymer behaved very differently; it formed a coarse suspension which was easily filtered. This was repeated one more time. The Kevlar model polymer and its rotaxanes were analysed by solid state NMR and DSC.

In another similar synthesis of the polyrotaxane of Kevlar, the polymerization was done for 11.5 hours at 100 °C. Purification of the polymer was done by pouring the reaction mixture into 300 ml 50:50 acetone:water and centrifugation. The liquid was decanted and this was repeated two more times using a little less acetone. The solid polymer was allowed to dry in air and then suspended in methanol and stirred for 0.5 hour, filtered, washed with methanol repeatedly and dried under vacuum for 12 hours. The polymer was analysed by solid state NMR and DSC.

One Phase Synthesis of Nylon 6.6:

Hexamethylenediamine (99%) was purified by sublimation under vacuum at 35-40 °C; mp: 43-44 °C (corrected); reported mp: 42-44 °C (Aldrich Catalog) . Adipoyl chloride was purified twice by distillation under vacuum; bp: 113-115 °C/2-3 torr; reported bp: 113-115 °C/2-3 torr (Aldrich Catalog).

0.8922 g (7.68×10^{-3} moles) of hexamethylenediamine (HMD) and 40.0 ml dry diglyme were mixed under nitrogen. HMD did not dissolve in diglyme so the mixture was heated using an oil bath at about 100 °C. HMD dissolved in about 10 minutes at this temperature. To this 2.14 ml (7.68×10^{-3} moles) of triethylamine was added using a syringe and then a preweighed vial containing 1.4053 g of adipoyl chloride was carefully dropped into the reaction mixture. The polymerization was very fast and it gelled instantly. Polymerization was allowed to continue for 14 hours at the same temperature. The polymerization mixture was cooled, filtered and then washed with acetone, water, THF and then with acetone and dried. The polymer weighed 1.73 g, yield 77.0 %. The polymer was characterized by TGA, DSC and FTIR.

One Phase Synthesis of Polyrotaxanes of Nylon 6.6:

1.0680 g (9.19×10^{-3} moles) HMD and 5.18 g (1.17×10^{-2} moles; 1.28 eq. of monomer) 30-c-10 were melted in a dry polymerization kettle under nitrogen and stirred for an hour at 50-

60 °C (using a water bath). The color turned from light cream to yellowish green within 10 minutes. To this then 10 ml of chloroform and triethylamine (2.8 ml, 2.02×10^{-2} moles; 2.2 eq. of monomer) were added, followed by addition of 1.6821 g (9.19×10^{-3} moles) adipoyl chloride in chloroform (in less than 10 seconds). The polymerization began immediately, giving an insoluble solid. The reaction is very exothermic and it caused the chloroform to evaporate rapidly under the nitrogen stream. Thus, 10 ml of dry DMF was added to the insoluble solid and the reaction mixture was stirred for 3.5 hours at room temperature. The reaction mixture was poured into 400 ml water, stirred for an hour and filtered and washed with water (5 x 50 ml). The polymer weighed 1.45 g (70 % yield). 1.0 g of the dry polymer was suspended in methanol and stirred for 1.5 hours, filtered and washed with methanol (5 x 50 ml). In this work up only 75 % of the polymer was recovered. The remainder (25 %) of the methanol soluble polymer was also recovered. The polymer was characterized by TGA, DSC and FTIR.

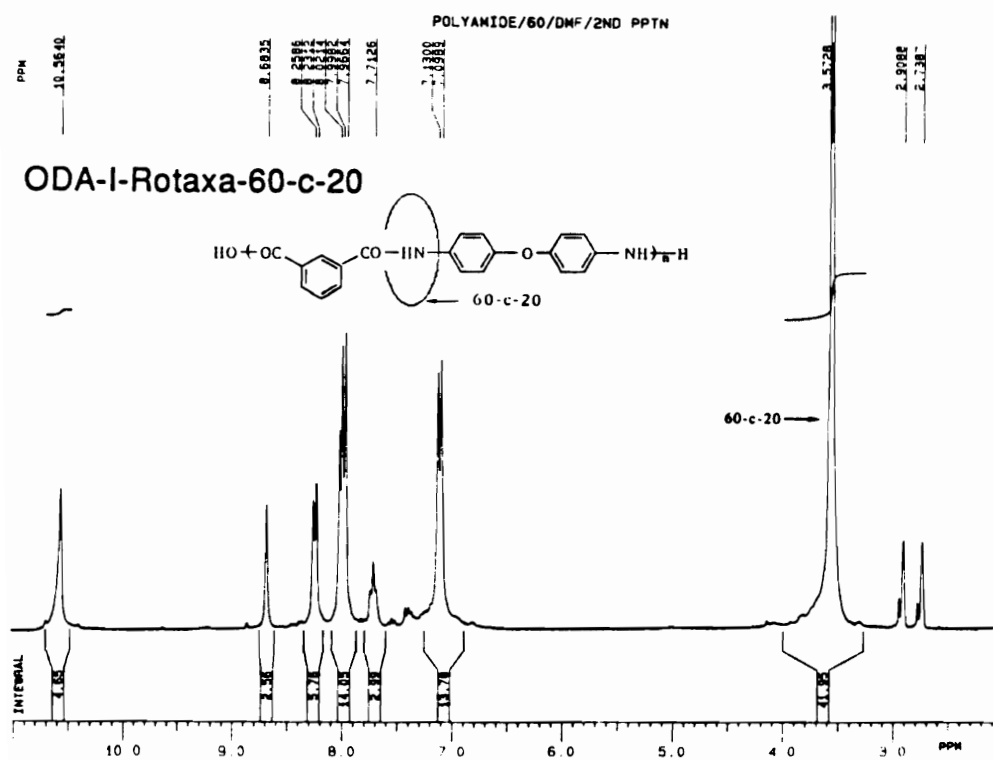
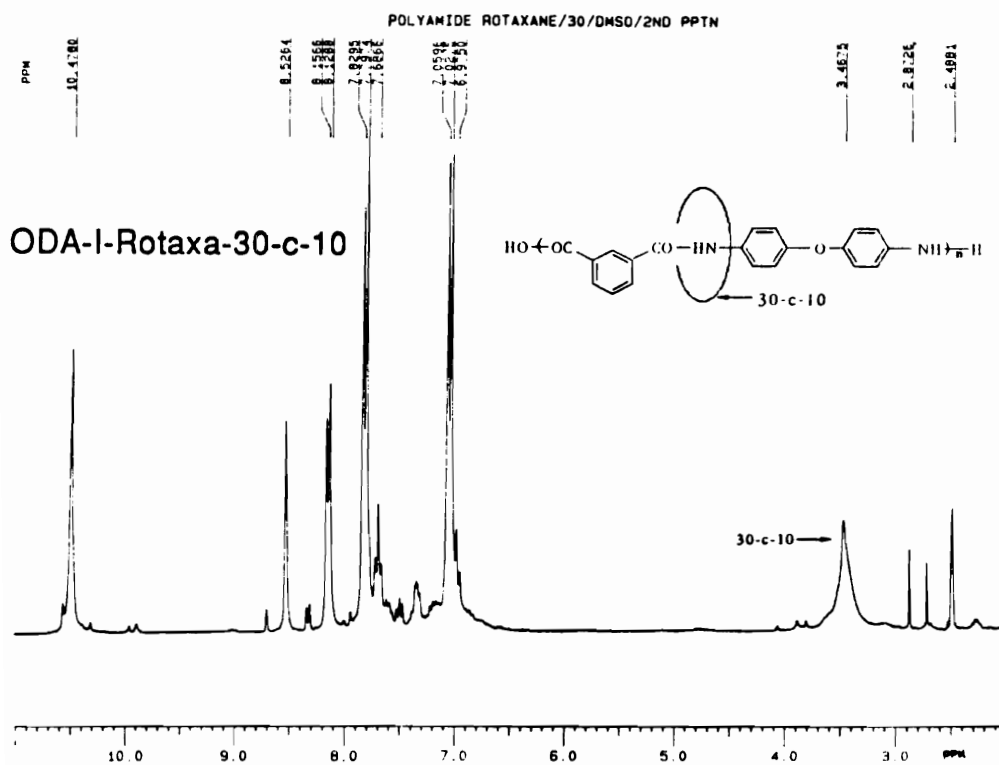


Figure VIII.1 ¹H (270 MHz) NMR of ODA-I-Rotaxa-30-c-10 and ODA-I-Rotaxa-60-c-20

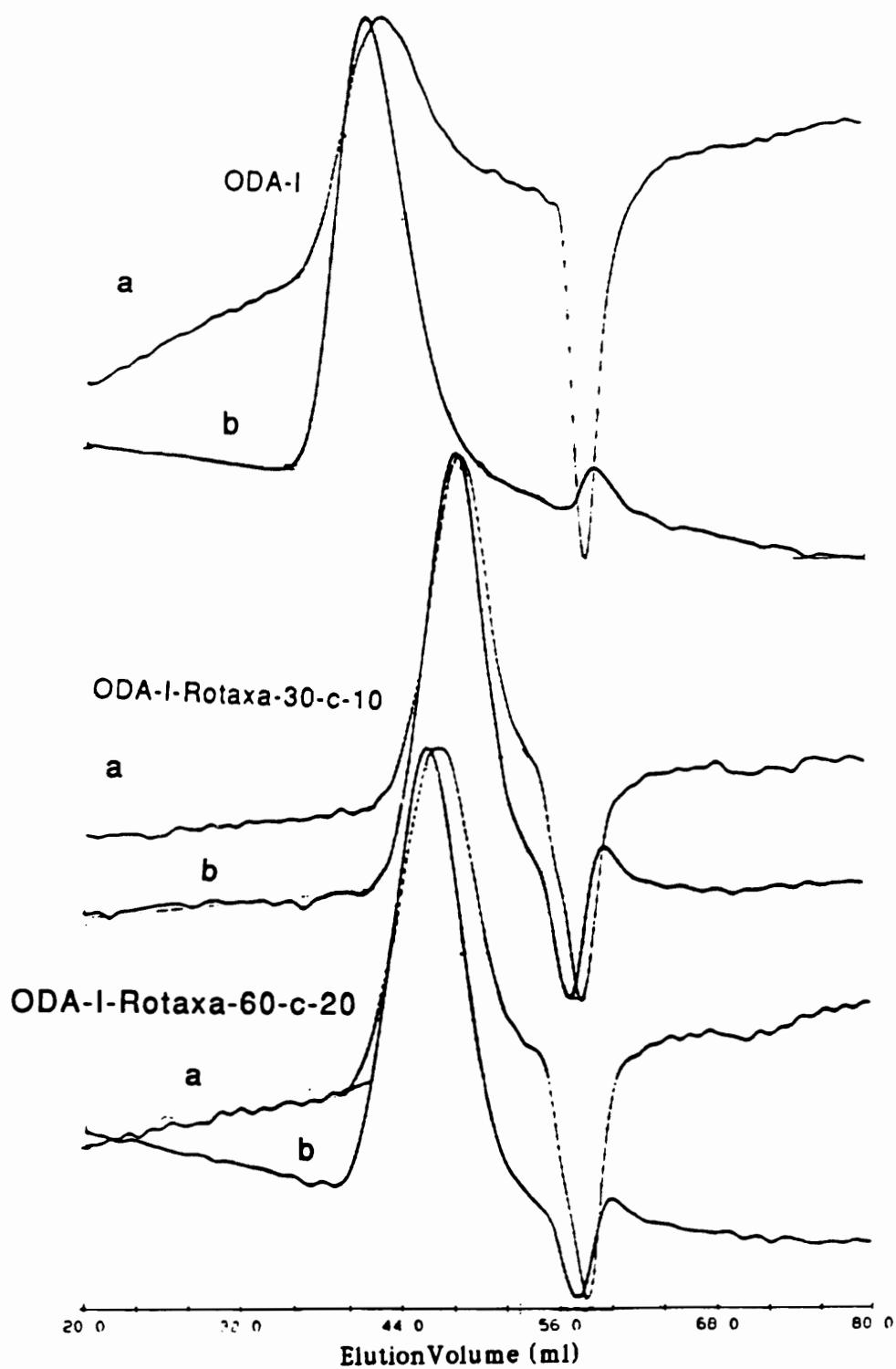


Figure VIII.2 GPC Traces of ODA-I, ODA-I-Rotaxa-30-c-10 and ODA-I-Rotaxa-60-c-20 (a) RI Trace, (b) Viscosity Trace

History Dependent Thermal Properties of Polyamide-Rotaxa-30-c-10

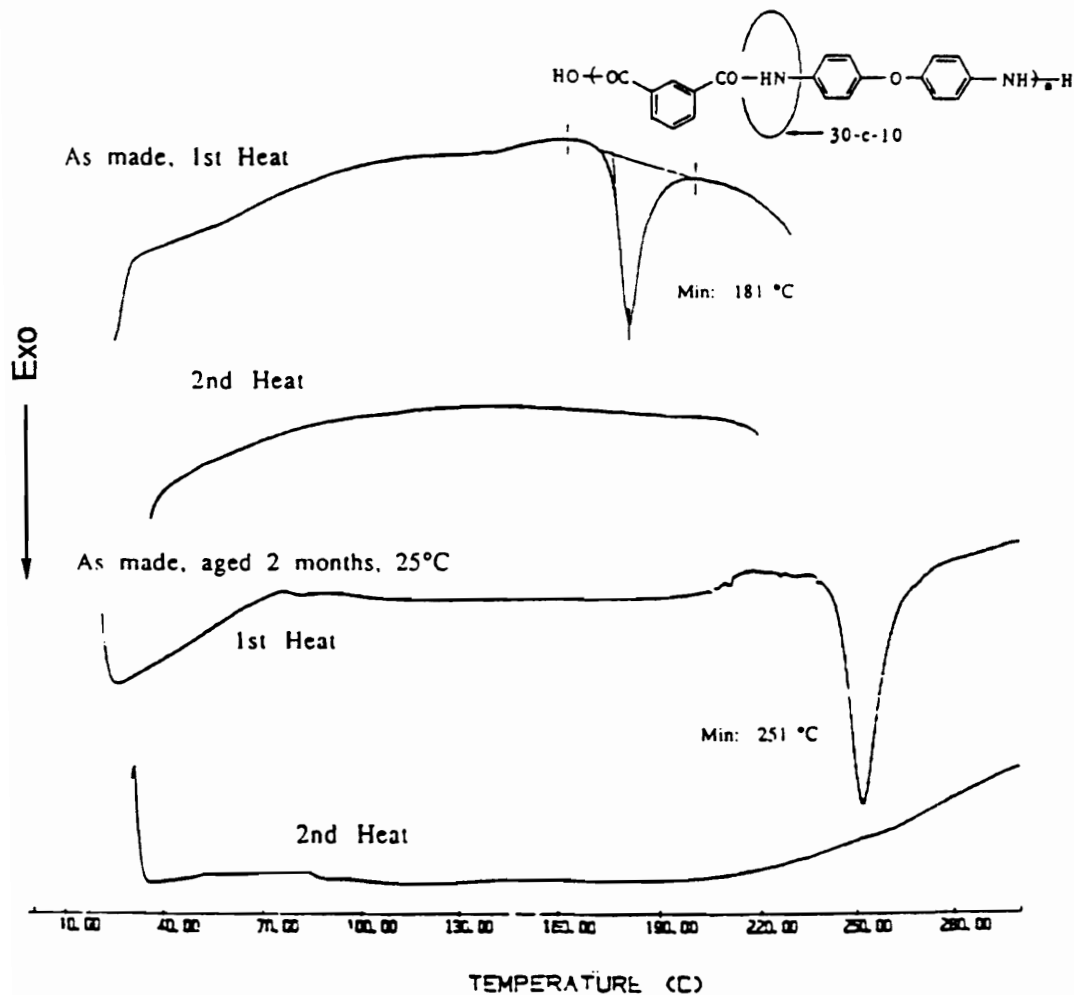


Figure VIII.3 DSC Traces of ODA-I-Rotaxa-30-c-10

History Dependent Thermal Properties of Polyamide-Rotaxa-60-c-20

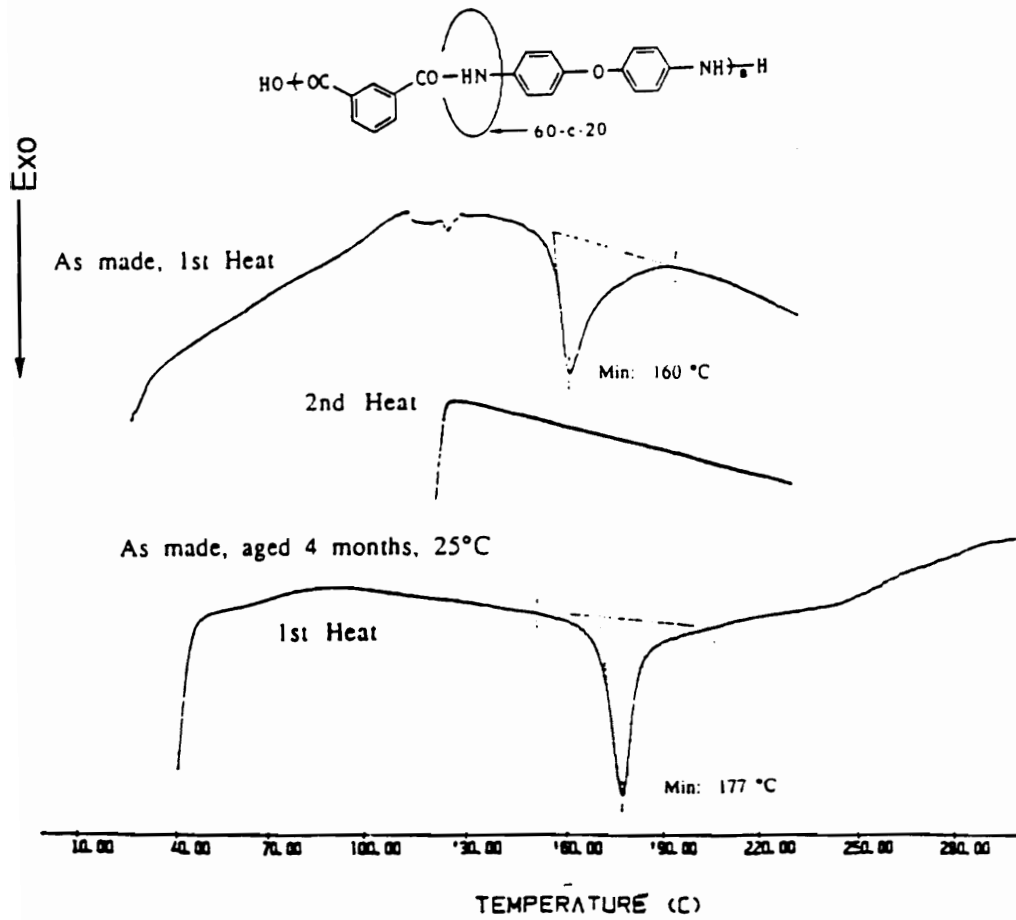


Figure VIII.4 DSC Traces of ODA-I-Rotaxa-60-c-20

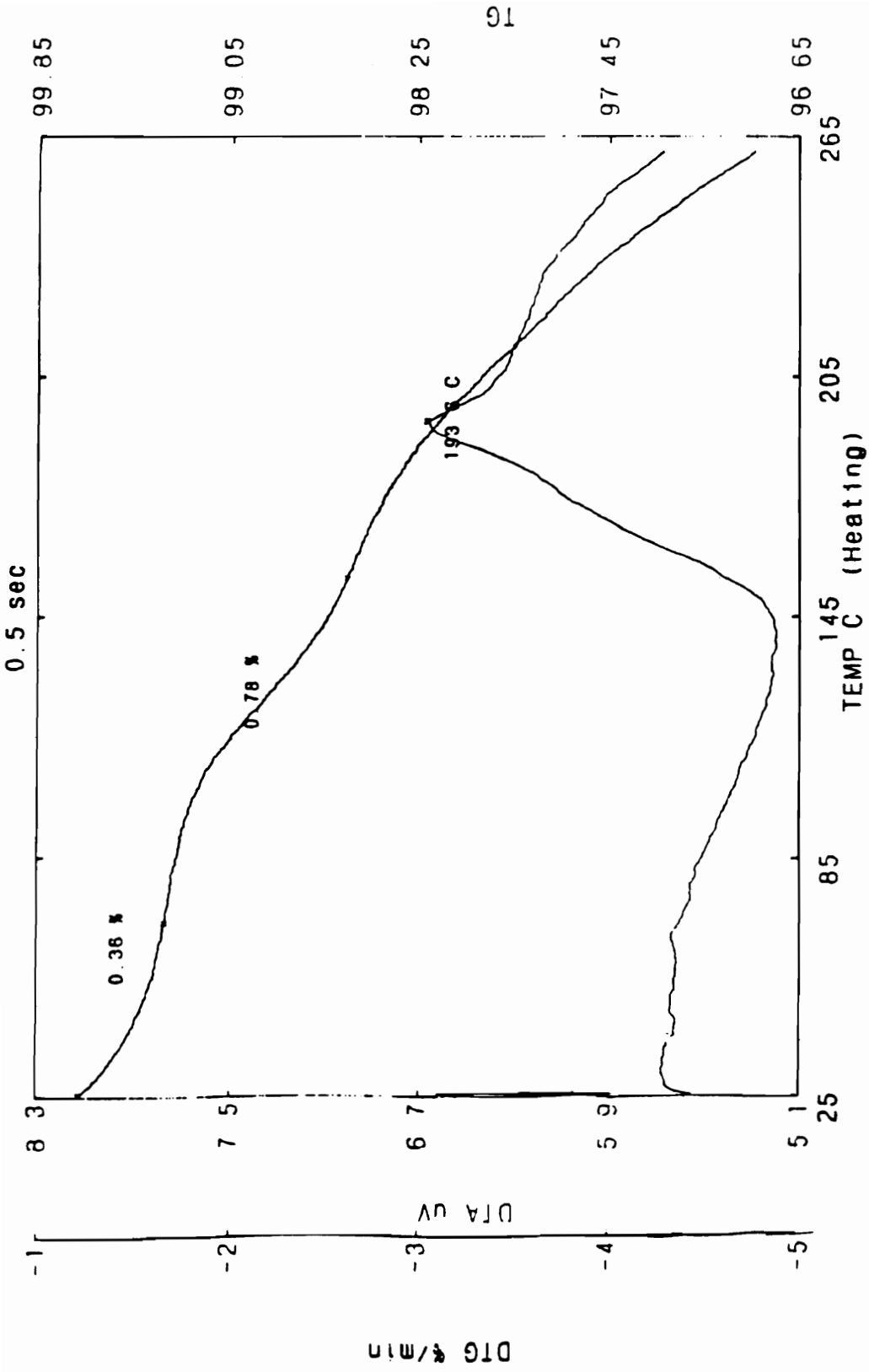


Figure VIII.5 DTA-TG Traces of ODA-I-Rotaxa-60-c-20

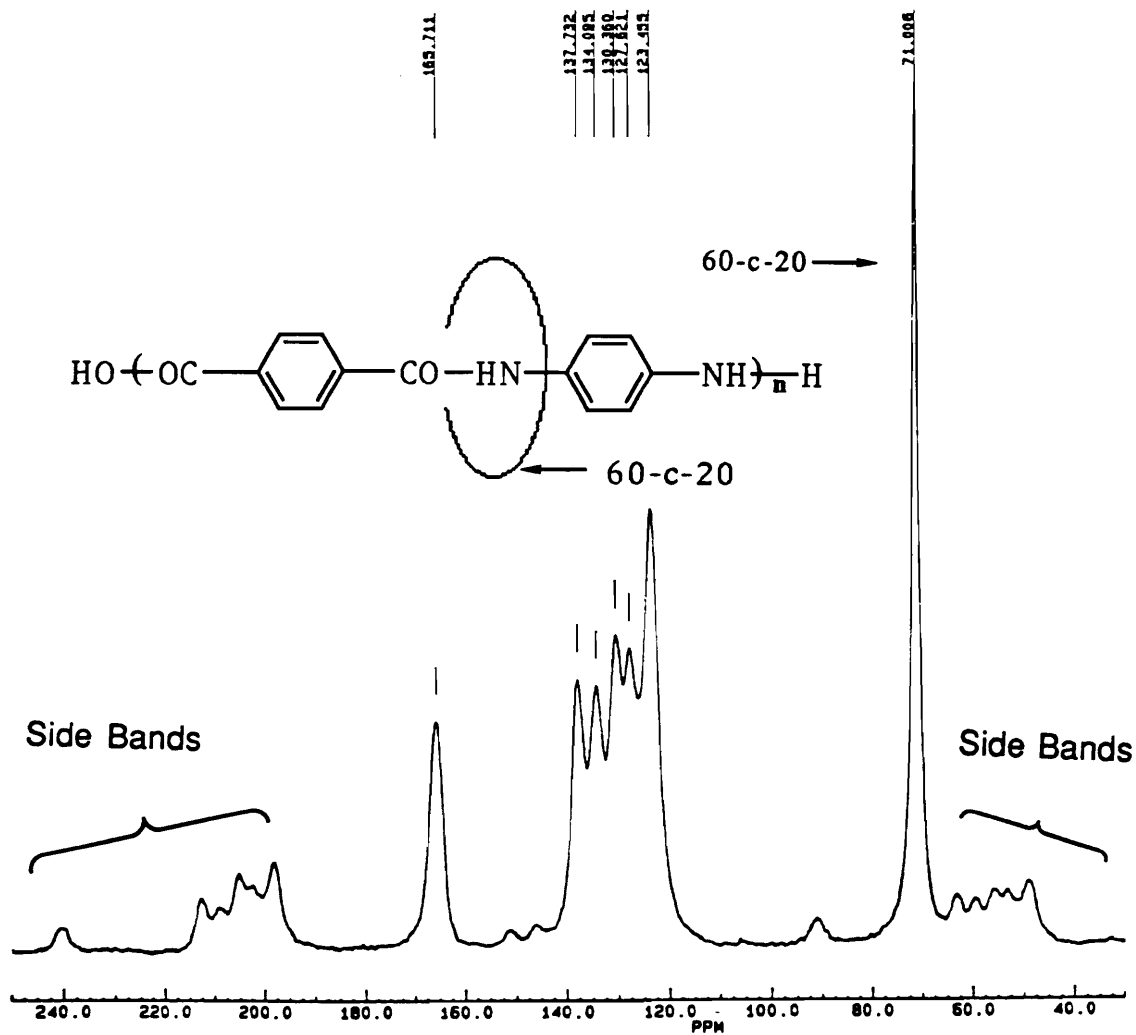


Figure VIII.6 ^{13}C Solid State NMR of PPD-T-Rotaxa-60-c-20

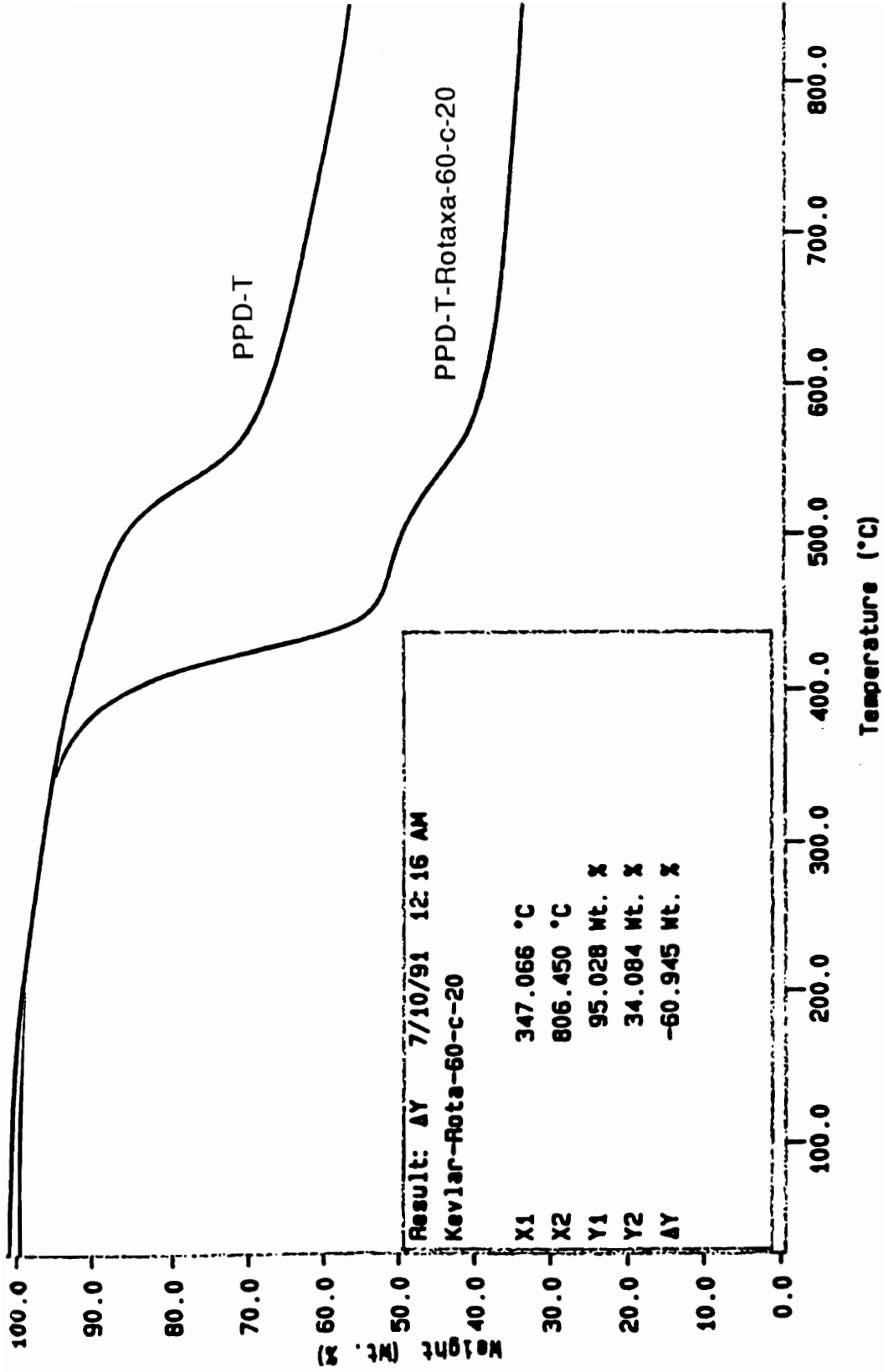


Figure VIII.7 TGA Traces of PPD-T and PPD-T-Rotaxa-60-c-20

References

1. J. Zimmerman, Encyclopedia of Polymer Science and Engineering, Second Edition, John Wiley & Sons, New York, NY, (1987), Vol. 11, 315.
2. J. Preston, Encyclopedia of Polymer Science and Engineering, Second Edition, John Wiley & Sons, New York, NY, (1987), Vol. 11, 381.
3. T. D. Greenwood, R. A. Kahley, J. F. Wolfe and J. J. Johnston, J. Polym. Sci., Polym. Chem. Ed., 1980, 18, 1047.
4. N. Yamazaki, M. Matsumoto and F. Higashi, J. Polym. Sci., Polym. Chem. Ed., 1975, 13, 1373.
5. N. Yamazaki and F. Higashi, Adv. Polym. Sci., 1981, 38, 1.
6. F. Higashi, Y. Nakano, M. Goto and H. Kakinoko, J. Polym. Sci., Polym. Chem. Ed., 1980, 18, 1099.
7. F. Higashi, S. I. Ogata and Y. Aoki, J. Polym. Sci., Polym. Chem. Ed., 1982, 20, 2081.
8. F. Higashi, Y. Taguchi and N. Kokubo, J. Polym. Sci., Polym. Chem. Ed., 1981, 19, 2745.
9. F. Higashi and Y. Taguchi, J. Polym. Sci., Polym. Chem. Ed., 1981, 19, 3345.
10. Y. Imai, M. Kajiyama, S. I. Ogata and M. Kakinoko, J. Polym. Sci., Polym. Chem. Ed., 1984, 22, 3183.
11. M. Ueda and A. Mochizuki, Macromolecules, 1985, 18, 2353.

12. M. Jaffe and R. S. Jones, High Performance Aramide Fibers; Handbook of Fiber Science and Technology, Vol III, High Technology Fibers, Part A; M. Lewin & J. Preston, Eds., Marcel Dekker Inc., New York, NY (1985).
13. P. C. Painter, Y. Park and M. M. Coleman, *Macromolecules*, 1988, 21, 66.
14. M. M. Coleman, D. J. Skrovanek, J. Hu and P. C. Painter, *Macromolecules*, 1988, 21, 59.
15. M. M. Coleman, D. J. Skrovanek and P. C. Painter, *Makromol. Chem., Makromol. Symp.*, 1986, 5, 21.
16. D. J. Skrovanek, P. C. Painter and M. M. Coleman, *Macromolecules*, 1986, 19, 699.
17. D. J. Skrovanek, S. E. Howe, P. C. Painter and M. M. Coleman, *Macromolecules*, 1985, 18, 1676.
18. M. M. Coleman, K. H. Lee, D. J. Skrovanek and P. C. Painter, *Macromolecules*, 1986, 19, 2149.
19. D. H. Williams, *Aldrichimica Acta*, 1991, 24(3), 71.
20. E. Schchori and J. Jaguar-Grodzinski, *J. Applied Polym. Sci.*, 1976, 20, 1665.
21. Y. Delaviz and H. W. Gibson, American Chemical Society, *Polymeric Materials Science and Engineering*, 1992, Volume. 66.

IX.	POLYSTYRENE ROTAXANES 210
IX.1	Introduction 211
IX.2	Results and Discussion 213
IX.3	Experimental 219

IX.1 Introduction

The syntheses of polyrotaxanes of styrene and acrylonitrile, with a variety of aliphatic crown ethers as well as dibenzo-34-c-10 were accomplished by free radical polymerization in our group (1). Further, several reports on the syntheses of polyrotaxanes of vinyl polymers have been published (2-6). These polymerizations were done under heterogeneous conditions.

High molecular weight polystyrene rotaxanes using crystalline cyclic urethanes comprising 34 and 40 atoms have been reported (2-3). Cyclic urethane swollen by neat styrene was polymerized thermally without any initiator. Further, the authors found that cyclic urethane complexed with $ZnCl_2$ prior to swelling with styrene favors polyrotaxane formation. Lower threading yields were obtained for the cyclic urethane with larger number of atoms, suggesting the possibility that unfavorable macrocycle conformations reduce the effective cavity size. The authors found the polyrotaxanes to be insoluble in benzene or DMSO, both of which are good solvents for polystyrene and cyclic urethanes. Further, estimates of the composition of the semi-crystalline polyrotaxanes were obtained by X-ray analyses. It may be possible that cyclic urethanes are distributed along the linear chain and that they aggregate to form ordered regions. No other data on characterization has been reported.

Synthesis of polyrotaxanes of polyvinylidene chloride was accomplished by radiation polymerization of the crystalline adduct of vinylidene chloride and β -cyclodextrin (4-6). The cyclodextrin content in the polymer was found to be about 80 % and the semi-crystalline polymer (molecular weight 20,000) was found to be soluble in DMF while polyvinylidene chloride is not.

In the syntheses of polyrotaxanes of styrene and acrylonitrile with a variety of aliphatic crown ethers and bis(p-phenylene)-34-crown-10 (BPP-34-c-10), an azo-free radical initiator containing bis(p-t-butylphenyl)phenylmethyl or tris(p-t-butylphenyl)methyl

groups were used. The termination of these polyrotaxanes by combination of the polymeric radicals yielded polyrotaxanes end blocked by bis(p-t-butylphenyl)phenyl-methyl or tris(p-t-butylphenyl)methyl groups. It was found that very small amounts of the macrocycles were incorporated (threaded) onto polystyrene (ca. about 3-5 weight % of 30-c-10, about 11 weight % of 42-c-14, about 12 weight % of 48-c-16, 8-10 % of weight 60-c-20, 8-10 weight % of BPP-34-c-10). The low incorporation of the macrocycles was attributed to the lack of any attractive interactions between the styrene monomer and the macrocycles and to the bulkiness of the propagating polystyryl radical, reducing the probability of the polymer chain threading to the macrocycle. In the syntheses of polyrotaxanes of polyacrylonitrile by free radical polymerization, about 38 weight % of the 60-c-20 macrocycle was threaded onto the linear polyacrylonitrile (1).

Threading of the polystyryl radical by the crown ethers does not proceed efficiently in the polymerization of polystyrene by the free radical method. The threading efficiency could be significantly improved if the polymerizations are done by ionic polymerizations such as anionic polymerization. In an anionic polymerization of styrene, the growing polystyryl anion has a metal ion (such as Na⁺ or Li⁺) associated with it and the crown ethers are known to complex with such metal ions, depending on the cavity size. Thus, if anionic polymerization of styrene is done in the presence of crown ether macrocycles (as solvent or cosolvent) the threading efficiencies of the macrocycles could be significantly improved. A similar template effect would also be operational in a cationic polymerization of styrene.

Thus, polyrotaxanes of polystyrene were prepared by anionic polymerizations using crown ether macrocycles (30-c-10 and 60-c-20 as cosolvents). In this preliminary study the goals were to study the feasibility of the use of crown ether macrocycles in anionic polymerization, to understand the threading behavior of small and large macrocycles onto polystyrene and to study the changes in the

properties as a result of the formation of the polyrotaxane architecture.

IX.2 Results and Discussion

Syntheses of polyrotaxanes of polystyrene were accomplished by anionic polymerization using sodium naphthalide as the initiator, since a bifunctional living polymer can be obtained using this initiator. Polyrotaxanes of polystyrene were prepared using 30-c-10 and 60-c-20 macrocycles and THF or THF:benzene mixture (55:45 V:V) as a cosolvent for the polymerizations. The use of THF or THF:benzene mixture as a cosolvent was necessary for the polymerizations to take place homogeneously since styrene and crown ethers are immiscible and further the initiator is prepared in THF and its use in polymerization requires polar polymerization solvents. The protic impurities in the crown ether solutions (in THF or THF:benzene) were titrated by addition of sodium naphthalide before addition of styrene to the polymerization mixture. The polymerizations were initiated using sodium naphthalide solution in THF. The living bi-ended polystyryl anions were end blocked using the chloro-functional blocking group, VI-13. A model end blocked polymer (target molecular weight 25,000) was also prepared using the THF:benzene mixture.

Polymerization of styrene in the presence of crown ethers did not yield the red color typical of living polystyryl anions; instead a light orange color was obtained. A report on anionic polymerizations of vinyl monomers containing dibenzo-18-c-6 or benzo-15-c-5 has been published (7). Polymerizations were initiated by addition of monomer solution in THF to the sodium tetramer of α -methylstyrene, causing a color change from dark red to light orange and the polymerizations were continued for 0.5 hours at $-50\text{ }^{\circ}\text{C}$. Further, the authors indicated that above $-50\text{ }^{\circ}\text{C}$ the living anions were terminated by an attack of the anions on the $-\text{PhO}-\text{C}-$ bond producing a stable phenoxy ion. In this study, the light orange color

obtained for living polymers is consistent with the reported results; however, no decomposition of the aliphatic crown ethers was found, as will be discussed later.

Figure IX-1 show the schematic of the syntheses of polyrotaxanes of polystyrene using 30-c-10 and 60-c-10. The polymers were precipitated from the reaction solution into methanol:water to remove unthreaded macrocycle and the polymers were analysed by proton NMR spectroscopy. The polymers were reprecipitated one more time into water to remove any remaining free macrocycle and the polymers were analysed by proton NMR to determine the repeat unit/macrocycle ratios. Two such precipitations were done for all the polymers. More reprecipitation of these polymers needs to be done until a constant repeat unit/macrocycle ratio is obtained.

Figure IX-2 shows the ^1H NMR spectrum of poly(styrene-rotaxa-30-c-10, IX-4, second precipitation). The two broad peaks from 7.2 and 6.3 ppm are due to the phenyl group protons of the polystyrene backbone. The single peak at 3.66 ppm is due to the methylene protons, $-\text{OCH}_2\text{CH}_2\text{O}-$, of the macrocycle (30-c-10). No decomposition of the macrocycles was observed by proton NMR in the precipitated products (1st pptn. and 2nd pptn.) since only one singlet corresponding to 30-c-10 or 60-c-20 was observed; oligo ethyleneoxy units yield multiplets in this region. The peaks between 1.2 - 2.2 ppm are due to the methine and methylene protons of the polystyrene backbone. Embedded in the polystyrene peaks are the peaks due to the protons of the blocking group (7.21-7.25, aromatic peaks; 3.4 ppm, $-\text{CH}_2$ protons alpha to the $-\text{Cl}$ from unreacted blocking group; 1.29 ppm, t-butyl groups). Table IX-1 show the conditions utilized for the synthesis of polyrotaxanes along with the results obtained for each precipitation.

As shown in the table IX-1, the repeat unit/macrocycle ratio of the polyrotaxanes is significantly higher for IX-2 and IX-3 compared with other polyrotaxanes; these repeat units/macrocycle ratios accounts for about 1 weight % 30-c-10 for IX-2 and much

Table IX-1 Synthesis and Characterization of Polyrotaxanes of Polystyrene

Target <Mn> Kg/mole	Styrene (moles/l)	Solvent ^a	Temp. °C	Monomer:crown (moles)	GPC <Mn> Kg/mole	PDI	Repeat Unit/ Macrocycle	Weight % Macrocycle	
							1st pptn.	2nd pptn.	
IX-1	25	0.23	M	10-15	25	1.08	---	---	0
IX-2	10	0.71	M	10-15	10	bimodal	297.4	317.5	1.0 % b
IX-3	25	0.77	M	10-15	25	2.0	726.0	780.6	0.7% b
IX-4	50	1.07	T	-30 to -40	28	bimodal	35.7	43.2	8.9% b
IX-5	50	1.28	T	RT	20	bimodal	60.1	68.5	5.8% b
IX-6	50	0.77	T	RT	16	2.0	34.5	208.7	3.9% c
IX-7	50	0.77	T	RT	16	2.0	132.6	249.2	3.3% c

a M = 55:45 (v:v) THF:benzene; T = THF

b 30-c-10

c 60-c-20

less for IX-3. However, for IX-4 and IX-5 these ratios correspond to 8.9 and 5.8 weight % 30-c-10 threaded onto polystyrene, respectively. Although the monomer:macrocycle feed ratio was the same for polyrotaxanes IX-2, IX-3 and IX-4, polyrotaxane IX-4 was prepared using THF instead of THF/benzene at slightly higher concentrations. It appears that THF favors threading relative to THF/benzene. Further for polyrotaxane IX-5 the monomer:macrocycle feed ratio was more than twice that for IX-2, but a higher repeat unit/macrocycle ratio was obtained for IX-2. This again is probably due to the solvent effect since polar THF was used for the synthesis of IX-5 while THF:benzene mixture was used in the synthesis of IX-2. Thus, a polar solvent helps in achieving higher threading yields as the cavity of the macrocycle is probably more expanded and may also enhance the template effect of complexation of the macrocycle with the metal ion. Further, higher polymerization temperature also seems to favor threading; despite the higher feed ratio of monomer:crown ether for IX-5 (polymerization temperature -30 to -40 °C), the weight % macrocycle threaded is comparable to IX-4 (polymerization at room temperature).

Poly(styrene-rotaxa-60-c-20) (IX-6, IX-7) showed relatively lower repeat unit/macrocycle ratio after the first precipitation compared with 30-c-10 rotaxanes, even though the monomer/macrocycle feed ratios were much higher and polymerizations were done using more dilute conditions. After the second precipitations 3.9 and 3.3 weight % 60-c-20 was found to be threaded onto polystyrene for IX-6 and IX-7, respectively. This large change may be due to dethreading of the macrocycle during the precipitation, since the blocking group used is not large enough to restrain such a large macrocycle. However, 60-c-20 showed higher threading efficiency than 30-c-10 due to the size factor.

The threading yields of the macrocycles are not significantly higher than those obtained by free radical polymerization (1). One major difference here is that polymerizations were done at much

higher dilution (ca. about 5-8 times) in this study compared to that by free radical method. If feasible, anionic polymerization in more concentrated solutions could significantly improve threading yields.

GPC analyses of the polymers were used to determine if target molecular weights were achieved. Figure IX-3 shows the GPC traces of IX-4 and IX-6. Figure IX-4 shows the GPC traces of 30-c-10 and 60-c-20. The model polymer, IX-1, showed a molecular weight of 24.5 K with a polydispersity of 1.08, consistent with the target molecular weight (25 K). All the poly(styrene-rotaxa-30-c-10) except IX-3 showed bimodal distributions and the major peaks in the GPC traces were relatively broad. GPC traces for poly(styrene-rotaxa-60-c-20) showed very broad molecular weights (polydispersity = 2.0) with a peak maximum at 33.0 ml, corresponding to a molecular weight of about 16.0 K; however, no bimodal distribution was observed. Further, GPC traces of the polyrotaxanes and model polymer showed a very small peak at 40.8 ml, corresponding to unreacted chloro-functional blocking group. This elution volume also corresponds to 30-c-10 (as indicated in chapter VII). Thus, the absence of free 30-c-10 could not be confirmed; however, no peak for 60-c-20 was detected in IX-6, demonstrating the absence of free 60-c-20.

The broad molecular weight distributions of the polyrotaxanes might be due to higher concentrations of the polymerization solutions. However, the bimodal nature of the peaks the polymers is surprising. The bimodal nature may be due initiator that was added to the solution of crown ether to titrate any impurities. However, it seems more likely that the bimodal distributions are due to two different initiating species. The complexation of one or more sodium ions of living polystyryl sodium with crown ethers could occur; propagation rates of the crown ether complexed and uncomplexed ion pairs would be significantly different, leading to the bimodal distributions. Studies on the effects of complexation of the cations of the living anionic polymers with macrocyclic species such as crown ethers (8) and cryptates (9-12) have been published.

These studies describe significant enhancement of the propagation rates of the living chain ends complexed with macrocyclic species.

In conclusion, it appears that crown ethers can be utilized in the synthesis of polyrotaxanes by anionic polymerization. The nature of the solvent appears to be highly influential in determining threading yields. The weight % macrocycles incorporated onto polymers are comparable with the earlier study by free radical polymerization; however, much more dilute solutions were used for the anionic polymerizations in this study. It is suggested that anionic polymerizations in more concentrated solutions (using a polar solvent) would significantly improve threading yields.

IX.4 Experimental

Measurements:

Proton NMR spectra were obtained on a Bruker WP 270 spectrometer using deuterated chloroform solutions with tetramethylsilane as an internal standard. GPC analyses of the polymers were done at 30 °C in THF using a Waters system (RI and UV detectors) after calibration with PS standards.

THF was distilled once from sodium-benzophenone and then styrene and n-butyllithium were added to it; the solution was freeze-thawed on the vacuum line (ca 10^{-5} torr) 5-6 times, distilled on the vacuum line and stored in a Vacuum Atmospheres glove box ($[H_2O] = 0.6$ ppm, $[O_2] = 1.0$ ppm).

Polystyryllithium solutions in benzene were freeze-thawed 3-4 times, distilled on the vacuum line and the pure solvent was stored in the glove box.

Styrene was passed through alumina, freeze-thawed 5-6 times on the vacuum line and distilled freshly before use. 30-c-10 and 60-c-20 were purified, dried thoroughly under vacuum at 50-60 °C for 24 hours, weighed accurately in a flask and taken to the glove box.

Sodium naphthalide was prepared in 250 ml THF by mixing 1.0 g (4.4×10^{-2} mole) sodium and 10.0 g (7.8×10^{-2} mole) naphthalene. It was allowed to stir for a day at 25 °C in the glove box and titrated against 0.50 N HCl before use.

Synthesis of Model Polystyrene (IX-1):

2.2 ml (2.0 g, 1.9×10^{-2} moles) styrene was dissolved in THF:benzene (55:45 v/v, 80.0 ml) and initiated using 2.0 ml of 0.077 M (1.5×10^{-4} moles) sodium naphthalide solution in THF. Polymerization was done at 10-15 °C for 30 minutes. Living polymer was end blocked with 0.116 g (2.3×10^{-4} moles) of VI-13 (1.5 eq. relative to the initiator). The dark red color of the living

polystyrene began to disappear slowly and it took about 10-15 minutes to obtain a light yellow solution. The polymer was precipitated into methanol and washed with ethanol so as to remove naphthalene.

Synthesis of Polyrotaxanes of Polystyrene (IX-2 to IX-7):

Polyrotaxanes were prepared using 30-c-10 and 60-c-20, using different solvents and at different temperatures. Following is the summary of the reaction conditions.

IX-2. Target Mol. Wt. 10 Kg/mole

Styrene: 2.0 g (1.9×10^{-2} moles)
Crown Ether: 5.0 g 30-c-10 (1.1×10^{-2} mole, 0.6 eq. per monomer)
Cosolvent: 15.0 ml, THF:benzene (55:45 v/v)
Sodium Naphthalide: 5.0 ml of 0.077 M (3.8×10^{-4} moles) in THF
Total Volume: 27 ml
Polymerization Temperature: 10-15 °C
Polymerization Time: 4 hours
Blocking Group, VI-13: 0.29 g, (5.8×10^{-2} , 1.5 eq. per initiator)

IX-3. Target Mol. Wt. 25 Kg/mole

Styrene: 2.0 g (1.9×10^{-2} moles)
Crown Ether: 5.0 g 30-c-10 (1.1×10^{-2} mole, 0.6 eq. per monomer)
Cosolvent: 16.0 ml, THF:benzene (50:50 v/v)
Sodium Naphthalide: 2.0 ml of 0.077 M (1.5×10^{-4} moles) in THF
Total Volume: 25 ml
Polymerization Temperature: 10-15 °C
Polymerization Time: 3 hours
Blocking Group, VI-13: 0.12 g, (2.3×10^{-4} , 1.5 eq. per initiator)

IX-4. Target Mol. Wt. 50 Kg/mole

Styrene: 4.0 g (3.8×10^{-2} moles)
Crown Ether: 10.0 g 30-c-10 (1.1×10^{-2} mole, 0.6 eq. per monomer)
Cosolvent: 20.0 ml THF
Sodium Naphthalide: 2.0 ml of 0.077 M (1.5×10^{-4} moles) in THF
Total Volume: 36 ml
Polymerization Temperature: -30 to -40 °C
Polymerization Time: 1.5 hours
Blocking Group, VI-13: 0.12 g, (2.3×10^{-4} , 1.5 eq. per initiator)

IX-5. Target Mol. Wt. 50 Kg/mole

Styrene: 4.0 g (3.8×10^{-2} moles)
Crown Ether: 4.0 g 30-c-10 (9.1×10^{-3} mole, 0.24 eq. per monomer)
Cosolvent: 20.0 ml THF
Sodium Naphthalide: 2.0 ml of 0.077 M (1.5×10^{-4} moles) in THF
Total Volume: 30 ml
Polymerization Temperature: RT
Polymerization Time: 2 hours
Blocking Group, VI-13: 0.12 g, (2.3×10^{-4} , 1.5 eq. per initiator)

IX-6 and IX-7. Target Mol. Wt. 50 Kg/mole

Styrene: 4.0 g (3.8×10^{-2} moles)
Crown Ether: 4.0 g 60-c-20 (4.5×10^{-3} mole, 0.12 eq. per monomer)
Cosolvent: 40.0 ml THF
Sodium Naphthalide: 2.0 ml of 0.077 M (1.5×10^{-4} moles) in THF
Total Volume: 50 ml
Polymerization Temperature: RT
Polymerization Time: 1.5 hours
Blocking Group, VI-13: 0.12 g, (2.3×10^{-4} , 1.5 eq. per initiator)

The crown ether was dissolved in the indicated solvent followed by addition of 2-7 drops of 0.077 M sodium naphthalide until the light green color persisted, to titrate any protic impurities that might be present in the crown ether. To this solution of the crown ether, the required amount of styrene was added and the

solution was stirred for 10-15 minutes followed by rapid (2 sec.) addition of sodium naphthalide using a syringe to initiate the polymerization. Upon addition of the initiator, the color of the polymerization solution became light orange in color, and not dark red at any time during the polymerization. All the polymerizations were done using these conditions and were continued for 1.5-4 hours. After the addition of the chloro functional blocking group, **VI-13**, the reactions were stirred overnight. The reaction mixtures were precipitated into methanol; however, they formed emulsions that were difficult to filter. Thus, part of the methanol was removed by rotary evaporation and water was added to the emulsions. The emulsions were filtered; the filtered solid was washed with water (4 x 100) and dried. The polyrotaxanes were reprecipitated from THF into water, filtered and dried. The polyrotaxanes were analysed by proton NMR and GPC.

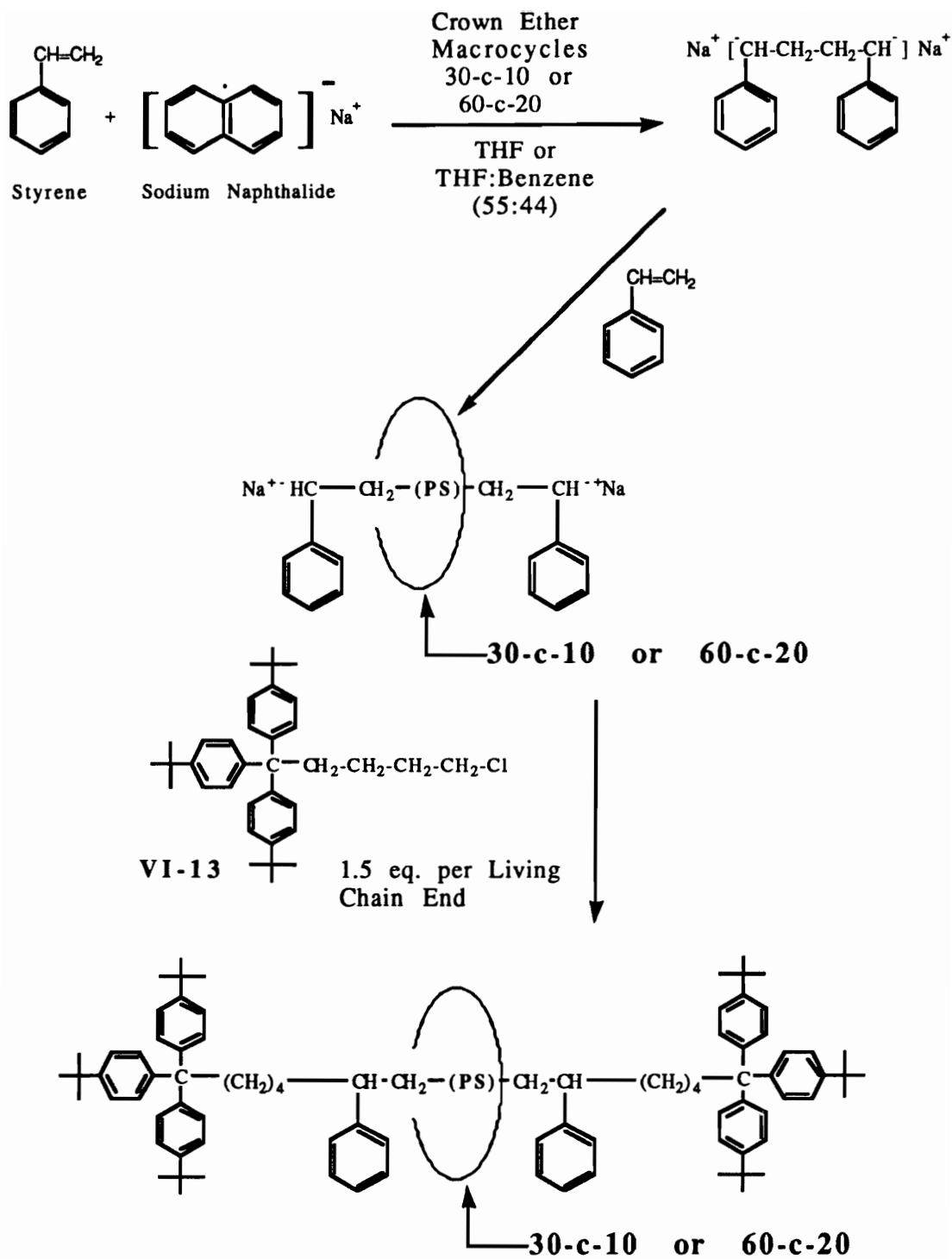


Figure IX.1 Schematic of the Syntheses of Polyrotaxanes of Polystyrene using 30-c-10 and 60-c-20

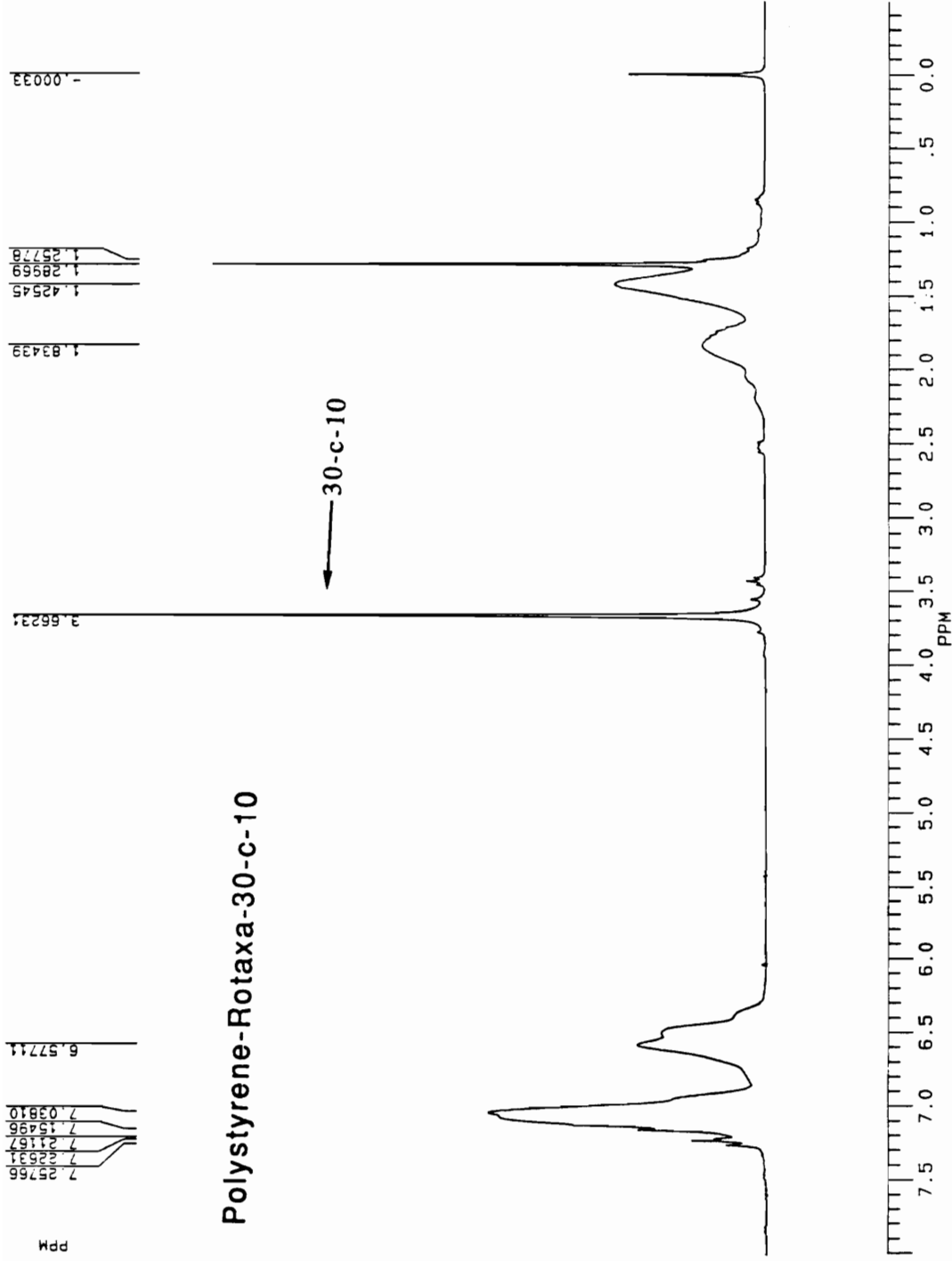


Figure IX.2 ¹H (270 MHz) NMR Spectrum of Polystyrene-Rotaxa-30-c-10 (IX-4)

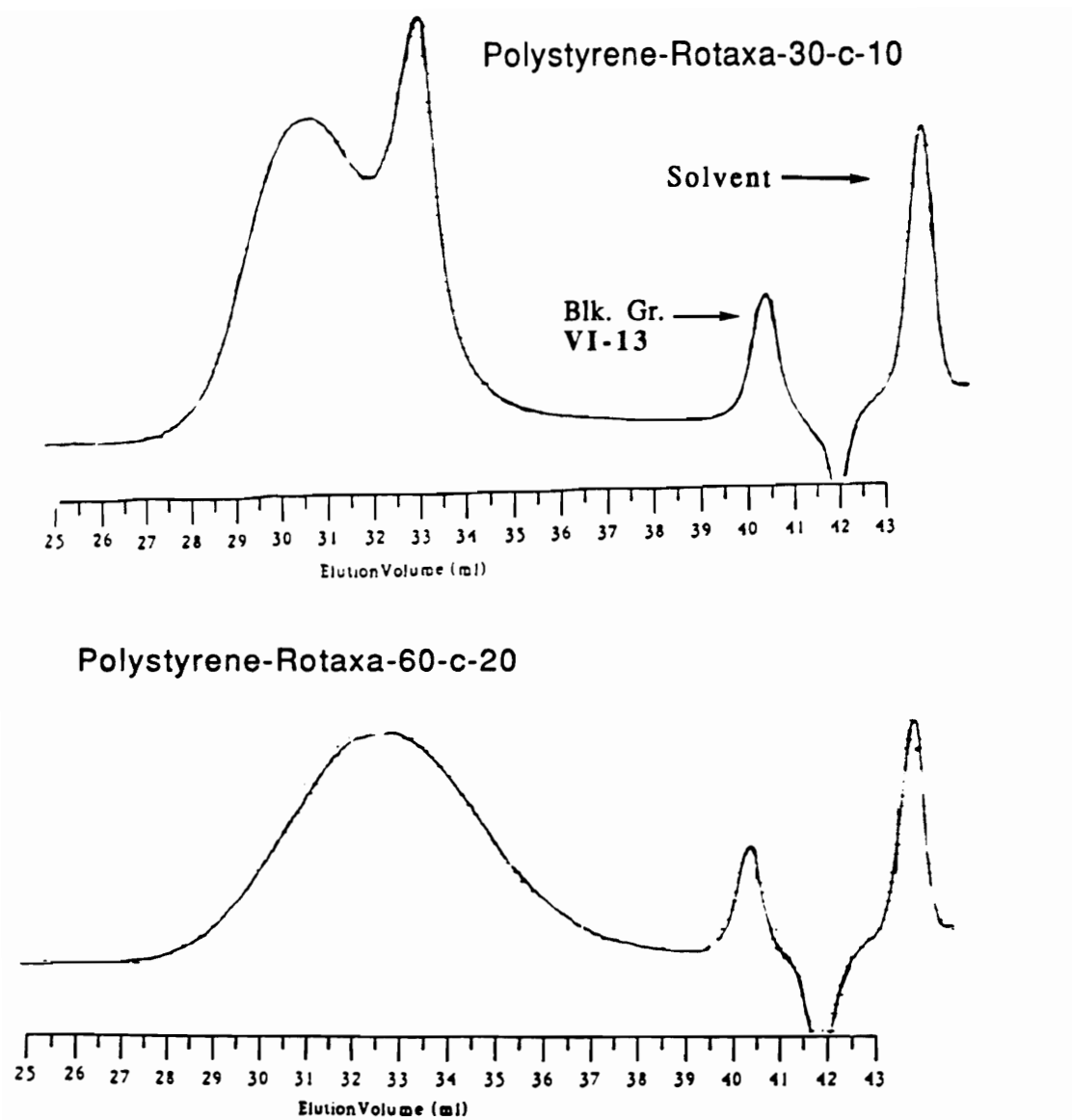


Figure IX.3 GPC Traces of Polystyrene-Rotaxa-30-c-10 (IX-4) and Polystyrene-Rotaxa-60-c-20 (IX-6) (UV Traces)

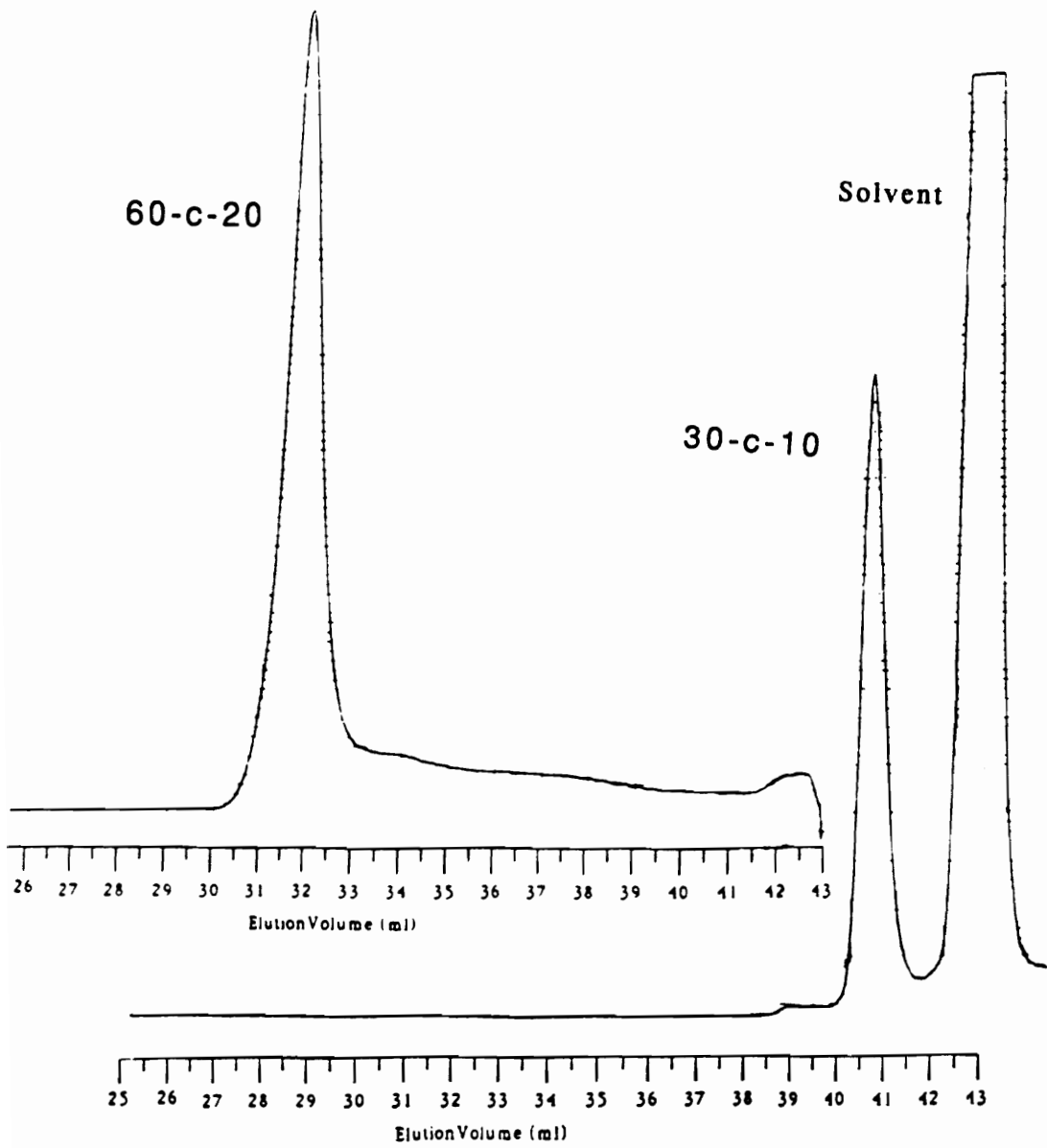


Figure IX.4 GPC Traces of 30-c-10 and 60-c-20 (RI Traces)

References

1. P. Engen, Ph. D. Thesis, Virginia Tech, 1991.
2. T. E. Lipatova, L. F. Kosyanchuk, Y. P. Gomza, V. V. Shilov, Y. S. Liptov, Dolk. Akad. Nauk. USSR, (Engl. Transl), 1982, 263, 140.
3. Y. S. Liptov, T. E. Lipatova, L. F. Kosyanchuk, Adv. Polym. Sci., 1989, 88, 49.
4. M. Maciejewski, M. Panasiewicz, D. Jarminska, J. Macromol. Sci.-Chem., 1978, A12, 701.
5. M. Maciejewski, J. Macromol. Sci.-Chem., 1979, A13, 77.
6. M. Maciejewski, A. Gwizdowski, P. Peczak, A. Pietrzak, J. Macromol. Sci.-Chem., 1979, A13, 87.
7. S. Kopolow, T. E. Hogen Esch and J. Smid, Macromolecules 1973, 6, 133.
8. J. Smid, "Anionic Polymerization, Kinetics, Mechanisms and Synthesis", J. E. McGrath, Ed; Am. Chem. Soc. Symp. Series 166, American Chemical Society, Washington, D.C., 1981, p. 79.
9. S. Slomkowski and S. Penczek, "Anionic Polymerization, Kinetics, Mechanisms and Synthesis", J. E. McGrath Ed; Am. Chem. Soc. Symp. Series 166, American Chemical Society, Washington, D.C., 1981, p. 271.
10. S. Boileau, "Anionic Polymerization, Kinetics, Mechanisms and Synthesis", J. E. McGrath Ed; Am. Chem. Soc. Symp. Series 166, American Chemical Society, Washington, D.C., 1981, p. 283.

11. S. Boileau, "Ring-Opening Polymerization, Kinetics, Mechanisms and Synthesis", J. E. McGrath Ed; Am. Chem. Soc. Symp. Series 286, American Chemical Society, Washington, D.C., 1985, p. 23.
12. J. Lacoste, F. Schue, S. Bywater and B. Kaempf, J. Poly. Sci., Poly. Lett. Ed., 1976, 14, 201.

X.	LIQUID CRYSTALLINE POLYROTAXANES 229
X.1	Introduction 230
X.2	Considerations of LC Systems 232
X.3	Results and discussion 233
	Model LC Polyester 235
	Polyrotaxanes of LC Polyester 238
X.4	Experimental 241

X.1 Introduction

Thermotropic liquid crystalline polymers are of commercial interest due to their unique properties such as thermo-oxidative stability, ductility, solvent resistance and high modulus. Further, these polymers have a unique position in the theoretical scheme of structural order in fluid phases (1). These properties make the thermotropic LC polymers useful for a broad range of applications from ultra high modulus fibers to electronic materials. It all began with Flory (2). He suggested that rigid-rod chain polymers in solution become liquid crystalline at a critical concentration (lyotropic LC polymers). He further suggested that as the molecular chains becomes more rodlike, a critical aspect ratio is reached, above which the molecules line up to pack in three dimensions efficiently.

Based on the packing of the LC polymers in bulk, they have been classified in four categories (2,3): (a) Rodlike, e.g., aromatic polyamides, esters, azomethines and benzbisoxazoles; (b) Helical, e.g., polypeptides, nucleotides, cellulose; (c) Side-chain mesogenics, e.g., vinylic polymers with crown ether as pendant units and (d) Block copolymers with alternating rigid and flexible units e.g., aromatic polyesters with n-alkane spacers.

In the latter type of thermotropic mesogenic polymer the liquid crystalline moiety (mesogen) is incorporated in the main polymer chain separated by n-alkyl or polyoxyethylene spacers of various lengths. Such polymers were described first by Roviello and Sirigu (4). Flexible aliphatic spacer groups are used to insulate the intermolecular interactions in the liquid crystalline portions and hence improve processibility of the polymers by lowering transition temperatures (1); however, the processing window in many of the polymers ($T_{\text{decomposition}} - T_{\text{melting}}$) is not broad enough to thermally process the polymer. This type of thermotropic main-chain LC polymers is made by incorporating rigid mesogenic units and flexible units in a monomer followed by polymerization of suitably

difunctionalized monomer(s) (with or without mesogenic units) by condensation polymerization to form a linear LC polymer.

The rigid unit consists most often of a number of aromatic rings connected in the para positions by short linkages such as ethers, amides, azomethines, ethers and esters, the latter being the most common one (2). Further, the rigid unit does not have to exhibit liquid crystallinity itself in order to be used as a mesogenic unit in a LC polymer (5). Various papers on the synthesis and characterization of LC polyesters containing flexible spacers of different lengths have been published (1-4,7). Similar work on the synthesis and characterization of LC polyethers containing alkyl spacers of various lengths has been published (5,8). One of the major disadvantages of these thermotropic LC polymers is that most of them can not be processed in solution because they are not soluble in common organic solvents, but need exotic solvents such as chlorinated aromatics or toxic acids; further, above T_m they tend to degrade very rapidly, thus they have limited high temperature stability.

It has been shown that by threading of macrocycles in sufficient quantities onto polymer chains, i.e., by formation of polyrotaxanes, solution and bulk properties of the polymer can be significantly altered (9,10). Thus, preparing polyrotaxanes of LC polymers may provide an alternative to render them soluble in some of the common organic solvents and get a handle on processibility.

Polyrotaxanes of thermotropic LC polymers could be prepared by incorporating highly soluble oligomeric crown macrocycles and other such macrocycles onto the LC polymer chains by threading them. The requirements of the macrocycles are that they should not adversely affect the LC nature of the polymer or high temperature stability. The resulting LC polyrotaxane may be soluble and may retain thermotropic LC nature. Further, it is anticipated that adverse effects of incorporation of macrocycles on LC polymers such as micro-phase separation could be avoided by selection of

appropriate macrocycle and/or by limiting macrocycle incorporation to sufficient but small quantities.

X.2 Considerations of LC Systems

Due to the broad nature of the subject, the following discussion is limited to the reasons for the selection of specific LC polymers for polyrotaxane synthesis, relevant literature review and characterization of the selected LC polymers.

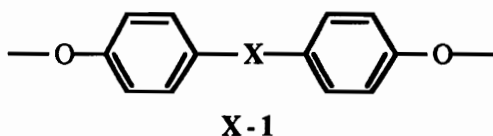
Based on the theoretical treatment of main chain LC polymers with flexible spacer groups, de Gennes predicted that such polymers would possess a nematic phase or would have the degree of order approaching the nematic state (3,11). It has been found (3) in some of the polymers that as the length of the flexible spacer increases, there is a higher chance to form the smectic phase; this may be due to longer spacer groups imparting a higher degree of mobility for mesogens to align themselves to form smectic layers (2-dimensional order). The advantages of the nematic LC polymers include useful solid state properties and processing ease (2). The nematic LC structure (1-dimensional order) is close to the extended-chain crystalline structure desired in the solid state to maximize properties such as highly uniaxial orientation for high modulus fibers, etc.

LC polyester exhibiting nematic behavior and having long flexible spacer groups were chosen to study changes in the properties brought about by the rotaxane formation.

It has been reported by Agam et al. that as the length of a small linear molecule increases, up to a limit, the threading efficiencies of a macrocycle on the linear backbone increase, in the absence of any attractive forces between the two (12). Thus, a monomer containing a longer alkyl group would thread more efficiently. n-Decyl was chosen as the flexible spacer group in the LC polyester, since monomers with n-decyl as spacer group should significantly improve threading efficiency. Further, melting

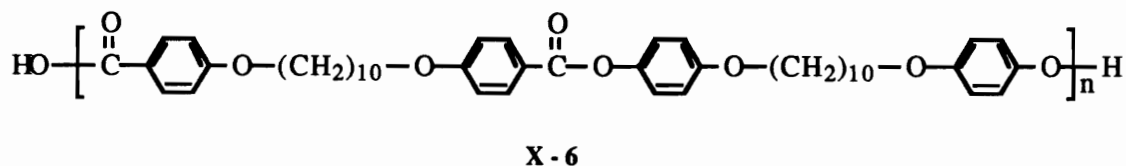
temperatures (T_m) of polymers are found to be lower as the length of the alkyl spacer increases in both odd and even series of spacer groups.

Various reports on the syntheses of LC polyesters containing mesogens and flexible spacers in the main chain have been published (1-4,7). The mesogenic groups that have been incorporated into such polymer chains include:



X = -COO-; -CH=CH-; -CH=C(CH₃)-; -C(CH₃)=N-N=C(CH₃)-;
X = -COO-(C₆H₄)-OCO-; nothing (i.e., 4,4'-dioxybiphenyl);
X = -CONH-; -CH=N-; -N=N-; -N(O)=N-; -C=C-

Griffin et al. (1) have reported the syntheses of main chain thermotropic LC polyesters using **X-1** (X = -COO-) as the mesogenic unit and alkyl spacers of various lengths. These polymers exhibited nematic mesophases. The polymer **X-6** was selected as a model polymer in the synthesis of polyrotaxanes. The polymer exhibited nematic mesophases and the T_m (melting temperature) and T_i (isotropization temperature) were reported to be 185 °C and 212 °C, respectively.

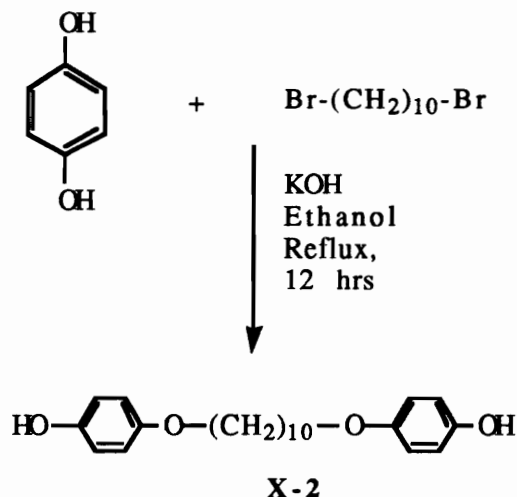


X.3 Results and Discussion

Synthesis of monomer 1,10-bis(p-hydroxyphenoxy)decane (**X-2**, referred to as c-10 bisphenol) was accomplished by reacting 1,10-dibromodecane with 10-fold excess hydroquinone as reported earlier

(1,3,13). Scheme X-1 shows the synthesis of X-2. C-10 bisphenol monomer was used for the LC polyester synthesis.

Scheme X-1 Synthesis of C-10 bisphenol (X-2)



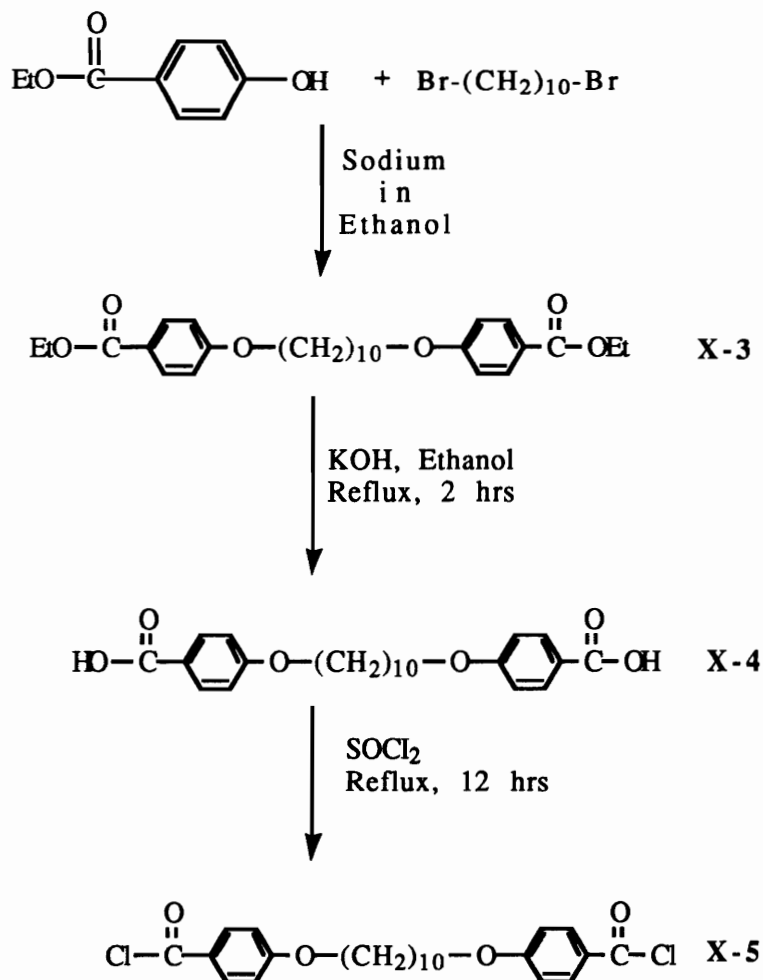
Synthesis of 1,10-bis(p-chloroformylphenoxy)decane (X-5, referred to as c-10 bis acid chloride), monomer for the synthesis of LC polyester is shown in Scheme X-2. Syntheses of X-3 and X-4 have been reported in the literature (1,3,13,14). Further, synthesis of X-5 has also been reported; however no details on the characterization such as melting point, etc., are reported.

In the reported synthesis of LC polyester X-6 (1) the authors utilized a biphasic method where c-10 bisphenol was suspended in aqueous sodium hydroxide solution and polymerized by addition of the other monomer in an organic solvent in the presence of a phase transfer catalyst.

This biphasic method is not suitable for the syntheses of polyrotaxanes since the crown ether macrocycle would preferentially stay in the large volume of aqueous phase due to its higher solubility as well as complexation with sodium, thus adversely affecting the threading efficiency. A homogeneous polymerization mixture is needed such that the crown ether

macrocycle can be used as a solvent for the polymerization, to maximize the threading efficiency. To prepare the model polymers diglyme was used as a solvent due to its structural resemblance to crown ether macrocycles

Scheme X-2 Synthesis of C-10 Bis Acid Chloride (X-5)



Model LC Polyester

Earlier attempts to synthesize LC polyester X-6 by the one phase method (diglyme as solvent) using c-10 bisphenol (X-2) and c-10 bis ester (X-3) by means of acid or base catalyzed

transesterification were not successful. The reactivity of aromatic esters and aromatic phenol is not sufficient to yield high molecular weight polymers. Hence, C-10 bisphenol and C-10 bis acid chloride were used to prepare the LC polyester in diglyme. A variety of conditions and bases were employed to obtain higher molecular weight polymer as indicated by their solid-nematic and nematic-isotropic transition temperatures. The reported solid to nematic (S-N) and nematic to isotropic (N-I) transition temperature are 185 °C and 212 °C. Table X-1 represents a summary of all the attempts.

Scheme X-3 represents the method that worked the best for the synthesis of the model LC polyester X-6. Polymerizations using KOH along with lower polymerization temperature gave much better results than any other base. A polymerization time of 14 hours was sufficient to produce polymer with higher transition temperatures. These polymers were analysed by FTIR, TGA, DSC and optical microscopy.

Scheme X-3 Synthesis of LC Polyester (X-6)

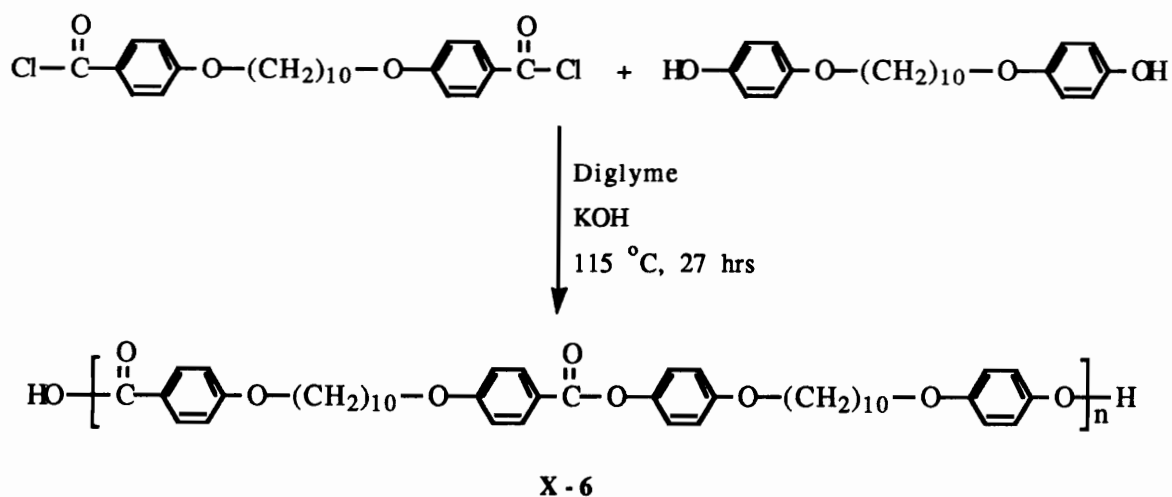


Table X-1 One Phase Syntheses of LC Polyester

<u>Trial</u>	<u>Base</u>	<u>Conditions</u>	<u>Color</u>	<u>Transitions</u>
1	pyridine	90 °C, 25 h; 135 °C, 93 h	Gray	143 °C, S-N 168°C, N-I
2	none	90 °C, 25 h; 135 °C, 93 h	white	132 °C, S-N 165°C, N-I
3	KOH	140 °C, 24 h	gray	160 °C, S-N 186°C, N-I
4	(Et) ₃ N	135 °C, 100 h	gray	141 °C, S-N 176 °C, N-I
5	(Et) ₃ N	115°C, 27 h	white	Broad peak at 187 °C
6	(Et) ₃ N	115 °C, 14 h;	white	180 °C, S-N 200 °C, N-I
7	KOH	115 °C, 27 h;	white	190 °C, S-N 231 °C, N-I
8	KOH	115 °C, 14 h;	white	190 °C, S-N 231 °C, N-I
9	----	Biphasic Method as reported (1)	white	186 °C, S-N 217 °C, N-I

The FTIR spectra of the polymers were identical and showed ester peaks at 1738 cm⁻¹. The ether peaks are seen between 1250-1265 cm⁻¹. In TGA the polymer showed onset of degradation at 275 °C (in air). DSC analyses (second heat) showed endothermic peaks at 190 °C and 231 °C, corresponding to solid-nematic and nematic-isotropic transitions. Other peaks at 123 °C and 169 °C are also seen in the second heating scan; however, no change in morphology

was seen by hot stage optical microscopy. A similar peak at 124 °C was seen in the first heat scan of DSC analysis of the polymer made by the biphasic method, but it disappeared in the second scan. These extra peaks seen in DSC may be due to some crystal-crystal transition. Further, Griffin et. al. (1) found that an even number of methylene groups as the flexible spacer in the diacid segment of the polymer chain have a larger isotropization enthalpy than polymers with an odd number of methylene groups and for most of the polymers, the enthalpies for solid-nematic transitions were lower than that for nematic-isotropic transitions.

From the intrinsic viscosity data (60:40 (v/v) phenol:tetrachloroethane) of similar LC polymers (polymer with one of the flexible spacers of 10 carbons, the other with 12 carbons), Griffin et al. (1) approximated the molecular weights to be in the range of 16000-20000 (1). Thus, the polymer synthesized in this study had higher molecular weights than that synthesized by the biphasic method (attempt 9, and that reported by Griffin et al.) as indicated by their thermal transition temperatures.

Polyrotaxane of LC Polyester

Synthesis of the polyrotaxane of LC polyester **X-7** is shown in Scheme **X-4**. This was accomplished by first stirring the c-10 bisphenol (**X-2**) with 20 equivalents of 30-c-10 at 50-60 °C for 20 hours followed by addition of c-10 bis acid chloride **X-5** and KOH. The polymerization was continued for 73 hours; polymer yield was about 90 %. A model LC polyester was also prepared under similar conditions. The IR spectrum of the LC polyester rotaxane was similar to that of the model LC polymer. In TGA, the onset of degradation was observed at 260 °C and 5 % weight loss at 330 °C for LC polyester rotaxane while the model polymer showed onset of degradation at 275 °C and 5 % weight loss at 346 °C.

Figure **X-1** shows the DSC traces of the model LC polyester **X-6** and its polyrotaxane **X-7**. The model LC polyester showed solid to nematic and nematic to isotropic transitions at 147 °C and 172 °C,

respectively, along with other transitions at 94 °C and 130 °C. The LC polyester rotaxane showed two transitions at 96 °C and 134 °C which may correspond to solid to nematic and nematic to isotropic transitions, respectively. These transitions need to be confirmed by optical microscopy. However, these transition temperatures suggest that both the polymers have lower molecular weights relative to the LC polyester prepared earlier in the study. Further, the lower transition temperatures of the polyrotaxane compared to that of model LC polyester could be due to the formation of polyrotaxane or due to the difference in molecular weight between the two polymers.

Scheme X-4 Synthesis of LC Polyester Rotaxane (X-7)

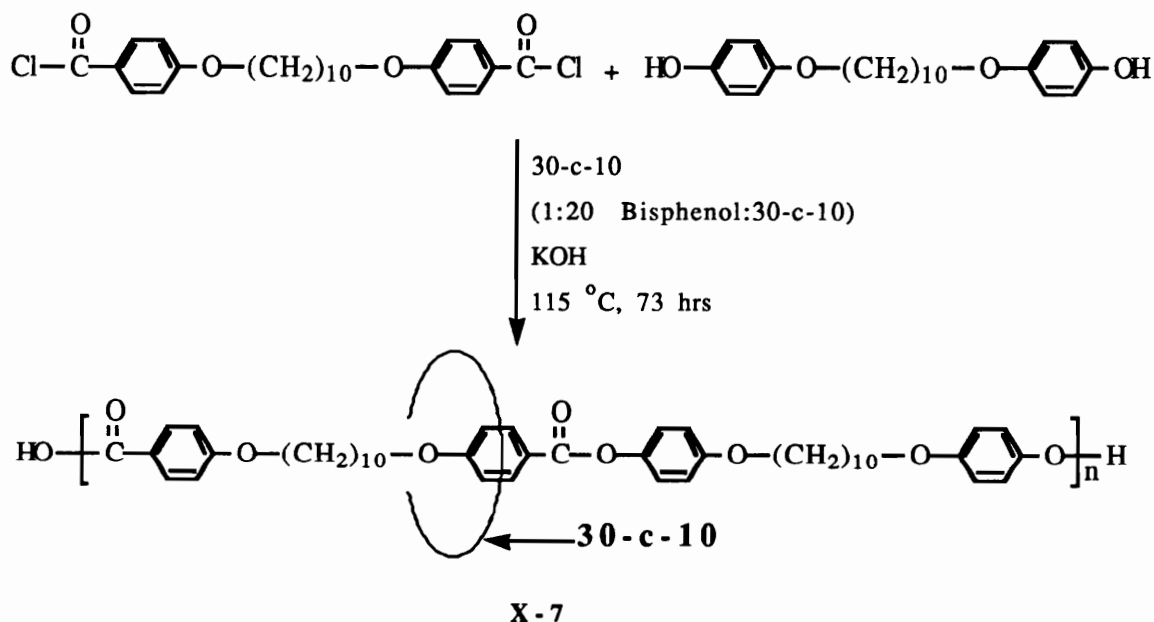


Figure X-2 shows the ^{13}C solid state NMR spectra of the LC polyester and its polyrotaxane. The peak corresponding to the carbons of the 30-c-10 appears at 70.08 ppm. One macrocycle was found to be present for every 15-17 repeat units, which accounts for about 3-5 weight % 30-c-10.

It appears from the TGA and DSC data that the polyrotaxane is of lower molecular weight than the model LC polymer as indicated

by the transition temperatures. From the solid state NMR of the polyrotaxane it appears that a very small amount of 30-c-10 has been incorporated.

Lower threading yields of 30-c-10 in polyrotaxane of LC polyester are surprising considering that in the polymerization mixture as many as 20 equivalents of 30-c-10 per monomer were used. Various factors such as size of the macrocycle and presence or absence of blocking group on the polymer play important roles in the syntheses of stable polyrotaxanes.

The threading of the 30-c-10 onto the monomers and polymers is governed by the statistical factors and one of the important statistical factors is the available cavity size of the macrocycle and the diameter of the linear polymer chain. As discussed in earlier chapters, the available cavity of 30-c-10 as seen in the solid state is small. In the melt state, the available cavity size may decrease as the number of possible conformations increases, resulting in decreased threading yield. Further, it has been found that the presence of aromatic groups in the polymer significantly reduces the statistical threading yields (15). Thus, the use of a large crown ether macrocycle such as 36-c-12, 42-c-14 or 60-c-20 would help increase the threading yields. Further, the use of the bipyridyl macrocycle, BP-28-N⁺⁴ (Chapter V), which is highly deficient in π electrons and could selectively form a rotaxane with c-10 bisphenol monomer (X-3) and the resulting monomeric rotaxane could be polymerized to form ionic LC polyester rotaxanes. This could also significantly increase threading yields in LC polyester.

The presence of blocking groups is essential in the formation of stable polyrotaxanes in the absence of any attractive forces between the repeat units of the polymer and the macrocycles. It may be the case in the above LC polyester that the threading yields of the macrocycle was significant and that the macrocycles dethreaded during the work up of the polyrotaxane. Further, the rigid rod type nature of the polymer could have made the dethreading of the macrocycles easier, along with the fact that no attractive

forces exist between the monomer repeat units of the LC polyester to slow the slippage of the macrocycle.

The phenol functional blocking group (VI-5) can be used to end block the LC polyrotaxanes. The phenol functional blocking group was not used in this study since the blocking group chemistry was not developed until this study was completed.

In conclusion, synthesis of LC polyester was accomplished by a one phase method and this procedure is suitable for the preparation of polyrotaxanes of LC polyester. Lower incorporation of 30-c-10 macrocycle onto LC polymer backbones is due to the smaller size of 30-c-10 and these results are consistent with the results obtained for polyamides and polystyrene rotaxanes; the threading yields could be significantly improved using a larger macrocycle. Further, liquid crystalline behavior of the polymers may have been retained by incorporation of low amounts of 30-c-10.

X.5 Experimental

Measurements:

Melting Points were taken in capillary tubes with a Haake-Buchler melting point apparatus and have been corrected. TGA data were obtained using Du Pont TGA 951 and Perkin-Elmer TGA-7 instruments at a scan rate of 10 °C/min. DSC data were obtained using Du Pont DSC 912 and Perkin-Elmer DSC-2 instruments at a scan rate of 10 °C/min. Proton NMR spectra were obtained on a Bruker WP 270 spectrometer using deuterated dimethyl sulfoxide solutions with tetramethylsilane as an internal standard. FTIR spectra were obtained on a Nicolet MX-1 instrument. Solid state ¹³C NMR spectra were obtained using a Bruker MSL-300 instrument.

Synthesis of 1,10-bis(p-hydroxyphenoxy)decane (X-2):

220.0 g (2.0 moles) hydroquinone were dissolved, by warming, in 400 ml solution of deaerated absolute ethanol of 0.5 g sodium dithionite. To this, 45.0 ml (0.2 moles, i.e., 60.0 g) of 1,10-

dibromodecane was added dropwise over 30 minutes and then 36.0 g of potassium hydroxide solution in 200 ml ethanol was added to the flask dropwise over one hour. The reaction was refluxed overnight. It was allowed to cool to room temperature and acidified with 50 ml of 30 % sulfuric acid. The solution containing some solid residue was then warmed and filtered hot. The insoluble monoalkylated product on the filter paper was washed with boiling ethanol. The filtrate was cooled and the C-10 bisphenol which recrystallized was filtered and washed with ethanol; yield = 47.5 g (66 %), mp: 149°C - 153° C. After the second recrystallization mp: 150-151°C. After the third recrystallization mp: 149.9-151.0°C. Reported mp: 151°C (I). FTIR (KBr): 3500-3200 (OH, broad), 2980-2860 (aliphatic), 1512, 1464 (aromatic), 1239 (aromatic-aliphatic ether, broad), 1022, 825, 769 cm⁻¹. NMR (DMSO-d₆): 6.6 (aromatic, m, 8H), 3.8 (O-CH₂, t, 4H), 1.1-1.9 (-CH₂, m, 16H).

Synthesis of 1,10-bis(p-Dicarbethoxyphenoxy)decane (X-3):

23.0 g (1.0 mole) sodium were added to 1.0 l absolute ethanol over a period of 6 hours. 166.0 g (1.0 mole) of ethyl p-hydroxybenzoate were added. After it dissolved, 150.03 g (112.4 ml, 0.5 moles) of 1,10-dibromodecane were added dropwise over a half hour. The solution was refluxed for 4 hours. It was allowed to cool, poured into 3 l of cold water, filtered, washed with water, ethanol and air dried. Crude Yield 178.6 g (76.6 %), crude mp: 109-112°C. After first recrystallization mp: 109-110°C, and after second recrystallization mp: 109.5-110.5°C. Reported mp: 110°C (16). FTIR (KBr): 3060-3030 (aromatic), 2980-2860 (aliphatic), 1705 (C=O), 1605, 1513 (aromatic), 1284 (aromatic-aliphatic ether) cm⁻¹.

Synthesis of 1,10-bis(p-Dicarboxyphenoxy)decane (X-4):

51.25 g of X-3 were dissolved in 1 l refluxing ethanol and 81.0 g KOH dissolved in 600 ml ethanol were added dropwise over a period of 3 hours. The reaction was refluxed for 4 more hours and then after cooling the reaction mixture containing precipitated acid was

dissolved in hot water and acidified using con. HCl. The acid which precipitated was filtered, washed thoroughly with water and air dried. The acid was again reprecipitated from aqueous basic solution; yield 37.2 g, 96.3 %, (after two purification); mp = 274-275°C, reported mp = 273-274 °C (16). FTIR (KBr): 3425 (OH), 3060-3030 (aromatic), 2980-2860 (aliphatic), 1718 (C=O), 1605, 1605, 1558, 1544 (aromatic), 1280-1240 (aromatic-aliphatic ether) cm⁻¹. The monomer was not soluble in deuterated solvents such as chloroform, acetone, etc.

Synthesis of 1,10-bis(p-Chloroformylphenoxy)decane (X-5):

To 36.5 g (0.09 moles) of X-4 was added 134.2 ml (219.0, 1.84 moles) of thionyl chloride and the reaction mixture was allowed to reflux for 16 hours. Thionyl chloride was then distilled under nitrogen and traces of thionyl chloride were removed under vacuum. The C-10 bis acid chloride was recrystallized from 1 l of 50:50 benzene:hexanes mixture. The dried C-10 bis acid chloride was transferred to the glove box. The yield after one recrystallization was 34.4 g, 84.65 %; mp = 89.9 - 90.9 °C. Synthesis of X-5 has been reported but no characterization data has been published (1,3)

Synthesis of LC Polyester X-6:

1.56 g (3.45×10^{-3} moles) of C-10 bis acid chloride, X-5, was weighed under nitrogen. To this, 1.24 g of C-10 bisphenol, X-2, (3.45×10^{-3} moles) was added followed by addition of 15-20 ml anhydrous diglyme under nitrogen. The reaction mixture was heated for half an hour at 100 °C to dissolve the monomers. To this 1.1 eq. of 87 % KOH was added and the reaction was continued for 27 hours at 115 °C. The reaction mixture was cooled and about 40 ml THF were added and refluxed. The solution was filtered hot and washed several times with THF. The precipitate was placed in 400 ml acetone and stirred for 1/2 hr and filtered and washed several times with acetone. The same was repeated with ethanol and then the

solid was washed with water, ethanol and dried under vacuum; yield: 2.19 g, 83 %.

Various reactions were done using this procedure by changing some condition and base. In some cases the polymer was Soxhlet extracted using acetone for 48 hours. The polymer was analysed by FTIR, TGA and DSC. FTIR (KBr): 3500-3100 (OH, broad), 3050-2850 (aromatic and aliphatic -C-H), 1512, 1464 (aromatic), 1738 (-C=O) 1283, 1253 (aromatic-aliphatic ether, broad), 825, 769 cm^{-1} . TGA: onset of degradation at 270 °C, 5 % weight loss at 330 °C. DSC: endotherms in second heat scan at 190°C (S-N transition), 231 °C (N-I transition).

One Phase Synthesis of LC Polyester Polyrotaxanes X-7:

To prepare the polyrotaxanes, the procedure reported above was modified. 0.605 g (1.69×10^{-3} moles) of C-10 bisphenol, **X-2**, and 15.0 g (3.40×10^{-2} moles) 30-c-10 (20 equivalents of C-10 bisphenol) were stirred at 50-60 °C for 20 hours. 0.762 g (1.69×10^{-3} moles) of C-10 bis acid chloride, **X-5**, was transferred to the polymerization mixture from a preweighed vial under nitrogen, followed by addition of 0.15 g (1.1 eq.) of KOH. The polymerization was done at 115 °C for 73 hours. A model LC polyester was also prepared using similar conditions. Work up was the same as described above. Yield: 1.11 g, 89.5 %. The polymers were analysed by FTIR, TGA, DSC and solid state NMR. Model LC polyester: FTIR (KBr): 3500-3100 (OH, broad), 3050-2850 (aromatic and aliphatic -C-H), 1512, 1464 (aromatic), 1738 (-C=O) 1283, 1253 (aromatic-aliphatic ether, broad), 825, 769 cm^{-1} . TGA: onset of degradation at 275 °C, 5 % weight loss at 346 °C. DSC: endotherms in second heat scan at 130 °C (S-N transition), 172 °C (N-I transition). ^{13}C NMR (solid state): 26.04, 32.84, 67.21 ppm (aliphatic), 109.92, 116.24, 123.21, 125.08, 132.50, 144.56, 155.49, 160.79, 162.32 (aromatic carbons). LC Polyester rotaxane: FTIR (KBr): 3500-3100 (OH, broad), 3050-2850 (aromatic and aliphatic -C-H), 1512, 1464

(aromatic), 1738 (-C=O) 1283, 1253 (aromatic-aliphatic ether, broad, pronounced), 825, 769 cm^{-1} . TGA: onset of degradation at 260 °C, 5 % weight loss at 330 °C. DSC: endotherms in second heat scan at 96 °C (S-N transition), 134 °C (N-I transition). ^{13}C NMR (solid state): 26.02, 32.87, 67.25 ppm (aliphatic), 70.08 ppm (30-c-10), 109.87, 116.33, 123.20, 124.96, 132.87, 144.60, 151.73, 155.41, 160.81, 162.40 (aromatic carbons)

Synthesis of LC Polyester (X-6) using Biphasic Method:

0.50 g KOH (8.14×10^{-3} moles) and 1.0 g benzyltriethyl ammonium chloride were dissolved in 150 ml water. To this 0.972 g (2.71×10^{-3} moles) of C-10 bisphenol, **X-2**, was added. An emulsion was formed which was then transferred completely to a Waring blender and stirred at very high speed for 10 minutes. 1.23 g (2.71×10^{-3} moles) of c-10 bis acid chloride, **X-5**, dissolved in 60.0 ml of dry dichloromethane was rapidly added to the blender. The flask was rinsed several times with dichloromethane into the blender. The contents of the blender were stirred at very high speed for 15 minutes. The resulting mixture was placed in 1.2 l of acetone, stirred overnight, filtered and the solid was washed several times with water and acetone. The polymer was air dried and then under vacuum at room temperature for 16 hours; yield 1.87 g, 89.2 %. FTIR: same as that reported for above polymer. The polymer was analysed by FTIR, TGA and DSC. FTIR (KBr): 3500-3100 (OH, broad), 3050-2850 (aromatic and aliphatic -C-H), 1512, 1464 (aromatic), 1738 (-C=O) 1283, 1253 (aromatic-aliphatic ether, broad), 825, 769 cm^{-1} . TGA: onset of degradation at 275 °C, 5 % weight loss at 330 °C. DSC: endotherms in second heat scan at 186 °C (S-N transition), 217 °C (N-I transition).

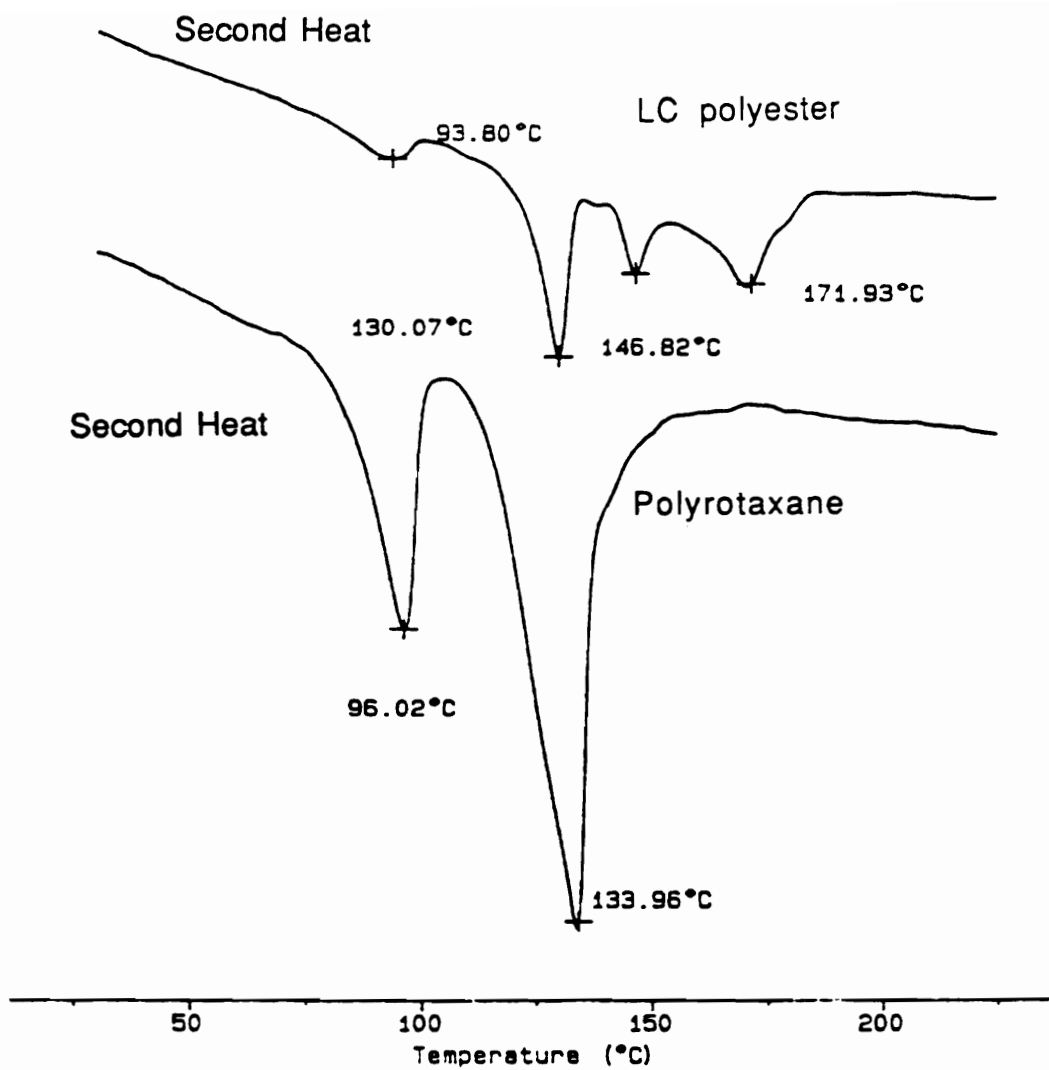


Figure X.1 DSC Traces of Model LC Polyester and its Polyrotaxane

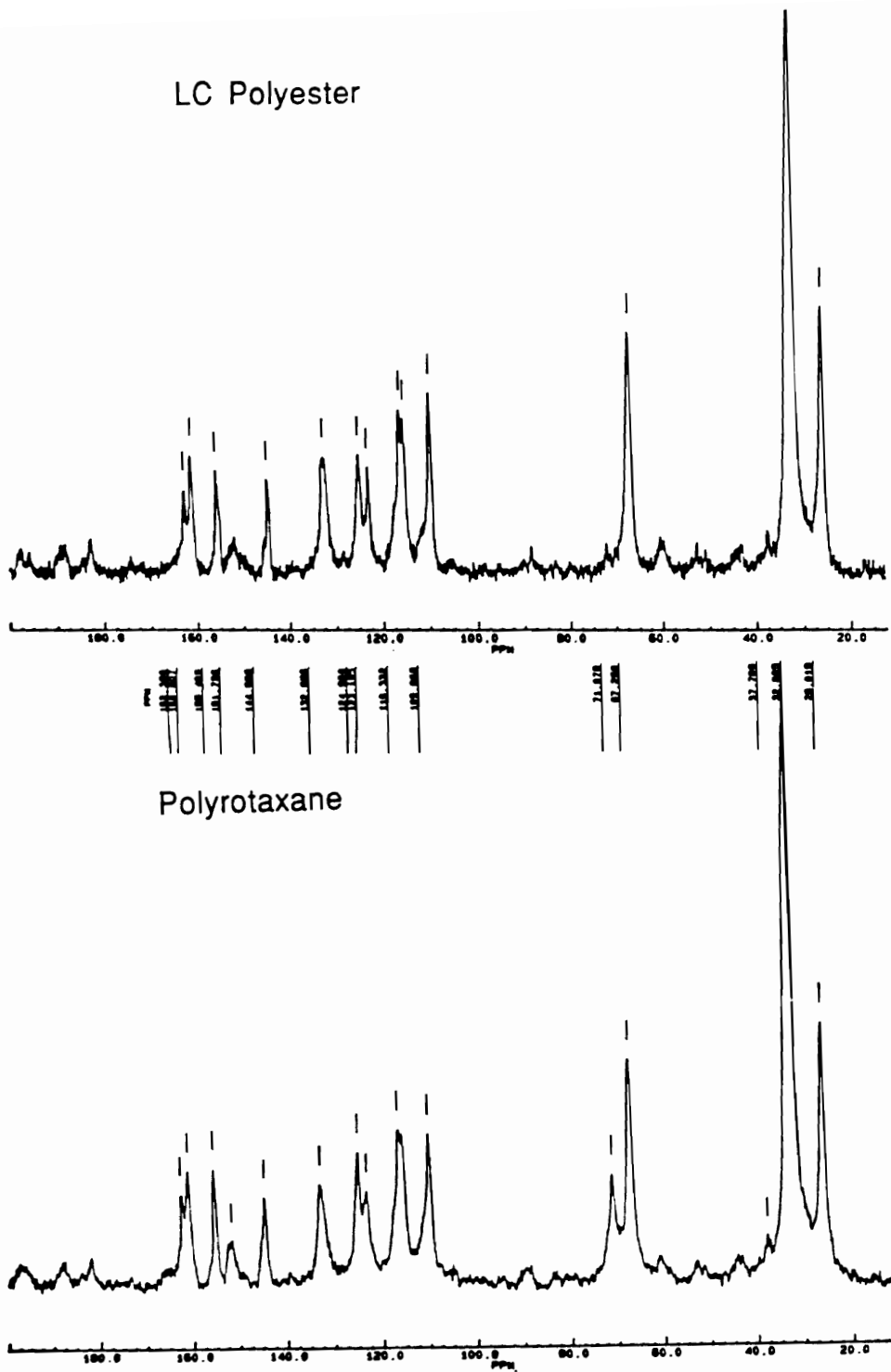


Figure X.2 ^{13}C Solid State NMR Spectra of LC polyester and its Polyrotaxane

References

1. A. C. Griffin and S. J. Havens, *J. Polym. Sci., Polym. Phys. Ed.*, 1981, 19, 951.
2. M. Jaffe, *Encyclopedia of Polymer Sci. and Eng.*, 1986, Vol. 7, 711.
3. J. I. Jin, S. Antoun, C. Ober and R. W. Lenz, *British Polym. J.*, 1980, 132.
4. A. Roviello and A. Sirigu, *J. Polym. Sci., Polym. Lett. Ed.*, 1975, 13, 455.
5. H. Jonsson, P. E. Werner, U. W. Gedde and A. Hult, *Macromolecules*, 1989, 22, 1863.
6. M. Laus, D. Caretti, A. S. Angeloni, G. Galli, and E. Chiellini, *Macromolecules*, 1991, 24, 1459.
7. C. H. Li and T. C. Chang, *J. Polym. Sci: Part A; Polym. Chem.*, 1991, 29, 361.
8. J. Ericsson, A. Hult, *Polym. Bull.*, 1987, 18, 295.
9. Y. X. Shen, Ph.D. Thesis, Virginia Tech, 1992.
10. J. Sze, M. S. Thesis, Virginia Tech, 1992.
11. P. G. de Gennes, *C. R. Acad. Sci. Paris*, 1975, Series B281, 101.
12. G. Agam, D. Gravier and A. Zilkha, *J. Am. Chem. Soc.*, 1976, 98, 5206.
13. J. Barberá, F. Navarro, L. Oriol, M. Piñol, and J. L. Serrano, *J. Polym. Sci: Part A; Polym. Chem.*, 1990, 28, 703.
14. H. Honsson, E. Wallgren, A. Hult and U. W. Gedde *Macromolecules*, 1990, 23, 1041.

15. P. T. Engen, Ph. D. Thesis, Virginia Tech, 1991.
16. H. B. Bonahoe, L. E. Benjamin, L. V. Fennoy and D. Greiff, J. Org. Chem., 1961, 26, 474.

XI	MICROSTRUCTURE OF POLYSTYRENE	.	.	.	250
XI.1	Introduction	.	.	.	251
XI.2	Results and Discussion	.	.	.	252
XI.3	Conclusions	.	.	.	263
XI.4	Experimental	.	.	.	264

XI.1 Introduction

Polyrotaxanes are two component systems in which a linear backbone polymer is threaded through macrocycles. This association of linear and cyclic species may result in polymers with improved solution, thermal and mechanical properties (1-8). Our goals were to synthesize cyclic polystyrene of low molecular weights (ca. 1500-2500) so as to have 30-50 ring atoms in the macrocycles and to use these macrocycles for making polyrotaxanes. Synthesis and characterization of low molecular weight cyclic polystyrene (molecular weight 2500) is reported in chapter-VI of this volume.

The synthesis and characterization of cyclic polystyrene has been reported in the literature. A broad range of molecular weights for cyclic polystyrene has been synthesized (4, 9-14).

Our early efforts to synthesize cyclic polystyrene using sodium naphthalide as initiator and dichlorodimethylsilane (DCDMS) as cyclization agent (difunctional terminator) presented us with two problems: (i) multiple peaks for the dimethylsilyl group protons in the ^1H NMR spectrum and (ii) incorporation of very low amounts of the terminator. The latter problem was corrected using better experimental and analytical techniques. However, the first problem of multiple peaks persisted.

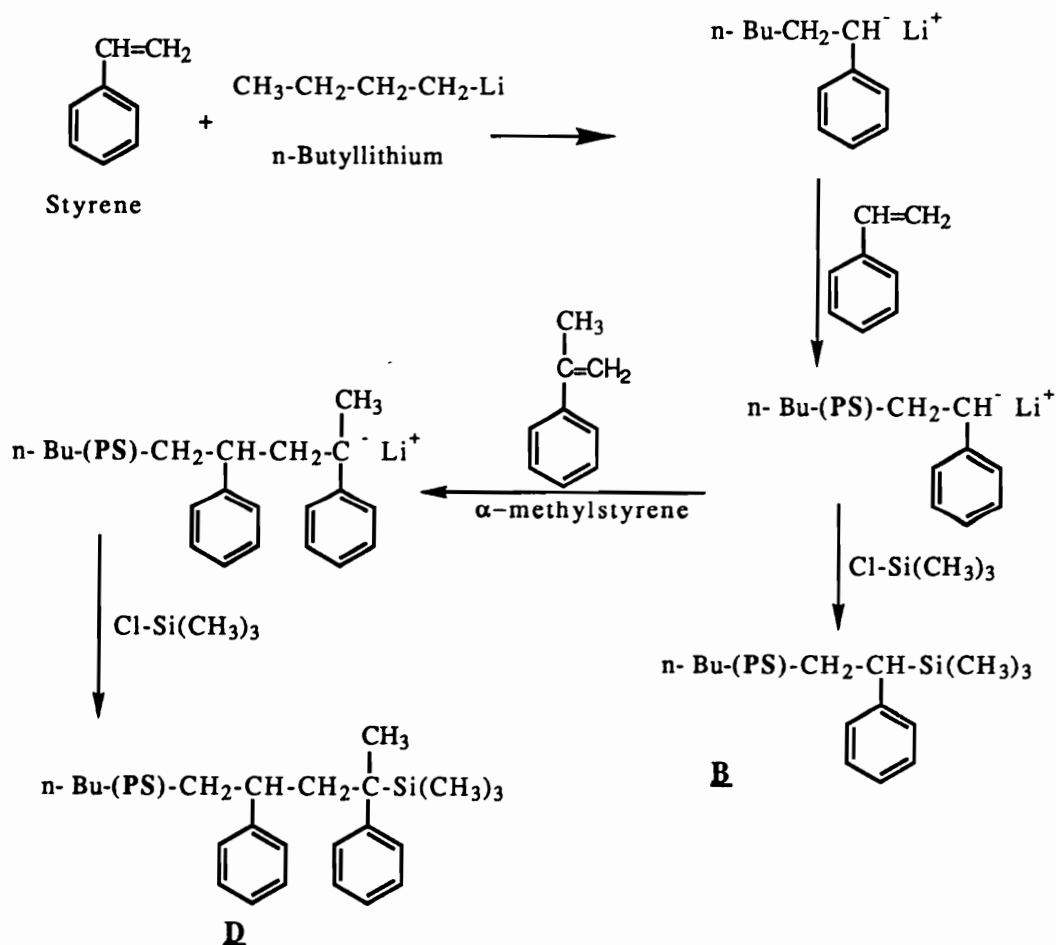
DCDMS has been used for the synthesis of cyclic polymers (10,12); however, there is no report on the characterization of the dimethylsilyl group incorporated into cyclic polymers. Further, multifunctional chlorosilanes have been extensively used for the synthesis of star-shaped polymers (15); however, no detailed characterization of incorporated silanes has been done. Thus the origin of the multiple peaks in our polymer was puzzling. Hence we decided to do model reactions by end capping the living polystyryl anions, prepared using *n*-butyllithium and sodium naphthalide as initiators, with chlorotrimethylsilane (CTMS) and chloromethyl methyl ether (CMME). The lower molecular weights of the model

polymers enabled us to study the nature of the end groups by spectroscopic methods.

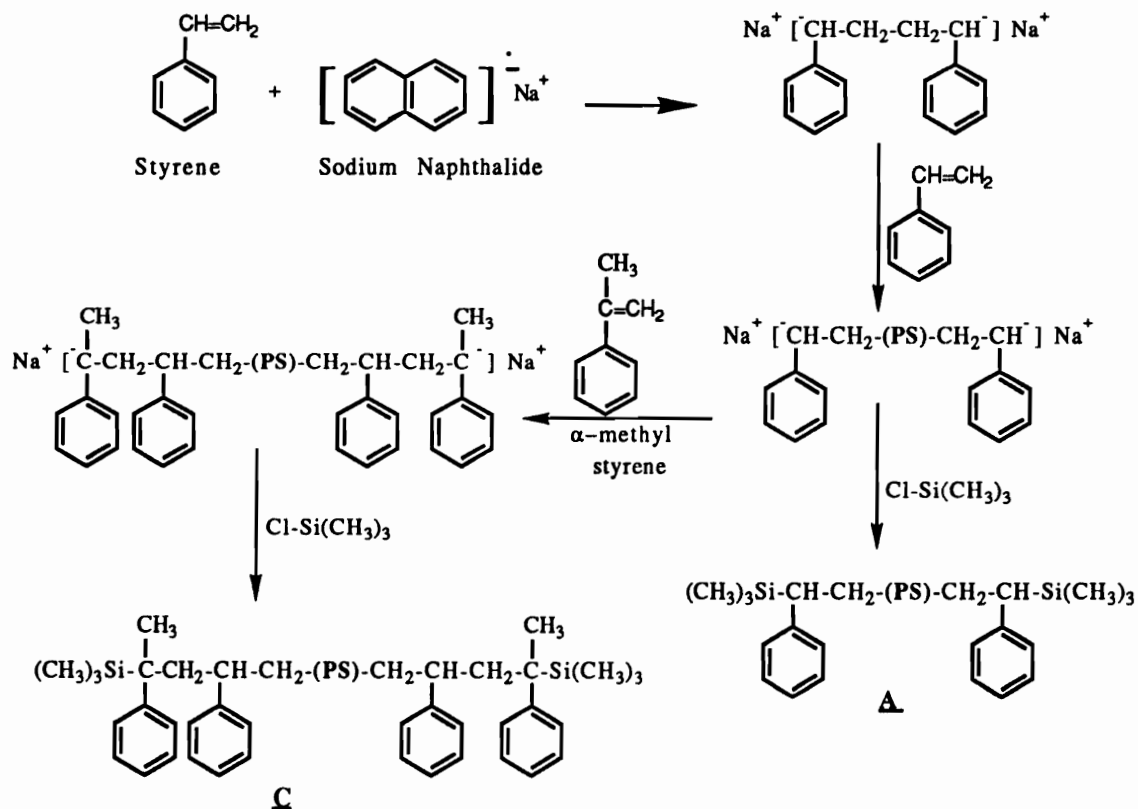
XI.2 Results and Discussion

Model polymers were prepared by anionic polymerization using n-butyllithium (Scheme XI-1) and sodium naphthalide (Scheme XI-2) as initiators.

Scheme XI-1
Model Reactions using n-Butyllithium as Initiator



Scheme XI-2
Model Reactions using Sodium Naphthalide as Initiator



n-Butyllithium and sodium naphthalide were used to initiate the polymerization of styrene to obtain mono- and bi-ended living polystyrene anions followed by end capping with CTMS (with and without incorporation of α -methylstyrene at the chain ends). The reactivity ratios of styrene and α -methylstyrene in anionic copolymerizations are 35.0 and 0.003, respectively, (16) because the methyl groups hinder the addition of α -methylstyrene unit to the α -methylstyryl anion. This permits incorporation of essentially only one α -methylstyrene unit at the chain end, thus allowing selective changes in the resulting living anion.

Typical target molecular weights for model polymers were in the range 1600-2500. Molecular weights obtained were within 10 %

of the target molecular weights. The molecular weight distributions were between 1.05-1.20. Integration values in ^1H NMR spectra of phenyl ring protons vs end group protons and GPC molecular weights were used to calculate percent end capping for the model polymers. The end capping yields were found to be between 92-96 %. The estimated error was $\pm 8\%$. A typical NMR spectrum of the model polystyrene initiated by sodium-naphthalide, end capped with CTMS is shown in Figure XI-1.

The ^1H , ^{13}C and ^{29}Si NMR spectra of $-\text{Si}(\text{Me})_3$ end groups of model polymers initiated with sodium naphthalide, with and without terminal α -methylstyrene units, are shown in Figure XI-2. The ^1H , ^{13}C and ^{29}Si NMR spectra of $-\text{Si}(\text{Me})_3$ end groups of model polymers initiated with n-butyllithium, with and without terminal α -methylstyrene units, are shown in Figure XI-3.

The multiple peaks observed in the ^1H NMR spectra of difunctional [A] and monofunctional [B] terminated samples were investigated further. The peaks are identical except that peaks for polymer [B] are shifted to lower field by 0.1 ppm. Four major peaks are seen in the region from -0.05 to -0.30 ppm, which are split further resulting into eight distinguishable peaks. The $-\text{Si}(\text{CH}_3)_3$ group protons of the corresponding α -methylstyrene terminated polymers [C] and [D] are identical; however, compared to [A] and [B] they are very different. A broad peak ranging from -0.05 ppm to -0.26 ppm shows three additional peaks embedded in it as they appear as shoulders on the main peak. Thus, it has four different peaks. Again, the peaks for polymer [B] are shifted downfield by about 0.1 ppm. Similar behavior was observed in ^{13}C and ^{29}Si NMR spectra for $-\text{Si}(\text{CH}_3)_3$ groups of model polymers. For model polymers [A] and [B], in both ^{13}C and ^{29}Si NMR spectra there were two major peaks, which were further split. In ^{13}C and ^{29}Si NMR spectra of [C] and [D] one major peak is seen and another peak of one fourth the size appears downfield. Further, in ^{29}Si NMR spectra peaks for model polymers [C] and [D] have shifted downfield by 5.8 ppm relative to those of [A] and [B].

The above results are surprising considering that $-\text{Si}(\text{CH}_3)_3$ group protons, carbons and silicons are equivalent and should appear as singlets in the respective NMR spectra. In a recent study (17) it was shown that $-\text{Si}(\text{CH}_3)_3$ group protons of 4-(trimethylsilyl)-methylstyrene and 4-bis(trimethylsilyl)methylstyrene do not exhibit any coupling with alpha methylene or methine protons and the carbon and proton nuclei produce singlets in respective NMR spectra. To ascertain that these results are not artifacts and to understand the origin of multiple peaks various parameters such as polymerization conditions, molecular weight and NMR parameters were studied.

Since model polymers [A]-[E] were prepared in a solvent mixture of THF:benzene (55:45 v/v) and the molecular weights were within 10 % of the target values; n-butyllithium is consumed essentially completely under our conditions. Due to the polar nature of the solvent mixture the initiation reaction involving solvent separated ion pairs is markedly more efficient than that reported for non-polar polymerization solvents such as benzene (18) and benzene-cyclohexane. Thus, the presence of n-C₄H₉-Si(CH₃)₃ from unreacted n-butyllithium by reaction with CTMS is unlikely in our systems; if present, it would be removed by precipitation.

Initiators: In this study two initiators were used, namely sodium naphthalide and n-butyllithium. The ¹H NMR peak patterns for Si(CH₃)₃ groups did not change with initiators. This also indicates that the peak pattern is not dependent on counter ions, e.g., Na⁺ and Li⁺.

Polymerization conditions: Typically a benzene:THF (45:55) mixture was employed for polymerization at 10-15 °C for 30 minutes. Changing polymerization times from 15 minutes to 1 hour or polymerizations temperature to 0-5 °C had no effect on the peak patterns observed. Changing the polymerization solvent to THF (10-15 °C, 30 minutes) had no effect on the peak pattern; however a broader molecular weight distribution was obtained.

Molecular Weight: Model polymers of molecular weight 1000-50,000 were studied to determine if longer or shorter chains had any effect on the peak patterns, but this was found not to be the case.

End Capping Agent: Three different batches of CTMS were used to see if any impurity may be responsible, but there was no change. Further, the end capping agent was changed from CTMS to CMME, to confirm that the multiple peaks are real. It was found that the -CH₂-O-CH₃ groups at the chain end showed similar behavior, i.e., multiple peaks for methyl and methylene peaks from 3.1 ppm to 3.4 ppm in the proton NMR spectrum.

NMR parameters: No changes were observed in the proton NMR peak pattern when the relaxation delay was varied between 2 and 16 seconds. To determine if the multiple peaks are due to long range coupling of -CH₂- and -CH- protons of the polystyrene chain with the protons of the -Si(CH₃)₃ end group, decoupling experiments in proton NMR were performed; no such coupling was found.

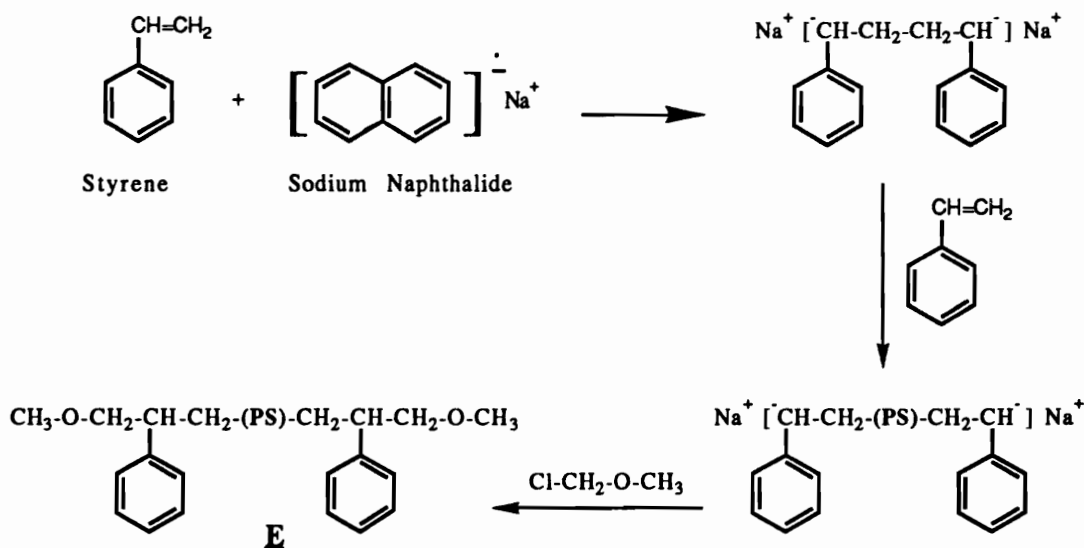
Incorporation of α -methylstyrene units at the chain ends changes the NMR peak pattern for model polymers; the only difference is that the methine proton on the last styrene repeat unit is replaced by a methyl group. The results indicate that -Si(CH₃)₃ groups are exposed to more than one environment at the chain ends. This led us to conclude that the eight peaks observed for polymers [A] and [B] in proton NMR spectra are due to stereoisomerism (tacticity) near the chain ends and that tetrad structures are seen. In principle, eight possible tetrad structures are possible at the chain ends, and in principle -Si(CH₃)₃ groups attached to different tetrad structure should have different chemical shifts. In fact, we have been able to resolve these peaks in proton NMR spectra.

Four peaks are observed in proton NMR of model polymers ([C] and [D]) with terminal α -methylstyrene units. This suggests that

the bulkier methyl group favors selective stereoisomer formation due to the steric factors, thus limiting the number of stereoisomers possible and that triad structures are seen. Further, ^{13}C and ^{29}Si spectra of these polymers show one major peak. This also supports the above conclusion that multiple peaks are due to tacticity at the chain ends. In a similar study multiple peaks due to ^{13}C end groups on poly(2-vinyl pyridine) have been attributed to stereoisomerism at the chain ends (19).

Living polystyrene prepared using sodium naphthalide was end capped with chloromethyl methyl ether (Scheme XI-3) [E] and analysed by ^1H and ^{13}C NMR spectroscopy.

Scheme XI-3
Model Polymer End Capped with Chloromethyl Methyl Ether



The ^1H and ^{13}C NMR spectra of $-\text{CH}_2\text{-O-CH}_3$ end groups of model polymers initiated with sodium naphthalide are shown in Figure XI-4. In proton NMR the $-\text{OCH}_3$ groups appear as multiple peaks (at least eight) from 3.1 ppm to 3.2 ppm while $-\text{OCH}_2$ peaks appear as diffuse multiplets from 3.2 ppm to 3.4 ppm. There is some overlapping of these signals; however, tacticity at the chain ends is

evident. The ^{13}C NMR spectrum in DMF shows two sharp peaks at 58.40 and 58.64 ppm corresponding to $-\text{OCH}_3$ carbons while $-\text{OCH}_2-$ carbons appear as multiple peaks from 76.7-78.6 ppm. The assignment of these peaks to $-\text{OCH}_3$ and $-\text{OCH}_2-$ carbons was confirmed by DEPT ^{13}C NMR.

As indicated above the peak pattern did not change with molecular weights from 1000 to 50,000. This suggests that stereoisomerism seen at the chain ends of model polymers [A] and [B] is related to the bulk tacticity of the polymer. Thus, it is possible to obtain information on bulk tacticity of these anionically prepared polymers by analyses of multiple peaks for $-\text{Si}(\text{CH}_3)_3$ in ^1H NMR.

Various attempts have been made to determine bulk tacticity of polystyrene prepared by anionic, cationic and free radical polymerization using ^{13}C NMR spectroscopy (20-33). Methylene and C(1) phenyl carbons of polystyrene have been probed to determine the probability of racemic dyad content (P_r). P_r values ranging from 0.5-0.79 had been reported for anionically prepared polystyrene. However, assignments of methylene or C(1) phenyl carbon peaks to tetrads and higher n -ads were questionable (20, 25, 27, 32-33). Sato et al. (29-33) prepared oligomeric polystyrene anionically and isolated various triads, tetrads and pentads. These were analysed by ^{13}C and ^1H NMR spectroscopy to correctly assign methylene and C(1) phenyl carbon peaks to various meso and racemic n -ads. Based on these results and Bernoullian statistics they found the value for P_r to be 0.56 for anionically prepared polystyrene. Other authors (23) have then correctly assigned the respective peaks, achieving the same values for P_r (0.50-0.54) within the experimental error.

The $-\text{Si}(\text{CH}_3)_3$ peaks of polymer [A] were computer resolved into sixteen peaks through deconvolution and relative peak areas were determined using pure Lorentzian peak shapes. Figure XI-5 shows the actual spectrum (top), the deconvoluted peaks (bottom) and full fit (center). The resonance frequencies and integral

data of the deconvoluted peaks are shown in Table XI-1. Estimated error is $\pm 1.0\%$.

Table XI-1 Frequencies and Integral Values of Deconvoluted Peaks

Line	Frequency (Hz)	Height (arb. units)	Linewidth (Hz)	Integral (arb. units)	% Integral
1	44.048	5.29	3.15	16.68	0.74
2	-44.811	31.70	4.04	128.19	5.71
3	-53.177	43.97	5.56	244.57	10.89
4	-57.065	10.69	2.38	25.43	1.14
5	-64.020	47.88	5.55	265.88	11.83
6	-68.250	57.02	4.20	239.70	10.67
7	-72.264	49.77	5.11	254.49	11.33
8	-78.443	11.33	7.06	79.98	3.56
9	-85.323	28.92	5.99	173.25	7.71
10	-88.350	32.27	4.41	142.25	6.33
11	-91.577	23.87	5.06	120.84	5.38
12	-94.961	44.80	4.27	191.19	8.51
13	-98.370	10.38	1.88	19.52	0.87
14	-104.315	13.27	2.04	27.06	1.20
15	-108.062	37.98	4.23	160.59	7.15
16	-111.007	42.88	3.66	157.06	6.99

^{13}C NMR data can not be used reliably for interpreting ^1H NMR peaks since the chemical shift order of various n-ads, even among the carbons of methylene and C(1) phenyl groups were different (33). Thus, assignments of these peaks to tetrad structures are based on ^1H NMR studies of PS oligomeric triads (29) and comparative study of syndiotactic, isotactic and atactic polystyrene by ^1H NMR (34). The methine protons of the mm triad of oligomeric PS appear down field (2.21 ppm), as much as 0.3 ppm relative to rr triad (2.54 ppm).

In the ^1H NMR spectrum of syndiotactic polymer, the methine protons appear 0.3 ppm upfield compared to isotactic polystyrene, while methylene protons appear 0.2 ppm upfield. Further, in atactic PS the respective methine and methylene proton chemical shifts are between those of syndiotactic and isotactic polystyrene.

According to Bernoullian statistics, the probabilities of stereochemical sequences in terms of higher -ads such as triads, tetrads and so on can be determined from dyad probabilities such as P_m (meso dyad) or P_r (racemic dyad) or vice versa. Here the following relationship applies:

$$P_m = (1 - P_r) \text{ or } P_r = (1 - P_m)$$

The total % dyad content can be obtained by multiplying the probability by 100.

Probabilities for tetrad stereochemical sequences were calculated from the racemic dyad probability using following relationships (24):

$$\begin{aligned} P_{mmmm} &= P_m^3 \\ P_{rmmm} &= P_m^2 P_r \\ P_{mmmr} &= P_m^2 P_r \\ P_{rmmr} &= P_m P_r^2 \\ P_{mrrm} &= P_m^2 P_r \\ P_{mrrr} &= P_m P_r^2 \\ P_{rrrm} &= P_m P_r^2 \\ P_{rrrr} &= P_r^3. \end{aligned}$$

Further, similar relationships were used for the pentad and hexad stereochemical sequences in order to compare the integral data of the deconvoluted peaks. A computer program in Basic language (on a Macintosh) was written to obtain probabilities of triad, tetrad, pentad and hexad stereochemical sequences using racemic dyad probabilities from 0.3 to 0.6 in the increment of 0.01. This made it easy to compare the experimental results to the calculated values.

Schematic representations of tetrad structures observed at the chain ends in the case of model polymers [A] and [B] are shown Figure XI-6, while those for the model polymers [C] and [D] are shown in Figure XI-7 in terms of triads. The stereochemical sequences are shown in terms of triads due to the reasons explained earlier.

The deconvoluted peaks 13-16 were assigned to rrr tetrads since they appear upfield, based on the above discussion, while peaks 1, 2 and 4 at low field were assigned to mmm tetrads. A P_r value of 0.55 was calculated from the integral values of peaks 13-16 assigned to rrr tetrad sequences, which agrees well with the reported P_r value of 0.56 for anionic polymerization (29-33).

From Bernoullian statistics, using $P_r = 0.55$, probabilities for other tetrads (rmm, mmm, rmm, mmm) were calculated and assigned. These are shown in Table XI-2; assignments with marks '#' and '*' may be interchanged.

Table XI-2 Statistical Analyses of Deconvoluted Multiple Peaks

Assignments	Peaks	Intensity (%)	
		Observed	$P_r=0.55$ †
mmm	1, 2 & 4	7.6	9.1
rmm & mmm#	3 & 5	22.7	22.3
mmr# & mmm*	6, 7, & 8	25.6	24.8
mrr & rmm*	9, 10, 11 & 12	27.9	27.3
rrr	13, 14, 15 & 16	16.2	16.6

† Calculated from Bernoullian Statistics

More than one peak has been assigned to the various tetrads observed because tetrad structures usually show splitting up to pentads and hexads; however, it is difficult to assign all these peaks

to higher -ads than tetrads without having oligomeric model compounds.

Thus, racemic dyad content in the bulk polymers was found to be 55 %. These results of bulk tacticity obtained from proton NMR are further supported by the integral ratios of the multiple peaks observed in carbon NMR for the end groups. Figure XI-8 show the carbon NMR spectra and the integral values of the end groups -Si(CH₃)₃ of polymers [A] and [B] and -OCH₃ end groups for polymer [E]. The ratio of integral values were found to be 52:48 (± 8), respectively, for two sharp peaks at 58.40 and 58.64 ppm corresponding to -OCH₃ carbons in ¹³C NMR spectrum of [E] in DMF (since the peaks are overlapping, the margin of error is much higher). Further, the ratio of integral values were also found to be 44:56 (± 1), respectively, for two Major peaks at -3.0 and -3.2 ppm corresponding to -Si(CH₃)₃ carbons in ¹³C NMR spectrum of [A] and [B].

The tacticity at the chain ends had no dependence on the molecular weight (as evident by similar peak patterns). This suggests that chain end tacticities also correspond to bulk tacticities of the polymer since experimental results are in close agreement with the reported racemic dyad content of 56 % for polystyrene prepared anionically.

Using a similar method it would be possible to analyse the multiple peaks observed in proton NMR for -CH₂-O-CH₃ end groups to obtain information on stereochemical sequences and bulk tacticity. This offers a new method, by incorporating specific groups at the chain ends, to determine bulk tacticity just by ¹H NMR without resorting to time consuming ¹³C NMR methods. Further, polymers of low molecular weights can also be analyzed as reliable models for higher molecular weight polymers where solubility in common NMR solvents is a problem. Furthermore, this suggests that in anionic polymerization, there is a bias, about 9 %, towards the formation of racemic dyads (racemic content 55 %) compared to that for free

radical polymerization of styrene, where the racemic dyad content was found to be about 46 % (24).

XI.3 Conclusions

Model studies of end capping of living polystyryl anions, with and without α -methylstyrene at the chain ends, with chlorotrimethylsilane and chloromethyl methyl ether were done. Low molecular weights of the model polymers enabled us to study the nature of the $-\text{Si}(\text{CH}_3)_3$ and $-\text{CH}_2\text{-O-CH}_3$ end groups by NMR spectroscopy. In ^1H NMR spectra multiple peaks for $-\text{Si}(\text{CH}_3)_3$ and $-\text{CH}_2\text{-O-CH}_3$ group protons were observed. However, $-\text{Si}(\text{CH}_3)_3$ peak patterns for polymers with and without α -methylstyrene at the chain ends were quite different. Various parameters such as initiator, solvent, temperature and molecular weights did not change the peak pattern. Trimethylsilyl end group protons and methine or methylene protons of the polystyrene chain were not coupled as determined by decoupling experiments. This study indicates that the multiple peaks are due to stereoisomerism at the chain ends. Selective stereoisomer formation due to steric factors is indicated when α -methylstyrene is the terminal unit before end capping the polymer. Further, the tacticity at the chain ends had no dependence on the molecular weight; thus, chain end tacticities also correspond to bulk tacticities of the polymer and hence this method provides a facile way to determine the bulk polymer tacticity. Deconvolution of the multiple peaks and statistical analyses indicated the probability of racemic dyad content, P_r , to be 0.55. This result is consistent with reported literature values for anionically prepared polystyrene. Thus, end group spectroscopy provides a means of determining bulk tacticity of the polymer.

XI.4 Experimental

Measurements:

GPC analyses of the polymers were done at 30 °C in THF using a Waters system (RI and UV detectors) after calibration with PS standards. ^1H , ^{13}C and ^{29}Si NMR spectra were obtained on a Varian Unity 400 MHz spectrometer using deuterated chloroform and dimethyl formamide solutions with tetramethylsilane as an external standard. Deconvolution of the proton NMR peaks was accomplished assuming pure Lorentzian peak shapes using built in software of the spectrometer. Routine proton NMR and integrations of the signals for each model polymer synthesized were done on a Bruker WP 270 spectrometer.

THF was distilled once from sodium-benzophenone and then styrene and n-butyllithium were added to it; the solution was freeze-thawed on the vacuum line (ca 10^{-5} torr) 5-6 times, distilled on the vacuum line and stored in a Vacuum Atmospheres glove box ($[\text{H}_2\text{O}] = 0.6$ ppm, $[\text{O}_2] = 1.0$ ppm).

Polystyryllithium solutions in cyclohexane and benzene were freeze-thawed 5-6 times, distilled on the vacuum line and the pure solvents were stored in the glove box.

CMME and CTMS were distilled under nitrogen and the middle fractions were freeze-thawed 5-6 times, distilled on the vacuum line and stored in the glove box.

Styrene was passed through alumina and titrated against dibutyl magnesium till light yellow color and distilled under a vacuum of 38 torr (N_2) at 57 °C. The middle fraction was freeze-thawed 5-6 times on the vacuum line and distilled freshly before use.

Sodium naphthalide was prepared in 30 ml THF by mixing 1.0 g sodium and 10.0 g naphthalene. It was allowed to stir for a day at 25 °C in the glove box and titrated against 0.5 N HCl before use.

Styrene was polymerized and then end capped with CTMS or CMME in the glove box. Styrene (4.0 ml) in THF:benzene (55:45 v/v, 110.0 ml) was initiated using n-butyllithium or sodium naphthalide. Polymerizations were done at 10-15 °C for 30 minutes. Living polymers were end capped with 2-3 equivalents (relative to the initiator) of the end capping agents. In some cases, 1.1-2.0 equivalents of α -methylstyrene were added to the living polystyrene and after 15 minutes the resulting living polymer was end capped with DCDMS. Polymers were precipitated into methanol and washed with ethanol so as to remove naphthalene.

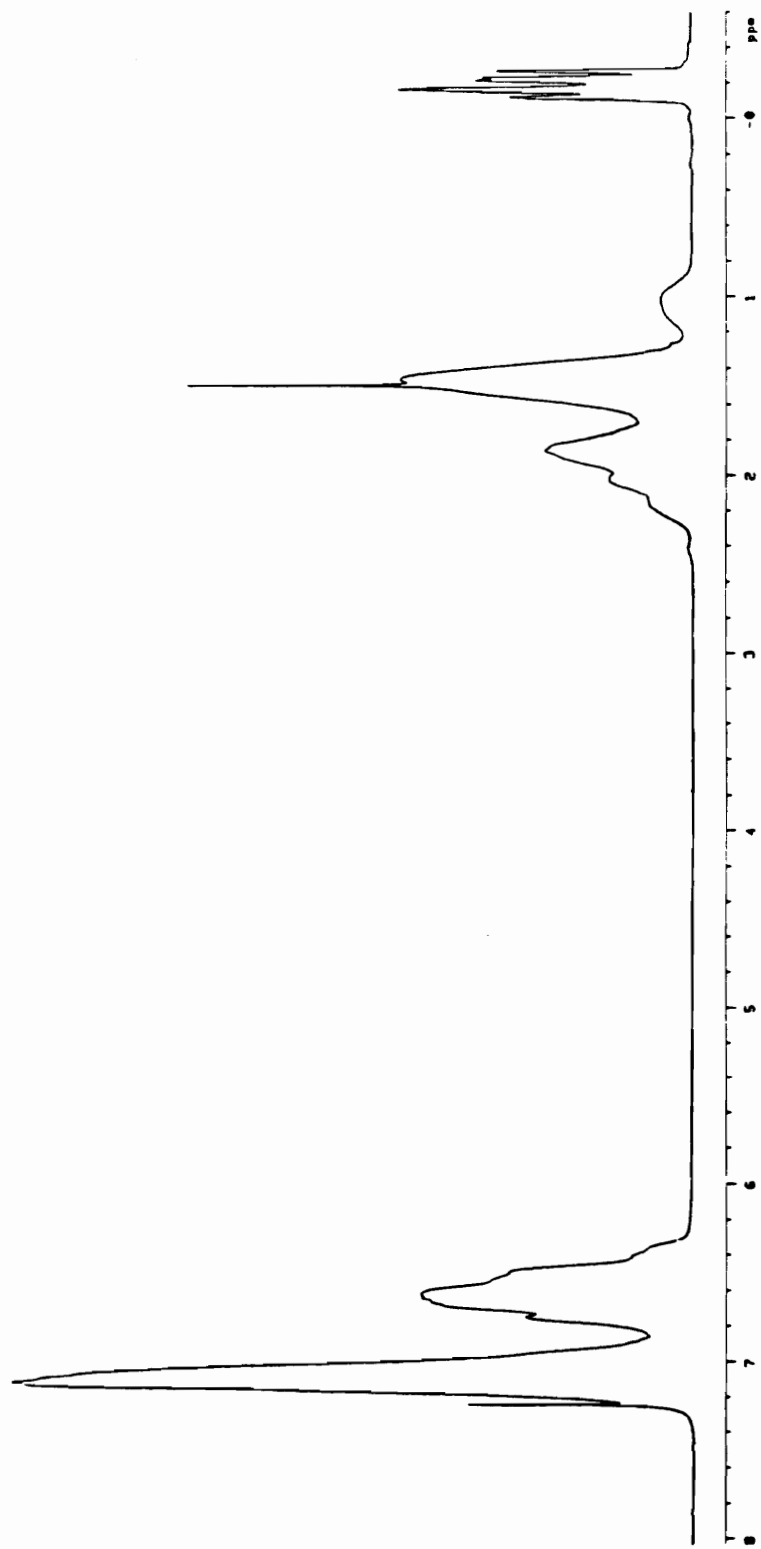
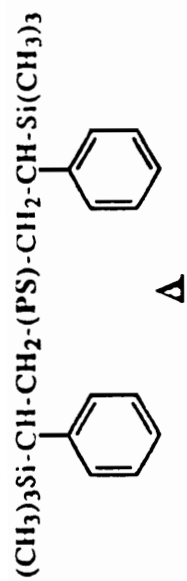


Figure XI.1 Typical ^1H (400 MHz) NMR of Model End Capped Polystyrene

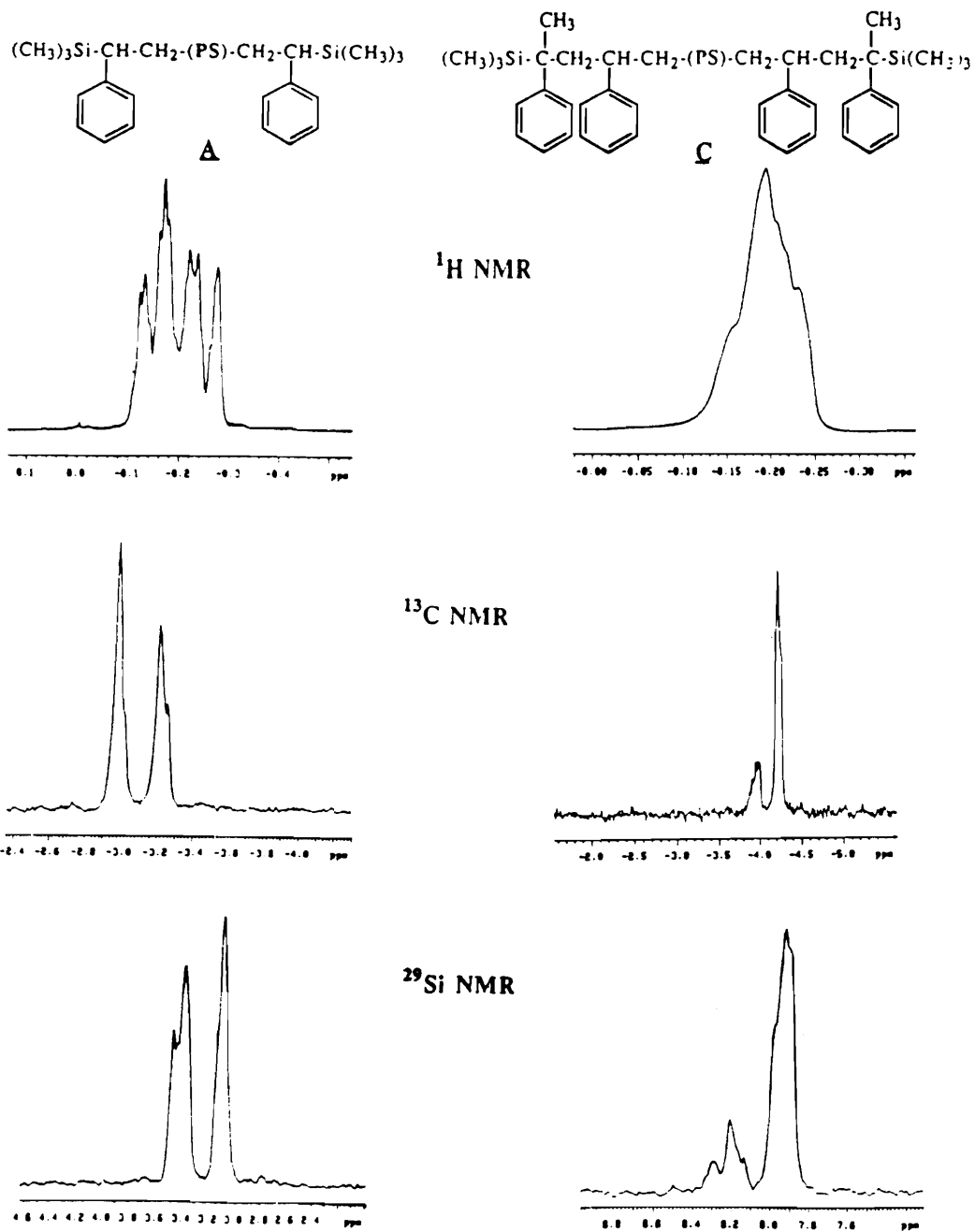


Figure XI.2 ^1H (400 MHz), ^{13}C and ^{29}Si NMR spectra of $-\text{Si}(\text{CH}_3)_3$ groups of model polymers [A] $M_n=2200$, $M_w/M_n=1.15$ and [C] $M_n=2300$, $M_w/M_n=1.15$

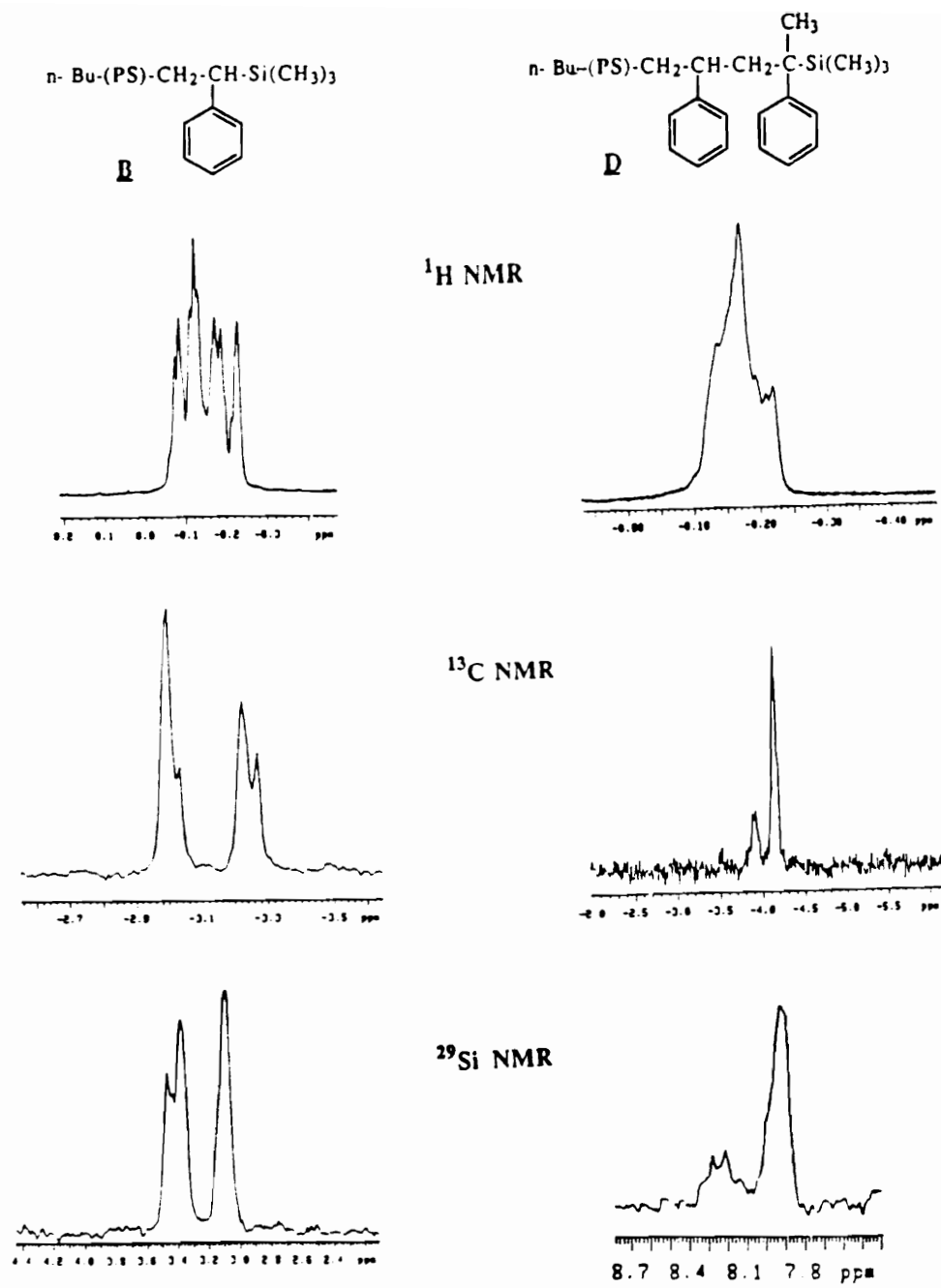


Figure XI.3 ^1H (400 MHz), ^{13}C and ^{29}Si NMR spectra of $-\text{Si}(\text{CH}_3)_3$ groups of model polymers [B] $M_n=1800$, $M_w/M_n=1.10$ and [D] $M_n=2500$, $M_w/M_n=1.09$

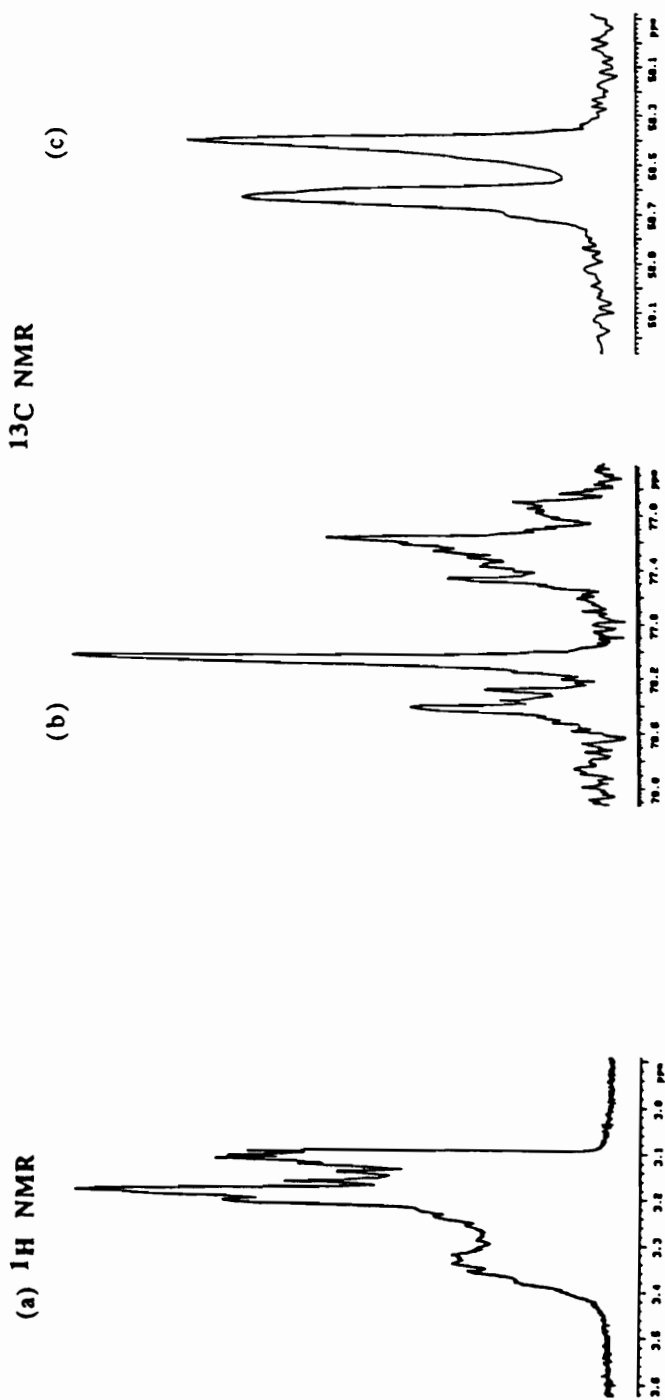


Figure XI.4 NMR Spectra of $-\text{CH}_2\text{-O-CH}_3$ groups of model polymer [E] $M_n=1800$, $M_w/M_n=1.12$: (a) ^1H NMR (400 MHz), (b) ^{13}C NMR: $-\text{CH}_2\text{-O-}$ groups and (c) ^{13}C NMR: $-\text{O-CH}_3$ groups

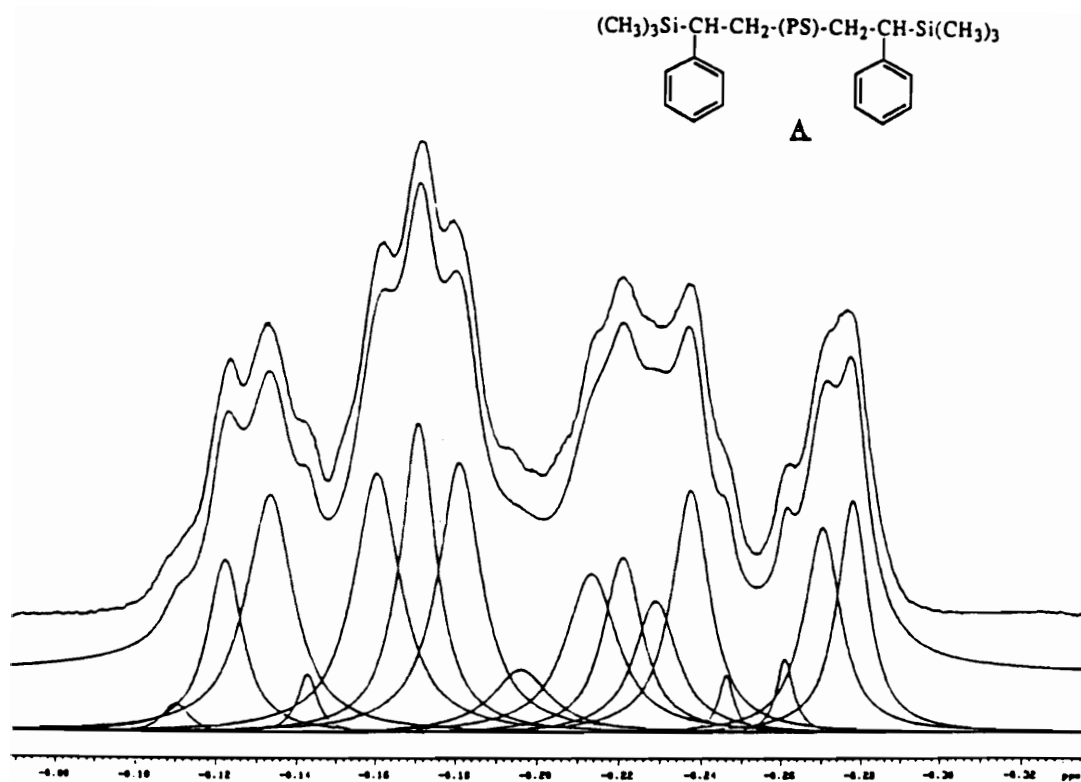


Figure XI.5 Deconvolution of the ^1H NMR spectrum of $-\text{Si}(\text{CH}_3)_3$ groups of the model polymer [A]. The actual spectrum (top), the deconvoluted peaks (bottom) and full fit (center) are shown

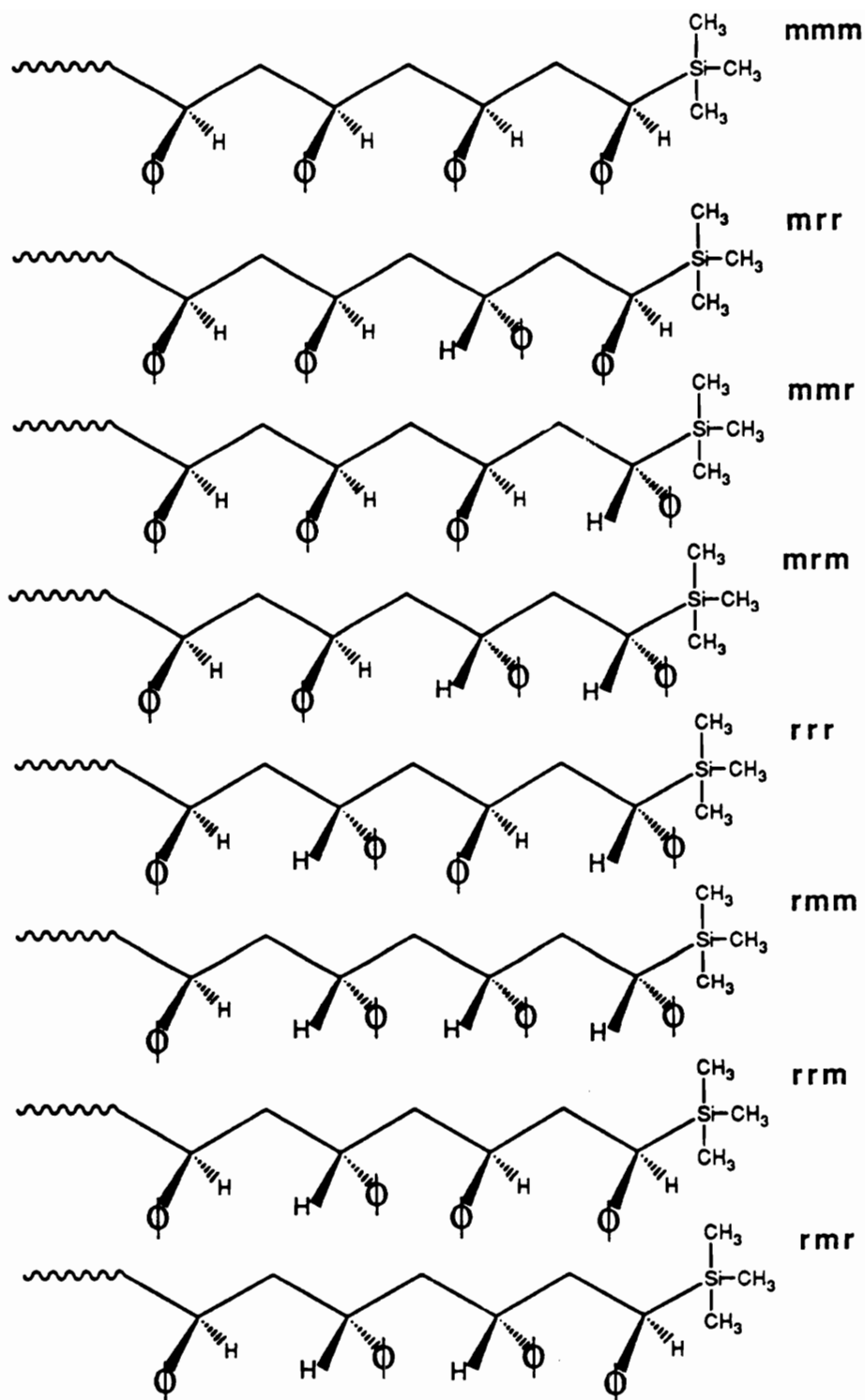


Figure XI.6 Schematic Representation of Tetrad Structures Observed for Model Polymers [A] and [B]

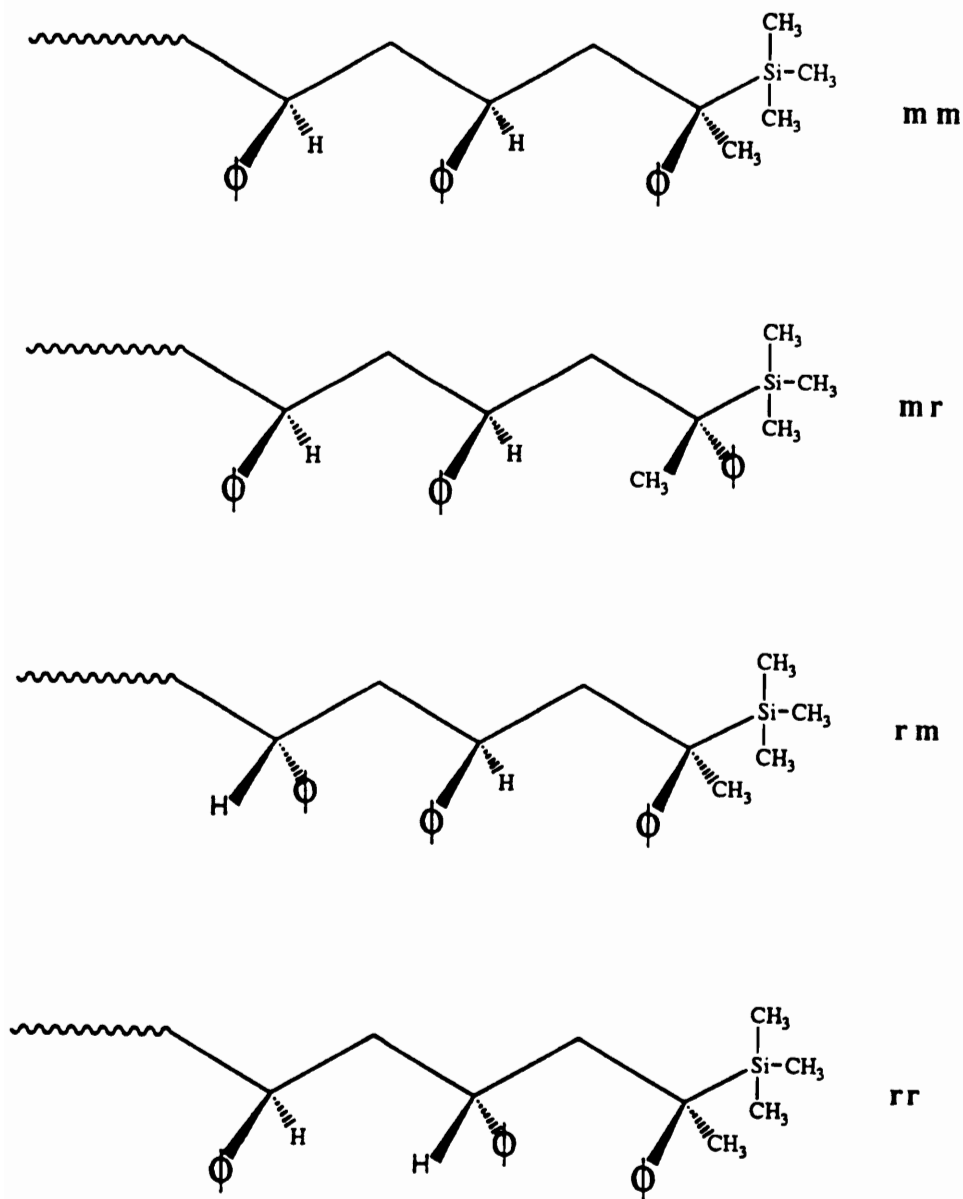


Figure XI.7 Schematic Representation of Triad Structures Observed for Model Polymers [C] and [D]

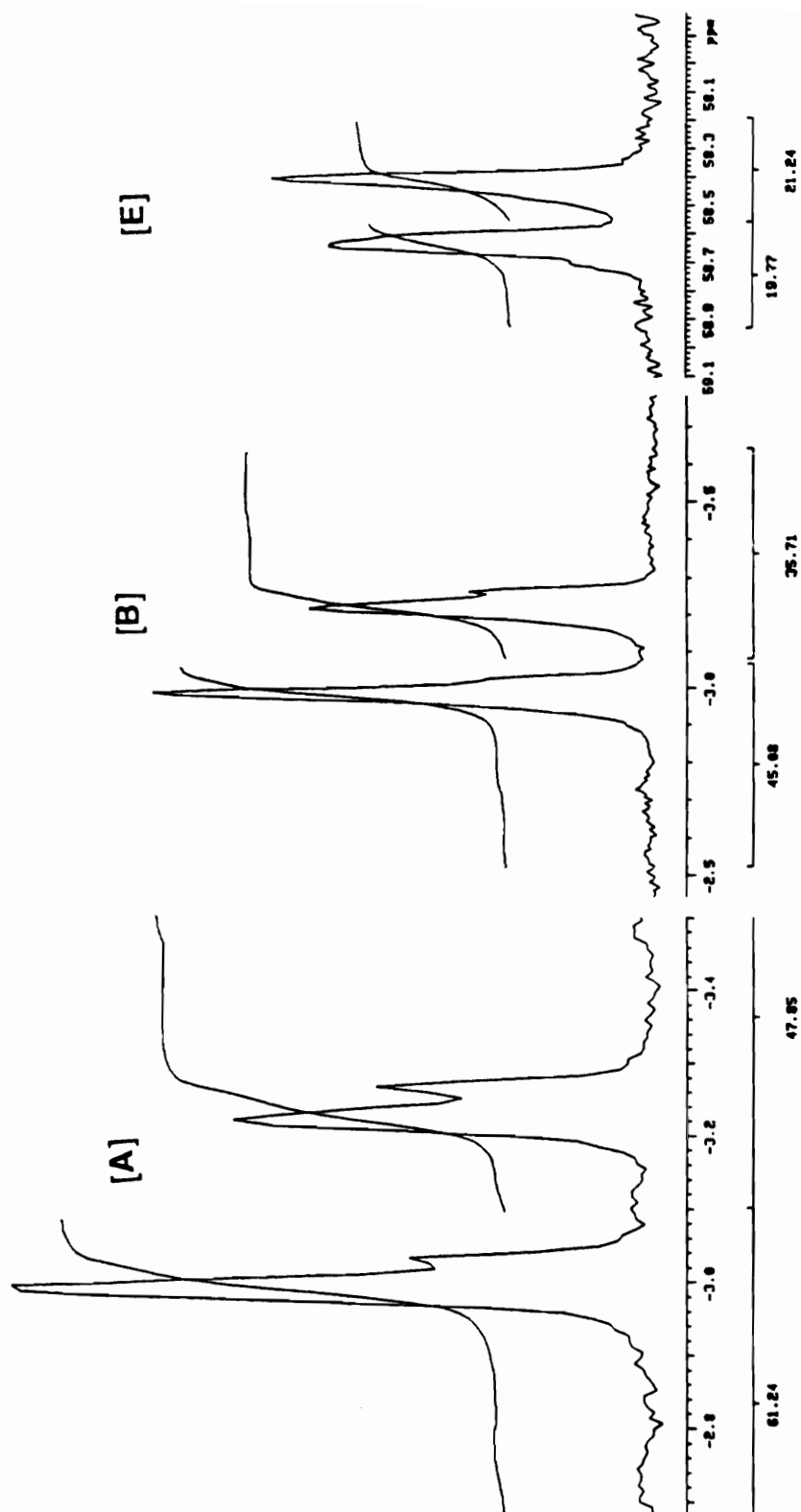


Figure XI.8 ^{13}C NMR Spectra of $-\text{Si}(\text{CH}_3)_3$ End Groups of Model Polymers [A] and [B] and $-\text{CH}_2\text{-O-CH}_3$ End Groups of Model Polymer [E] with Integration Values

References

1. H. W. Gibson, P. R. Lecavalier and P. T. Engen, Amer. Chem. Soc., Polymer Preprints, 1988, 29(1), 248.
2. P. R. Lecavalier, P. T. Engen, Y. X. Shen, S. Jordar, T. C. Ward, and H. W. Gibson, Amer. Chem. Soc., Polymer Preprints, 1989, 30(1), 189.
3. H. W. Gibson, M. C. Bheda, P. T. Engen, Y. X. Shen, J. Sze, C. Wu, S. Joardar, T. C. Ward and P. R. Lecavalier, Amer. Chem. Soc., Polymer Preprints, 1990, 31(1), 79.
4. M. C. Bheda and H. W. Gibson, Amer. Chem. Soc., Polymer Preprints, 1990, 31(1), 588.
5. P. R. Lecavalier, Y. X. Shen, C. Wu and H. W. Gibson, Amer. Chem. Soc., Polymer Preprints, 1990, 31(2), 659.
6. H. W. Gibson, M. C. Bheda, P. T. Engen, Y. X. Shen, J. Sze, C. Wu, T. C. Ward and P. R. Lecavalier, Makromol. Chem., Symp. Vol., 1991, 42/43, 395.
7. C. Wu, P. R. Lecavalier, Y. X. Shen and H. W. Gibson, Chem. Mater., 1991, 3, 569.
8. C. Wu, M. C. Bheda, C. Lim, Y. X. Shen, J. Sze and H. W. Gibson, Polym. Comm., 1991, 32 (7), 204.
9. P. Rempp, C. Strazielle and P. Lutz, Encyclopedia of Polymer Science and Engineering., John Wiley & Sons, New York., 1987, Vol 9, p 183.

10. G. B. McKenna, B. J. Hostetter, N. Hadjichristidis, L. J. Fetters and D. J. Plazek, *Macromolecules*, 1989, 22, 1834.
11. J. J. Ma and R. P. Quirk, *Amer. Chem. Soc., Polymer Preprints*, 1988, 29(2), 10.
12. J. Roovers and P. Toporowski, *Macromolecules*, 1983, 16, 843.
13. G. Hild, C. Strazielle and P. Rempp, *Eur. Polym. J.*, 1983, 19, 721.
14. D. Geiser and H. Hocker, *Macromolecules*, 1980, 13, 653.
15. R. W. Pennisi and L. J. Fetters, *Macromolecules*, 1988, 21, 1094 and references listed therein.
16. D. N. Bhattacharya, C. L. Lee, J. Smid and M. Szwarc, *J. Am. Chem. Soc.*, 1963, 85, 533.
17. Y. Nagasaki and T. Tsuruta, *Makromol. Chem., Rapid Commun.*, 1986, 7, 437.
18. D. J. Worsfold and S. Bywater, *Can. J. Chem.*, 1960, 38, 1891 and K. F. O'Driscoll, E. N. Ricchezza and J. E. Clark, *J. Polym. Sci, Part A*, 1965, 3, 3241.
19. A. H. Soum and T. E. Hogen-Esch, *Macromolecules*, 1985, 18, 690.
20. J. C. Randall, *J. Poly. Sci., Poly. Phy. Ed.*, 1976, 14, 2083.

21. K. Matsuzaki, T. Uryu, K. Osada and T. Kawamura, *Macromolecules*, 1972, 5, 816.
22. T. Uryu, T. Kawamura and K. Matsuzaki, *J. Poly. Sci., Poly. Chem. Ed.*, 1979, 17, 2019.
23. T. Uryu, T. Kawamura and K. Matsuzaki, *Makromol. Chem., Rapid Commun*, 1982, 3, 661.
24. H. J. Harwood, T. K. Chen and F. T. Lin in "NMR & Macromolecules", J. C. Randall Ed; ACS Symposium Series # 247, American Chemical Society, Washington D.C., 1984.
25. A. E. Tonelli, *Macromolecules*, 1983, 16, 604.
26. A. E. Tonelli, *Macromolecules*, 1979, 12, 252.
27. D. L. Trumbo, T. K. Chen and H. J. Harwood, *Macromolecules*, 1981, 14, 1138.
28. S. Suparno, J. Lacoste, S. Raynal, J. Sledz and F. Schue, *Polymer Journal*, 1981, 4, 313.
29. Y. Tanaka, H. Sato, K. Saito and K. Miyashita, *Makromol. Chem., Rapid Commun*. 1980, 1, 551.
30. H. Sato and Y. Tanaka, *Makromol. Chem., Rapid Commun*. 1982, 3, 175.
31. H. Sato and Y. Tanaka, *Makromol. Chem., Rapid Commun*. 1982, 3, 181.

32. H. Sato and Y. Tanaka, J. Poly. Sci., Poly. Phy. Ed., 1983, 21, 1667.
33. H. Sato and Y. Tanaka in "NMR & Macromolecules", J. C. Randall Ed; ACS Symposium Series # 247, American Chemical Society, Washington D.C., 1984, page 183.
34. N. Ishihara, T. Seimiya, M. Kuramoto and M. Uoi, Macromolecules, 1986, 19, 2464.

XII. SUMMARY AND PROSPECTS 278

The important findings of this study are summarized in this chapter along with suggestions and possible future applications of polyrotaxanes.

1. Synthesis of polyrotaxanes of a variety of chemical structures can be accomplished using the statistical threading method and high threading yields can be achieved.
2. Availability of pure macrocycles in large quantities was the major limiting factor in the synthesis of polyrotaxanes. In this study, it was demonstrated that crown ether macrocycles can be prepared in large quantities and can be purified relatively easily and inexpensively to obtain glycol free, polymerization grade (99+ % pure) crown ethers. Pure crown ether macrocycles were isolated in about 40 % yield. The yields of these macrocycles can be further improved by optimizing the reaction conditions such as temperature, dilution, controlled cyclization conditions by using a syringe pump, and so on.

Further, it was found that in the synthesis of 30-c-10, the macrocycle of twice the size, i.e., 60-c-20, is also formed in about 12 % yield. This was of great advantage and a step forward in the synthesis of polyrotaxanes, since the large macrocycles can easily be threaded onto polymer backbones. Furthermore, taking advantage of this knowledge, 36-c-12, 42-c-14 and 48-c-16 were prepared in high yields in our group by optimization of the reaction conditions.

3. Cyclic polystyrene of molecular weight 2500 were prepared in about 50 % yield (isolated yield about 38 %) to provide diversity in the nature of the macrocycles since it is non-polar. Cyclic polystyrene was not utilized in this study for the synthesis of polyrotaxanes; however, it is suggested that such macrocycles can be utilized in the synthesis of polyrotaxanes of

polyaramides such as PPD-T and ODA-I, to increase the hydrophobic content of the polymer systems, without altering the chemical structure of the linear polymer. This could result in soluble polyaramides as indicated in Chapter VIII. Further, significant incorporation of cyclic polystyrene macrocycles onto linear polybutadiene and its comparative study with styrene-butadiene block copolymers would be interesting. The resulting polybutadiene-cyclic polystyrene polyrotaxane can be cross-linked (by cross linking the polybutadiene chains) to various degrees thus, limiting the phase separation of the two components and this could result in much higher impact resistant polymers for use in specialty coatings and other applications.

4. The ionic bipyridyl macrocycle BP-28-N⁺⁴ was prepared in this study in about 13 % yield. The yield of the macrocycle was not affected by use of a template at any concentration. It is believed that another major component of the product (about 42 % yield) having similar proton and carbon NMR spectra is the macrocycle of twice the size, i.e., BP-56-N⁺⁸; however, it has not been proven. This macrocycle can selectively form pre-rotaxanes (as discussed in chapter I) which could be polymerized under appropriate conditions. This macrocycle was not utilized in the synthesis of polyrotaxanes in this study; however, preliminary studies on the synthesis of conductive mono-rotaxanes were done (not included in the thesis due primarily to the preliminary nature of the work). It also seems feasible to expand this concept to polymers such as polyimides to prepare conductive polyrotaxanes. Further, this ionic bipyridyl macrocycle can be utilized to incorporate ionic groups in polymeric systems by polyrotaxane synthesis. The ionic content of such polyrotaxanes prepared by template threading method can be controlled by selective incorporation of macrocycles onto the polymer backbone.

5. Chemistries for monofunctional blocking groups derived from tris(*p*-*t*-butylphenyl)methane containing various functionalities such as phenol, acid, acid chloride, vinyl, hydroxy and chloro were developed. Further, a similar blocking group with an amine functionality was also prepared.
6. Studies on the threading tendencies of flexible and rigid small molecules revealed that both thread 30-c-10 equally well in statistical threading. The rotaxane yields for rigid and flexible molecules were about 10 %. Further, studies on threading of preformed poly(tetrahydrofuran) of different molecular weights by 30-c-10 revealed that threading increases with a decrease in molecular weight due to larger concentration of chain ends per unit volume. Studies on threading of preformed poly(butadiene) by 30-c-10 showed that compatibility of the linear polymer and the macrocycles was not an important factor in the threading yields since similar threading yields were obtained for poly(THF) and poly(BD) of similar molecular weights. Further, it is clear that threading of the polymers is more efficient than for the small molecules on a macrocycle per backbone atom basis. This means that 'model' reactions using small molecules may not be very successful in assessing the structures of polyrotaxanes.
7. Significant changes in the thermal properties of polyaramides were observed upon incorporation of crown ether macrocycles onto the polymer chains. ODA-I-Rotaxa-30-c-10 and ODA-I-Rotaxa-60-c-20 showed interplay of intermolecular and intraannular hydrogen bonding interactions in the polyrotaxanes and the polyrotaxanes showed behavior analogous to thermosetting polymers. PPD-T-Rotaxa-60-c-20 did not show any expected solubility improvement despite very high incorporation of macrocycles; however, very fine suspensions of

polyrotaxanes were obtained and this could help in processing of insoluble PPD-T polymer.

8. It appears that crown ethers can be utilized in the syntheses of polyrotaxanes by anionic polymerization. In the syntheses of polyrotaxanes of polystyrene by anionic polymerization, various factors such as the nature of the solvent, the polymerization temperature, etc., highly influenced the threading yields of the crown ether macrocycles. The weight % macrocycles incorporated (ca. about 9 % 30-c-10) onto polymers are comparable with the earlier study by free radical polymerization; however, much more dilute solutions were used for the anionic polymerizations in this study. It is suggested that anionic polymerizations in more concentrated solutions (using a polar solvent) would significantly improve threading yields.
9. Polyrotaxane of LC polyester showed very little incorporation of 30-c-10 due to the small size of the macrocycle as well as lack of blocking groups at the chain ends. Due to low incorporation of the macrocycles, no significant improvements in the properties were observed. It is suggested that using ionic bipyridyl macrocycle would selectively thread the monomer c-10 bisphenol, which can be polymerized to yield either the LC polyether or the LC polyester. Thus ionic LC polyrotaxanes can be produced. Large crown ethers such as 42-c-14 would also help in achieving higher threading yields in LC polyrotaxanes.
10. Model polymers of low molecular weights enabled us to study the nature of the $-\text{Si}(\text{CH}_3)_3$ and $-\text{CH}_2\text{-O-CH}_3$ end groups and hence determine microstructure of polystyrene by NMR spectroscopy. Various parameters were studied and the results indicate that multiple peaks are due to chain end tacticity. Selective stereoisomer formation is indicated when α -methylstyrene is

the terminal unit before end capping the polymer. The tacticity at the chain ends had no dependence on the molecular weight and hence provides a facile way to determine the bulk polymer tacticity. Deconvolution of the multiple peaks and statistical analyses indicated the probability of racemic dyad content, P_r , to be 0.55 and similar results were obtained from the integral values of the carbon NMR peaks of the end groups. These results are consistent with reported literature values.

Appendix A Vacuum Line Set Up and Operation.	284
---	------------

The inert gas atmosphere system was set up as shown in Figure A-1. The molecular sieves (5 Å) (for removal of water from the inert gas) were dried for 15 hours at 138°C, in the vacuum oven. A glass wool layer about 1/2" thick was placed in the bottom of the column, followed by a 1/2" layer of Drierite® (blue when dry, red when moist). The column was then filled with dry molecular sieves (5 Å) followed by 1/2" layer of Drierite® and 1" layer of glass wool. The catalyst for the removal of oxygen was filled in the catalyst column. Nitrogen and hydrogen gas cylinders were fixed to the wall and copper tubings from the gas cylinders led to the inert atmosphere system. From the mercury column of the inert gas system, a Tygon® tube line led to the hood.

The cold-cathode manometer console was connected to the vacuum line and a pressure reading of 1.1×10^{-5} torr was recorded at the lowest setting of the sensitivity parameter (0.6). The sensitivity parameter can be varied from 0.6 to 2.5; the recommended setting is 1.0. Further, there is no proportional increase in the pressure with increasing setting and that setting at 0.6 gives fairly accurate readings on the vacuum.

The catalyst, for the removal of oxygen from the inert gas, was regenerated as follows. A mixture of 5-10 % hydrogen in nitrogen was passed over the catalyst that was heated to about 140°C. The catalyst turned jet black color upon activation. It took almost 83 hours to complete the activation process. The drying tower, for the removal of moisture from the inert gas, was evacuated for over 80 hours to remove any traces of moisture present. Thus the vacuum line was ready for use.

The catalyst needs to be regenerated periodically as the color of the catalyst begins to turn greenish in color.

Periodic cleaning of the internal parts of the cold cathode is necessary to obtain accurate reading of the vacuum. This can be done by removing the cold cathode from the vacuum line, taking the snap rings out form the slots and washing the internal parts with hexanes or dichloromethane. Thoroughly dry all the parts before

reinstalling them back in the cold cathode. It may be necessary to replace internal parts if they are corroded. These parts can be obtained from INFICON (see the manual).

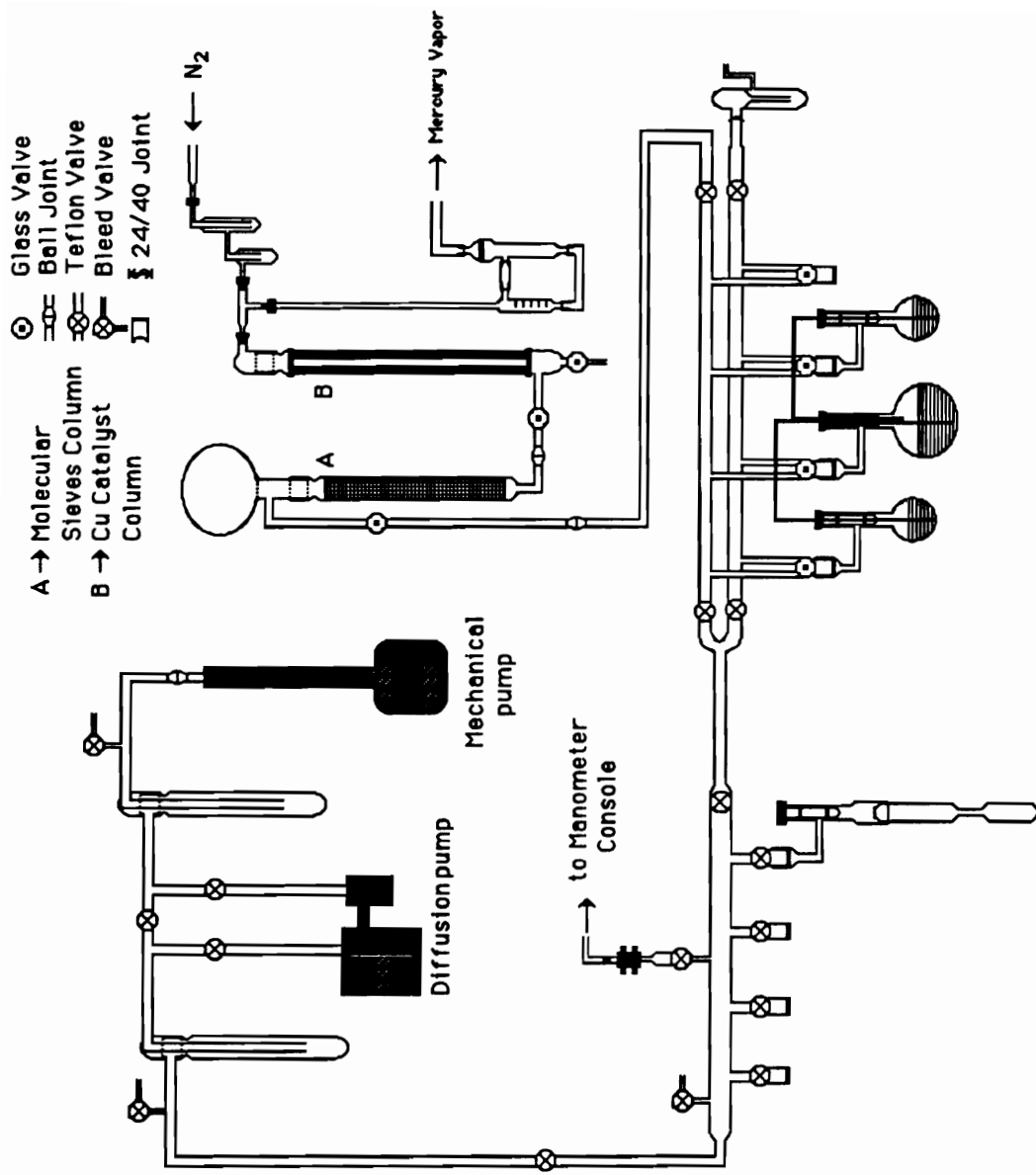


Figure A-1 Vacuum Line Setup

VITA 288

Mukesh C. Bheda was born in Siddhpur, India on July 1, 1960. In 1980, he obtained his Bachelor of Science in chemistry and zoology from University of Bombay, India. He completed his Masters of Science degree (non thesis) in 1982 with organic chemistry as major at University of Bombay, India. During the year of 1982, he worked as Technical Manager for an electroplating plant in Bombay, India.

In 1983, he joined Central Michigan University, Mt. Pleasant, MI, where, he worked with Dr. Dale J. Meier at Michigan Molecular Institute, Midland, MI on modification of block copolymers for thesis research and obtained a M. S. degree in Chemistry (polymer science major) in 1985. After taking a year long medical leave, he joined Dr. Harry W. Gibson's group in December 1987 at Virginia Polytechnic Institute and State University, Blacksburg, VA, for thesis research on novel molecular architectures: polyrotaxanes and catenanes.

A handwritten signature in black ink, appearing to read "Mukesh C. Bheda". The signature is written in a cursive, flowing style with a large initial 'M' and a long, sweeping tail.